Proceedings of the

Fortieth
DOE Solar Photochemistry
P.I. Meeting

Gaithersburg Marriott Washingtonian Center
Gaithersburg, Maryland
June 4-7, 2018

Chemical Sciences, Geosciences, and Biosciences Division
Office of Basic Energy Sciences
Office of Science
U.S. Department of Energy

FOREWORD

The 40th Department of Energy Solar Photochemistry Principal Investigators' Meeting, sponsored by the Chemical Sciences, Geosciences, and Biosciences Division of the Office of Basic Energy Sciences, is being held June 4-7, 2018 at the Washingtonian Marriott in Gaithersburg, Maryland. These proceedings include the meeting agenda, abstracts of the formal presentations and posters, and a list of participants.

The Solar Photochemistry Program supports fundamental, molecular-level research on solar energy capture and conversion in the condensed phase and at interfaces. This conference is the annual meeting of the grantees who conduct research with support from this Program. The gathering is intended to facilitate the exchange of ideas and foster collaboration among these researchers.

The meeting this year features presentations by the two Solar Photochemistry PIs who also serve as a Director of a current Energy Frontier Research Center (EFRC). Tom Meyer leads the UNC Center for Solar Fuels, which has the mission "To conduct research on dye sensitized photoelectrosynthesis cells for water splitting and tandem cells for the reduction of carbon dioxide to carbon-based solar fuels." Mike Wasielewski leads the Argonne-Northwestern Solar Energy Research (ANSER) Center that seeks "To revolutionize our understanding of molecules, materials, and methods necessary to create dramatically more efficient technologies for solar fuels and electricity production." Both will tell us about the many impressive discoveries and research accomplishments within their EFRCs over the past nine years.

This is the first PI Meeting since Mark Spitler retired in January of this year, after managing the Solar Photochemistry Program for over a decade and participating as a PI for many years before joining BES. Mark's vast scientific knowledge combined with his impressive ability to identify, foster, and oversee outstanding research has played a critical role in achieving the high quality and ongoing impact of the Program. I have been fortunate to work alongside Mark and am honored to continue managing a program with such a long tradition of excellence.

I would like to express my appreciation to Justin Johnson of the National Renewable Energy Laboratory, Teresa Crockett of the Office of Basic Energy Sciences, and Connie Lansdon of the Oak Ridge Institute for Science and Education for their assistance with the preparation of this volume and coordination of the meeting logistics. I am also grateful to all of the participants in this meeting, especially the speakers and poster presenters who have contributed so much to the continued success of the Solar Photochemistry Program.

Chris Fecko
Chemical Sciences, Geosciences,
and Biosciences Division
Office of Basic Energy Sciences

TABLE OF CONTENTS

Session VII – Molecular Catalysts for Photochemistry

Session VIII – Photocatalytic Assemblies

Session IX – Supramolecular Systems

Abstracts of Poster Presentations

40th DOE SOLAR PHOTOCHEMISTRY
P.I. MEETING

June 4-7, 2018

Washingtonian Marriott
Gaithersburg, MD

PROGRAM

Monday, June 4

3:00 – 6:00 p.m. Registration

Monday Evening, June 4

5:30 p.m. Working Dinner (*Welcome and Scientific Overview of the Meeting*)

Session I
Ultrafast Molecular Phenomena
Chris Fecko, Chair

7:00 p.m. Electronic Structures of Metal Centers in OER Catalyst Models and Electron/Energy Relays in the Excited State Supramolecular Dinuclear Transition Metal Complexes Revealed by In Situ and Transient X-ray Spectroscopy
Lin X. Chen, Argonne National Laboratory

7:30 p.m. Ultrafast Electron Transfer and Exciton-Vibration Coupling
Gregory D. Scholes, Princeton University

8:00 p.m. Organic Macromolecules for Long-Range and Efficient Transport Properties in Light Energy Conversion Applications
Theodore Goodson III, University of Michigan

8:30 p.m. Chromophores for Enhanced NIR Absorption and High Excited State Redox Potential
Mark Thompson and Stephen Bradforth, University of Southern California

9:00 p.m. No Host Reception

Tuesday Morning, June 5

7:15 a.m. Continental Breakfast

Session II
Introductory Session
Chris Fecko, Chair

8:30 a.m. Opening Remarks
Bruce Garrett and Chris Fecko, DOE Basic Energy Sciences

9:00 a.m. Making Solar Fuels: UNC EFRC for Solar Fuels
Thomas J. Meyer, University of North Carolina at Chapel Hill

9:45 a.m. Highlights from the Argonne-Northwestern Solar Energy Research (ANSER) Center
Michael R. Wasielewski, Northwestern University

10:30 a.m. Break

Session III
Singlet Fission
Libai Huang, Chair

11:00 a.m. Optimal Packing of Chromophores for Singlet Fission
Josef Michl, University of Colorado – Boulder

11:30 a.m. Harvesting the Triplet Pair from Singlet Fission
Xiaoyang Zhu, Columbia University

12:00 p.m. Determination of Vibrational Motions Driving Photoinduced Electron Transfer Reactions in Molecular Crystals and Organic Thin Films
Renee R. Frontiera, University of Minnesota

12:15 p.m. Working Lunch (*Discussions about morning scientific presentations*)

Tuesday Afternoon, June 5

4:00 p.m. Program Information
Chris Fecko, DOE Basic Energy Sciences

Session IV
Semiconductor (Photo)electrochemistry
Shannon Boettcher, Chair

4:30 p.m. Electrochemical Kinetics and Mass-Transport at Single Catalytic Nanoparticles
Michael V. Mirkin, Queens College – CUNY

5:00 p.m. Observing Nanoscale Photochemical Charge Separation with Surface Photovoltage Spectroscopy
Frank E. Osterloh, University of California – Davis

5:30 p.m. Investigation of Oxide-Based Photocathodes for Use in Solar Fuel Production
Kyoung-Shin Choi, University of Wisconsin - Madison

Tuesday Evening, June 5

6:00 p.m. Working Dinner (*Discussions about afternoon scientific presentations*)

7:30 – 10:00 p.m. Posters (*Odd numbers*)

Wednesday Morning, June 6

7:15 a.m. Continental Breakfast

Session V
Semiconductor Interfacial Processes
Stephen Maldonado, Chair

8:30 a.m. Surface Chemistry and Heterogeneous Processes in Solar-Driven Pyridine-Catalyzed CO_2 Reduction
Bruce E. Koel, Princeton University

9:00 a.m. Probing Interfacial Processes on Semiconductors Using Lab-Based Ambient Pressure XPS
Sylwia Ptasinska, University of Notre Dame

9:30 a.m. Modulating Primary Photochemical Events in Group IV Nanocrystals Through Surface Chemistry
Nathan R. Neale, National Renewable Energy Laboratory

10:00 a.m. Break

Session VI
Photodriven Nanoparticle Dynamics
Prashant Kamat, Chair

10:30 a.m. Controlling 2D Transition Metal Dichalcogenides Optoelectronic and Catalytic Properties
Elisa M. Miller, National Renewable Energy Laboratory

11:00 a.m. Surface P-doping and Hot Hole Photochemistry in CdSe Quantum Dots
David F. Kelley, University of California - Merced

11:30 a.m. Ultrafast Dynamics of Photocatalytic Hydrogen Evolution on Monolayer-Rich Tungsten Disulfide
Jao van de Lagemaat, National Renewable Energy Laboratory

12:00 p.m. Working Lunch (*Discussions about morning scientific presentations*)

Wednesday Afternoon, June 6

Session VII
Molecular Catalysts for Photochemistry
Rich Eisenberg, Chair

3:00 p.m. Artificial Photosynthesis: From Rational Catalyst Design to Solar Fuels Generation
Javier J. Concepcion, Brookhaven National Laboratory

3:30 p.m. The Design and Synthesis of Polypyridine Metal Complexes as Catalysts for the Decomposition of Water into its Elements
Randolph Thummel, University of Houston

4:00 p.m. Measuring and Increasing Water Oxidation Catalyst Viability
Douglas B. Grotjahn, San Diego State University

4:15 p.m. Break

4:45 p.m. From the Fundamentals Radiation Chemistry of Acetonitrile to Mechanistic Pulse Radiolysis Studies of CO_2 Reduction Catalysts
David C. Grills, Brookhaven National Laboratory

5:15 p.m. Photosynthetic Systems for Solar Fuel Production: A Combined Study of Molecular Catalysts by Advanced EPR and DFT Modeling
Oleg G. Poluektov, Argonne National Laboratory

Wednesday Evening, June 6

6:00 p.m. Dinner on the Town

7:30 – 10:00 p.m. Posters (*Even numbers*)

Thursday Morning, June 7

7:15 a.m. Continental Breakfast

Session VIII
Photocatalytic Assemblies
Jerry Meyer, Chair

8:30 a.m. Mechanisms of Photocatalytic Assemblies for Solar Fuel Production
Victor S. Batista, Charles A. Schmuttenmaer, Yale University

9:15 a.m. Polyoxometalate Systems, Interfacial Electron Transfer, and Multi-Electron Catalysis
Tianquan Lian, **Djamaladdin G. Musaev, Craig L. Hill**, Emory University

10:00 a.m. Coupled Transport-Transformation Phenomena in a Dye-Sensitized Solar Conversion System
Frances Houle, Lawrence Berkeley National Laboratory

10:15 a.m. Break

Session IX
Supramolecular Systems
Phil Castellano, Chair

10:45 a.m. Well-defined Plasmonic-Excitonic Hybrid Nanosystems as Plexitonic Model Systems
Dorthe M. Eisele, City University of New York

11:00 a.m. Water Oxidation in Catalyst Modified Metal Organic Frameworks
Amanda J. Morris, Virginia Tech University

11:30 a.m. Fundamental Studies of Light-Induced Charge Transfer, Energy Transfer, and Energy Conversion with Supramolecular Systems
Joseph T. Hupp, Northwestern University

12:00 p.m. Closing Remarks
Chris Fecko, DOE Basic Energy Sciences

Electronic Structures of Metal Centers in OER Catalyst Models and Electron/Energy Relays in the Excited State Supramolecular Dinuclear Transition Metal Complexes Revealed by In-situ and Transient X-ray spectroscopic Studies

Ryan G. Hadt, Dugan Hayes, Lars Kohler, Karen L. Mulfort and Lin X. Chen
(in collaboration with Nocera Group)

Chemical Sciences and Engineering Division
Argonne National Laboratory
Lemont, Illinois 60439

Electronic Structures of Metal Centers in an OER Catalyst Model. One of the challenges in solar fuels generation is generating multiple redox equivalents for the oxygen evolution reaction (OER) (i.e., $2H_2O \rightarrow O_2+4H^+ +4e^-$) that is a four-electron, four-proton coupled process. Earth-abundant first-row transition metal oxides of cobalt, nickel, and their mixed-metal forms can drive this half-reaction at relatively low overpotentials. In collaboration with Nocera Group, we used a combination of in situ and ex situ X-ray absorption and emission spectroscopies as well as quantum mechanical calculations on OER thin films and their molecular and heterogeneous inorganic analogs. These studies provided insights into the electronic structures of the high-valent states involved in the mechanisms of O-O bond formation and for the high-valent states to drive the bond-forming and bond-breaking steps of OER reactions. Using a Co_4O_4 cluster as a model for the Co-based OER anode, CoPi, which has a similar topology and can host a stable, but electronically delocalized, mixed-valent Co(IV) state, we employed complementary X-ray spectroscopies, X-ray absorption (XAS) and 1s3p resonant inelastic X-ray scattering (K_β RIXS), to effectively extract Co(IV) contributions within a spectroscopically active background (**Figure 1**). Co K- and L-edge X-ray absorption directly probe the 3d-manifold of effectively localized Co(IV), providing a handle on the covalency of the dπ-based redox active molecular orbital (MO) of Co_4O_4. K_β RIXS is shown to be highly sensitive to metal cluster oxidation state and oxo-mediated metal-metal coupling in high-valent, delocalized mixed-valent species. We also probed the doubly oxidized $Co(III)_2(IV)_2$ state of the Co_4O_4 cluster, which features a cofacial $Co(IV)_2$ site and is thus a molecular model of the active site in Co-OEC. Spectroelectrochemical X-ray absorption data further reveal systematic spectral changes with successive oxidations of the cubane, as well as a feature ~7 eV above the pre-edge for the doubly oxidized cubane. Density functional theory calculations suggest the ground state of the doubly oxidized cube is best

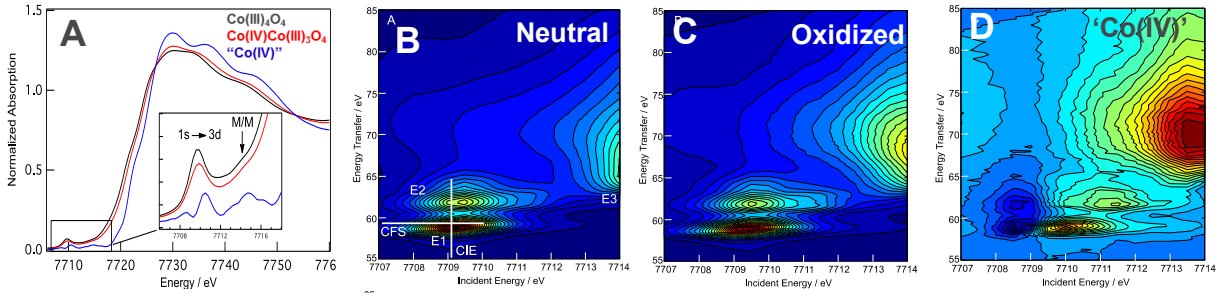

Figure 1. A) XAS spectra of the model Co_4O_4 cluster from which the corresponding oxidized Co(IV) can be extracted; complementary RIXS spectra for neutral B) oxidized C) Co_4O_4; D) the difference spectrum from C) - B) with scaling factor to reveal the "Co(IV)" spectrum.

represented by a localized, antiferromagnetically coupled $Co(IV)_2$ dimer. The exchange coupling in the cofacial $Co(IV)_2$ site allows for parallels to be drawn between the electronic structure of the Co_4O_4 cubane model system and the high valent active site of the Co-OEC, with specific emphasis on contributions to O–O bond formation.

Electron and Energy Relays in the Excited State Supramolecular Dinuclear Transition Metal Complexes. The rational design of multinuclear transition metal complexes (TMCs) for photochemical catalysis of homogeneous and/or heterogeneous multi-electron reactions (e.g. for producing solar fuels) requires a detailed understanding of the often unique and convoluted excited state charge and energy transfer dynamics in this class of compounds. Optical spectroscopic features of various metal sites are often indistinct or overshadowed by the strong ligand orbital dominated π to π^* transition and the transfer of charges to and from shared ligands generally complicate obtaining a comprehensive picture of the dynamics of multinuclear complexes. Using combined optical and X-ray transient spectroscopic measurements, excited state electron electron relays in tetrapyridophenazine-bridged heteroleptic dinuclear Cu(I) bis(phenanthroline) complexes have been investigated as an exemplary system. Our approach combines the synthesis of heterodinuclear analogues of the homodinuclear targets with ultrafast optical and multi-edge X-ray transient absorption (XTA) spectroscopies and theoretical calculations to disentangle the excited state dynamics at individual metal sites by taking advantage of the element specificity in XAS and theoretical methods. We have been able to observe and quantify intermetallic charge and energy transfer in an asymmetric dinuclear Cu-Ru complex (**Figure 2**) in which the redox potentials of the copper sites are offset by a few hundred meV. Intriguingly, we observe charge transfer in the direction opposite to that predicted only from the ground state redox potentials, and we attribute this behavior to an even greater difference in reorganization energies. We also demonstrate the ability of this complex to effectively shuttle energy away from short-lived to long-lived excited states, an unexpected property that could be of great use in the design of broadly absorbing and multifunctional mutimetallic photocatalysts. This work provides an important step toward developing both a fundamental conceptual picture and a practical experimental handle with which synthetic chemists, spectroscopists, and theoreticians may collaborate to engineer cheap and efficient photocatalytic materials capable of performing Coulombically demanding chemical transformations.

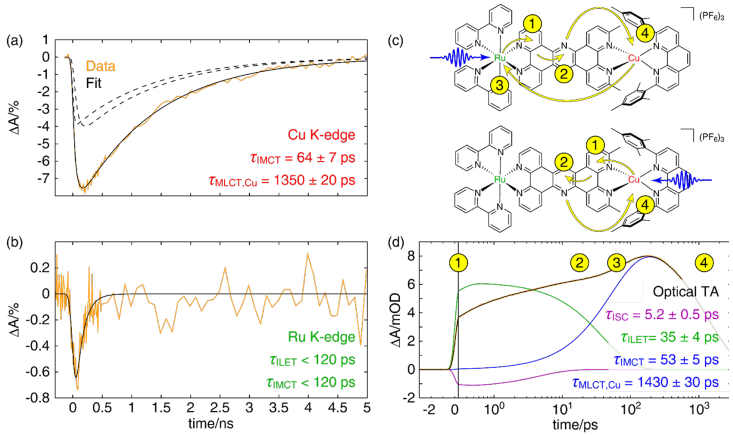

Figure 2. (a) Copper K-edge XTA kinetic trace (orange) of the depletion of the Cu(I) species following 400 nm excitation. (b) Corresponding ruthenium K-edge XTA kinetic trace (orange). (c) Scheme depicting electron transfer pathways in **$CuMe_2$-RuH_2** following optical excitation into the MLCT bands of the Ru(II) (top) or Cu(I) (bottom) center. (d) optical TA kinetic trace (orange) of **$CuMe_2$-RuH_2** taken at a probe wavelength of 605 nm following excitation at 415 nm and a fit (black) to a three-component model that includes ISC (purple), ILET (green), and IMCT and ground state recovery (blue) processes.

DOE Sponsored Publications 2015-2018 (Solar Photochemistry Program)

1. The Role of Excited State Vibrational Dynamics on Electronic Coherence in a Binuclear Pyrazolate-Bridged Platinum (II) Phenylpyradine Complex, Joseph J. Radler, David B. Lingerfelt, Felix N. Castellano, Lin X. Chen, Xiaosong Li, in press, *J. Phys. Chem. A.* (Featured article) (2018).
2. Ligand mediation of vectorial charge transfer in Cu(I)diimine chromophore—acceptor dyads, Dugan Hayes, Lars Kohler, Lin X. Chen, Karen L. Mulfort, *J. Phys. Chem. Lett.*, 9, 2070-2076 (2018).
3. Coherent Vibrational Wavepacket Dynamics in Platinum(II) Dimers and Their Implications, Pyosang Kim, Matthew S. J. Kelley, Arnab Chakraborty, George C. Schatz, Felix N. Castellano, Lin X. Chen, in press *J. Phys. Chem. C* (invited) (2018).
4. The nature of the long-lived excited state in Ni^{II} phthalocyanine complex investigated by X-ray transient absorption spectroscopy, Jiyun Hong, Megan L. Shelby, Dugan Hayes, Xiaoyi Zhang, Lin X. Chen, (invited) in press, *ChemSusChem.*(2018).
5. Phonon-Driven Oscillatory Plasmonic Excitonic Nanomaterials, Matthew S. Kirschner, Wendu Ding, Yuxiu, Craig T. Chapman, Aiwen Lei, Xiao-Min Lin, Lin X. Chen, George C. Schatz, Richard D. Schaller, *Nano Lett.* 18, 442−448 (2018).
6. Electron and Energy Relays Along MLCT State Pathways of Superamolecules with Multiple Metal Centers Revealed by Optical and X-ray Transient Absorption Spectroscopy, D. Hayes, L. Kohler, R. G. Hadt, X. Zhang, C. Liu, K. L. Mulfort, L. X. Chen. *Chem. Sci.,* 9, 860-875 (2018).
7. In situ characterization of cofacial Co(IV) centers in Co_4O_4 cubane: Modeling the high-valent active site in oxygen-evolving catalysts, C. N. Brodsky, R. G. Hadt, D. Hayes, B. J. Reinhart, N. Li, L. X. Chen, D. G. Nocera, *Proc. Natl. Acad. Sci. USA* 114, 3855-3860 (2017).
8. Ultrafast dynamics of two copper bisphenanthroline complexes measured by x-ray transient absorption spectroscopy. M. S. Kelley, M. L. Shelby, M. W. Mara, K. Haldrup, D. Hayes, R. G. Hadt, X. Zhang, A.B. Stickrath, R. Ruppert, J.-P. Sauvage, D. Zhu, H. T. Lemke, M. Chollet, G.C. Schatz, L. X. Chen, (invited) *J. Phys. B-Atomic Molecular and Optical Physics* 50, 154006 (2017).
9. Transient Melting and Recrystallization of Semiconductor Nanocrystals Under Multiple Electron-Hole Pair Excitation, M. S. Kirschner, D. C. Hannah, B.T. Diroll, X. Zhang, M. J. Wagner, D. Hayes, A. Y. Chang, C. E. Rowland, C. M. Lethiec, G.C. Schatz, L. X. Chen, R. D. Schaller, *Nano Lett*. 17, 5314-5320 (2017).
10. Synthesis, structure, and excited state kinetics of heteroleptic Cu(I) complexes with a new sterically demanding phenanthroline ligand. L. Kohler, R. G. Hadt, D. Hayes, L. X. Chen, K. L. Mulfort, *Dalton Trans*. 46, 13088-13100 (2017).
11. Influence of iron doping on tetravalent nickel content in catalytic oxygen evolving films. N. Li, D. K. Bediako, R. G. Hadt, D. Hayes, T. J. Kempa, F. von Cube, D. C. Bell, L. X. Chen, D. G. Nocera, *Proc. Natl. Acad. Sci. USA*, 114, 1486-1491 (2017).

12. Can Excited State Electronic Coherence Be Tuned via Molecular Structural Modification? A First-Principles Quantum Electronic Dynamics Study of Pyrazolate-Bridged Pt(II) Dimers, D. B. Lingerfelt, P. J. Lestrange, J. J. Radler, S. E. Brown-Xu, P. Kim, F. N. Castellano, L. X. Chen, X. Li, *J. Phys. Chem. A* 121, 1932-1939 (2017).
13. Exciton Absorption Spectra by Linear Response Methods: Application to Conjugated Polymers, M. A. Mosquera, N. E. Jackson, T. J. Fauvell, M. S. Kelley, L. X. Chen, G. C. Schatz, M. A. Ratner, *J. Am. Chem. Soc.* 139, 3728-3735 (2017).
14. Chapter 10. "Ultrafast Photochemical Reaction Trajectories Revealed by X-ray Transient Absorption Spectroscopy Using X-ray Free Electron Laser Sources", Lin X. Chen, in *X-Ray Free Electron Lasers: Applications in Materials, Chemistry and Biology*, Ed. U. Bergmann, V. Yachandra, J. Yano, (invited) pp. 201 – 224, Royal Chem. Soc. Publishing (2017).
15. Using coherence to enhance function in chemical and biophysical systems, Scholes, G. D.; Fleming, G. R.; Chen, L. X.; Aspuru-Guzik, A.; Buchleitner, A.; Coker, D. F.; Engel, G. S.; van Grondelle, R.; Ishizaki, A.; Jonas, D. M.; Lundeen, J. S.; McCusker, J. K.; Mukamel, S.; Ogilvie, J. P.; Olaya-Castro, A.; Ratner, M. A.; Spano, F. C.; Whaley, K. B.; Zhu, X. *Nature* 543, 647-656 (2017).
16. Electronic and nuclear contributions to time-resolved optical and X-ray absorption spectra of hematite and insights into photoelectrochemical performance Electronic and nuclear contributions to time-resolved optical and X-ray absorption spectra of hematite and insights into photoelectrochemical performance, Dugan Hayes, Ryan G. Hadt, Jonathan D. Emery, Amy A. Cordones, Alex B. Martinson, Megan L. Shelby, Kelly A. Fransted, Peter D. Dahlberg, Jiyun Hong, Xiaoyi Zhang, Qingyu Kong, Robert W. Schoenlein, Lin X. Chen. *Energ. Env. Sci*., 9, 3754 - 3769 (2016).
17. X-ray Spectroscopic Characterization of Co(IV) and Metal---Metal Interactions in Co4O4: Electronic Structure Contributions to the Formation of High---Valent States Relevant to the Oxygen Evolution Reaction, Ryan G. Hadt, Dugan K. Hayes, Casey N. Brodsky, Andrew M. Ullman, Diego M. Casa, Mary H. Upton, Daniel G. Nocera, Lin X. Chen, *J. Am. Chem. Soc*., 138, 11017–11030 (2016).
18. Photocatalytic Hydrogen Evolution from Water Photocatalysts Based on Cobalt-chelating Conjugated Polymers for Hydrogen Evolution from Water, Lianwei Li, Ryan G. Hadt, Shiyu Yao, Zhengxu Cai, Qinghe Wu, Bill Pandit, Waiyip Lo, Lin X. Chen, Luping Yu, *Chem. Mat.*, 28. 5394-5399 (2016).
19. Butterfly deformation modes in a photo-excited pyrazolate-bridged Pt-complex measured by time-resolved X-ray scattering in solution, Kristoffer Haldrup, Asmus Dohn, Megan L. Shelby, Michael W. Mara, Andrew B. Stickrath , Michael R. Harpham, Jier Huang, Xiaoyi Zhang, Klaus B. Møller, David M. Tiede and Lin X. Chen, *J. Phys. Chem. A*. 120 7475–7483 (2016).
20. Rational Design of Porous Conjugated Polymers and Roles of Residual Palladium for Photocatalytic Hydrogen Production, Li, L.; Cai, Z.; Wu, Q.; Lo, W.-Y.; Zhang, N.; Chen, L. X.; Yu, L. *J. Am. Chem. Soc*. 38, 7681–7686 (2016).

21. Imaging Ultrafast Excited State Pathways in Transition Metal Complexes by X-ray Transient Absorption and Scattering Using X-ray Free Electron Laser Source, Lin X. Chen, Megan L. Shelby, Patrick J. Lestrange, Nicholas E. Jackson, Kristoffer Haldrup, Michael W. Mara, Andrew B. Stickrath, Diling Zhu, Henrik Lemke, Matthieu Chollet, Brian M. Hoffman, Xiaosong Li, *Faraday Discussions* 194, 639-658 (2016).
22. Synthesis, structure, ultrafast kinetics, and light-induced dynamics of CuHETPHEN chromophores, Lars Kohler Dugan K. Hayes, Jiyun Hong, Megan L. Shelby, Kelly A. Fransted, Tyler J. Carter, Lin X. Chen, Karen L. Mulfort, *Dalton Trans*., 45, 9871 - 9883 (2016).
23. Sequential Double Excitations from Linear-response Time-dependent Density Functional Theory Mart´ın A. Mosquera, Lin X. Chen, Mark A. Ratner, and George C. Schatz, *J. Chem. Phys.* 144, 204105 (2016).
24. Size Dependent Coherent Phonon Plasmon Modulations and Dephasing in Gold Bipyramids and Nanojavelins, Matthew S. Kirschner, Clotilde M. Lethiec, Xiao-Min Lin, George C. Schatz, Lin X. Chen, and Richard D. Schaller, *ACS Photonics* 3, 758-763 (2016).
25. Ultrafast Processes in the Relaxation of a Nickel(II) Porphyrin Described by Femtosecond X-ray Absorption Spectroscopy, Megan L. Shelby, Patrick J. Lestrange, Nicholas E. Jackson, Michael W. Mara, Kristoffer Haldrup, Andrew B. Stickrath, Diling Zhu, Henrik Lemke, Brian M. Hoffman, Xiaosong Li, Lin X. Chen, *J. Am. Chem. Soc*. 138, 8752–8764 (2016).
26. The Photophysical and Morphological Implications of Single-Strand Conjugated Polymer Folding in Solution, Thomas J. Fauvell, Tianyue Zheng, Nicholas E. Jackson, Mark A. Ratner, Luping Yu, Lin X. Chen, *Chem*. *Mater*, 28, 2814–2822 (2016).
27. Pyrazolate-Bridged Pt(II) Dimers with Tunable Pt-Pt Distances Enable Control Over the Excited State Properties and Dynamics, Samantha E. Brown-Xu, Matthew S. Kelley, Kelly A. Fransted, Felix N. Castellano, Lin X. Chen, *J. Phys. Chem. A.* 120, 543–550 (2016).
28. Chapter 9. X-ray Transient Absorption Spectroscopy, L. X. Chen, in "*X-Ray Absorption and X-Ray Emission Spectroscopy: Theory and Applications*", Vol. I, Jeroen A. van Bokhoven and Carlo Lamberti, Eds., (Invited) pp. 213-250, Wiley (2016).
29. Electron Injection from Copper Diimine Sensitizers into TiO2: Structural Effects and Their Implications for Solar Energy Conversion Devices, Michael W. Mara, David N. Bowman, Onur Buyukcakir, Megan L. Shelby, Kristoffer Haldrup, Jier Huang, Michael R. Harpham, Andrew B. Stickrath, Xiaoyi Zhang, J. Fraser Stoddart, Ali Coskun, Elena Jakubikova, Lin X. Chen, *J. Am. Chem. Soc.*137, 9670- 9684 (2015).
30. Interplays of Excited State Structures and Dynamics in Copper(I) Diimine Complexes: Implications and Perspectives, M. W. Mara, K. A. Fransted, L.X. Chen, (Invited) Coord. Chem. Rev., 282, 2-18 (2015).

Ultrafast Electron Transfer and Exciton-Vibration Coupling

Gregory D. Scholes and Shahnawaz Rafiq
Department of Chemistry
Princeton University
Princeton, NJ 08544

Introduction. A primary motivation for the first stage of this proposed research program was to work out how to think about 'coherence' in electron transfer reactions. To this end we strove to ascertain different experimental windows to the underlying dynamical processes that govern electron transfer reactions. A particular motivation for such studies is to establish how chemical design at the molecular level influences, and induces the *interplay* among, electronic coupling between molecules, interactions with the environment, and intramolecular vibrations. The key point of the proposal was that we should investigate the *interplay* of factors, which is a hallmark of the attribute loosely called 'coherence'. Our essential approach aimed to revisit the insights concluded in seminal papers on the theory of electron transfer reactions and use new experimental probes based on multidimensional electronic spectroscopy to explore these fundamental aspects of electron transfer dynamics. Some highlights of this research will be reported.

Exciton-Vibration Coupling in Organometallic Complexes. In collaboration with the Chirik group we have been studying the photophysics of bi-molybdenum complexes that bind nitrogen. We imagined that these complexes would be good model systems for exploring the coupling between electronic and nuclear degrees of freedom, and such studies have the potential to lead us to new ways of thinking about stimulating chemical bond activations. In work to date we have resolved the photophysics of representative complexes and have discovered that the excited state lifetime lengthens incredibly upon cryogenic cooling. In subsequent work, see below, we have explored how excitations couple to vibrational degrees of freedom, motivated by the hypothesis that we may be able to work out how to vibronically control the initial steps of reactions.

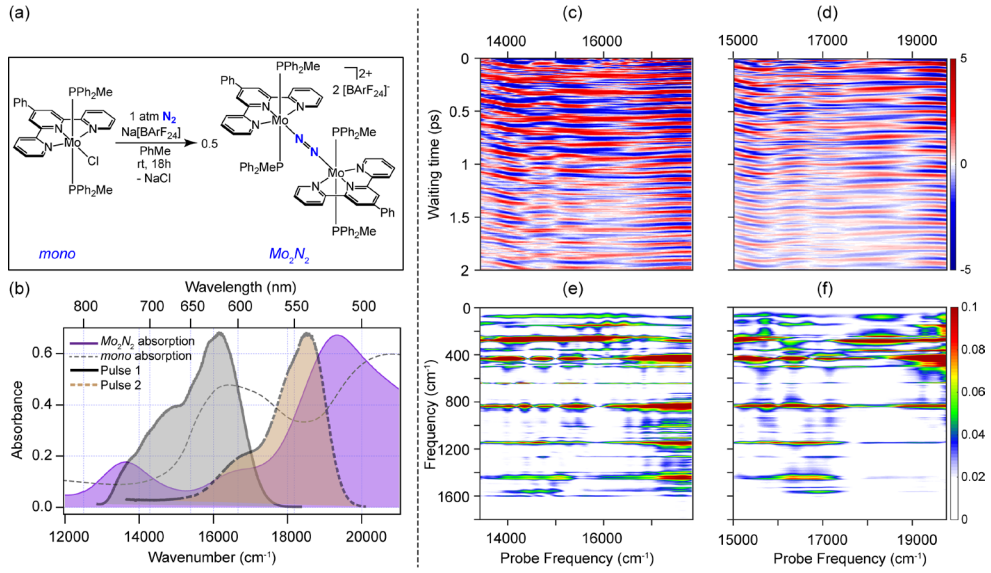

Figure 1. (a) Synthesis of the dinitrogen bridged bimetallic complex ***Mo_2N_2*** from monomer. (b) Violet color shaded filled curve is the absorption spectrum of ***Mo_2N_2*** in diethyl ether. Dashed grey line is the monomer absorption. Solid and dashed bordered shaded curves are the two laser pulse spectra used for broadband pump-probe and two-dimensional electronic spectroscopy. Residual oscillation maps (c) and (d) from the BBPP measurements of ***Mo_2N_2*** complex with pulse 1 and pulse 2 are shown. (e) and (f) are the images obtained after Fourier transform of the oscillations in (c) and (d). Integrated FT is shown in supporting information, figure S1.

Organized vibrational energy flow is indispensable to chemical reactions because reactions ultimately involve the breaking and making of chemical bonds, a process that can be accelerated by putting energy into relevant vibrational degrees of freedom. Ultrafast coherence spectroscopies, Fig 1, augmented by quantum chemical calculations, were used to analyze the choreographed nuclear motions in electronically excited transition-metal pincer complex supporting dinitrogen. The design of the end-on bridged bimetallic molybdenum complex (M-N=N-M) is aimed at functionalizing notoriously unreactive molecular nitrogen. The possibility that photoexcited states might influence bond activation is explored. A striking vibrational coupling mechanism, connecting in-plane breathing motion of the light-harvesting terpyridine ligands with the stretching motion of the dinitrogen bridge, is revealed by accidental Fermi-resonance upon isotopic nitrogen substitution. The coupling is significantly enhanced in the photoexcited state. This anharmonicity-driven coupling is well recognized for driving efficient vibrational energy transfer between the molecular vibrations and in the present case, we hypothesize it can be used to deposit energy into the dinitrogen stretch.

These results will be compared to our studies with the Doyle group, where we have examined the photophysics of Ni(dtbbpy) aryl halide complexes using ultrafast transient absorption spectroscopy. In these studies, we identified an notable density of metal-to-ligand charge transfer (MLCT), ligand-to-ligand charge transfer (LLCT), and π–π* transitions spanning the visible and UV spectral regions. Resonance with any transition led to the generation of a long-lived ^{3}MLCT state. Notably, even ligand-localized π–π* transitions underwent rapid-excitation energy transfer to give the ^{3}MLCT state. This work leads us to the study of photoactivated reductive elimination chemistry and questions concerning the two electron transfers involved and their interplay with bond making and breaking.

Ultrafast Electron Transfer. Generation of coherent superposition of vibrational states in the reactant state does not necessarily deem the transformation of reactant into the product state vibrationally coherent. Vibrational coherences can dephase prior to the underlying photophysical or photochemical dynamics, as in stilbenes, and they are sometimes seen as spectator modes that are orthogonal to the reaction coordinate. Effective off-diagonal coupling between the vibrational superposition on the reactant state and the vibrational states on the product state in comparison to the energy gap fluctuations due to solvation effects decides the level of the interaction between the two potentials. A stronger coupling will enable strongly correlated interaction and the process will have stronger coherent contribution, and in case the effective coupling is negligible than the solvent fluctuations, the correlation parameter will be insignificant and the process will be predominantly incoherent. In the latter case, the initial superposition on the reactant state will evolve on its own with its dephasing decided by the vibrational cooling and intramolecular vibrational relaxation occurring on the reactant state. However, as per the Bixon-Jortner modification of electron transfer theory, the transfer can still occur from the lowest vibrational quantum of the high frequency mode on the reactant state towards the vibrational quanta lying at a resonant energy on the product potential and thereby enhance the rate of electron transfer. We have studied various molecular systems is supported and have observed that dephasing times of high frequency modes and low frequency torsional modes can correlate with electron transfer rates. These results and prospects for future studies will be reported.

DOE Sponsored Publications 2015-2018

1. Shahnawaz Rafiq & Gregory D. Scholes "Slow Intramolecular Vibrational Relaxation Leads to Long-lived Excited State Wavepackets" J. Phys. Chem. A 120, 6792–6799 (2016).

2. Christopher Grieco, Grayson Doucette, Ryan Pensack, Marcia Payne, Adam Rimshaw, Gregory Scholes, John Anthony, John Asbury, "Dynamic Exchange During Triplet Transport in Nanocrystalline TIPS-Pentacene Films" J. Am. Chem. Soc. 138, 16069–16080 (2016).

3. Jean-Luc Brédas, Edward H. Sargent & Gregory D. Scholes "Coherent Solar Energy Conversion" Nature Mater. 16, 35–44 (2017). Invited review.

4. Shahnawaz Rafiq and Gregory D. Scholes, "Is back-Electron Transfer Process in Betaine-30 Coherent?" Chem. Phys. Lett. 683, 500–506 (2017). Ahmed Zewail Commemorative Issue

5. Marius Koch, Mykhaylo Myahkostupov, Daniel Oblinsky, Siwei Wang, Sofia Garakyaraghi, Felix Castellano, and Gregory D. Scholes, "Charge Localization after Ultrafast Photoexcitation of a Rigid Perylene Perylenediimide Dyad Visualized by Transient Stark Effect" J. Am. Chem. Soc. 139, 5530–5537 (2017).

6. YunHui L. Lin, Marius Koch, Alyssa N. Brigeman, David M. E. Freeman, Lianfeng Zhao, Hugo Bronstein, Noel C. Giebink, Gregory D. Scholes, Barry P. Rand "Enhanced sub-bandgap efficiency of a solid-state organic intermediate band solar cell using triplet-triplet annihilation" Energy. Environ. Sci. 10, 1465-1475 (2017).

7. Bryan Kudisch, Margherita Maiuri, Vicente M. Blas-Ferrando, Javier Ortiz, Ángela Sastre-Santos, Gregory D. Scholes, "Solvent-dependent Photo-induced Dynamics in a Non-rigidly Linked Zinc Phthalocyanine-Perylenediimide Dyad Probed by Ultrafast Spectroscopy" PCCP. 19, 21078–21089 (2017).

8. Jacob C. Dean, Ruomeng Zhang, Rawad K. Hallani, Ryan D. Pensack, Samuel N. Sanders, Daniel G. Oblinsky, Sean R. Parkin, Luis M. Campos, John E. Anthony and Gregory D. Scholes, "Photophysical characterization and time-resolved spectroscopy of a anthradithiophene dimer: exploring the role of conformation in singlet fission" PCCP. 19, 23162-23175 (2017).

9. Lianfeng Zhao, Yao-Wen Yeh, Nhu L. Tran, Fan Wu, Zhengguo Xiao, Ross A. Kerner, YunHui L. Lin, Gregory D. Scholes, Nan Yao, Barry P. Rand, "In-situ Preparation of Metal Halide Perovskite Nanocrystal Thin Films for Improved Light Emitting Devices" ACS Nano. 11, 3957-3964 (2017). DOI: 10.1021/acsnano.7b00404

10. Marius Koch, Mykhaylo Myahkostupov, Daniel Oblinsky, Siwei Wang, Sofia Garakyaraghi, Felix Castellano, and Gregory D. Scholes, "Charge Localization after Ultrafast Photoexcitation of a Rigid Perylene Perylenediimide Dyad Visualized by Transient Stark Effect" J. Am. Chem. Soc. 139, 5530–5537 (2017).

11. Elango Kumarasamy, Samuel N. Sanders, Murad J. Y. Tayebjee, Amir Asadpoordarvish, Timothy J. H. Hele, Eric G. Fuemmeler, Andrew B. Pun, Lauren M. Yablon, Jonathan Z. Low, Daniel W. Paley, Jacob C. Dean, Bonnie Choi, Gregory D. Scholes, Michael L. Steigerwald, Nandini Ananth, Dane R. McCamey, Matthew Y. Sfeir, and Luis M. Campos, "Tuning Singlet Fission in π-Bridge-π Chromophores" J. Am. Chem. Soc. 139, 12488–12494 (2017).

12. Benjamin J. Shields, Bryan Kudisch, Gregory D. Scholes and Abigail G. Doyle “Long-Lived Charge-Transfer States of Nickel(II) Aryl Halide Complexes Facilitate Bimolecular Photoinduced Electron Transfer” J. Am. Chem. Soc. 140, 3035–3039 (2018).

13. Christopher Grieco, Eric R. Kennehan, Hwon Kim, Ryan D. Pensack, Alyssa N. Brigeman, Adam Rimshaw, Marcia M. Payne, John E. Anthony, Noel C. Giebink, Gregory D. Scholes, and John B. Asbury, “Direct Observation of Correlated Triplet Pair Dynamics during Singlet Fission Using Ultrafast Mid-IR Spectroscopy” J. Phys. Chem. C. 122, 2012–2022 (2018).

14. Shahnawaz Rafiq, Máté Bezdek, Marius Koch, Paul Chirik, Gregory D. Scholes, “Ultrafast Photophysics of a Dinitrogen Bridged Molybdenum Complex” J. Am. Chem. Soc. Revised manuscript submitted (2018).

Organic Macromolecules for Long-Range and Efficient Transport Properties in Light Energy Conversion Applications

Theodore Goodson III

Department of Chemistry, Department of Macromolecular Science and Engineering, University of Michigan, Ann Arbor, Michigan 48109

Organic conjugated molecules for light harvesting applications have received great attention due to their versatility, simple fabrication process ability and relatively low manufacturing costs. While there has been great improvement of light conversion efficiency in certain materials, there still remain questions concerning the structural and inhomogeneity of the transport processes. In this regard, understanding the fast processes (fs) at a local level (nm) in these systems is crucial in the design criteria for better light conversion efficiency. In this presentation, the results of fast photo-physical dynamics of organic light harvesting materials will be described. These materials have been analyzed using time-resolved spectroscopy as well as a nonlinear ultrafast time resolved microscopy. Charge transport dynamics of light harvesting polymers which have different electron withdrawing and accepting groups have been investigated. The heteroatom effect embedded in conjugated polymers has also been investigated for increasing charge transport properties. Ultra-fast interferometric microscopic measurements were carried out to investigate the role of coherent energy transport in these organic photovoltaic materials.

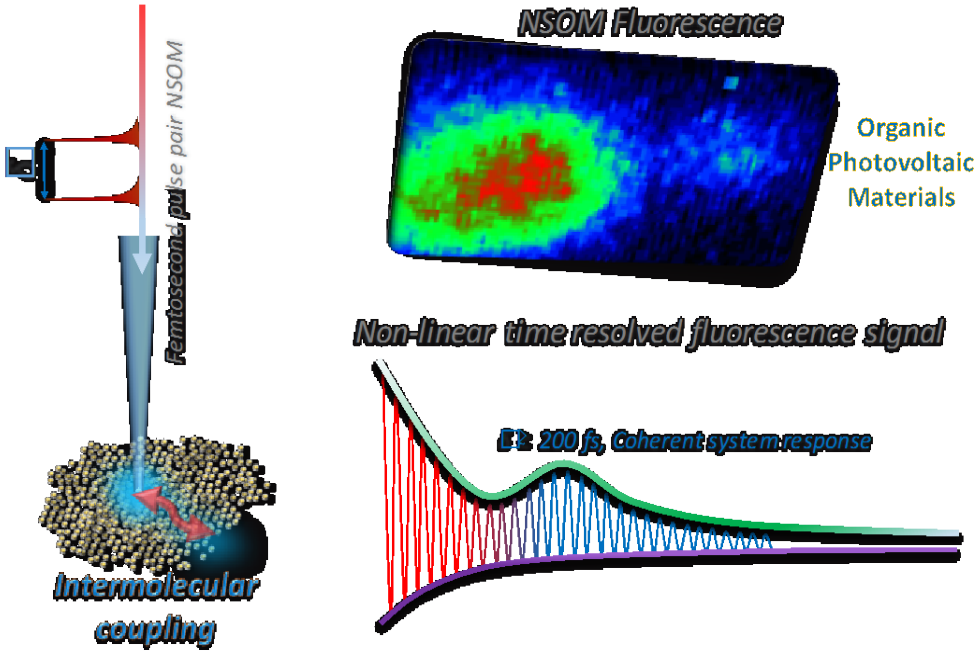

Schematic of two-photon time-resolved NSOM interferometry.

DOE Sponsored Publications 2015-2018

1. Cai, Z.X.; Vazquez, R.J.; Zhao, D.L.; Li, L.W.; Lo, W.Y.; Zhang, N.; Wu, Q.H.; Keller, B.; Eshun, A.; Abeyasinghe, N.; Banaszak-Holl, H.; Goodson III, T.; Yu, L. Two Photon Absorption Study of Low-Bandgap, Fully Conjugated Perylene Diimide-Thienoacene-Perylene Diimide Ladder-Type Molecules *Chem. Mater.* **2017**, *29*, 6726-6732.
2. Idowu, M.A.; Yau, S.H.; Varnavski, O.; Goodson III, T. Evolution of the Dynamics of As-Deposited and Annealed Lead Halide Perovskites *ACS Photonics*, **2017**, *4,* 1195–1206.
3. Yik, B.J.; Guo, M.; Kwon, Y.; Goodson III, T. New Approaches for Energy Storage with Hyperbranched Polymers *J. Phys. Chem. C* **2017,** *121,* 7108-7122.
4. Vazquez, R.J.; Kim, H.; Kobilka, B.M.; Hale, B.J.; Jeffries-EL, M.; Zimmerman, P.M. Goodson, T. Evaluating the Effect of Heteroatoms on the Photophysical Properties of Donor-Acceptor Conjugated Polymers Based on 2,6-Di(thiophen-2-yl)benzo[1,2-b:4,5-b']difuran: Two-Photon Cross Section and Ultrafast Time-Resolved Spectroscopy *J. Phys. Chem. C* **2017,** *121,* 14382-14392.
5. Keller, B.; McLean, A.; Kim, B.G.; Chung, K.; Kim, J.; Goodson III, T Ultrafast Spectroscopic Study of Donor-Acceptor Benzodithiophene Light Harvesting Organic Conjugated Polymers *J. Phys. Chem. C* **2016**, *120*, 9088-9096.
6. Varnavski, O.; Abeyasinghe, N.; Aragó, J.; Serrano-Pérez, J.J.; Enrique Ortí, E.; López Navarrete, J.T.; Takimiya, K.; Casanova, D.; Casado, J.; Theodore Goodson III, T. High Yield Ultrafast Intramolecular Singlet Exciton Fission in a Quinoidal Bithiophene *J. Phys. Chem. Lett.*, **2015**, *6*, 1375-1384.
7. Adegoke, O.O.; Jung, I.H.; Orr, M..; Yu, L.; Goodson III, T. Effect of the Acceptor Strength on the Optical and Electronic Properties in Conjugated Polymers for Solar Applications *J. Am. Chem. Soc.* **2015,** *137*, 5759-5769.
8. Varnavski, O.; Kim, T.; Cai, Z.; Yu, L.; Goodson III, T. Ultra-fast Coherent Energy Transport in Organic Photovoltaic Materials Measured at Nanoscale" to *J. Am. Chem. Soc. (submitted)* **2018**
9. Carlotti, B.; Cai, Z.; Kim, H.; Sharapov, VV.; Madu, I.K.; Zhao D.; Chen W.; Zimmerman, P.M.; Yu, L.; Goodson III, T. " Charge Transfer and Aggregation Effects on the Performance of Planar vs. Twisted Non-Fullerene Acceptor Isomers for Organic Solar Cells "*Chem. Mater. (submitted)* **2018**
10. Vazquez, R.J.; Kim, H.; Zimmerman, P.M.; Goodson III, T. Evidence of Delayed Fluorescence in the Nanosecond Regime by a Purely Organic Chromopohore *J. Am. Chem. Soc. (submitted)* **2018**
11. Kim, H.; Keller, B.; Ho-Wu, R.; Abeyasinghe, N.; Varquez, R.J.; Goodson III, T.; Zimmerman, P.M. Enacting Two-Electron Transfer from a TT State of Intermolecular Singlet Fission to *J. Am. Chem. Soc.(submitted)* **2018**

Chromophores for Enhanced NIR Absorption and High Excited State Redox Potential

Mark Thompson, Stephen Bradforth, Jessica Golden, Laura Estergreen, Abegail Tadle
Department of Chemistry
University of Southern California
Los Angeles, CA 90089

The goal of our program is to prepare chromophores that give strong absorption in the NIR and give long lifetime charge separated states. Achieving both of these in the same dye is often precluded by energy gap law considerations. The approach we have taken here is to split this into two tasks, *i.e.* NIR absorbance and strategies for achieving long lifetimes for these dyes. The text below will cover the use of dipyridyl-methene based dyes to achieve red and NIR absorption. Our approach to achieving long lifetime for these dyes is to couple them into orthogonal dimers to drive Symmetry Breaking Charge Transfer (SBCT) and form charge separated excited states from the initially localized excited state. The SBCT transition takes place on the ps time scale, outcompeting both emission and nonradiative decay.

We have investigated a relatively unexplored family of dyes, based on dipyridyl-methenes (DIPYRs), Figure 1.[1] Benzanulation of DIPYR leads to an expected red shift and a marked enhancement in photoluminescence efficiency (Φ_{PL}). The low Φ_{PL} for DIPYR is due to a near degeneracy of the S_1 and T_2 states giving rapid intersystem crossing, which is not the case for the benzannulated versions. Our modeling values correlate well the experimental singlet and triplet energies for the three DIPYR compounds. We have two other dipyridyl-methene dyes in process (*i.e.* Aα-DIPYR and dbl-DIPYR) and will have data to present at the review in June. Both compounds are expected to give strong absorption in the NIR.

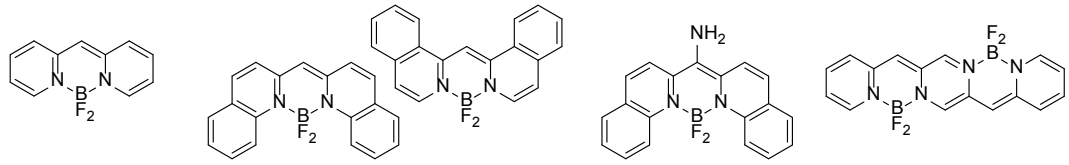

	DIPYR	α-DIPYR	γ-DIPYR	Aα-DIPYR	dbl-DIPYR
EXP.: λ Abs./PL-S_1/PL-T_1 (nm)	481/484/577	520/520/638	500/504/626	--	--
Theory (DFT): S_1/T_1 (nm)	461 / 587	533 / 668	515 / 658	760 /	1060 / 1810
EXP: ε (10^4 $M^{-1}cm^{-1}$) / Φ_{PL}	2.9 / 0.17	11 0.77	8.7 / 0.80	--	--

Figure 1: Photophysical properties of DIPYR dyes.

A key design criterion for our dye studies is that they are capable of chelating to a metal center or fusing into a dimer by linking two dyes at their *meso*-carbons. This criterion is very important for the second part of our approach to useful NIR dyes, which is to form a long-lived excited state. We are extending our previous work with chromophore dimers, using SBCT to rapidly transition from a localized excited state to a charge separated state. (Our work of course builds on that of other researchers that showed an orthogonal relationship between planar dyes might give rise to rapid SBCT in polar solvents.)[2] We have found that for both Zn(dipyrrin)$_2$ and *meso*-bridged BODIPY compounds (Figure 2 a and b) excitation initially gives an excited state localized on a single dipyrrin that transitions to an inter-dye charge separated state on the ps time scale, and that charge separated state lives for 0.5-2 ns.[3] In polar solvents, the charge transfer process in these

dimers out-competes both radiative and nonradiative decay from the dye alone, and ps rates are expected for NIR dyes as well. A NIR "dye-dimer" will be rapidly converted to a pair of oxidized and reduced dyes that can be used to drive electrochemical processes.

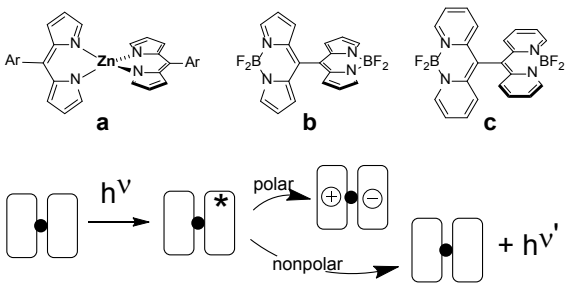

Figure 2: Dimer structure types used to study symmetry breaking charge transfer and a schematic representation of the decay process for SBCT materials in polar and non-polar media.

We have recently examined *meso*-bridged dimers of DIPYR dyes (Figure 2 c) and found that the SBCT process takes place on the sub-ps time scale in both polar and nonpolar solvents.[4] This is believed to be due to an intermediate step for the DIPYR dimers, which may occur at very early times. This intermediate state is the partial charge transfer state (PCT) where charge density is pushed onto the *meso*-bridge of the dimer complex. In 9,9'-bianthryl this partial charge transfer state is observed at very early times in polarized transient absorption studies.[5] The PCT state has a very different torsion potential which once populated leads to oscillations in the torsional angle for the dimer; this has been observed in both polar and nonpolar solvents.[6] However, in 9,9'-bianthryl, this PCT state does not result in a complete separation of charges in nonpolar solvents. In the DIPYR dimers, where the molecular framework itself is more polarizable, the PCT may act as a doorway state to a complete separation of charges, even in a nonpolar environment. In contrast, for the $Zn(DIP)_2$ complexes, the orbital energies at the Zn(II) center preclude electron density developing in the center of the excited chromophore. Thus, Zn complexes should not have a partial charge transfer state, which would otherwise result in a change in the torsional angle.

Based on their lack of SBCT in nonpolar solvents, it appears that both the $Zn(dipyrrin)_2$ and BODIPY dimer systems do not involve initial formation of a PCT state. It is interesting to note that the nature of the HOMO and LUMO for the DIPYR and BODIPY dimers differ markedly. The HOMO of DIPYRs have significant density on the *meso*-carbon, while BODIPY dyes have a node at the *meso*-carbon,[1] suggesting it is the hole that migrates from dye*→SBCT. Passage from the locally excited to PCT state typically occurs on timescales that are shorter than current resolution of 150 fs. In order to increase the time resolution and gain dynamic and spectral information about the PCT, new transient absorption measurements of the DIPYR dimers and BODIPY dimers will be made exploiting a noncolinear optical parametric amplifier to improve time resolution. Polarized transient absorption will also be carried out to unravel the direction of charge transfer in the symmetry breaking processes.

1. Golden, J. H.; Facendola, J. W.; Sylvinson M. R, D.; Baez, C. Q.; Djurovich, P. I.; Thompson, M. E., *The Journal of Organic Chemistry* **2017,** *82*, 7215-7222.

2. (a) Rettig, W.; Zander, M., *PCCP* **1983,** *87*, 1143-1149; (b) Giaimo, J. M.; Gusev, A. V.; Wasielewski, M. R., *J. Am. Chem. Soc.* **2002,** *124*, 8530-8531.

3. (a) Whited, M. T.; Patel, N. M.; Roberts, S. T.; Allen, K.; Djurovich, P. I.; Bradforth, S. E.; Thompson, M. E., *Chem. Commun.* **2012,** *48*, 284-286; (b) Trinh, C.; Kirlikovali, K. O.; Das, S.; Ener, M. E.; Gray, H. B.; Djurovich, P. I.; Bradforth, S.; Thompson, M. E., *The Journal of Physical Chemistry C* **2014**.

4. Golden, J. H.; Estergreen, L.; Porter, T.; Tadle, A. C.; Sylvinson M. R, D.; Facendola, J. W.; Kubiak, C. P.; Bradforth, S. E.; Thompson, M. E., *ACS Applied Energy Materials* **2018,** *1*, 1083-1095.

5. Takaya, T.; Hamaguchi, H.; Iwata, K., *J. Chem. Phys.* **2009,** *130*, 014501

6. Hashimoto, S.; Yabushita, A.; Kobayashi, T.; Okamura, K.; Iwakura, I., *Chem. Phys.* **2018**.

Papers from this DOE funded program, October 2016 – present:

1. Golden, J. H.; Facendola, J. W.; Sylvinson M. R, D.; Baez, C. Q.; Djurovich, P. I.; Thompson, M. E., *Boron Dipyridylmethene (DIPYR) Dyes: Shedding Light on Pyridine-Based Chromophores*. *The Journal of Organic Chemistry* **2017**, *82*, 7215-7222.
2. Golden, J. H.; Estergreen, L.; Porter, T.; Tadle, A. C.; Sylvinson M. R, D.; Facendola, J. W.; Kubiak, C. P.; Bradforth, S. E.; Thompson, M. E., *Symmetry-Breaking Charge Transfer in Boron Dipyridylmethene (DIPYR) Dimers*. *ACS Applied Energy Materials* **2018**, *1*, 1083-1095.
3. Das, S.; Thornbury, W. G.; Bartynski, A.; Thompson, M. E.; Bradforth, S. E., *Manipulating Triplet Yield Through Control Of Symmetry Breaking Charge Transfer*, *Journal of Physical Chemistry Letters*, submitted.

Making Solar Fuels
UNC EFRC for Solar Fuels

Thomas J. Meyer, Leila Alibabaei, Benjamin D. Sherman, Matthew V. Sheridan, M. Kyle Brennaman, Animesh Nayak , Michael S. Eberhart ,Ying Wang, Renato N. Sampaio, Ludovic Troian-Gautier, Kyung-Ryang Wee, Melissa K. Gish, [#]Javier J. Concepcion, James F. Cahoon, Gerald J. Meyer, John M. Papanikolas

Department of Chemistry, University of North Carolina at Chapel Hill, Chapel Hill, NC 27599
[#]Chemistry Division, Brookhaven National Laboratory, Upton, NY 11973

In one approach to solar energy conversion, the separate half reactions for water oxidation or reduction, or the reduction of CO_2 to carbon fuels, occur at the separate half reactions in Dye Sensitized Photoelectrosynthesis Cells (DSPEC). Significant progress has been made for both electrodes and in their integration for water oxidation splitting and CO_2 reduction in nanoparticle oxide films. For water oxidation based on TiO_2 modified films, significant advances have come from the use of core/shell structures and surface stabilization of external molecular structures by Atomic Layer Deposition (ALD). Significant advances have also occurred in the design of molecular structures that both absorb light, and following excitation, activate catalysts for water oxidation. The new designs include examples of integrated electrodes with core/shell overlayer

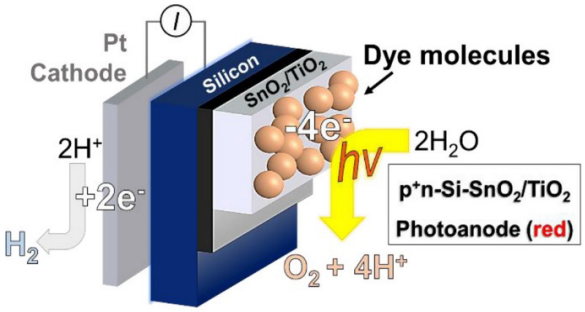

Figure 1. All-in-One Derivatized Tandem p^+n-Silicon−SnO_2/TiO_2 Water Splitting Photoelectrochemical Cell

oxide structures on Si with co-excitation of the Si resulting in H_2 production (Figure 1), and an integrated DSSC-DSC design (Figure 2), with the second electrode a dye-sensitized solar cell for low energy visible light absorption. For coupled photocathode structures, significant advances have been made with NiO electrodes based on surface modification and molecular structures that avoid back electron transfer with the NiO surface, and on surface catalysis in aqueous solutions.

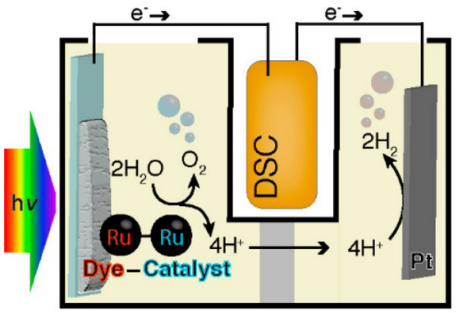

Figure 2. Dye-Sensitized Photoelectrochemical Tandem Cell for Light-Driven Hydrogen Production from Water

References

1. Sherman, B. D.; Sheridan, M. V.; Dares, C. J.; Meyer, T. J. Two Electrode Collector-Generator Method for the Detection of Electrochemically or Photoelectrochemically Produced O_2. *Anal. Chem.* **2016,** *88*, 7076-7082. DOI: 10.1021/acs.analchem.6b00738
2. Brennaman, M. K.; Dillon, R. J.; Alibabaei, L.; Gish, M. K.; Dares, C. J.; Ashford, D. L.; House, R. L.; Meyer, G. J.; Papanikolas, J. M.; Meyer, T. J. Finding the Way to Solar Fuels with Dye-Sensitized Photoelectrosynthesis Cells. *J. Am. Chem. Soc.* **2016,** *138* (40), 13085-13102. DOI: 10.1021/jacs.6b06466
3. Gish, M. K.; Lapides, A. M.; Brennaman, M. K.; Templeton, J. L.; Meyer, T. J.; Papanikolas, J. M. Ultrafast Recombination Dynamics in Dye-Sensitized SnO_2/TiO_2 Core/Shell Films. *J. Phys. Chem. Lett.* **2016,** *7* (24), 5297-5301. DOI: 10.1021/acs.jpclett.6b02388
4. Sherman, B. D.; Sheridan, M. V.; Wee, K.-R.; Marquard, S. L.; Wang, D.; Alibabaei, L.; Ashford, D. L.; Meyer, T. J. A Dye-Sensitized Photoelectrochemical Tandem Cell for Light Driven Hydrogen Production from Water *J. Am. Chem. Soc.* **2016,** *138* (51), 16745-16753. DOI: 10.1021/jacs.6b10699
5. Sheridan, M. V.; Hill, D. J.; Sherman, B. D.; Wang, D.; Marquard, S. L.; Wee, K.-R.; Cahoon, J. F.; Meyer, T. J. All-in-One Derivatized Tandem p^+n-Silicon-SnO_2/TiO_2 Water Splitting Photoelectrochemical Cell. *Nano Lett.* **2017,** *17* (4), 2440-2446. DOI: 10.1021/acs.nanolett.7b00105
6. Wang, Y.; Marquard, S. L.; Wang, D.; Dares, C. J.; Meyer, T. J. Single-Site, Heterogeneous Electrocatalytic Reduction of CO_2 in Water as the Solvent. *ACS Energy Lett.* **2017,** *2* (6), 1395-1399. DOI: 10.1021/acsenergylett.7b00226
7. Dillon, R. J.; Alibabaei, L.; Meyer, T. J.; Papanikolas, J. M. Enabling Efficient Creation of Long-Lived Charge-Separation on Dye-Sensitized NiO Photocathodes. *ACS Appl. Mater. Interfaces* **2017,** *9* (32), 26786-26796. DOI: 10.1021/acsami.7b05856
8. Eberhart, M. S.; Wang, D.; Sampaio, R. N.; Marquard, S. L.; Shan, B.; Brennaman, M. K.; Meyer, G. J.; Dares, C.; Meyer, T. J. Water Photo-Oxidation Initiated by Surface-Bound Organic Chromophores. *J. Am. Chem. Soc.* **2017,** *139* (45), 16248-16255. DOI: 10.1021/jacs.7b08317
9. Alibabaei, L.; Dillon, R. J.; Reilly, C. E.; Brennaman, M. K.; Wee, K.-R.; Marquard, S. L.; Papanikolas, J. M.; Meyer, T. J. Chromophore-Catalyst Assembly for Water Oxidation Prepared by Atomic Layer Deposition. *ACS Appl. Mater. Interfaces* **2017,** *9* (44), 39018–39026. DOI: 10.1021/acsami.7b11905
10. Wang, D.; Marquard, S. L.; Troian-Gautier, L.; Sheridan, M. V.; Sherman, B. D.; Wang, Y.; Eberhart, M. S.; Farnum, B. H.; Dares, C. J.; Meyer, T. J. Interfacial Deposition of Ru(II) Bipyridine-Dicarboxylate Complexes by Ligand Substitution for Applications in Water Oxidation Catalysis. *J. Am. Chem. Soc.* **2018,** *140* (2), 719-726. DOI: 10.1021/jacs.7b10809
11. Wang, Y.; Wang, D.; Dares, C. J.; Marquard, S. L.; Sheridan, M. V.; Meyer, T. J. CO_2 reduction to acetate in mixtures of ultrasmall $(Cu)_n$,$(Ag)_m$ bimetallic nanoparticles. *Proc. Natl. Acad. Sci. USA* **2018,** *115* (2), 278-283. DOI: 10.1073/pnas.1713962115
12. Sheridan, M. V.; Wang, Y.; Wang, D.; Troian-Gautier, L.; Dares, C. J.; Sherman, B. D.; Meyer, T. J. Light-Driven Water Splitting Mediated by Photogenerated Bromine. *Angew. Chem. Int. Ed.* **2018,** *57* (13), 3449-3453. DOI: 10.1002/anie.201708879

Highlights from the Argonne-Northwestern Solar Energy Research (ANSER) Center

Michael R. Wasielewski, Director

Northwestern University, Evanston, IL 60208

Over the past nine years, ANSER Center research has sought to revolutionize our understanding of the molecules, materials, and physical phenomena necessary to create dramatically more efficient technologies for solar fuels and electricity production. ANSER Center objectives are to answer the following four fundamental questions essential to both solar fuels and solar electricity production: 1) How can multi-scale predictive theory and computational modeling lead to the design and discovery of novel organic, inorganic, and hybrid systems? 2) How do molecular and materials structure and order determine the efficiency of light capture, charge separation, and long-range charge transport? 3) What are the fundamental multi-scale temporal and spatial requirements for efficient charge transport across interfaces to deliver multiple redox equivalents to catalysts and electrodes? 4) How can molecular and materials properties be tailored to exploit hierarchical assembly for solar fuels and electricity systems scalable from the nanoscale to the mesoscale?

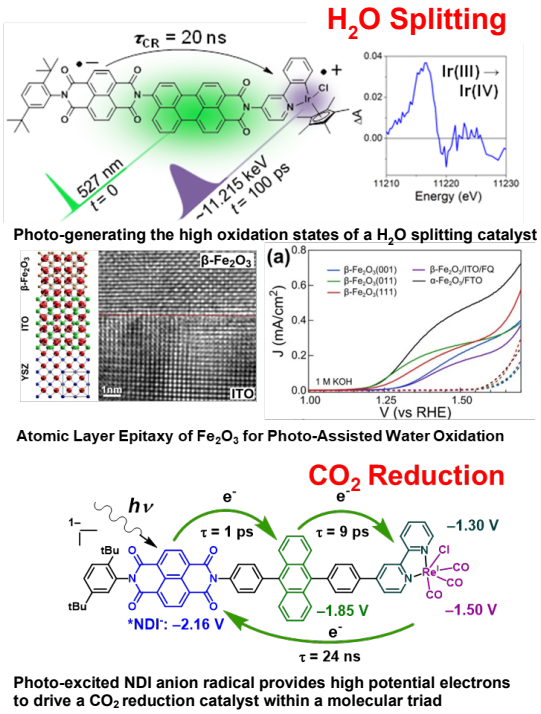

Fig.1. Structural and mechanistic studies of molecules and materials for water splitting and CO_2 reduction.

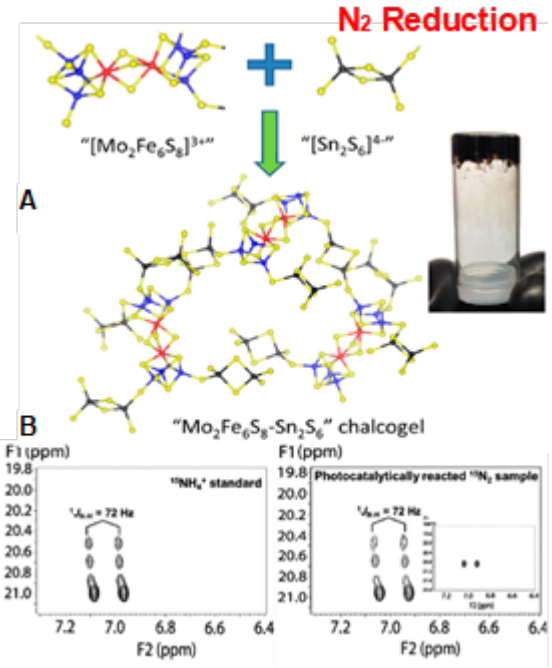

Fig. 2. A) Biomimetic FeMoS-chalcogel catalyst. B) Photochemical N_2 conversion to NH_3 as observed by ^{1}H-^{15}N 2D-NMR spectra.

Multi-step photo-driven electron transfer has been used to produce the highly oxidizing or reducing states of catalysts for water splitting and CO_2 reduction (**Fig.1**).[1-5] The structures of these short-lived energy-demanding redox states have been determined using ultrafast time-resolved X-ray absorption, IR and stimulated Raman spectroscopies. The fundamental relationships between structure and catalytic mechanisms have been determined by following multi-step, photo-initiated, proton-coupled electron transfer one charge at a time. The results have led to new insights into catalytic mechanisms for energy-demanding solar fuels formation reactions.

We have demonstrated the photochemical conversion of nitrogen to ammonia (nitrogen-fixation) under ambient conditions using a biomimetic FeMoS-chalcogel as the catalyst (**Fig. 2**).[6] These results provide important insights into how catalyst structure and environment determine performance for this energy intensive process. Nitrogen fixation is one of the most important biological and industrial processes on Earth. The development of light-driven nitrogen fixation to produce ammonia under mild, energy efficient conditions is critical to food production as well as the use of ammonia as a source of hydrogen, thereby a solar fuel.

Solution deposition of vertically oriented highly stable 2D perovskites ($(BA)_2(MA)_3Pb_4I_{13}$) results in solar cell efficiencies >12% (**Fig. 3**).[7] A new inverted perovskite PV cell design uses an ultrathin (13 nm) oxide electron extraction layer produced by atomic layer deposition both to transport electrons efficiently and protect the perovskite resulting in high stability toward degradation by water.[8] In addition, we have demonstrated low-toxicity, lead-free solution-processed solid-state photovoltaic cells based on a $CH_3NH_3SnI_3$ and Cs_2SnI_6 perovskite semiconductors as the light harvester having efficiencies >8%.[9-12] This combination of advances in efficiency, stability, and low toxicity make it possible to fabricate robust perovskite solar cells.

We have discovered the structural and mechanistic requirements for achieving power conversion efficiencies exceeding 10% in organic photovoltaics (OPVs) utilizing robust non-fullerene electron acceptors (**Fig. 4**).[13-15] These new acceptors achieve high electron mobilities and at the same time avoid generating exciton and/or charge traps sites in the materials that degrade performance. OPVs have the advantage of being thin, flexible, and can be readily fabricated using printing techniques. Achieving high OPV efficiencies with long device lifetimes requires eliminating photochemical degradation. Eliminating unstable fullerene acceptors makes it possible to increase photon harvesting efficiency and greatly increase OPV lifetime.

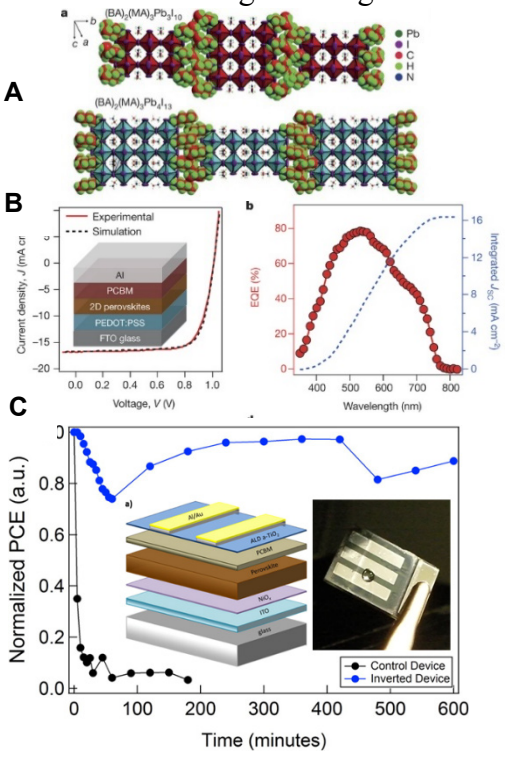

Fig. 3. A) Structure of 2D perovskites. B) Performance, bandgap and photoluminescence for a 2D perovskite solar cell. C) Device performance in the presence of water for an inverted perovskite solar cell.

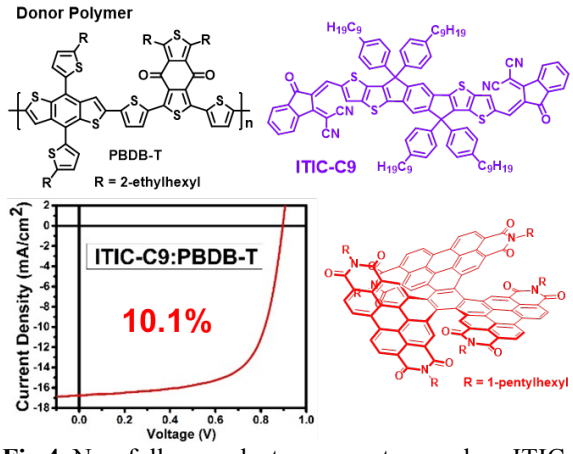

Fig.4. Non-fullerene electron acceptors such as ITIC and PDI derivatives have proven to be the key to achieving high performance organic photovoltaics.

Selected ANSER Center References:

1. Martinez, J. F.; La Porte, N. T.; Mauck, C. M.; Wasielewski, M. R., Photo-Driven Electron Transfer from the Highly Reducing Excited State of Naphthalene Diimide Radical Anion to a CO_2 Reduction Catalyst within a Molecular Triad. *Faraday Discuss.* **2017**, *198*, 235-249.
2. Michaelos, T. K.; Shopov, D. Y.; Sinha, S. B.; Sharninghausen, L. S.; Fisher, K. J.; Lant, H. M. C.; Crabtree, R. H.; Brudvig, G. W., A Pyridine Alkoxide Chelate Ligand That Promotes Both Unusually High Oxidation States and Water-Oxidation Catalysis. *Acc. Chem. Res.* **2017**, *50*, 952-959.
3. Hayes, D., et al., Electronic and Nuclear Contributions to Time-Resolved Optical and X-Ray Absorption Spectra of Hematite and Insights into Photoelectrochemical Performance. *Energy Environ. Sci.* **2016**, *9*, 3754-3769.
4. Yang, K. R., et al., Solution Structures of Highly Active Molecular Ir Water-Oxidation Catalysts from Density Functional Theory Combined with High-Energy X-Ray Scattering and EXAFS Spectroscopy. *J. Am. Chem. Soc.* **2016**, *138*, 5511-5514.
5. Vagnini, M. T.; Mara, M. W.; Harpham, M. R.; Huang, J.; Shelby, M. L.; Chen, L. X.; Wasielewski, M. R., Interrogating the Photogenerated Ir(IV) State of a Water Oxidation Catalyst Using Ultrafast Optical and X-Ray Absorption Spectroscopy. *Chem. Sci.* **2013**, *4*, 3863-3873.
6. Banerjee, A.; Yuhas, B. D.; Margulies, E. A.; Zhang, Y.; Shim, Y.; Wasielewski, M. R.; Kanatzidis, M. G., Photochemical Nitrogen Conversion to Ammonia in Ambient Conditions with Femos-Chalcogels. *J. Am. Chem. Soc.* **2015**, *137*, 2030-2034.
7. Tsai, H., et al., High-Efficiency Two-Dimensional Ruddlesden–Popper Perovskite Solar Cells. *Nature* **2016**, *536*, 312–316.
8. Kim, I. S.; Martinson, A. B. F., Stabilizing Hybrid Perovskites against Moisture and Temperature via Non-Hydrolytic Atomic Layer Deposited Overlayers. *J. Mater. Chem. A* **2015**, *3*, 20092-20096.
9. Ke, W. J.; Priyanka, P.; Vegiraju, S.; Stoumpos, C. C.; Spanopoulos, I.; Soe, C. M. M.; Marks, T. J.; Chen, M. C.; Kanatzidis, M. G., Dopant-Free Tetrakis-Triphenylamine Hole Transporting Material for Efficient Tin-Based Perovskite Solar Cells. *J. Am. Chem. Soc.* **2018**, *140*, 388-393.
10. Dolzhnikov, D. S.; Wang, C.; Xu, Y.; Kanatzidis, M. G.; Weiss, E. A., Ligand-Free, Quantum-Confined Cs_2SnI_6 Perovskite Nanocrystals. *Chem. Mater.* **2017**, *29*, 7901-7907.
11. Mao, L. L., et al., Role of Organic Counterion in Lead- and Tin-Based Two-Dimensional Semiconducting Iodide Perovskites and Application in Planar Solar Cells. *Chem. Mater.* **2016**, *28*, 7781-7792.
12. Ma, L.; Hao, F.; Stoumpos, C. C.; Phelan, B. T.; Wasielewski, M. R.; Kanatzidis, M. G., Carrier Diffusion Lengths of over 500 nm in Lead-Free Perovskite $CH_3NH_3SnI_3$ Films. *J. Am. Chem. Soc.* **2016**, *138*, 14750-14755.
13. Wang, G., et al., Photoactive Blend Morphology Engineering through Systematically Tuning Aggregation in All-Polymer Solar Cells. *Adv. Ener. Mater.* **2018**, 1702173.
14. Eastham, N. D., et al., Hole-Transfer Dependence on Blend Morphology and Energy Level Alignment in Polymer: ITIC Photovoltaic Materials. *Adv. Mater.* **2017**, *29*, 1704263.
15. Hartnett, P. E., et al., Ring-Fusion as a Perylenediimide Dimer Design Concept for High-Performance Non-Fullerene Organic Photovoltaic Acceptors. *Chem. Sci.* **2016**, *7*, 3543-3555.
16. Guo, X., et al., Polymer Solar Cells with Enhanced Fill Factors. *Nat. Photon.* **2013**, *7*, 825-833.

Optimal Packing of Chromophores for Singlet Fission

Eric Buchanan, Milena Jovanovic, Alexandr Zaykov, Zdeněk Havlas, Josef Michl
Department of Chemistry and Biochemistry
University of Colorado
Boulder, CO 80309-0215, U.S.A.
and
Institute of Organic Chemistry and Biochemistry
Academy of Sciences of the Czech Republic
Prague, Czech Republic

Singlet fission is a process in which a singlet excited and a ground state chromophore are transformed into two triplet excited chromophores, and its use in solar cells promises a considerable increase in cell efficiency. Only a few organic solids are presently known to perform singlet fission with a triplet yield close to 200% and most if not all of these are not suitable for practical use. In most cases, singlet fission is only slightly exothermic or even somewhat endothermic, and therefore not sufficiently competitive against other processes that depopulate the singlet excited state. We have developed a simplified theory that allows us to search for optimal packing in any new material at which singlet fission is likely to be the fastest and competing processes the slowest. We do this by searching fully the six-dimensional space of dimer geometries to identify all local maxima of the matrix element squared that enters the Fermi golden rule for the rate of singlet fission, taking due care of the impenetrability of the two molecules. This requires calculations at billions of geometries but the theory is sufficiently simple that they can be completed in a matter of hours or at most days, depending on the size of the chromophore. At the optimal dimer geometries we then evaluate the Boltzmann averaged contributions from the two exciton levels to the rate of singlet fission, and also the biexciton binding energy. A practical realization of the packing geometries identified as optimal will require either advanced crystal engineering or covalent dimer synthesis. Results will be illustrated for dimers of tetracene and of an indigoid industrial dye, cibalackrot.

DOE Sponsored Publications 2015-2018

1. Wen, J.; Havlas, Z.; Michl, J. "Captodatively Stabilized Biradicaloids as Chromophores for Singlet Fission", *J. Am. Chem. Soc.* **2015**, *137*, 165.

2. Akdag, A.; Wahab, A.; Beran, P.; Rulíšek, L.; Dron, P. I.; Ludvík, J.; Michl, J. "Covalent Dimers of 1,3-Diphenylisobenzofuran for Singlet Fission: Synthesis and Electrochemistry", *J. Org. Chem.* **2015**, *80*, 80.

3. Schrauben, J. N.; Zhao, Y.; Mercado, C.; Dron, P. I.; Ryerson, J. M.; Michl, J.; Zhu, K; Johnson, J. C. "Singlet Fission-Induced Photocurrent in a Dye-Sensitized Solar Cell", *ACS Appl. Mater. Interfaces* **2015**, *7*, 2286.

4. Havlas, Z.; Michl, J. “Guidance for Mutual Disposition of Chromophores for Singlet Fission”, *Isr. J. Chem.* **2016**, *56*, 96.

5. Schrauben, J.; Akdag, A.; Wen, J.; Ryerson, J.; Havlas, Z.; Michl, J.; Johnson, J. C. “Excitation Localization/Delocalization Isomerism in a Strongly Coupled Covalent Dimer of 1,3-Diphenylisobenzofuran”, *J. Phys. Chem. A* **2016**, *120*, 3473.

6. Dron, P. I.; Ramešová, Š.; Holloran, N. P.; Pospíšil, L.; Michl, M. “Redox Behavior of 2,3-Diamino-1,4-naphthoquinone and its *N*-Alkylated Derivatives”, *Electroanalysis* **2016**, *28*, 2855.

7. Johnson, J. C.; Michl, J. “1,3-Diphenylisobenzofuran: a Model Chromophore for Singlet Fission”, *Top. Curr. Chem.* **2017**, *375*, 80.

8. Buchanan, E. A.; Havlas, Z.; Michl, J. “Singlet Fission: Optimization of Chromophore Dimer Geometry”, in *Advances in Quantum Chemistry: Ratner Volume, Volume 75*; Sabin, J. R.; Brändas, E. J., Eds.; Elsevier: Cambridge, MA, 2017, p. 175.

9. Dron, P.; Michl, J.; Justin, J. C. “Singlet Fission and Excimer Formation in Disordered Solids of Alkyl-substituted 1,3-Diphenylisobenzofurans”, *J. Phys. Chem. A* **2017**, *121*, 8596.

10. Buchanan, E. A.; Michl, J. “Packing Guidelines for Optimizing Singlet Fission Matrix Elements in Non-Covalent Dimers”, *J. Am. Chem. Soc.* **2017**, *139*, 15572.

11. Grotjahn, R.; Maier, T. M.; Michl, J.; Kaupp, M. “Development of a TDDFT-Based Protocol with Local Hybrid Functionals for the Screening of Potential Singlet Fission”, *J. Chem. Theory Comput.* **2017**, *13,* 4984.

12. Tarábek, J.; Wen, J.; Dron, P. I.; Pospíšil, L. Michl, J. “EPR Spectroscopy of Radical Ions of a 2,3-Diamino-1,4-naphthoquinone Derivative”, *J. Org. Chem.*, in press.

13. Wen, J.; Han, B.; Havlas, Z.; Michl, J. “An MS-CASPT2 Calculation of the Excited Electronic States of an Axial BODIPY Dimer”, submitted for publication.

Harvesting the Triplet Pair from Singlet Fission

Xiaoyang Zhu, Colin Nuckolls

Department of Chemistry
Columbia University
New York, NY 10027

Singlet fission is a photophysical process in which a singlet excited state, S_1, in a molecular system is converted to two triplet excited states, $2xT_1$, via a triplet pair intermediate, $^1(TT)$. This research program explores chemical strategies for the application of singlet fission to solar energy harvesting and photocatalysis. During this funding period, the PIs have studied singlet fission mechanisms, synthesized new molecules with potential for singlet fission, and explored the concept of two-electron transfer from intra-molecular singlet fission.

Using model systems, Fig. 1, of pentacene dimers (BP0 and BB1) and pentacene monomer or dimer (BP0) covalently linked to an electron acceptor, we probe spectroscopic signature and charge transfer properties of the $^1(TT)$ state. We use the redox-active molecular cluster $Fe_8O_4pz_{12}Cl_4$ (pz = pyrazolate), labeled $[Fe_8O_4]$, as an electron acceptor partly because of the energetic alignment which should facilitate easy electron transfer from the T_1 state in pentacene. The $^1(TT)$ state is characterized in the near-IR region by a distinct excited state absorption (ESA) spectral feature, which closely resembles that of the S_1 state. We assign these to $^1(TT) \rightarrow S_2$' and $S_1 \rightarrow S_2$" transitions; S_2' and S_2" are the antisymmetric and symmetric linear combinations, respectively, of the S_2 state localized on each pentacene. The $^1(TT) \rightarrow S_2$' transition is an indicator of the inter-triplet electronic coupling strength, as inserting a phenylene spacer or twisting the dihedral angle between the two pentacene chromophores decreases the electronic coupling and diminishes this peak. We show that electron transfer from pentacene to $[Fe_8O_4]$ occurs efficiently from an individual T_1 state in pentacene. In contrast, the $^1(TT)$ state has a much longer lifetime of 0.42 ns in both BP0 and $[Fe_8O_4]$-BP0, indicating negligible electron transfer to $[Fe_8O_4]$ in the latter. Thus, the chemical property of the $^1(TT)$ state is distinctively different from that of an individual T_1 state and the triplets in the $^1(TT)$ state are more tightly bound than previously predicted in the literature. These findings suggest that reducing inter-triplet electronic coupling in $^1(TT)$ might be needed for the efficient charge transfer.

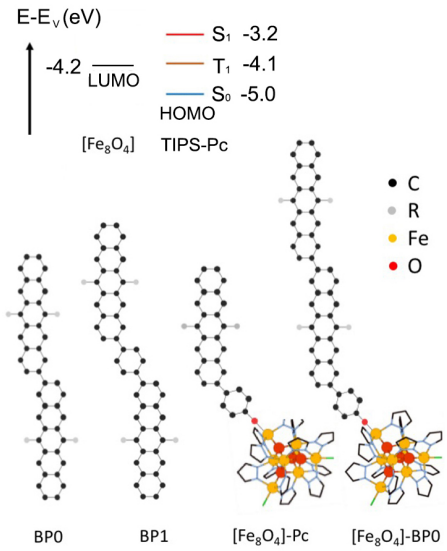

Fig. 1. The model systems for intramolecular singlet fission and charge harvesting. BP0, BP1, $[Fe_8O_4]$-Pc, $[Fe_8O_4]$-BP0. The inset shows estimated ionization potential (IP) and electron affinity (EA) from electrochemical oxidation/reduction potentials of $[Fe_8O_4]$ and TIPS-pentacene.

In the second major achievement, the PIs clarified a much-debated puzzle on the singlet fission mechanism, i.e., the coherent vs. the incoherent singlet fission mechanism, in the model system of

singlet fission in crystalline hexacene.[3] Using time-resolved two-photon photoemission (TR-2PPE) and transient absorption (TA) spectroscopies, the PIs showed that different experiments probe different aspects of the same problem. This system was chosen because the ^{1}(TT) at ~0.89 eV is well separated from the singlet state (S_1) at 1.48 eV and the triplet state (T_1) at 0.44 eV, thus allowing unambiguous identification of the ^{1}(TT) state in TR-2PPE spectroscopy, as shown in Fig. 2a. The ^{1}(TT) state decays to 2xT_1 with a time constant of 270 fs, Fig. 2b. However, the decay of S_1 and the formation of ^{1}(TT) occur on different time scales of 180 fs and <50 fs, respectively. The PI carried out theoretical analysis based on incoherent rate equations and quantum dynamics simulations, in collaboration with Hiroyuki Tamura and David Beljonne. These calculations suggest that a vibrationally excited ^{1}(TT) is resonant and forms an initial quantum superposition with S_1. Ultrafast dephasing of this superposition leads to populations of S_1 and ^{1}(TT) states; the former is further converted to ^{1}(TT) in an incoherent rate process, Fig. 2c. Both coherent and incoherent singlet fission mechanisms likely coexist in crystalline hexacene and this may also reconcile different experimental observations in other acenes.

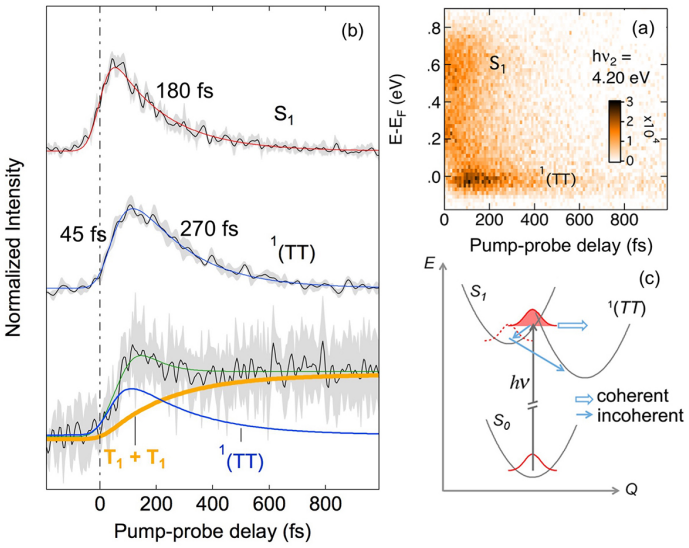

Fig. 2. (a) TR-2PPE spectroscopy unambiguously detects the ***S_1*** and ***^{1}(TT)*** from singlet fission in crystalline hexacene. The population dynamics of the the ***S_1, ^{1}(TT)*** and ***T_1*** states reveal the coexistence of coherent and incoherent singlet fission, (c).

In the third direction, we explored fused perylenediimide (PDI) as potential candidates to extract the electrons from materials made for singlet fission and for singlet fission itself also. The latter was initially motivated by reports of singlet fission in thin films of modified PDIs, but our spectroscopic measurements showed no singlet fission in these PDI dimers and oligomers. The two classes of materials are (1) fused, helical systems that exhibit strong chiroptic properties and (2) cove-edged graphene ribbons that exhibit best-in-class performance in photovoltaics and photodetectors. These are shown schematically in Figs. 3a&b depicting a twistacene, fused donor-acceptor system and a helicene, fused donor-

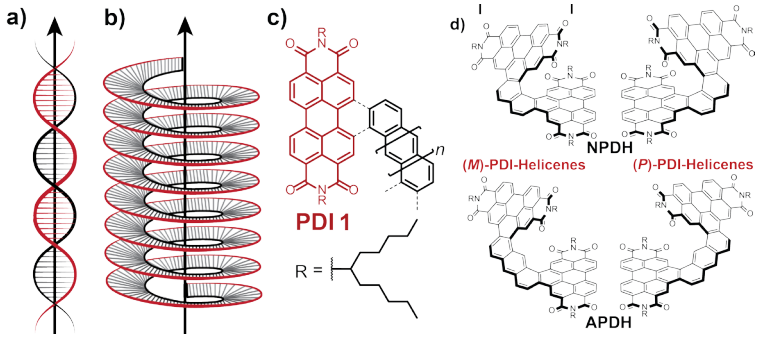

Fig. 3. Fused donor-acceptor PDI-nanoribbons to make (a) twistacenes or (b) helicenes. (c) Acene is a donor that is fused with the bay of the PDI yields PDI-helicenes (n = 0 and 1). (d) Fusion with two PDI moieties forms (M)- and (P)-NPDH and (M)- and (P)-APDH.

acceptor system. Our first project on this class of molecule details the synthesis and characterization of two new helicenes that result from the double fusion along one of the zigzag edges of an acene with the bay of two PDI monomers (Fig.3c, n = 0 and 1).[5] Specifically, double fusion with naphthalene or anthracene forms naphthyl- or anthracenyl-linked PDI-dimer helicene (NPDH and APDH, respectively). We separated the left- (M) and right-handed (P) helicenes of both compounds (Fig. 3d) and discovered that NPDH resists racemization at very high temperatures (>250 °C). The enantiomers of APDH interconvert at room temperature. Intermolecular π-to-π stacking mediates the self-assembly of single-handed supramolecular helixes of APDH in the solid state. The large gap separating the PDI subunits of APDH minimizes intramolecular π-to-π contact. Conversely, the [6]helicene core of NPDH positions its PDI subunits within 3.2 Å of one another. This proximity facilitates the intramolecular collision of their π-electron clouds, which enhances the delocalization of electrons added to NPDH. Our ongoing studies have extended this helicene to form longer versions and the remarkable finding is that the chiroptic properties and the electronic delocalization continue in this new, exciting material. The second type of fused donor acceptor systems we have also explored twistacene ribbons,[6] that are long (~5 nm), atomically precise, and soluble. The design is based on the benzannulation of electron deficient perylene diimide oligomers with an electron rich alkoxy pyrene subunit. These nanoribbons are exceptional electron acceptors, and organic photovoltaics fabricated with the ribbons show efficiencies of ~8% without optimization. We have found that these materials are very efficient in optoelectronic devices, including photodetectors.[7]

We are currently exploring two-electron transfer from pentacene dimers covalently linked to modified PDI electron acceptors. Preliminary experiments revealed the critical importance of energetic alignment and dynamic competition. We are exploring new strategies based on molecular strain to tune the energetics of singlet fission and charge transfer.

DOE Sponsored Publications 2015-2018

1. Zhang, B.; Trinh, M. T.; Fowler, B.; Ball, M.; Xu, Q.; Ng, F.; Steigerwald, M. L.; Zhu, X. Y.; Nuckolls, C.; Zhong, Y. Rigid, Conjugated Macrocycles for High Performance Organic Photodetectors. *J. Am. Chem. Soc.* **2016**, *138*, 16426–16431.
2. Schuster, N. J.; Paley, D. W.; Jockusch, S.; Ng, F.; Steigerwald, M. L.; Nuckolls, C. Electron Delocalization in Perylene Diimide Helicenes. *Angew. Chemie Int. Ed.* **2016**, *55*, 13519–13523.
3. Fuemmeler, E. G.; Sanders, S. N.; Pun, A. B.; Kumarasamy, E.; Zeng, T.; Miyata, K.; Steigerwald, M. L.; Zhu, X.-Y.; Sfeir, M. Y.; Campos, L. M.; *et al.* A Direct Mechanism of Ultrafast Intramolecular Singlet Fission in Pentacene Dimers. *ACS Cent. Sci.* **2016**, *2*, 316–324.
4. Trinh, M. T.; Pinkard, A.; Pun, A. B.; Sanders, S. N.; Kumarasamy, E.; Sfeir, M. Y.; Campos, L. M.; Roy, X.; Zhu, X.-Y. Distinct Properties of the Triplet Pair State from Singlet Fission. *Science Adv.* **2017**, *3*, e1700241.
5. Monahan, N. R.; Sun, D.; Tamura, H.; Williams, K. W.; Xu, B.; Zhong, Y.; Kumar, B.; Nuckolls, C.; Harutyunyan, A. R.; Chen, G.; Dai, H.-L.; Beljonne, D.; Rao, Y.; Zhu, X.-Y. Dynamics of the triplet pair state reveals the likely co-existence of coherent and incoherent singlet fission in crystalline hexacene. *Nature Chem*. **2017**, *9*, 341-346.

6. Williams, K. W.; Monahan, N. R.; Evans, T. J. S.; Zhu, X.-Y. Direct Time-Domain View of Auger Recombination in a Semiconductor. *Phys. Rev. Lett.* **2017**, *118*, 87402.
7. Sisto, T. J.; Zhong, Y.; Zhang, B.; Trinh, M. T.; Miyata, K.; Zhong, X.; Zhu, X. Y.; Steigerwald, M. L.; Ng, F.; Nuckolls, C. Long, Atomically Precise Donor-Acceptor Cove-Edge Nanoribbons as Electron Acceptors. *J. Am. Chem. Soc.* **2017**, *139*, 5648–5651.
8. Zhong, Y.; Sisto, T. J.; Zhang, B.; Miyata, K.; Zhu, X. Y.; Steigerwald, M. L.; Ng, F.; Nuckolls, C. Helical Nanoribbons for Ultra-Narrowband Photodetectors. *J. Am. Chem. Soc.* **2017**, *139*, 5644–5647.
9. Castro, E.; Sisto, T. J.; Romero, E. L.; Liu, F.; Peurifoy, S. R.; Wang, J.; Zhu, X.; Nuckolls, C.; Echegoyen, L. Cove-Edge Nanoribbon Materials for Efficient Inverted Halide Perovskite Solar Cells. *Angew. Chemie* **2017**, *129*, 14840–14844.
10. Kang, H. S.; Sisto, T. J.; Peurifoy, S.; Arias, D.; Zhang, B.; Nuckolls, C.; Blackburn, J. L. Production of Long-Lived Separated Charges at Heterojunctions between Semiconducting Single-Walled Carbon Nanotubes and Perylene Diimide Electron Acceptors. *J. Phys. Chem. C* **2018**, *submitted*.
11. Miyata, K.; Conrad-Burton, F. S.; Geyer, F. L.; Zhu, X.-Y. Understanding Singlet Fission. *Chem. Rev.* **2018**, *to be submitted.*

Determination of vibrational motions driving photoinduced electron transfer reactions in molecular crystals and organic thin films

Kajari Bera, Stephanie M. Hart, Christopher C. Rich, Renee R. Frontiera
Department of Chemistry
University of Minnesota
Minneapolis, MN 55455

The objective of this research is to develop an understanding of how nuclear motions can be used to drive and control photo-induced charge transfer and singlet fission reactions in molecular crystals and thin films. By following the structural evolution of reacting molecules and nanostructures on the timescale of their nuclear motion, we will determine what interplay of nuclear coordinates is most efficient in driving electron transfers, a necessary first step in most photovoltaic and photocatalytic processes. We will identify which nuclear coordinates effectively promote desirable electron transfer processes, or ineffectively dissipate photon energy into unwanted thermal energy, thus guiding the design and implementation of molecular systems tailored for high efficiency processes.

We use femtosecond stimulated Raman spectroscopy (FSRS), a vibrational technique capable of obtaining structural information on the femtosecond time scale, to determine the structure, anharmonicity and vibrational wavepacket dynamics of reacting molecules. This enables us to map out reaction coordinates on excited state potential energy surfaces, leading to a complete understanding of how different nuclear coordinates play a role in driving wavepackets, promoting reaction pathways, and dissipating energy. FSRS has previously been used to determine a wide variety of reaction mechanisms, but applications to ultrafast

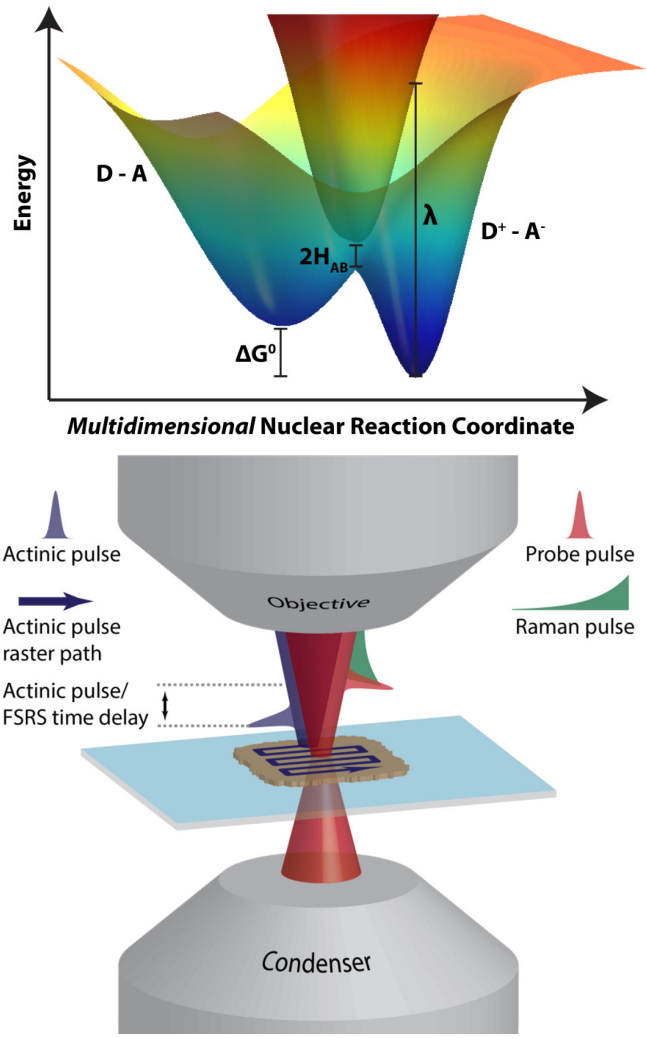

Figure 1. (Top) Schematic depiction of FSRS probing to map out reaction coordinates of highly reactive potential energy surfaces. (Bottom) Depiction of spatially-offset FSRS microscopy.

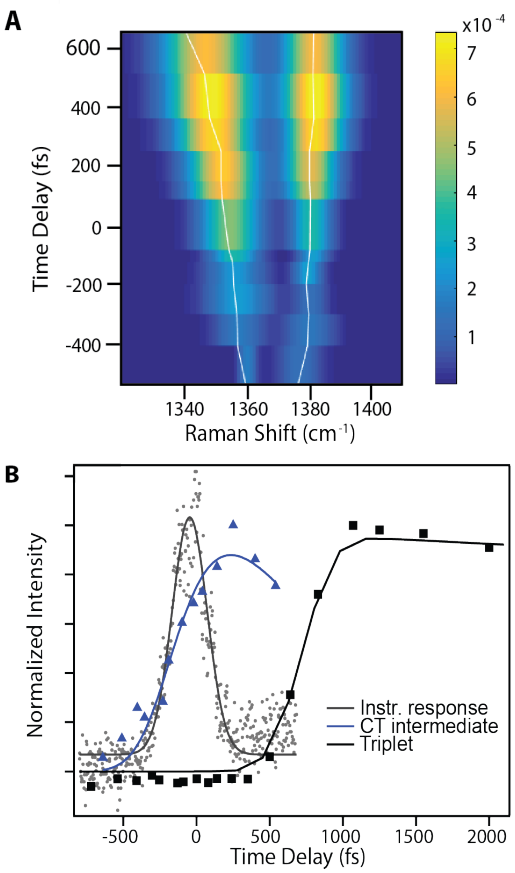

Figure 2A. Femtosecond stimulated Raman spectra of the singlet fission process in crystalline pentacene, showing evidence for a charge-transfer intermediate by the evolution of anionic and cationic vibrational features. B. Kinetics for charge-transfer intermediate preceding formation of triplets in crystalline pentacene singlet fission.

electron transfer and singlet fission in films and solid systems have not previously been possible. We have implemented a variety of unique experimental upgrades to extend the FSRS technique, including an inverted microscope, a pulse shaper, and spatially-offset microscopy. These technical advances have been crucial in extending our ability to examine structural changes in systems not compatible with existing FSRS instrumentation, such as molecular crystals and non-transparent films.

Our initial investigations in this area examined the mechanism of singlet fission in crystalline pentacene. Surprisingly, we found evidence for a state with strong charge-transfer character persisting for approximately 1 picosecond prior to triplet formation. This state is characterized by excited state Raman features that are red- and blue-shifted from the ground state features, corresponding to states with strong cationic and anionic character. Based on comparison with TD-DFT calculations, we hypothesize that these features arise due to partial transfer of electron density from one pentacene molecule to a neighboring molecule, which ultimately results in formation of a correlated triplet pair. This surprising insight into the mechanism of singlet fission in crystalline pentacene highlights the utility of structurally-sensitive time-resolved methods to determine reaction coordinates on highly complex potential energy surfaces.

Our ongoing investigations are focused on determining the mechanism of singlet fission in TIPS-pentacene thin films, understanding the role of vibrational coherences in driving photoinduced charge transfer in potassium TCNQ, and developing spatially-offset FSRS microscopy to probe the effects of nuclear motions in promoting long-range charge transport. Ultimately we aim to determine how complex film morphologies and nuclear motions relate to photovoltaic and photocatalytic device performance.

DOE Sponsored Publications

1. Hart, S. M., Silva, W. R., Frontiera, R. R., "Femtosecond stimulated Raman evidence for charge-transfer character in pentacene singlet fission", ***Chemical Science***, 2018, 9, 1242.

Electrochemical kinetics and mass-transport at single catalytic nanoparticles

Tong Sun, Dengchao Wang, Je Hyun Bae, Alexander Nepomnyashchii, and Michael V. Mirkin
Department of Chemistry and Biochemistry
Queens College-CUNY
Flushing, NY 11367

Our Department of Energy supported research is aimed at developing nanoelectrochemical methodology for quantitative studies of charge-transfer processes at single catalytic nanoparticles (NP). In the past year, we focused on developing the tunneling mode of scanning electrochemical microscopy (SECM) and applying SECM to reactivity mapping of semiconductor interfaces.

Microscopic understanding of electron tunneling between NPs and electrodes is essential for rational design of nanostructured interfaces for electrocatalysis and energy conversion. The tunneling mode of SECM enables studying long-distance electron transfer between the NP and the nanoelectrode tip as a function of the separation distance *(d)*. Our SECM experiments at unbiased Au NPs showed the transition from bipolar feedback response (Fig. 1A) to electron tunneling at very short distances between the NP and the tip nanoelectrode (Fig. 1B). Au NPs were immobilized on a flat, insulating glass surface. In a feedback mode experiment, a nm-sized SECM probe approaches a metal NP in solution containing redox mediator (e.g., a reduced form R; Figure 1A), and the tip potential (E_T) is such that the mediator oxidation occurs at the rate governed by diffusion. When the tip is relatively far from the NP (e.g., > ~3-4 nm), the floating NP potential (E_p) is determined by local concentrations of the reduced and oxidized forms of the reversible redox mediator according to the Nernst equation. The unbiased NP behaves as a bipolar electrode, with the regeneration of the redox mediator ($O + e^- = R$) occurring at the top half of the NP facing the tip, and the opposite reaction ($R - e^- = O$) – at the bottom half of the NP. When the tip is brought within the tunnelling distance from the NP, E_p shifts from its open-circuit value toward the E_T value, and the NP begins to act as a part of the tip electrode, e.g., by oxidizing the reduced form of the mediator (Fig. 1B). With no voltage applied between the tip and the substrate, the tip current (i_T) is due to the diffusion of redox species to the NP surface.

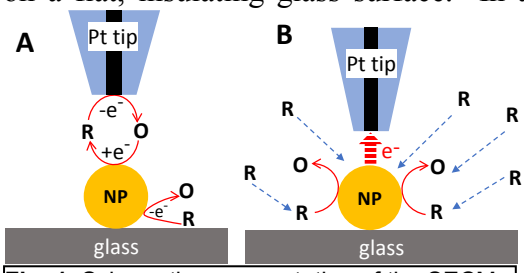

Fig. 1. Schematic representation of the SECM feedback at the floating metal NP (A) and tunnelling experiment (B) in which the overall charge-transfer process involves diffusion of redox species to the NP, faradaic reaction at its surface, and tunnelling between the tip and NP.

Fig. 2 shows the transition from the SECM feedback response (Fig. 1A) to electrochemical tunneling (Fig. 1B) observed with a Pt tip (radius, a = 30 nm) approaching a 50-nm-radius Au NP. At d > ~3nm, positive feedback current was produced by regeneration of ferrocenemethanol (Fc) mediator at the Au NP (solid line in Fig. 2A) in quantitative agreement with the simulated approach curve (open circles). The current increased sharply when the tip approached the NP to within ~3 nm distance. The zoom in (Fig. 2B) shows an abrupt change in the slope of the i_T vs. d curve corresponding to the onset of tunneling. After this point, ~10 experimental points were recorded over the tip displacement distance of ~3 nm, and the tunneling constant, $\beta = 1.0$ A^{-1} extracted by fitting this portion of the current-distance curve to the theory (triangles). The i_T eventually levelled off and slightly decreased after the tip made hard contact with the NP and started to push it. The

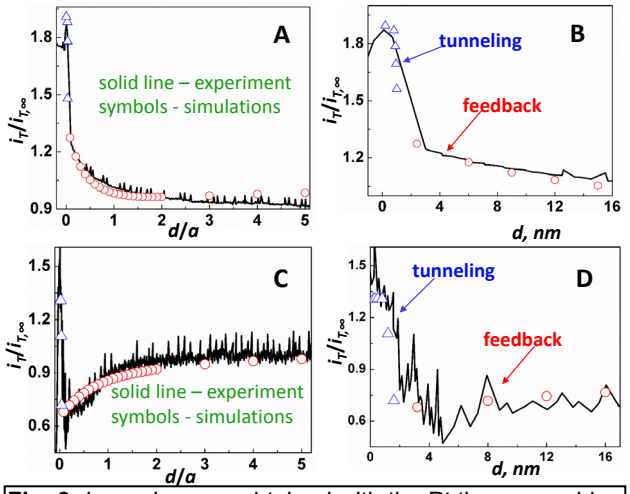

Fig. 2. i_T vs. d curves obtained with the Pt tip approaching an Au NP anchored to the glass surface in solution containing 1 mM Fc (A) or 1 mM $HClO_4$ (C). (B) and (D) Zoom in of the tunneling region in A and C, respectively.

maximum measured current equals the diffusion limiting current of Fc to the Au NP. Overall, this data represents a quantitative electrochemical experiment on the sub-nm spatial scale.

The i_T vs. d curve in Fig. 2C (and its zoom in, Fig. 2D) were obtained with the hydrogen evolution reaction occurring at the tip. The mediator regeneration in this case (i.e., HOR at the Au NP) was kinetically slow, and negative SECM feedback was observed for d > ~3 nm. The sharp current increase corresponds to the onset of tunneling, and the source of the current is the HER at the Au NP. The tunneling i_T vs. d curve fits well the theory (triangles in Fig. 2D). Much smaller, 10-nm-radius NPs were also probed using smaller tips. This technique enables measurement of the current flowing at a single NP without attaching it to the electrode surface. It can also be useful for probing 2D catalytic nanoflakes and other nanostructures.

Another objective of our research was to develop an SECM setup for nanoscale photoelectrochemical experiments at semiconductor/solution interfaces. Nb doped TiO_2 single crystals were used as our first model. We mapped a simple outer-sphere electron transfer reaction (oxidation of Fc; Fig. 3) and the oxygen evolution reaction at Nb:TiO_2 surfaces irradiated with the UV light. One question was whether the photoelectrochemical reactivity of Nb:TiO_2 surfaces may be non-uniform due to significant niobium segregation in the crystal. The SECM reactivity map in Fig. 3A shows stable tip current recorded over a large (9 x 9 μm^2) area of the crystal. Minor reactivity variations (~5%) were irreproducible in the consecutive images of the same area (Fig. 3B), suggesting the random nature of these variations and the overall uniform distribution of Nb throughout the crystal on the sub-micrometer scale. These initial experiments showed that nano-SECM is a suitable technique for investigating morphology of photocatalysts. The higher-resolution SECM photoelectrochemical experiments, including reactivity mapping of terraces, steps and electrodeposited Pt NPs on TiO_2 surfaces, as well as kinetic experiments at individual TiO_2 nanocrystals are currently underway in our laboratory.

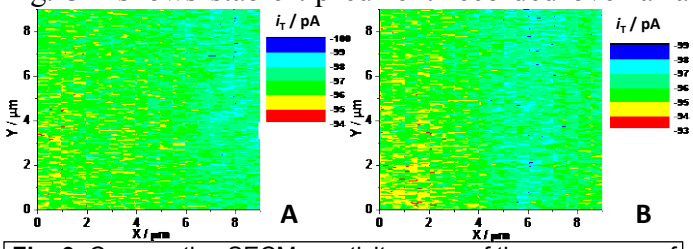

Fig. 3. Consecutive SECM reactivity maps of the same area of the 0.5 % doped Nb:TiO_2 (110) n-type rutile single crystal in 1 mM Fc solution. a = 500 nm. d = 500 nm; λ = 350 nm.

DOE Sponsored Publications 2017-2018

1. Sun, T.; Wang, D.; and Mirkin, M. V. "Tunnelling Mode of Scanning Electrochemical Microscopy (SECM): Probing Electrochemical Processes at Single Nanoparticles", *Angew. Chem. Int. Ed.,* **2018**, DOI: 10.1002/anie.201801115.

2. Sun, T.; Wang, D.; and Mirkin, M. V. "Electrochemistry at a Single Nanoparticle: from Bipolar Regime to Tunnelling", *Faraday Discuss.*, **2018**, in press.

Observing Nanoscale Photochemical Charge Separation with Surface Photovoltage Spectroscopy, 03/01/2016 - 02/28/2018

Frank E. Osterloh
Department of Chemistry
University of California
Davis, CA 95616

Project Scope: The use of Surface Photovoltage Spectroscopy (SPS) to the observation of light induced charge transfer processes dates back to the work by Brattain and Bardeen in 1953 at Bell Labs. The technique offers high sensitivity and the ability to interrogate charge transfer without any applied electrochemical bias and in the absence of added redox couples or liquid electrolytes. This makes it possible to observe the intrinsic photochemistry of materials. Here we employ SPS for the study of photochemical charge separation in a series of well-defined molecular, polymeric, and nanocrystalline light absorbers. We ask how nanoscale photochemical charge separation depends on the absorption coefficient, the built-in potential, the acceptor-donor separation, the light intensity and the environment. **Recent Results:** In a collaborative study with Prof. Gerko Oskam (CINVESTAV-IPN, Meŕida, Mexico) we used SPS to probe energetics and photochemical charge transfer efficiency in fluorenyl-thiophene dye (OD-8)-sensitized ZnO films and using I^-/I_3^- or $[Co(2,2'\text{-bipyridyl})_3]^{3+/2+}$ redox couples. Without a redox couple, charge separation at the ZnO/dye interface is only 4% effective, likely due to the short electron hole separation distance. In the presence of the redox couples, charge separation approaches 26–54% of the theoretical limit, emphasizing the importance of the dye regeneration reaction.[1, 2] In a related study we used SPS together with photoelectrochemical measurements to characterize photochemical charge separation in 1-6 nm diameter graphitic quantum dots (GQQ). The GQDs behave as p-type semiconductors, based on the positive photovoltage on Al, Au and fluorine doped tin oxide (FTO) substrates, and generate mobile charge carriers under excitation of defect states at 1.80 eV and under band gap excitation at 2.63 eV. Chemical reduction with hydrazine removes some defects, increasing the effective band gap to 2.92 eV, and allowing photochemical reactions to proceed with sacrificial electron donors and acceptors. These results are relevant to the use of CQDs as photocathode and in photovoltaics. In another study SPS was used to study photochemical charge transfer between $BiVO_4$ and Cu_2O nanoparticles. Layered particle films produced a negative photovoltage that confirms a tandem junction at the Cu_2O – $BiVO_4$ particle interface. The results are relevant to the construction of artificial photosynthesis system based on abundant materials. SPS was also used to provide the first photovoltage measurements for the $Rh/SrTiO_3$:$Rh/BiVO_4$ direct contact particle tandem which can split water into stoichiometric amounts of H_2 and O_2 with an apparent quantum efficiency of 1.29 % at 435 nm and a solar to hydrogen conversion efficiency of 0.028 %. According to SPS, a photovoltage forms above 2.20 eV, the effective band gap of the tandem and reaches its maximal value of -2.45 V at 2.85 eV illumination (435 nm, 2.50 mW cm^{-2}), which corresponds to 58% of the theoretical limit of the absorber configuration. Charge separation is 80% reversible with approximately 20% of the charge carriers being trapped in surface states. [3]A collaborative project with Kazunari Domen in Japan employed SPS to observe photochemical charge transfer in $La_5Ti_2CuS_5O_7$ and $SrNbO_2N$ photocatalysts for water oxidation and reduction. For $SrNbO_2N$, hole trapping at a Co-Pi cocatalyst and hole injection into methanol could be observed, while for Sc-doped $La_5Ti_2CuS_5O_7$

inversion of the photovoltage on gold and titanium substrates was indicative of a space charge layer in the material. [4] **Future plans.** The project application 'Surface Photovoltage Studies on Inorganic Tandem Photocatalysts for Overall Water Splitting' will use SPS to map the energy and location of charge trapping defects in inorganic pigments and to measure the ability of solid-solid and solid-liquid interfaces to facilitate charge transport and separation. The magnitude and spatial extent of electric fields in the particles will also be determined.

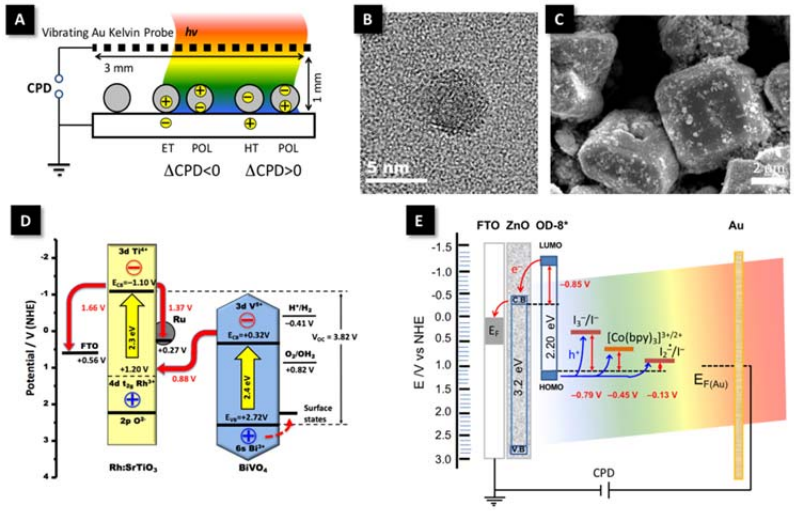

Figure: A) SPS measurement configuration. B) EM images of CQDs and C) $Rh/SrTiO_3$:$Rh/BiVO_4$ direct contact particle tandem photocatalyst. D) Corresponding energy scheme for tandem on FTO substrate. E) Energy scheme for charge separation in fluorenyl-thiophene dye-sensitized photoelectrochemical cell.

DOE Sponsored Publications 2016-2018

1. Rodríguez-Pérez, M., E. Canto, R. García-Rodríguez, A.T. De Denko, G. Oskam, and F. Osterloh, *Surface Photovoltage Spectroscopy Resolves Interfacial Charge Separation Efficiencies in ZnO Dye-Sensitized Solar Cells.* J. Phys. Chem. C, 2018. **122**(5): p. 2582-2588. https://doi.org/10.1021/acs.jpcc.7b11727
2. Canto-Aguilar, E.J., M. Rodriguez-Perez, R. Garcia-Rodriguez, A.T.D. Denko, F.E. Osterloh, and G. Oskam, *ZnO-based dye-sensitized solar cells: Effects of redox couple and dye aggregation.* Electrochimica Acta, 2017. **258**: p. 396-404. https://doi.org/10.1016/j.electacta.2017.11.075
3. Melo, M.A., Z. Wu, B.A. Nail, A.T. De Denko, A.F. Nogueira, and F.E. Osterloh, *Surface Photovoltage Measurements on a Particle Tandem Photocatalyst for Overall Water Splitting.* Nano Letters, 2018. **18**: p. 805-810. https://doi.org/10.1021/acs.nanolett.7b04020
4. Kodera, M., J. Wang, B.A. Nail, J. Liu, H. Urabe, T. Hisatomi, M. Katayama, T. Minegishi, F.E. Osterloh, and K. Domen, *Investigation of charge separation in particulate oxysulfide and oxynitride photoelectrodes by surface photovoltage spectroscopy.* Chemical Physics Letters, 2017. **683**: p. 140-144. https://doi.org/http://dx.doi.org/10.1016/j.cplett.2017.03.012
5. Zhao, J., B.A. Nail, M.A. Holmes, and F.E. Osterloh, *Use of Surface Photovoltage Spectroscopy to Measure Built-in Voltage, Space Charge Layer Width, and Effective Band Gap in CdSe Quantum Dot Films.* J. Phys. Chem. Lett., 2016: p. 3335-3340. https://doi.org/10.1021/acs.jpclett.6b01569
6. Tan, H.L., A. Suyanto, A.T.D. Denko, W.H. Saputera, R. Amal, F.E. Osterloh, and Y.H. Ng, *Enhancing the Photoactivity of Faceted BiVO4 via Annealing in Oxygen-Deficient Condition.* Particle & Particle Systems Characterization, 2017. **34**(4): p. 1600290. https://doi.org/10.1002/ppsc.201600290
7. Boltersdorf, J., I. Sullivan, T.L. Shelton, Z. Wu, M. Gray, B. Zoellner, F.E. Osterloh, and P.A. Maggard, *Flux Synthesis, Optical and Photocatalytic Properties of n-type Sn2TiO4: Hydrogen and Oxygen Evolution under Visible Light.* Chemistry of Materials, 2016. **28**(24): p. 8876-8889. https://doi.org/10.1021/acs.chemmater.6b02003
8. Osterloh, F.E., *Photocatalysis versus Photosynthesis: A Sensitivity Analysis of Devices for Solar Energy Conversion and Chemical Transformations.* ACS Energy Letters, 2017: p. 445-453. https://doi.org/10.1021/acsenergylett.6b00665

Investigation of Oxide-Based Photocathodes for Use in Solar Fuel Production

Garrett P. Wheeler, Allison C. Cardiel, and Kyoung-Shin Choi
Department of Chemistry
University of Wisconsin-Madison
Madison, WI 53706

The overall objective of our project is to bring about a marked advancement in the synthesis and understanding of polycrystalline photoelectrodes for use in solar fuel production. Identifying inexpensive and easily processable semiconductors that can achieve high solar energy conversion efficiencies and developing facile synthesis methods to produce them as high performance photoelectrodes are critical steps to considerably reduce the production cost of solar fuels. We achieve these goals by developing simple and practical electrochemical synthesis methods/conditions that can produce promising semiconductors as high quality photoelectrodes with systematically varying compositions and morphologies. Our synthesis methods enabled us to accurately evaluate their photoelectrochemical properties and develop effective strategies to address their primary limitations. During the current funding period, we have focused on the investigation of oxide-based photocathodes. The most significant achievements we have made are summarized below.

Developing Fe-based photocathodes. Most p-type oxides that have been studied as photocathodes for a water splitting photoelectrochemical cell (PEC) contain Cu^{+} or Cu^{2+} ions. However, the presence of Cu^{+} or Cu^{2+} ions in these oxides is a common source for their photoinstability. Therefore, we aimed to develop photocathodes that did not contain Cu ions and can be potentially more photostable. Perovskite-type lanthanum iron oxide, $LaFeO_3$, is p-type and has a bandgap of ~2.1 eV, allowing for the utilization of a large portion of the visible solar spectrum. Furthermore, its conduction band minimum (CBM) and valence band maximu (VBM) straddle the water reduction potential and water oxidation potential, enabling overall water splitting. We have developed and optimized electrochemical synthesis methods for the preparation of high surface area nanoporous $LaFeO_3$ photocathodes (Figure 1a-b). Since the nanoporous morphology significantly reduces the distance that the minority carriers need to travel to reach the electrode/electrolyte interface, photocurrent onset potentials very close to the flatband potential (1.45 V vs. RHE) could be achieved for both photoelectrochemical reduction of O_2 and water. Furthermore, we confirmed that $LaFeO_3$ is photostable without the aid of a

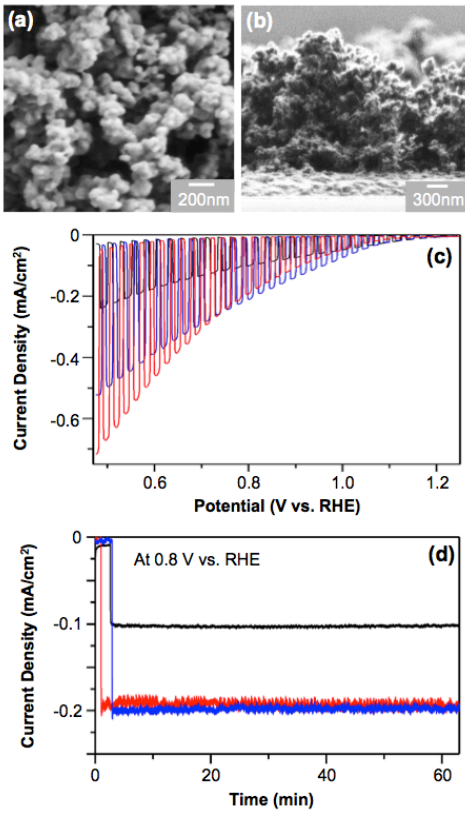

Figure 1. (a-b) SEM image of a nanoporous $LaFeO_3$ electrode; (c) J-V and (d) J-t plots of $LaFeO_3$ (black), $K_xLa_{1-x}FeO_3$ (blue), and $LaMg_xFe_{1-x}O_3$ (red) for photoelectrochemical O_2 reduction in 0.1 M KOH (pH 13) solution with O_2 purging under AM1.5G illumination.

protection layer. Currently, we are investigating doping both the La site and Fe site of $LaFeO_3$ to enhance its charge transport properties (Figure 1c-d).

We have also investigated another Fe-containing p-type oxide, $Ca_2Fe_2O_5$. The bandgap of $Ca_2Fe_2O_5$ is 1.9 – 2.0 eV, and its CBM and VBM are also ideally located to achieve overall water splitting. However, $Ca_2Fe_2O_5$ has never been investigated as a photocathode in a water splitting PEC prior to our investigation. We developed a synthesis procedure to prepare polycrystalline $Ca_2Fe_2O_5$ electrodes and evaluated their photoelectrochemical properties and stabilities. $Ca_2Fe_2O_5$ is chemically stable in solutions ranging from pH 5 to pH 11. However, we discovered that unlike $LaFeO_3$, $Ca_2Fe_2O_5$ is not photostable, and it will require a protection layer to achieve stable photocurrent generation. This result suggested that not all Fe^{3+}-containing p-type oxides are photostable and that the thermodynamics and kinetics of photoreduction of Fe^{3+} in Fe^{3+}-containing photocathodes can be significantly affected by the crystal structure and composition of each compound.

Improving photocurrent generation and photostability of CuO and Cu_2O. While investigating ternary-oxide based photocathodes that do not contain Cu, we concurrently investigated strategies to further improve the photoelectrochemical properties and photostabilities of Cu-containing photocathodes (e.g. CuO and Cu_2O). Cupric oxide, CuO, is a well-known p-type oxide with a bandgap of 1.2 – 1.8 eV. Due to its smaller bandgap, it should be able to achieve a higher photocurrent than Cu_2O, which has been intensively studied as a water splitting cathode. However, CuO has received less attention than Cu_2O for use as a photocathode in solar water splitting PECs. We have developed a synthesis method to produce nanofibrous CuO that significantly increased electron-hole separation, which directly enhanced its photocurrent generation (Figure 2). We have also discovered that Li doping can further increase photocurrent generation (Figure 2c, red line). Density Functional Theory (DFT) calculations showed that Li can serve as a shallow acceptor, effectively increasing the hole concentration of CuO.

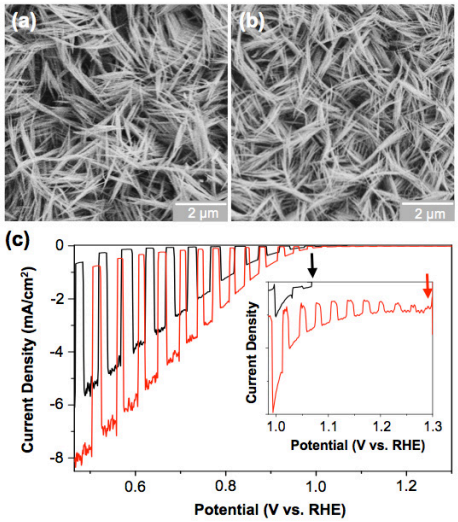

Figure 2. SEM images of nanofibrous (a) CuO and (b) Li-doped CuO; (c) J-V plots (scan rate = 10 mV/s) of CuO (black) and Li-doped CuO (red) for O_2 reduction in 0.1 M KOH (pH 13) solution with O_2 purging under AM1.5G illumination. The inset shows a more positive photocurrent onset potential caused by Li doing.

We are also developing strategies to suppress photocorrosion of CuO and Cu_2O. To date, TiO_2 and ZnO layers deposited by atomic layer deposition (ALD) have been used as protection layers to stabilize CuO and Cu_2O photocathodes. We have developed electrochemical methods to deposit thin conformal coatings of TiO_2 and ZnO on photoelectrodes, which enhance the stabilities of photoelectrodes without interfering with electron or hole transfer from the photoelectrodes to solution species. Our methods may offer a practical alternative to ALD. We will continue to develop effective and practical strategies to enhance photoelectrochemical properties and photostabilities of Fe- and Cu-based photocathodes.

DOE Sponsored Publications 2015-2018

1. Kang, D.; Kim, T. W.; Kubota, S.; Cardiel, A.; Cha, H. G.; Choi, K.-S. "Electrochemical Synthesis of Photoelectrodes and Catalysts for Use in Solar Water Splitting" *Chem. Rev.* **2015**, *115*, 12839–12887.

2. Cha, H. G.; Choi, K.-S. "Combined Biomass Valorization and Hydrogen Production in a Photoelectrochemical Cell" *Nat. Chemistry*, **2015**, *7*, 328–333.

3. Papa, C. M.; Cesnik, A. J.; Evans, T. C.; Choi, K.-S. "Electrochemical Synthesis of Binary and Ternary Niobium-Containing Oxide Electrodes Using the p-Benzoquinone/Hydroquinone Redox Couple" *Langmuir*, **2015,** *31*, 9502–9510.

4. Kim, T. W.; Choi K.-S. "Improving Photoelectrochemical Performance and Stability of $BiVO_4$ in Basic Media by Adding a $ZnFe_2O_4$ Layer" *J. Phys. Chem. Lett*. **2016**, *7*, 447–451.

5. Roylance, J. J.; Kim, T. W.; Choi K.-S., "Efficient and Selective Electrochemical and Photoelectrochemical Reduction of 5-hydroxymethylfurfural to 2,5-bis(hydroxymethyl)furan Using Water as the Hydrogen Source" *ACS Catalysis* **2016**, *6*, 1840–1847.

6. Kang, D.; Hill, J. C.; Park, Y.; Choi, K.-S. "Photoelectrochemical properties and photostabilities of high surface area $CuBi_2O_4$ and Ag-doped $CuBi_2O_4$ photocathodes" *Chem. Mater.* **2016**, *28*, 4331-4340.

7. Kang, D.; Lee, D.; Choi, K.-S. "Electrochemical Synthesis of Highly Oriented, Transparent, and Pinhole-Free ZnO and Al-Doped ZnO Films and Their Use in Heterojunction Solar Cells" *Langmuir*, **2016**, *32*, 10459-10466.

8. Lumley, M. A.; Choi, K.-S. "Investigation of Pristine and (Mo, W)-Doped $Cu_{11}V_6O_{26}$ for Use as Photoanodes for Solar Water Splitting" *Chem. Mater.* **2017**, *29*, 9472–9479.

9. Cardiel, A. C.; McDonald, K. J.; Choi, K.-S. "Electrochemical Growth of Copper Hydroxy Double Salt Films and Their Conversion to Nanostructured p-type CuO photocathodes" *Langmuir* **2017**, *33*, 9262-9270.

10. Wheeler, G. P.; Choi, K.-S. "Photoelectrochemical Properties and Stability of Nanoporous p-Type $LaFeO_3$ Photoelectrodes Prepared by Electrodepostion" *ACS. Energy Lett.* **2017**, *2*, 2378-2382.

11. Wheeler, G. P.; Choi, K.-S. "Investigation of p-type $Ca_2Fe_2O_5$ as a Photocathode for Use in a Water Splitting Photoelectrochemical Cell" **2018**, Under revision.

12. Wheeler, G. P.; Choi, K.-S. "Enhancing Charge Transport Properties of Nanoporous p-Type $LaFeO_3$ Photocathodes by Doping of La and Fe sites" **2018**, Manuscript in preparation.

13. Smart, T; Cardiel, A.; Choi, K.-S.; Ping, Y. "Enhanced Hole Conduction in CuO by Li Doping: A Combined Theoretical and Experimental Study" **2018**, Manuscript in preparation.

14. Lee, D. K.; Lumley, M. A.; Lee, D. H.; Choi, K.-S. "Ternary Oxide-Based Photoelectrodes for Use in a Water Splitting Photoelectrochemical Cell" **2018**, Manuscript in preparation (Invited, to be submitted to *Chem. Soc. Rev.* by 07/01/2018).

Surface Chemistry and Heterogeneous Processes in Solar-Driven Pyridine-Catalyzed CO_2 Reduction

Zhu Chen, Coleman X. Kronawitter, Xiaofang Yang, Denis Potapenko, and Bruce E. Koel
Department of Chemical and Biological Engineering
Princeton University
Princeton, NJ 08544

The goal of this research is to provide new insights into the role of the semiconductor electrode surface in the mechanism of solar-driven pyridine (C_5H_5N; Py)-catalyzed CO_2 reduction. As an example of utilizing a molecular catalyst to increase the efficiency or selectivity for CO_2 reduction by photoelectrocatalysis, high selectivity for the conversion of CO_2 to methanol or formic acid has been reported when pyridine was dissolved in the electrolyte of a photoelectrochemical cell employing p-GaP, p-CdTe, or p-$CuInS_2$ photocathodes. In order to improve the efficiency of these reactions, it is important to understand the mechanism by which pyridine catalyzes CO_2 conversion. Our research includes a surface science approach to investigate surface chemistry, defining reaction centers and identifying and characterizing key surface-bound intermediates, and determine the role of heterogeneous processes in this catalysis. A fundamental understanding is important for the continued optimization of solar-driven CO_2 reduction. This talk will focus on our foundational studies of small molecule adsorption on GaP(110) surfaces utilizing ambient pressure photoelectron spectroscopy (APPES) and STM. Later we will move beyond surface science experiments to operando FTIR investigations of surface-bound species during CO_2 reduction.

Identification of Surface-Bound Hydride from Water Dissociative Adsorption on GaP(110). Surface-bound species on GaP(110) formed upon interaction with water were spectroscopically identified at ambient pressures up to 0.5 Torr H2O using synchrotron-based APPES, as shown in Figure 1. These APPES experiments were performed at the APPES end station of the CSX-2 beamline at the National Synchrotron Light Source II at Brookhaven National Laboratory (BNL). The interaction of GaP(110) with H_2O induces formation of a partially dissociated adlayer, characterized by the presence of both Ga−OH and molecular H_2O species. The P 2p core level indicates formation of a negatively charged hydride that is remarkably stable in the presence of water, which is notable given the critical role of hydride transfer to catalysts and CO_2 during chemical fuel synthesis reactions in aqueous environments.

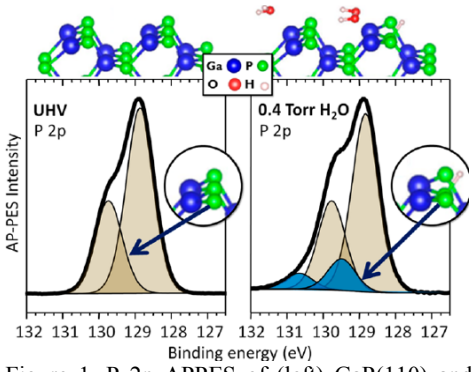

Figure 1. P 2p APPES of (left) GaP(110) and (right) GaP(110) at 0.4 torr H_2O. The P 2p components in blue indicate surface P-H. Diagram of dissociation of H_2O on GaP(110).

Investigation of the Adsorption Geometry and Electronic Structure of Pyridine on GaP(110). Using LT-STM at the Center for Functional Nanomaterials at BNL, facilitated by the discovery of a images of the gallium sublattice (for unoccupied state images) and the phosphorous sublattice (for occupied state images) on conductive *p*-type Zn:GaP(110). On this surface we examined the surface state that allowed some conductivity at 5 K, we routinely obtained atomic resolution bonding geometry of pyridine after adsorption at 20 and 300 K. The results as shown in Figure 2

showed that pyridine adsorbs in a tilted configuration at exposed unsaturated Ga (Lewis acid) sites. DFT results confirmed that the tilted geometry was the most favorable because it maintains the tetrahedral coordination of Ga in the zinc blende lattice. Furthermore, the combined experimental and theoretical results established that pyridine adsorbs through a dative bond between surface Ga unoccupied p orbitals and the lone pair of electrons on the pyridine N, consistent with expectations. The STM images reported in this study were the highest resolution ever obtained by STM for a single chemisorbed pyridine molecule and these images matched very closely simulated images obtained from the results of DFT calculations. By examining the distribution of unoccupied molecular orbitals with high spatial and energy resolution, we showed that scanning probe techniques can be used to positively identify the sites on pyridine that, in the context of frontier orbital theory, are susceptible to nucleophilic attack, consistent the known acid-base chemistry of N-heterocycles. These sites are especially relevant to pyridine-catalyzed CO_2 reduction, because they are proposed to be attacked by coadsorbed nucleophilic hydrides, creating the hydride-shuttling capability of partially reduced N-heterocycles such as dihydropyridine. This indicates that STM can be used to explore the local reaction centers of adsorbed ambidentate electrophiles and nucleophiles relevant to artificial photosynthesis, and more broadly to generate critical mechanistic information for various heterogeneous acid−base reactions.

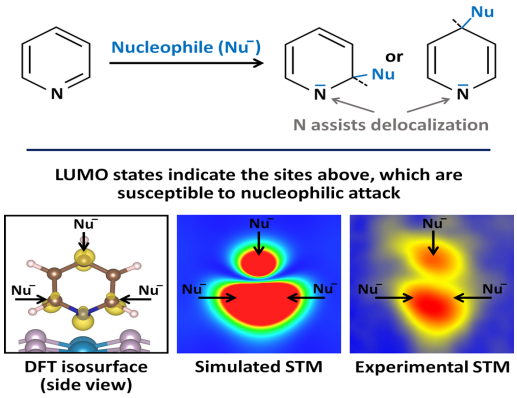

Figure 2. (Top) Schematic for hydrogenation of pyridine by nucleophiles. (Bottom) From left to right, DFT calculations of pyridine geometry on GaP(110), simulated STM image of pyridine adsorption on GaP(110), and constant-height STM image of pyridine on GaP(110) obtained at 5 K, 2.0 V. Arrows indicate the ortho- and para- sites susceptible to nucleophilic attack.

Observation of Pyridinium Hydrogenation by Operando FTIR. We identified hydrogenated pyridine products (pyridinium $C_5H_5NH^+$, for pH<pKa) by electrochemical reduction on a platinum electrode in an electrolyte solution with and without dissolved CO_2, providing clear evidence of the formation of a hydrogenated pyridine product, piperidine (piperidinium $C_5H_{10}NH_2^+$) from the changes in the CH_2 stretching, CH_2 bending, and ring modes under reducing conditions, as shown in Figure 3. The electrocatalytic hydrogenation proceeds by a heterogeneous chemical step involving adsorbed pyridine and adsorbed H, with the latter formed by the one-electron discharge of a proton on the platinum surface. Piperidine is the fully hydrogenated product of pyridine, and so the partially hydrogenated intermediate dihydropyridine must exist transiently during CO_2 reduction. Thus, partially hydrogenated N-heterocycles remain good candidates for active hydrogen-shuttling species in CO_2 reduction catalysis. More generally, the observed mild potentials required for electrocatalytic hydrogenation of stable organics implies that engineered transfer hydrogenations of organic adsorbates can be a viable approach for achieving selective CO_2 reduction to fuels.

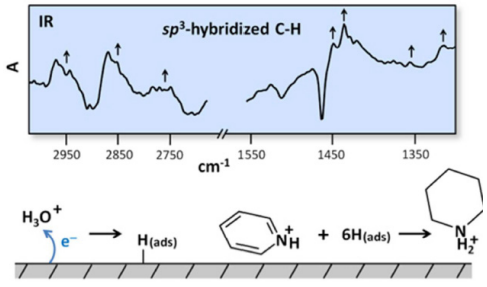

Figure 3. Schematic showing a proposed mechanism of electrocatalytic hydrogenation of pyridinium. IR spectrum of species formed during CO_2 reduction in the near surface region.

DOE Sponsored Publications 2015-2018

1. "Observation of surface-bound negatively charged hydride and hydroxide on GaP(110) in H_2O environments", C. X. Kronawitter, M. Lessio, P. Zhao, C. Riplinger, J. A. Boscoboinik, D. E. Starr, P. Sutter, E. A. Carter, and B. E. Koel, *J. Phys. Chem. C,* **119** (31), 17762–17772 (2015). DOI: 10.1021/acs.jpcc.5b05361

2. "Orbital-resolved imaging of the adsorbed state of pyridine on a III-V semiconductor identifies atomic sites susceptible to nucleophilic attack", C. X. Kronawitter, M. Lessio, P. Zahl, A. B. Muñoz-García, P. Sutter, E. A. Carter, and B. E. Koel, *J. Phys. Chem. C,* **119**, 28917– 28924 (2015). DOI: 10.1021/acs.jpcc.5b08659

3. "Electrocatalytic hydrogenation of pyridinium enabled by surface proton transfer reactions", C. X. Kronawitter, Z. Chen, P. Zhao, X. Yang, and B. E. Koel, *Catal. Sci. Technol.,* **7**, 831-837 (2017). DOI: 10.1039/C6CY02487D

4. "Adsorption and dissociation of methanol on GaP(110) surfaces studied by ambient pressure photoelectron spectroscopy", Z. Chen, X. Yang, I. Waluyo, and B.E. Koel, *J. Phys. Chem. C,* to be submitted.

5. "Adsorption, bonding, and thermal stability of pyridine on GaP(110) surfaces using ambient pressure photoelectron spectroscopy", Z. Chen, X. Yang, I. Waluyo, and B.E. Koel, *J. Phys. Chem. C,* to be submitted.

Probing Interfacial Processes on Semiconductors Using Lab-Based Ambient Pressure XPS

Sylwia Ptasinska
Radiation Laboratory and Department of Physics
University of Notre Dame
Notre Dame, Indiana 46556

Water splitting is a clean and sustainable process for the production of hydrogen as a chemical fuel. A photoelectrochemical (PEC) solar cell, which contains a semiconductor photoanode and a cathode, is commonly used to split water into O_2 via water oxidation by holes generated at the photoanode, and into H_2 via water reduction by electrons at the cathode. The development of PEC devices remains a challenging task, as many of the most efficient materials, such as III-V semiconductors, are unstable under harsh operating conditions, including high temperature, high current, reactive electrolyte and reaction products. In particular, highly-oxidized surfaces are composed of oxygen species that trap charge carriers and lead to the photocorrosion of these electrodes. Thus, better understanding of the interfacial chemistry on III-V semiconductors, under *in situ* and *operando* conditions, is essential for enhancing our knowledge of the water splitting mechanisms and for improving the efficiency and stability of PEC devices.

By performing lab-based ambient pressure X-ray Photoelectron Spectroscopy (AP-XPS) studies, we were able to follow the physicochemical processes occurring on the surface of Ga-based semiconductors, such as GaAs, GaP, and Ga-N, over a wide range of pressures and temperatures (ultra-high-vacuum (UHV) – 5 mbar, 298 – 873 K); identify the multiple oxides, including the intermediate species that were formed, i.e., Ga_2O; and track changes in both the thickness of oxides and the work function of the surface (Figure 1).

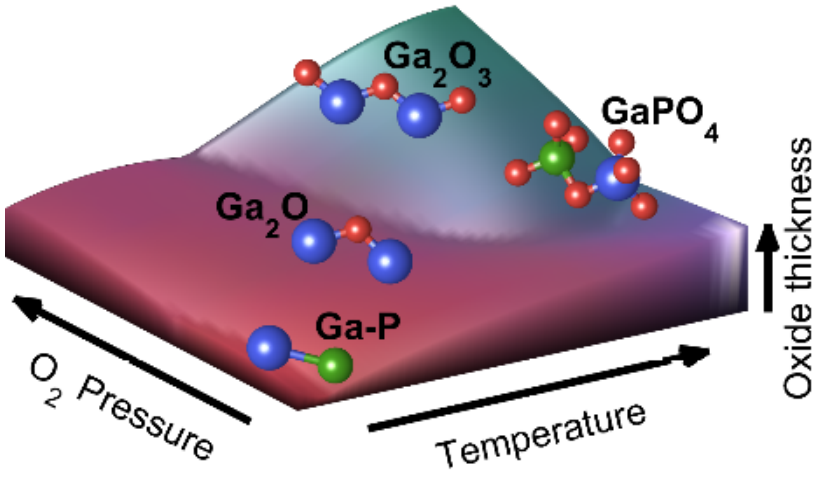

Figure 1. Tracking surface oxides. The chemical evolution of various oxide species on the GaP(111) surface can be monitored by lab-based ambient pressure X-ray photoelectron spectroscopy. The activation energies of the oxide species formation, the work function and the thickness of oxide layers can be estimated under elevated O_2 pressure and temperature conditions.

In addition to our experimental efforts, information from simulation and modeling has been provided; in particular, first-principles molecular dynamics simulations allowed for accessing complex interfacial chemical processes, while high-level electronic structure theory, such as many-body perturbation theory within the GW approximation, provided an accurate description of interfacial electronic properties due to its ability to treat the electronic structure of both semiconductors and aqueous solutions on the same footing. From these calculations the valence band maxima (VBM) were computed for hydrated pristine and hydroxylated GaP surfaces are presented in Figure 2.

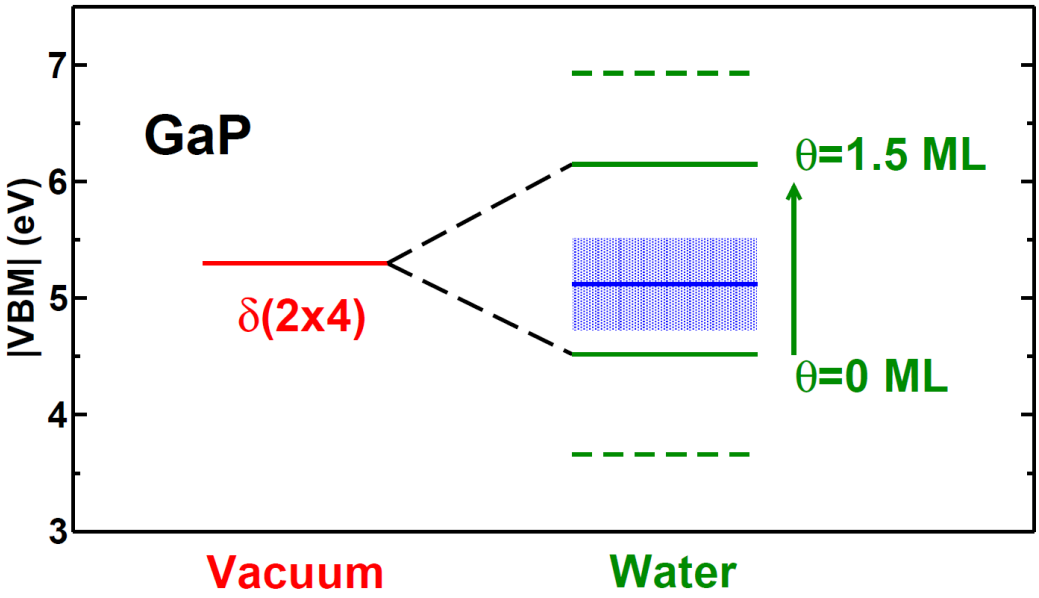

Figure 2. Absolute values of the valence band maximum of GaP in vacuum (mixed-dimer δ (2 × 4) surfaces), and in the presence of liquid water, including mixed-dimer δ (2 × 4) (θ = 0) and hydroxylated (θ = 1.5 ML) surfaces. Results computed for surfaces with a monolayer of water molecules and hydroxyls in vacuum are presented by dashed lines. Experimental results obtained for pH=0–14 and neutral water are represented by filled boxes, and the solid blue lines.

Currently, we are extending our investigation on interfacial processes to other III-V semiconductors, i.e., InP. Our preliminary results show that the formation of In-O-P is thermodynamically more favorable than that of In-O-In. While the latter species can be preferentially generated in a kinetics-governed non-equilibrated environment such as under UHV conditions.

Our study provides a basis for molecular-level understanding of the processes that occur in a PEC solar cell performing water splitting, during which electrode corrosion is minimized, while an efficient charge transfer at the electrolyte/electrode interface is maintained.

DOE Sponsored Publications 2015-2018

1. X. Zhang, S. Ptasińska - *Evolution of surface-assisted oxidation of GaAs (100) by gas-phase N_2O, NO, and O_2 under near-ambient pressure conditions.* Journal of Physical Chemistry C 119 (2015) 262-270
2. X. Zhang, S. Ptasinska - *Distinct and dramatic water dissociation on GaP (111) tracked by near ambient pressure XPS.* Physical Chemistry Chemical Physics 17 (2015) 3909-3918
3. W. Huang, J. Manser, P.V. Kamat, S. Ptasinska - *Evolution of Chemo-structural Composition and Photovoltaic Efficiency of $CH_3NH_3PbI_3$ Perovskite under Ambient Conditions.* Chemistry of Materials 28 (2016) 303-3011
4. X. Zhang, S. Ptasinska - *Heterogeneous Oxygen-containing Species Formed via Oxygen or Water Dissociative Adsorption onto a Gallium Phosphide Surface.* Topics in Catalysis 59 (2016) 564-573
5. W. Huang, S. Ptasinska - *Functionalization of Graphene by Atmospheric Pressure Plasma Jet in Air or H_2O_2 environments.* Applied Surface Science 367 (2016) 160-166
6. X. Zhang, S. Ptasinska – *Electronic and chemical structure of the H_2O/GaN(0001) interface under ambient conditions.* Scientific Reports 6 (2016) 24848
7. X. Zhang, S. Ptasinska - *High pressure Induced Pseudo-Oxidation of Copper Surface by Carbon Monoxide*. ChemCatChem 8 (2016) 1632
8. T. Jiang, X. Zhang, S. Vishwanath, X. Mu, V. Kanzyuba, D.A Sokolov, S. Ptasinska, D.B Go, H. Xing, T. Luo - *Covalent Bonding Modulated Graphene-Metal Interfacial Thermal Transport.* Nanoscale 8 (2016) 10993-11001
9. W. Huang, J.S. Manser, S. Sadhu, P.V Kamat, S. Ptasinska - *Direct Observation of Reversible Transformation of $CH_3NH_3PbI_3$ and NH_4PbI_3 Induced by Polar Gaseous Molecules.* Journal of Physical Chemistry Letters 7 (2016) 7 5068-5073
10. T.X.T. Sayle, F. Caddeo, X. Zhang, T. Sakthivel, S. Das, S. Seal, S. Ptasinska, D.C. Sayle - *Structure–Activity Map of Ceria Nanoparticles, Nanocubes, and Mesoporous Architectures.* Chemistry of Materials 28 (2016), 7287-7295
11. A.R. Milosavljević, W. Huang, S. Sadhu, S. Ptasinska - *Low-Energy Electron-Induced Transformations in Organolead Halide Perovskite*. Angewandte Chemie International Edition 128 (2016) 10237-10241
12. X. Zhang, Ch-G. Wang, W. Ji, S. Ptasinska - *Evolution of CH_3NO_2/Si interfacial chemistry under reaction conditions: a combined experimental and theoretical study.* Chemical Communications 53 (2017) 3342-3345
13. L.V. Trandafilovic, D.J. Jovanovic, X. Zhang, S. Ptasinska, M.D. Dramicanin, - *Enhanced photocatalytic degradation of methylene blue and methyl orange by ZnO:Eu nanoparticles.* Applied Catalysis B-environmental, 203 (2017) 740-752
14. J. Yang, Y. Pang, W. Huang, S.K. Shaw, J. Schiffbauer, M.A. Pillers, X. Mu, S. Luo, T. Zhang, Y. Huang, G. Li, S. Ptasinska, M. Lieberman, T. Luo - *Functionalized Graphene Enables Highly Efficient Solar Thermal Steam Generation.* ACS Nano 11 (2017) 5510-5518
15. W. Huang, S. Sadhu, S. Ptasinska - *Heat-and Gas-Induced Transformation in $CH_3NH_3PbI_3$ Perovskites and Its Effect on the Efficiency of Solar Cells.* Chemistry of Materials 29 (2017) 8478-8485
16. X. Liu, S.-K. Bac, P. Sapkota, C. Gorsak, X. Li, S. Dong, S. Lee, S. Ptasinska, J.K. Furdyna, M. Dobrowolska - *In situ annealing of III1-x Mn x V ferromagnetic semiconductors.* Journal of Vacuum Science & Technology B 36 (2018) 02D102.

17. T.A. Pham, X. Zhang, B.C. Wood, D. Prendergast, S. Ptasinska, T. Ogitsu - *Integrating Ab Initio Simulations and X-ray Photoelectron Spectroscopy: Towards A Realistic Description of Oxidized Solid/Liquid Interfaces.* Journal of Physical Chemistry Letters 9 (2018) 194-203
18. X. Zhang, Y.-S. Chen, P.V. Kamat, S. Ptasinska - *Probing Interfacial Electrochemistry on a Co_3O_4 Water Oxidation Catalyst Using Lab-Based Ambient Pressure XPS*. Journal of Physical Chemistry C (2018) DOI: 10.1021/acs.jpcc.8b01012

Modulating Primary Photochemical Events in Group IV Nanocrystals Through Surface Chemistry

Lance M. Wheeler, Nicholas C. Anderson, Gerrard M. Carroll, Rens Limpens, Matthew C. Beard, Nathan R. Neale
Chemistry and Nanoscience Center
National Renewable Energy Laboratory
Golden, CO 80401

We have been exploring the surface functionalization of group IV (Si, Ge) and III–V ($In_xGa_{1-x}P$, etc.) nanocrystals (NCs) to understand how surface chemistry influences the primary photochemical events (charge generation, separation, and recombination) as well as inter-NC charge transfer. These studies are all enabled by plasma synthesis that provides clean, highly reactive NC surfaces. Subsequent surface chemistry manipulation yields NCs largely free from competing surface defect states that are thus amenable to detailed optical characterization studies.

For example, spectroscopic interrogation of plasma-synthesized Si NCs have provided insight into their electron-phonon interactions, quasi-direct optical transitions, and exciton formation dynamics. Doped Si NCs are easily accessible using this technique, which has allowed us to probe the degree of interaction between free carriers and photogenerated electron-hole pairs. In addition, we have demonstrated cationic ligand exchange reactions on plasma-synthesized Ge NCs that enables effective electronic coupling and thus inter-particle charge transport in Ge NC films. Finally, very recent work has shown that we can use the plasma method to control the morphology of $In_xGa_{1-x}P$ NCs from hollow to solid, demonstrating the viability of this method in accessing difficult-to-synthesize semiconductor nanostructures.

In this presentation, we will first focus on our work to understand the mechanism of ligand functionalization for Si NCs synthesized using the nonthermal plasma process. FTIR and solution-phase 1D NMR spectroscopies are used to characterize the Si NC surfaces before and after ligand functionalization. In contrast to conventional hydrosilylation reactions with alkenes—where homolytic cleavage of Si−H surface bonds typically initiates Si–C alkyl bond formation—we find the dominant initiation step for plasma-synthesized Si NCs is abstraction of a surface silyl radical, $\bullet SiH_3$, as shown in Figure 1. We will additionally discuss collaborative work using solid-state 2D multidimentional NMR spectroscopy to quantify the proportion of the three surface hydride species before and after functionalization with alkyl groups (Figure 2).

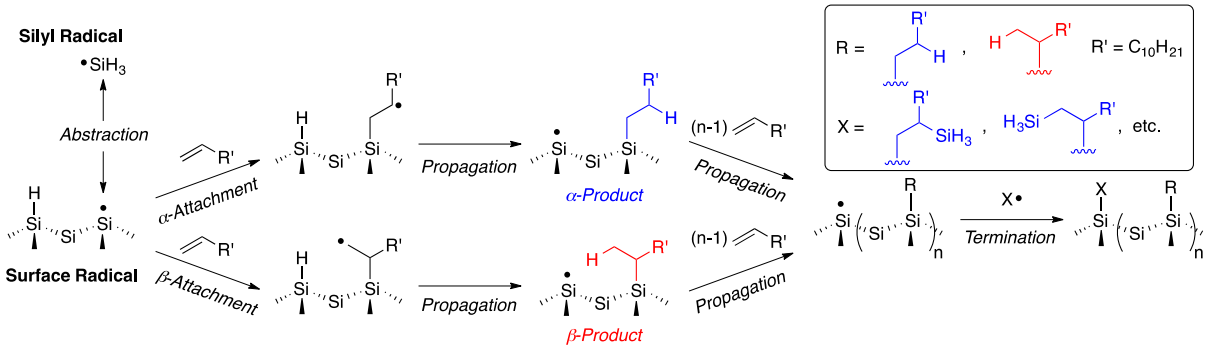

Figure 1. New mechanism for silicon surface functionalization based on silyl radical ($\bullet SiH_3$) abstraction.

We recently leveraged this deep understanding of the surface chemistry to reveal a new way to modulate the emission properties in Si NCs. The optical properties of Si NCs are a subject of intense study and continued debate. The photoluminescence (PL) in particular is known to depend strongly on the surface chemistry, with electron-hole recombination pathways derived from the Si NC band-edge, surface-state defects, or combined NC-conjugated ligand hybrid states.

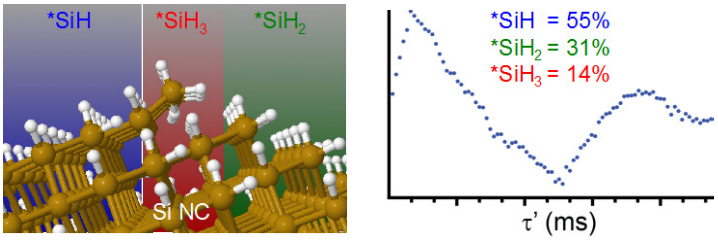

Figure 2. Model showing unique Si NC surface hydrides *SiH_x and proportion of monohydride *SiH, dihydride *SiH_2, and trihydride, or silyl, *SiH_3 groups as revealed by multidimensional solid-state NMR spectroscopy. The asterisk (*) denotes an atom on the Si NC surface.

For the second key thrust of this presentation, we will describe the effect of three different *saturated* surface functional groups—alkyls, amides, and alkoxides—on the photogenerated charge dynamics in nonthermal plasma-synthesized Si NCs. We find a systematic and *size-dependent* high-energy (blue) shift in the PL spectrum of Si NCs with amide and alkoxy functionalization relative to alkyl (Figure 3). Extensive surface chemistry characterization shows that our radical-based method developed for alkyl group functionalization (*Si–CR) of the native hydride-terminated surface also provides amide- (*Si–NHR) and alkoxy- (*Si–OR) functionalized Si NCs with a surface coverage of 3–4 ligands nm^{-2} irrespective of ligand type. Time-resolved PL and transient absorption spectroscopies reveal no change in the excited-state dynamics between Si NCs functionalized with alkyl, amide, or alkoxide ligands, showing for the first time that saturated ligands—not only surface-derived charge transfer states or hybridization between NC and low-lying ligand orbitals—are responsible for tuning the Si NC optical properties. These results suggest that the atom bound to the Si NC surface strongly interacts with the Si NC electronic wave function and modulates the Si NC quantum confinement, revealing a potentially broadly applicable correlation between the primary photochemical events in quantum-confined structures and the ligand binding group.

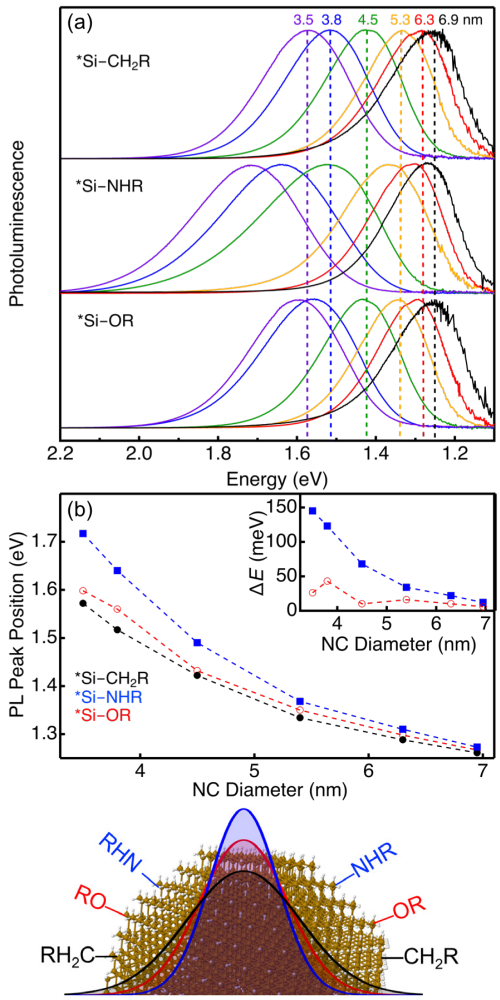

Figure 3. The degree of quantum confinement in Si nanocrystals (NCs) can be controlled by the nature of the ligand head group as evidenced by systematic differences in the size-dependent emission spectra with alkyl *$Si–CH_2R$, amide *Si–NHR, and alkoxide *Si–OR surface functionalization.

DOE Sponsored Publications 2015-2018

1. "Tuning Quantum Confinement in Colloidal Silicon Nanocrystals with Saturated Surface Ligands," G. M. Carroll, R. Limpens, N. R. Neale, *Nano Letters*, **18**, ASAP (2018). DOI: http://dx.doi.org/10.1021/acs.nanolett.8b00680

2. "Morphological Control of $In_xGa_{1-x}P$ Nanoparticles Synthesized in a Nonthermal Plasma," N. D. Bronstein, L. M. Wheeler, N. C. Anderson, N. R. Neale, *Chemistry of Materials*, **30**, ASAP (2018). DOI: http://dx.doi.org/10.1021/acs.chemmater.8b01358

3. "Negligible Electronic Interaction Between Photo-Excited Electron-Hole Pairs and Free Electrons in Phosphorus-Boron Co-Doped Silicon Nanocrystals," R. Limpens, M. Fujii, N. R. Neale, T. Gregorkiewicz, *The Journal of Physical Chemistry C*, **122**, 6397 (2018). DOI: http://dx.doi.org/ 10.1021/acs.jpcc.7b12313

4. "Switchable Photovoltaic Windows Enabled by Reversible Photothermal Complex Dissociation from Methylammonium Lead Iodide," L. M. Wheeler, D. T. Moore, R. Ihly, N. Stanton, E. M. Miller, R. C. Tenent, J. L. Blackburn, N. R. Neale, *Nature Communications*, **8**, 1722 (2017). DOI: http://dx.doi.org/10.1038/s41467-017-01842-4

5. "Characterization of Silicon Nanocrystal Surfaces by Multidimensional Solid-State NMR Spectroscopy," M. P. Hanrahan, E. L. Foust, T. L. Windus, L. M. Wheeler, N. C. Anderson, N. R. Neale, A. J. Rossini, *Chemistry of Materials*, **29**, 10339 (2017). DOI: http://dx.doi.org/10.1021/acs.chemmater.7b03306

6. "Silicon Photoelectrode Thermodynamics and Hydrogen Evolution Kinetics Measured by Intensity-Modulated High-Frequency Resistivity Impedance Spectroscopy," N. C. Anderson, G. M. Carroll, R. T. Pekarek, S. T. Christensen, J. van de Lagemaat, N. R. Neale, *The Journal of Physical Chemistry Letters*, **8**, 5253 (2017). DOI: http://pubs.acs.org/doi/abs/10.1021/acs.jpclett.7b01311

7. "Covalent Surface Modification of Gallium Arsenide Photocathodes for Water Splitting in Highly Acidic Electrolyte," L. E. Garner, K. X. Steirer, J. L. Young, N. C. Anderson, E. M. Miller, J. S. Tinkham, T. G. Deutsch, A. Sellinger, J. A. Turner, N. R. Neale, *ChemSusChem*, **10**, 676 (2017). DOI: http://dx.doi.org/10.1002/cssc.201601408

8. "Semiconductor-to-Metal Transition in Rutile TiO_2 Induced by Tensile Strain," E. E. Benson, E. M. Miller, S. U. Nanayakkara, D. Svedruzic, S. Ferrere, N. R. Neale, J. van de Lagemaat, B. A. Gregg, *Chemistry of Materials*, **29**, 2173 (2017). http://dx.doi.org/10.1021/acs.chemmater.6b04881

9. "A Graded Catalytic-Protective Layer for an Efficient and Stable Water-Splitting Photocathode," J. Gu, J. A. Aguiar, S. Ferrere, K. X. Steirer, Y. Yan, C. Xiao, J. L. Young, M. Al-Jassim, N. R. Neale, J. A. Turner, *Nature Energy*, **2**, 16192 (2017). DOI: http://dx.doi.org/10.1038/nenergy.2016.192

10. "Proton Reduction Using a Hydrogenase-Modified Nanoporous Black Silicon Photoelectrode," Y. Zhao, N. C. Anderson, M. W. Ratzloff, D. W. Mulder, K. Zhu, J. A. Turner, N. R. Neale, P. W. King, H. M. Branz, *ACS Applied Materials & Interfaces*, **8**, 14481 (2016). DOI: http://dx.doi.org/10.1021/acsami.6b00189

11. "Revealing the Semiconductor-Catalyst Interface in Buried Platinum Black Silicon Photocathodes," J. A. Aguiar, N. C. Anderson, N. R. Neale, *Journal of Materials Chemistry A*, **4**, 8123 (2016). DOI: http://dx.doi.org/10.1039/C6TA02505F

12. "Quasi-Direct Optical Transitions in Silicon Nanocrystals with Intensity Exceeding the Bulk," B. G. Lee, J.-W. Luo, N. R. Neale, M. C. Beard, D. Hiller, M. Zacharias, P. Stradins, A. Zunger, *Nano Letters*, **16**, 1583 (2016). DOI: http://dx.doi.org/10.1021/acs.nanolett.5b04256

13. "Size Dependent Exciton Formation Dynamics in Colloidal Silicon Quantum Dots," M. R. Bergren, P. K. B. Palomaki, N. R. Neale, T. E. Furtak, M. C. Beard, *ACS Nano*, **10**, 2316 (2016). DOI: http://dx.doi.org/10.1021/acsnano.5b07073

14. "All-Inorganic Germanium Nanocrystal Films by Cationic Ligand Exchange," L. M. Wheeler, A. W. Nichols, B. D. Chernomordik, N. C. Anderson, M. C. Beard, N. R. Neale, *Nano Letters*, **16**, 1949 (2016). DOI: http://dx.doi.org/10.1021/acs.nanolett.5b05192

15. "Water Reduction by a p-$GaInP_2$ Photoelectrode Stabilized by an Amorphous TiO_2 Coating and a Molecular Cobalt Catalyst," J. Gu, Y. Yan, J. L. Young, K. X. Steirer, N. R. Neale, J. A. Turner, *Nature Materials*, **15**, 456 (2015). http://dx.doi.org/10.1038/NMAT4511

16. "Understanding Semiconductor Interfacial Carrier Dynamics by Direct Observation of Photo-Induced Transient Electric Fields," Y. Yang, J. Gu, J. L. Young, E. M. Miller, J. A. Turner, N. R. Neale, M. C. Beard, *Science*, **350**, 1061 (2015). http://dx.doi.org/10.1126/science.aad3459

17. "Silyl Radical Abstraction in the Functionalization of Plasma-Synthesized Silicon Nanocrystals," L. M. Wheeler, N. C. Anderson, P. K. B. Palomaki, J. L. Blackburn, J. C. Johnson, N. R. Neale, *Chemistry of Materials,* **27**, 6869 (2015). http://dx.doi.org/10.1021/acs.chemmater.5b03309

18. "Synthesis, Optical, and Photocatalytic Properties of Cobalt Mixed-Metal Spinel Oxides $Co(Al_{1-x}Ga_x)_2O_4$," K. Lee, D. A. Ruddy, G. Dukovic, N. R. Neale, *Journal of Materials Chemistry A,* **3**, 8115 (2015). http://dx.doi.org/10.1039/C4TA06690A

19. "Oxidatively Stable Nanoporous Silicon Photocathodes with Enhanced Onset Voltage for Photoelectrochemical Proton Reduction," Y. Zhao, N. C. Anderson, K. Zhu, J. A. Aguiar, J. A. Seabold, J. van de Lagemaat, H. M. Branz, N. R. Neale, J. Oh, *Nano Letters*, **27**, 2517 (2015). http://dx.doi.org/10.1021/acs.nanolett.5b00086

20. "Quantum Confined Electron-Phonon Interaction in Silicon Nanocrystals," D. M. Sagar, J. M. Atkin, P. K. B. Palomaki, N. R. Neale, J. L. Blackburn, J. C. Johnson, A. J. Nozik, M. B. Raschke, M. C. Beard, *Nano Letters*, **15**, 1511 (2015). http://dx.doi.org/10.1021/nl503671n

21. "All First Row Transition Metal Oxide Photoanode for Water Splitting Based on $Cu_3V_2O_8$," J. A. Seabold and N. R. Neale, *Chemistry of Materials*, **27**, 1005 (2015). http://dx.doi.org/10.1021/cm504327f

22. "Semiconducting properties of spinel tin nitride and other IV_3N_4 polymorphs," C. M. Caskey, J. A. Seabold, V. Stevanovic, M. Ma, W. A. Smith, D. S. Ginley, N. R. Neale, R. M. Richards, S. Lany, A. Zakutayev, *Journal of Materials Chemistry C*, **3**, 1389 (2015). http://dx.doi.org/10.1039/C4TC02528H

Controlling 2D Transition Metal Dichalcogenides Optoelectronic and Catalytic Properties

Hanyu Zhang, Eric E. Benson, Sanjini U. Nanayakkara, Jeffrey L. Blackburn, Elisa M. Miller
Materials and Chemical Science & Technology
National Renewable Energy Laboratory
Golden, CO 80401

Quantum-confined transition metal dichalcogenides (TMDCs) are interesting for energy harvesting and solar conversion systems due to their unique optical and electronic properties, where they have the formula MX_2 (M = Mo or W and X = S, Se, or Te). We aim to control these TMDC properties for charge transfer at interfaces by functionalizing, doping, and/or straining the surface. We have developed synthesis strategies that enable both top-down (solution or mechanical exfoliation) or bottom up (chemical vapor deposition, CVD) approaches to make nanosheets or monolayers, respectively.

In particular, metallic molybdenum disulfide (MoS_2) nanosheets are promising for the hydrogen evolution reaction (HER) due to their high reactivity, earth abundance, low-cost, and non-toxicity, which makes MoS_2 a candidate to replace platinum for HER. We modify the fundamental electronic properties of metallic (1T phase) MoS_2 nanosheets through covalent chemical functionalization, and thereby directly influence the HER kinetics, surface energetics, and stability.[1] Chemically-exfoliated, metallic (1T) MoS_2 nanosheets are functionalized with organic phenyl rings containing electron donating or withdrawing groups (Figure 1a). Using X-ray photoelectron spectroscopy (XPS) and diffuse reflectance infrared Fourier transform spectroscopy (DRIFTS), we confirm that the functional group is attached to the S and not the Mo, as is depicted in Figure 1a. We find that MoS_2 functionalized with the most electron donating functional group (p-$(CH_3CH_2)_2NPh$-MoS_2) is the most efficient catalyst for HER in this series, with initial activity similar to the pristine metallic phase of MoS_2 (Figure 1b). With regards to the entire studied series, the overpotential and Tafel slope for catalytic HER are both directly correlated with the electron donating strength (Hammett parameter) of the pendant group on the phenyl ring. The results are consistent with a mechanism involving ground-state electron donation or withdrawal to/from the MoS_2 nanosheets, which modifies the electron transfer kinetics and catalytic activity of the MoS_2 sheet. Furthermore, the p-$(CH_3CH_2)_2NPh$-MoS_2 thin film has the shallowest workfunction and as the functional groups become more electron withdrawing the workfunction increases, which is due to the dipole on the surface.

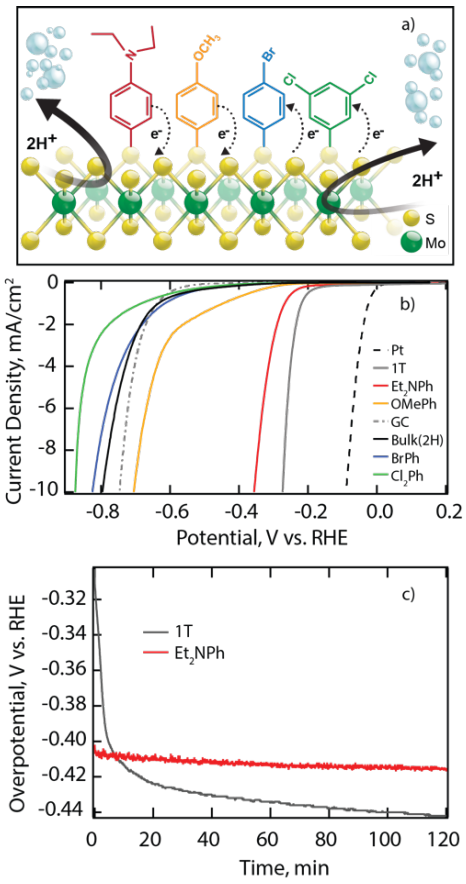

Figure 1. Functionalized metallic MoS_2 nanosheets. a) the functional groups range from electron donating to electron withdrawing, which influences the HER activity and stability of the nanosheets.

In addition, we explore the stability and degradation mechanism for the 1T MoS_2 nanosheets. We show that the functional groups preserve the metallic phase of the MoS_2 films, inhibiting conversion to the thermodynamically stable semiconducting state (2H) when annealed at 150 °C for 24 h in a nitrogen atmosphere. We propose that this protection is critical to maintaining the catalytically active state of 1T MoS_2 nanosheets. We are interested in understanding how the conversion from 1T to 2H occurs, and we have begun using high-resolution microscopy techniques to map this transition, which is done with our collaborator Michael Mirkin (CUNY-Queens College). In addition to "shelf-stability", the functionalized MoS_2 films also have in-situ HER durability. Figure 1c highlights how the p-$(CH_3CH_2)_2$NPh-MoS_2 outperforms the unfunctionalized metallic MoS_2 under continuous H_2 evolution conditions within 10 min. Our next steps in this project are to probe the degradation mechanism more thoroughly. We plan to examine the surface after HER to learn what chemical changes are occurring on the surface via XPS, DRIFTS, and other spectroscopies. This will be essential to design durable MoS_2 HER catalysts. Moreover, we have also begun studying other functionalized TMDC nanosheets for HER.

Our group is also interested in exploring TMDC monolayers as model systems for quantum-confined 2D direct-gap semiconductors. We can synthesize up to 50-μm MoS_2 monolayer triangles, and we are currently exploring how to grow large area (~1 cm) MoS_2 by systematically changing the CVD growth conditions. We are also collaborating with Young-hee Lee's group (Sungkyunkwan University) to learn about environmental effects on the optoelectronic properties of WS_2, where they are providing the 20-μm WS_2 monolayer triangles. In the literature, there is a wide range of reported optoelectronic properties for TMDC monolayers; however, there is not a good understanding of environmental effects on optical (photoluminescence, PL) and electrical (conductivity) properties. We have determined that the PL of WS_2 monolayers is enhanced with O_2 and H_2O exposure, with the effects being distinct for each molecular adsorbent. In a controlled environment, we measure the effects of O_2 adsorption on WS_2 by using dry air. O_2 adsorption onto WS_2 is light-induced (532 nm), drastically increases the emission intensity, and shifts the peak potion to lower energy, which consists of the trion and exciton (Figure 2). In contrast, H_2O adsorption onto WS_2 occurs without light exposure and increases the emission peak while shifting the peak to higher energy. Both adsorbents can be removed by annealing the WS_2 monolayer in a N_2 environment and the pristine WS_2 monolayer can be recovered. We hypothesize that the adsorption for both H_2O and O_2 is occurring at defect sites on the edges, which leads to differences in the emission intensity between the center and edge. This work is ongoing to decipher the different surface adsorption mechanisms for H_2O and O_2.

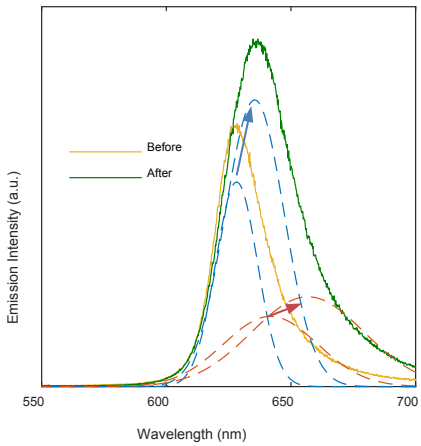

Figure 2. Changes to the optical properties of monolayer WS_2 following exposure to O_2 and 532-nm photons. The emission peak is deconvoluted, where the exciton is the blue dashed trace and the trion is the red dashed trace.

DOE Sponsored Publications 2015-2018

1. E. E. Benson, H. Zhang, S. A. Shuman, S. U. Nanayakkara, N. D. Bronstein, S. Ferrere, J. L. Blackburn, E. M. Miller, "Balancing the Hydrogen Evolution Reaction, Surface Energetics, and Stability of Metallic MoS_2 Nanosheets via Covalent Functionalization," *JACS*, 140, 441 (2018). DOI: 10.1021/jacs.7b11242

2. M. A. Todt, A. E. Isenberg, S. U. Nanayakkara, E. M. Miller, J. B. Sambur, "Single Nanoflake Photoelectrochemistry Reveals Champion and Spectator Flakes in Exfoliated $MoSe_2$ Films," *The Journal of Physical Chemistry C*, 122, 6539 (2018). DOI: 10.1021/acs.jpcc.7b12715

3. A. D. Martinez, E. M. Miller, A. G. Norman, R. R. Schnepf, N. Leick, C. Perkins, P. Stradins, E. S. Toberer, and A. Tamboli, Growth of Amorphous and Epitaxial $ZnSiP_2$-Si alloy films on Si, *Journal of Materials Chemistry C*, 6, 2696 (2018). DOI: 10.1039/C7TC05545E

4. L. M. Wheeler, D. T. Moore, R. Ihly, N. J. Stanton, E. M. Miller, R. C. Tenent, J. L. Blackburn, N. R. Neale, "Switchable Photovoltaic Windows Enabled by Reversible Photothermal Complex Dissociation from Methylammonium Lead Iodide," *Nature Communications,* 8*,* 1722 (2017). DOI: 10.1038/s41467-017-01842-4

5. B. Dou, E. M. Miller, J. A. Christians, E. M. Sanehira, T. R. Klein, F. S. Barnes, S. E. Shaheen, S. M. Garner, S. Ghosh, A. Mallick, D. Basak, and . F. A. M. van Hest, "High Performance Flexible Perovskite Solar Cells on Ultra-thin Glass: Implications of the TCO," *Journal of Physical Chemistry Letters*, *8* (19), 4960 (2017). DOI: 10.1021/acs.jpclett.7b02128

6. C. L Melamed, B. R. Ortiz, P. Gorai, A. D. Martinez, W. E. McMahon, E. M. Miller, V. Stevanović, A. C. Tamboli, A. G. Norman, and E. S. Toberer, "Large Area Atomically Flat surfaces via Exfoliation of Bulk Bi_2Se_3 Single Crystals," *Chemistry of Materials*, 29, 8472 (2017). DOI: 10.1021/acs.chemmater.7b03198

7. D. M. Kroupa, B. K. Hughes, E. M. Miller, D. T. Moore, N. C Anderson, B. D. Chernomordik, A. J. Nozik, and M. C. Beard, "Synthesis and Spectroscopy of Silver-Doped PbSe Quantum Dots," *Journal of the American Chemical Society*, 139, 10382 (2017). DOI: 10.1021/jacs.7b04551

8. E. E. Benson, E. M. Miller, S. Nanayakkara, D. Svedruzic, S. Ferrere, N. Neale, J. van de Lagemaat, and B. Gregg, "Semiconductor-to-Metal Transition in Rutile TiO_2 Induced by Strain," *Chemistry of Materials*, 29, 2173 (2017). DOI: 10.1021/acs.chemmater.6b04881

9. D. M. Kroupa, M. Vörös, N. P. Brawand, B. W. McNichols, E. M. Miller, J. Gu, A. J. Nozik, A. Sellinger, G. Galli, and M. C. Beard, "Tuning Colloidal Quantum Dot Band Edge Positions through Solution-Phase Surface Chemistry Modification," *Nature Communications*, 8, 15257 (2017).
DOI: 10.1038/ncomms15257

10. L. Garner, K. X. Steirer, J. L. Young, N. C. Anderson, E. M. Miller, J. S. Tinkham, T. G. Deutsch, A. Sellinger, J. A. Turner, N. R. Neale, "Covalent Surface Modification of Gallium Arsenide Photocathodes for Water Spitting in Highly Acidic Electrolyte," *ChemSusChem* 10, 767 (2017).
DOI: 10.1002/cssc.201601408

11. Y. Yang, M. Yang, D. T. Moore, Y. Yan, E. M. Miller, K. Zhu, and M. C. Beard, "Top and Bottom Surfaces Limit Carrier Lifetime in Lead Iodide Perovskite Films," *Nature Energy,* 2, 16207 (2016).
DOI:10.1038/nenergy.2016.207

12. A. E. Maughan, A. M. Ganose, M. M. Bordelon, E. M. Miller, D. O. Scanlon, and J. R. Neilson. "Defect Tolerance to Intolerance in the Vacancy-ordered Double Perovskite Semiconductors," *Journal of the American Chemical Society*, 138, 8453 (2016).
DOI: 10.1021/jacs.6b03207

13. E. M. Miller, D. M. Kroupa, J. Zhang, P. Schulz, A. Marshall, A. Kahn, J. M. Luther, M. C. Beard, C. L. Perkins, and J. van de Lagemaat, "Revisiting the Valence and Conduction Band Size Dependence of PbS Quantum Dot Thin Films," *ACS nano*, 10, 3302 (2016).
DOI: 10.1021/acsnano.5b06833

14. Y. Yang, J. Gu, J. L. Young, E. M. Miller, J. A. Turner, N. R. Neale, M. C. Beard, "Semiconductor interfacial carrier dynamics via photoinduced electric fields," *Science*, 350, 1061 (2015).
DOI: 10.1126/science.aad3459

Surface P-doping and Hot Hole Photochemistry in CdSe Quantum Dots

David Morgan, Youhong Zeng, Ke Gong and David F. Kelley
Chemistry and Chemical Biology
University of California, Merced
5200 North Lake Road, Merced, CA 95343

Much of the excited state dynamics of CdSe and CdSe/CdS quantum dots is determined by the density of surface states and the particle Fermi level, both of which can be controlled by particle surface treatments. In the present studies we examine these dynamics in the case where there is a high density of mid-gap surface states and the Fermi level is only slightly above the valence band edge. In this case, valence band electrons undergo thermal promotion to empty surface states, resulting in particles that are surface p-doped or "surface charged", as indicated in Scheme 1.

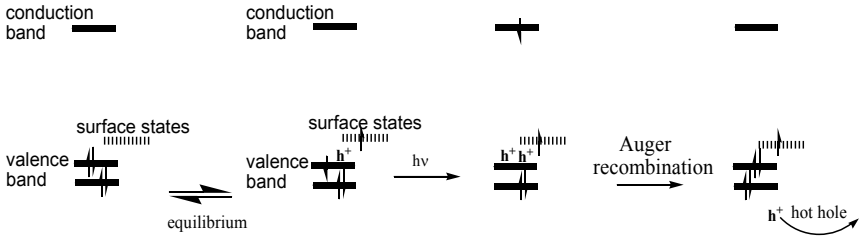

Scheme 1. Surface charging results in an electron in a surface state and a valence band hole. Following photoexcitation, the trion (two holes and one electron) can undergo a Auger process, producing a hot, photochemically active hole.

A surface charged particle can absorb a photon to form what is essentially a positively charged trion. The trion has different absorption and luminescence characteristics than the exciton, and can be spectroscopically identified in time-resolved absorption and luminescence studies, as shown in figure 1. Specifically, the trions show a relatively large ground state bleach in the TA kinetics and weak luminescence. These spectroscopic characteristics can be understood in terms of the electronic structure having valence band state filling from two holes.

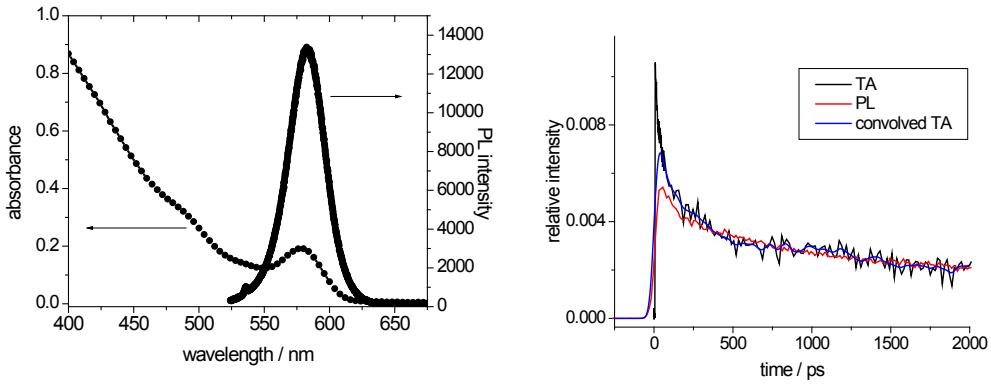

Figure 1. Static (left) and time-resolved (right) absorption and luminescence results for surface charged CdSe/CdS quantum dots.

The trions can undergo a relatively fast Auger process (see figure 1) and are therefore nonluminescent. Figure 2 shows that one-photon excitation of surface charged CdSe/CdS quantum dots in room temperature chloroform results in a delayed and reversible photodarkening of the sample. Since the surface charged particles are dark, here is little or no prompt loss of photoluminescence intensity. Subsequent photodarkening takes place on the tens of minutes timescale. This is assigned to the production of a hot hole being transferred to a surface ligand, followed by dissociation to form a QD^-/L^+ ion pair. The newly-formed positively charged ligand can react with another QD in solution causing photodarkening. Other photochemical pathways are also available in polar solvents. Charge recombination occurs on a slower timescale and reverses the loss of photoluminescence intensity.

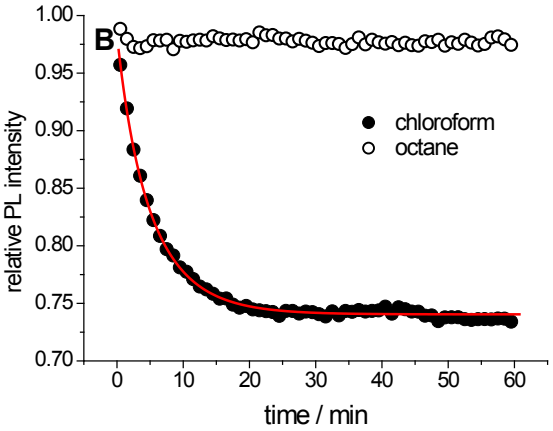

Figure 2. PL kinetics for CdSe/CdS quantum dots suspended in octane and chloroform solvents following 30 seconds of one-photon irradiation. The red curve is calculated from a diffusive mechanism for formation and subsequent reaction of positively charged ligands in solution.

DOE Sponsored Publications 2015-2018

1. David Morgan, Ke Gong, Anne Myers Kelley and David F. Kelley, "Biexciton Dynamics in Alloy Quantum Dots", *J Phys. Chem. C*, **121**, 18307 (2017).
2. Youhong Zeng and David F. Kelley, "Surface Charging in CdSe Quantum Dots: Infrared and Transient Absorption Spectroscopy", *J Phys. Chem. C*, **121**, 16657 (2017).
3. Youhong Zeng and David F. Kelley, "Excited Hole Photochemistry of CdSe/CdS Quantum Dots" *J. Phys. Chem. C,* **120**, 17853 (2016).
4. Gary A. Beane, Ke Gong and David F. Kelley, "Auger and Carrier Trapping Dynamics in Core/Shell Quantum Dots Having Sharp and Alloyed Interfaces", *ACS Nano*, **10**, 3755 (2016).
5. Ke Gong, Gary Beane and David F. Kelley, **"**Strain Relaxation in Metastable CdSe/CdS Quantum Dots", *Chemical Physics*, **471**, 18 (2016).
6. Youhong Zeng and David F. Kelley, "Two-Photon Photochemistry of CdSe Quantum Dots", *J. Phys. Chem. C, **117***, 20268 (**2015).**
7. Ke Gong and David F. Kelley, "Surface Charging and Trion Dynamics in CdSe-based Core/Shell Quantum Dots", *J. Phys. Chem. C,***119**, 9637 (2015).
8. Ke Gong and David F. Kelley, "Lattice Strain Limit for Uniform Shell Deposition in Zincblende CdSe/CdS Quantum Dots", *J. Phys. Chem. Lett*, **6**, 1559 (2015).

Ultrafast dynamics of photocatalytic hydrogen evolution on monolayer-rich tungsten-disulfide

Jeremy Dunklin, Hanyu Zhang, Ye Yang, Jao van de Lagemaat
Chemistry and Nanoscience Center
National Renewable Energy Laboratory
Golden, Colorado, 80401

We demonstrate a transient absorption spectroscopy (TAS) and photochemical study of carrier lifetimes and photocatalytic activity for direct photocatalytic hydrogen evolution in monolayer-rich aqueous transition metal dichalcogenides (TMD) dispersions. TMDs such as MoS_2 and WS_2 are corrosion-resistant, visible bandgap semiconductors with extraordinarily strong optical absorption that might be very interesting for large-scale solar energy conversion.[1] Many groups have studied these systems as efficient electrocatalysts[2] or used them with other light absorbers or senistizers. However very few have studied these 2-dimensional semiconductors as active, direct photochemical systems. While their electronic structure and excitonic transitions are now well-understood, less is known about ultra-fast carrier dynamics following light excitation and how these transient light-induced species can be harnessed in aqueous photochemical systems.

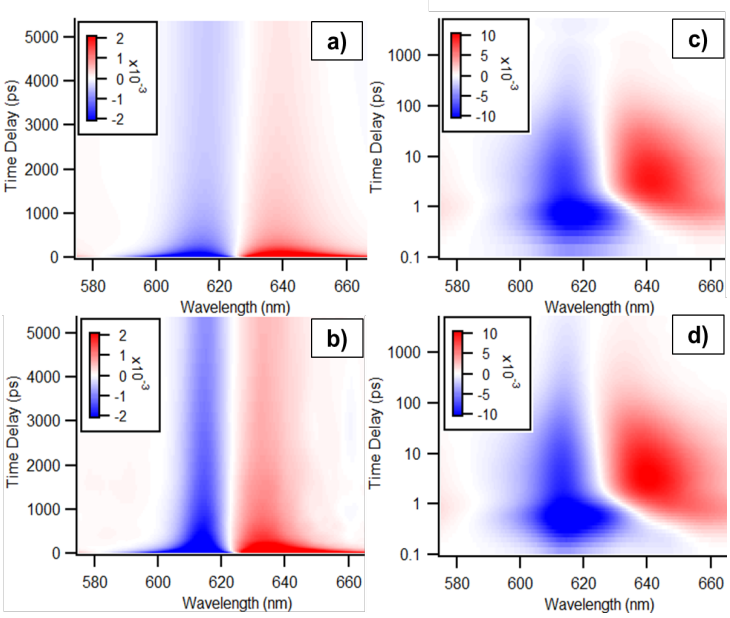

Fig. 1. Transient absorption spectroscopy of monolayer function of wavelength and probe delay for a) & c) WS_2 reference and b) & d) WS_2 in 1 mM ascorbic acid showing the much longer lifetime in the presence of ascorbic acid hole capturing agent.

Contrary to most work reported in the literature, in this work, we utilize a novel protocol[3] for production of WS_2 samples containing 60% monolayers by volume. The mean length of the WS_2 nanosheets is 30 nm, which is similar to the charge diffusion length in TMDs. This suggests that photogenerated charges are likely to reach catalytically active edges sites. Fig. 1 shows representative TAS results for aqueous dispersions of monolayer enriched WS_2 on both a linear and logarithmic timescale using 100 fs bandwidth 530 nm excitation pulses at about 10^4 to 10^5 nJ/cm^2 excitation densities. The interpretation of transient spectral features remains controversial as photobleaching has been alternatively ascribed to state filling, stimulated emission, or exciton self-energy renormalization while photoinduced absorption bands have been attributed to carrier-induced broadening and bi-excitons. Short (<ps) timescale kinetics have been explained using exciton formation, bandgap renormalization, trapping, cooling, and trions. The most closely aligned study confirmed that excitons are the primary photo-excited species which subsequently break up to form charges.[4] We

modeled our results using global fitting to a simple kinetic scheme which translates to a series of exponential decays with varying contributions at each wavelength. The scheme considers exciton formation, decay into free carriers, carrier trapping, radiative and non-radiative decay, hole capture and water reduction by free or trapped electrons. Using this global fitting scheme allows us to extract ranges of rate constants for the major processes occurring upon photoexcitation. It is clear from Fig.1 that the addition of a hole-capture agent prolongs the photoexcitation at longer-time scales ,while the early-time behavior is not strongly impacted. Extracted rate constants from global fitting quantified this as a 3 to 4-fold increase in free/trapped carrier lifetimes. The hole capture agent is needed as holes in WS_2 are not energetic enough to oxidize water.

Fig. 2. shows hydrogen evolved from aqueous dispersions of monolayer enriched WS_2 as a function of time in both the absence and presence of ascorbic acid. It is believed that adding ascorbic acid allows the electron to escape recombination and to then reduce water to form hydrogen, as supported by the aforementioned increase in TA times. Because of the low hydrogen production efficiency, we can estimate the relative time constants for electron transfer, recombination, and hole capture.

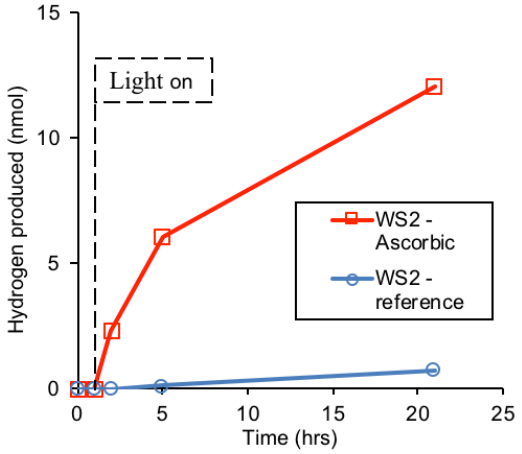

Fig. 2 Hydrogen production from aqueous dispersion of monolayer-enriched WS_2 nanosheets.

In conclusion, we demonstrate that photochemical water reduction using WS_2 that is not under bias or sensitized is possible. We observed hydrogen production from aqueous dispersions of WS_2 and studied the dynamics and kinetics of photoexcitation and charge transfer processes using ultrafast transient absorption. To understand the observed dynamics we need to consider exciton formation, free (observed as trions) and trapped charges, radiative and non-radiative recombination, hole transfer and electron transfer. The results of this study are pertinent not just to the use of WS_2 as a photocatalyst but also to its use as an electrocatalyst in water-splitting systems.

References:

(1) Yu, X.; Sivula, K. Toward Large-Area Solar Energy Conversion with Semiconducting 2D Transition Metal Dichalcogenides. *ACS Energy Lett.* **2016**, *1* (1), 315–322.

(2) Liu, P.; Zhu, J.; Zhang, J.; Xi, P.; Tao, K.; Gao, D.; Xue, D. P Dopants Triggered New Basal Plane Active Sites and Enlarged Interlayer Spacing in MoS_2 Nanosheets toward Electrocatalytic Hydrogen Evolution. *ACS Energy Lett.* **2017**, *2* (4), 745–752.

(3) Backes, C.; Szydłowska, B. M.; Harvey, A.; Yuan, S.; Vega-Mayoral, V.; Davies, B. R.; Zhao, P. L.; Hanlon, D.; Santos, E. J. G.; Katsnelson, M. I.; et al. Production of Highly Monolayer Enriched Dispersions of Liquid-Exfoliated Nanosheets by Liquid Cascade Centrifugation. *ACS Nano* **2016**, *10* (1), 1589–1601.

(4) Vega-Mayoral, V.; Vella, D.; Borzda, T.; Prijatelj, M.; Tempra, I.; Pogna, E. A. A.; Dal Conte, S.; Topolovsek, P.; Vujicic, N.; Cerullo, G.; et al. Exciton and Charge Carrier Dynamics in Few-Layer WS_2. *Nanoscale* **2016**, *8* (10), 5428–5434.

DOE Sponsored Publications 2015-2018

1. Oleksandr S.Bushuyev, Phil De Luna, Cao Thang Dinh, Ling Tao, Genevieve Saur, Jao van de Lagemaat, Shana O. Kelley, Edward H. Sargent, "What Should We Make with CO_2 and How Can We Make It?", *Joule*, March 2018, doi:10.1016/j.joule.2017.09.003

2. Haridas Mundoor, Ghadah H. Sheetah, Sungoh Park, Paul J. Ackerman, Ivan I. Smalyukh, and Jao van de Lagemaat, "Tuning and Switching a Plasmonic Quantum Dot "Sandwich" in a Nematic Line Defect", *ACS Nano*, **2018**, 12, 2580, doi:10.1021/acsnano.7b08462

3. Nicholas C. Anderson, Gerard M. Carroll, Ryan T. Pekarek, Steven T. Christensen, Jao van de Lagemaat, Nathan R. Neale, "Silicon Photoelectrode Thermodynamics and Hydrogen Evolution Kinetics Measured by Intensity-Modulated High-Frequency Resistivity Impedance Spectroscopy", *J. Phys. Chem. Lett.* **2017**, 8, 5253, doi:10.1021/acs.jpclett.7b01311

4. Daniel H. Weingarten, Michael D. LaCount, Jao van de Lagemaat, Garry Rumbles, Mark T. Lusk, and Sean E. Shaheen, "Experimental demonstration of photon upconversion via cooperative energy pooling", *Nature Comm.* **2017**, 8, 14808, doi:10.1038/ncomms14808

5. Eric E. Benson, Elisa M. Miller, Sanjini U. Nanayakkara, Drazenka Svedruzic, Suzanne Ferrere, Nathan R. Neale, Jao van de Lagemaat, Brian A. Gregg, "Semiconductor-to-Metal Transition in Rutile TiO_2 Induced by Tensile Strain", *Chem. Mater.* **2017**, 19, 2173, doi:10.1021/acs.chemmater.6b04881

6. Mengjin Yang, Yining Zeng, Zhen Li, Dong Hoe Kim, Chun-Sheng Jiang, Jao van de Lagemaat, Kai Zhu, "Do grain boundaries dominate non-radiative recombination in $CH_3NH_3PbI_3$ perovskite thin films?, *Phys. Chem. Chem. Phys*. **2017**, 19, 5043, doi:10.1039/C6CP08770A

7. Ye Yang, Mengjin Yang, Kai Zhu, Justin C. Johnson, Joseph J. Berry, Jao van de Lagemaat, Matthew C. Beard, "Large polarization-dependent exciton optical Stark effect in lead iodide perovskites", *Nature Comm.* **2016**, 7, 12613, doi:10.1038/ncomms12613

8. Elisa M. Miller, Daniel M. Kroupa, Jianbing Zhang, Philip Schulz, Ashley R. Marshall, Antoine Kahn, Stephan Lany, Joseph M. Luther, Matthew C. Beard, Craig L. Perkins, Jao van de Lagemaat, "Revisiting the valence and conduction band size dependence of PbS quantum dot thin films", *ACS Nano*, **2016**, 10, 3302, doi:10.1021/acsnano.5b06833

9. Ye Yang, David P. Ostrowski, Ryan M. France, Kai Zhu, Jao van de Lagemaat, Joseph M. Luther, Matthew C. Beard, "Observation of a hot-phonon bottleneck in lead-iodide perovskites", *Nature Phot.* **2016**, 10, 53, doi:10.1038/nphoton.2015.213

10. Paul J. Ackerman, Haridus Mundoor, Ivan I. Smalyukh, Jao van de Lagemaat, "Plasmon–Exciton Interactions Probed Using Spatial Coentrapment of Nanoparticles by Topological Singularities", *ACS Nano*, **2015**, 9, 12392, doi:10.1021/acsnano.5b05715

11. Chun-Sheng Jiang, Mengjin Yang, Yuanyuan Zhou, Bobby To, Sanjini U. Nanayakkara, Joseph M. Luther, Weilie Zhou, Joseph J. Berry, Jao van de Lagemaat, Nitin P. Padture, Kai Zhu, Mowafak M. Al-Jassim, "Carrier separation and transport in perovskite solar cells studied by nanometre-scale profiling of electrical potential", *Nature Comm.* **2015**, 6, 8397, doi:10.1038/ncomms9397

12. Sanjini U. Nanayakkara, Jao van de Lagemaat, Joseph M. Luther, "Scanning probe characterization of heterostructured colloidal nanomaterials", *Chem. Rev.* **2015**, 115, 8157, doi:10.1021/cr500280t

13. Michael D. LaCount, Daniel Weingarten, Nan Hu, Sean E. Shaheen, Jao van de Lagemaat, Garry Rumbles, David M. Walba, Mark T. Lusk, "Energy pooling upconversion in organic molecular systems", *J. Phys. Chem. A*, **2015**, 119, 4009, doi:10.1021/acs.jpca.5b00509

14. Yixin Zhao, Nicholas C. Anderson, Kai Zhu, Jeffrey A. Aguiar, Jason A. Seabold, Jao van de Lagemaat, Howard M. Branz, Nathan R. Neale, J. Oh, "Oxidatively stable nanoporous silicon photocathodes with enhanced onset voltage for photoelectrochemical proton reduction", *Nanolett.* **2015**, 15, 2517, doi:10.1021/acs.nanolett.5b00086

15. Paul J. Ackerman, Jao van de Lagemaat, Ivan I. Smalyukh, "Self-assembly and electrostriction of arrays and chains of hopfion particles in chiral liquid crystals", *Nature Comm.* **2015**, 6, 6012, doi:10.1038/ncomms7012

16. Taiyang Zhang, Mengjin Yang, Eric E. Benson, Zijian Li, Jao van de Lagemaat, Joseph M. Luther, Yanfa Yan, Kai Zhu, Yixin Zhao, "A facile solvothermal growth of single crystal mixed halide perovskite $CH_3NH_3Pb(Br_{1-x}Cl_x)_3$", *Chem. Comm.* **2015**, 51, 7820, doi:10.1039/C5CC01835H

Artificial Photosynthesis: From Rational Catalyst Design to Solar Fuels Generation

Yan Xie, Lei Wang, David W. Shaffer, David J. Szalda, Javier J. Concepcion
Chemistry Division
Brookhaven National Laboratory
Upton, NY 11973

The generation of solar fuels *via* artificial photosynthesis is a sustainable approach to address many of the challenges of our energy present and future. It requires the development of integrated systems that combine many features including light absorption, charge separation, water oxidation and water/CO_2 reduction catalysis. Local and bulk proton management, in combination with product separation, are also key requirements for efficient and safe operation. We will discuss our progress towards these efforts with a major focus on oxidative and reductive catalysis. On the oxidation side, we will present a new family of single-site water oxidation catalysts that outperforms all previously reported molecular catalysts at low pH. This is the result of careful catalyst design to enhance fundamental aspects in the water oxidation mechanism, from catalyst activation to the key O-O bond formation and O_2 evolution steps. Our catalysts are "hybrid" systems that combine important features from bda-based catalysts and multifunctional bpa-catalysts, Figure 1. The carboxylate group from the bda systems allows water coordination at the Ru(III) state, Figure 2, and enables intramolecular proton-coupled electron transfer (*i*-PCET). The multifunctional phosphonate group from the bpa systems facilitates O-O bond formation by significantly lowering the activation energy for this step *via* intramolecular atom-proton transfer (*i*-APT). In addition, the phosphonate group also provides low energy pathways for oxidative activation steps and oxidation steps preceding O_2 evolution *via* *i*-PCET.

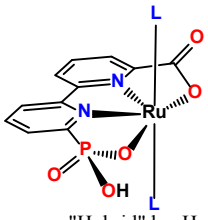

Figure 1. "Hybrid" bpcH catalysts.

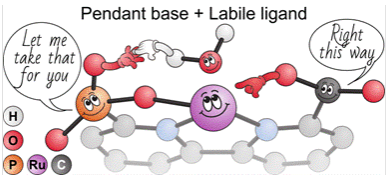

Figure 2. bda side allows *i*-PCET; bpa side allows *i*-APT.

On the reductive site, we will present a family of catalysts that selectively reduce CO_2 to formate in aqueous solution at the lowest overpotential reported to date for this reaction. CO_2 reduction to formate usually involves prior formation of a metal hydride M-H followed by hydride transfer to CO_2 or hydride insertion into the M-H bond. Pathways involving CO_2 binding to the metal center often lead to CO as the reduction product. We will present a new mechanism based on a combination of experimental results and DFT calculations where CO_2 binding to the metal results in exclusive formation of formate. This mechanism operates under two regimes: a kinetically slow, low overpotential regime and a faster one with higher overpotential. The lower overpotential regime is limited by a

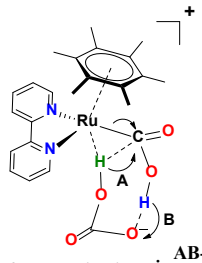

Figure 3. Isomerization *via* AB-PCET_I

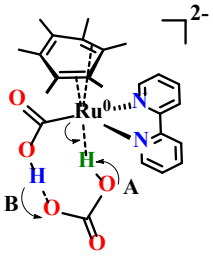

Figure 4. Hydride formation *via* AB-PCET_II

chemical step where a metallocarboxilic acid undergoes and acid-base proton-coupled electron transfer (AB-PCET) isomerization to a metal-formate adduct stabilized by a M---$HCOO^-$ agostic interaction, Figure 3. The higher overpotential mechanism is limited by an electron transfer step involving further reduction of the metallocarboxilic acid intermediate. This ET step leads to an η^6-η^4 ring slippage, followed by another AB-PCET step that generates an unprecedented metallocarboxylate hydride intermediate (H-M-CO_2, Figure 4). From the latter, intramolecular hydride transfer (*i*-HT) takes place to generate formate, Figure 5.

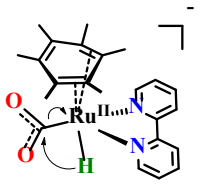

Figure 5. Intramolecular hydride trasnfer (*i*-HT)

We will also present an update in photochemical water oxidation as well as our most recent developments in Dye Sensitized Photoelectrochemical Cells (DSPECs) to carry out artificial photosynthesis and split water into O_2 and H_2 using sunlight.

DOE Sponsored Publications 2015-2018

1. "O−O Radical Coupling: From Detailed Mechanistic Understanding to Enhanced Water Oxidation Catalysis", Xie, Y.; Shaffer, D. W.; Concepcion, J. J. *Inorg. Chem.* **2018**, Accepted, ACS Editor's Choice Article.
2. "Improved Stability and Performance of Visible Photoelectrochemical Water Splitting on Solution-Processed Organic Semiconductor Thin Films by Ultrathin Metal Oxide Passivation", Wang, L.; Yan, D.; Shaffer, D. W.; Ye, X.; Layne, B. H.; Concepcion, J. J.; Liu, M.; Nam, C.-Y. *Chem. Mater.* **2018**, *30*, 324.
3. "Light-Driven Water Splitting by a Covalently Linked Ruthenium-Based Chromophore-Catalyst Assembly", Sherman, B. D.; Xie, Y.; Sheridan, M. V.; Wang, D.; Shaffer, D. W.; Meyer, T. J.; Concepcion, J. J. *ACS Energy Lett.* **2017**, *2*, 124.
4. "Lability and Basicity of Bipyridine-Carboxylate-Phosphonate Ligand Accelerate Single-Site Water Oxidation by Ruthenium-Based Molecular Catalysts", Shaffer, D. W.; Xie, Y.; Szalda, D. J.; Concepcion, J. J. *J. Am. Chem. Soc.* **2017**, *139*, 15347.
5. "O-O bond formation in ruthenium-catalyzed water oxidation: single-site nucleophilic attack vs. O-O radical coupling", Shaffer, D. W.; Xie, Y.; Concepcion, J. J. *Chem. Soc. Rev.* **2017**, *46*, 6170.
6. "Water Oxidation by Ruthenium Complexes Incorporating Multifunctional Bipyridyl Diphosphonate Ligands", Xie, Y.; Shaffer, D. W.; Lewandowska-Andralojc, A.; Szalda, D. J.; Concepcion, J. J. *Angew. Chem., Int. Ed.* **2016**, *55*, 8067.
7. "Manipulating the Rate-Limiting Step in Water Oxidation Catalysis by Ruthenium Bipyridine-Dicarboxylate Complexes", Shaffer, D. W.; Xie, Y.; Szalda, D. J.; Concepcion, J. J. *Inorg. Chem.* **2016**, *55*, 12024.
8. "Proton-Coupled Electron Transfer in a Strongly Coupled Photosystem II-Inspired Chromophore-Imidazole-Phenol Complex: Stepwise Oxidation and Concerted Reduction", Manbeck, G. F.; Fujita, E.; Concepcion, J. J. *J. Am. Chem. Soc.* **2016**, *138*, 11536.
9. "Mechanism of water oxidation by [Ru(bda)(L)2]: the return of the "blue dimer"", Concepcion, J. J.; Zhong, D. K.; Szalda, D. J.; Muckerman, J. T.; Fujita, E. *Chem. Commun.* **2015**, *51*, 4105.

The Design and Synthesis of Polypyridine Metal Complexes as Catalysts for the Decomposition of Water into its Elements

Ruifa Zong, Nattawut Kaveevivitchai, Debashis Basu, Lianpeng Tong, Husain Kagalwala, Liubov, Lifshits, Lanka Wickramasinghe, Elamparuthi Ramasamy, and Randolph Thummel
Department of Chemistry
University of Houston
Houston, Texas 77204-5003

The main goal of this project continues to be the development of a homogeneous catalyst for the photochemical (solar) decomposition of water into its elements. Early work established that certain mononuclear Ru^{II} polypyridine complexes could function as quite effective water oxidation catalysts. The dpp complex **1** was particularly interesting because it seemed likely that a water molecule would attack the oxidized metal center in the equatorial plane to create a seven-coordinate species. We found that smaller first row transition metals preferred to bind tridentate, leaving a peripheral pyridine unbound as evidenced by X-ray and NMR analysis of the Zn-dpp complex **2**. To provide a more square planar tetradentate environment we incorporated an additional sp^2 center into the quaterpyridine backbone, creating the ppq ligand **3**. We found that **3** formed a well organized tetradentate complex with Co^{II} and this material was an excellent water reduction catalyst, using $[Ru(bpy)_3]Cl_2$ as a photosensitizer and ascorbic acid as a sacrificial electron donor. Treatment of ppq with $FeCl_3$ led to the formation of an oxo-bridged dimer **5** that, in the presence of Ce^{IV} as a sacrificial electron acceptor, proved to be a potent water oxidation catalyst.

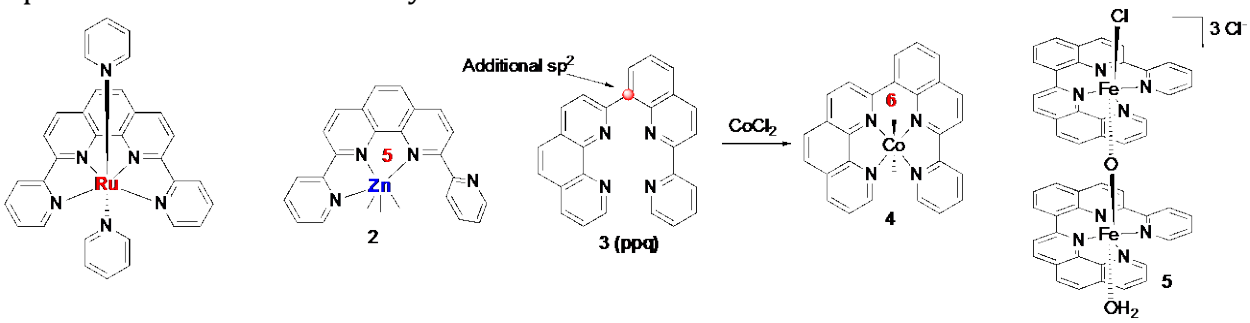

We prepared a series of tetradentate ligands closely related to ppq, all of which formed Fe^{III} complexes similar to **5**. The degree of interaction between the Fe centers was quite sensitive to the structure of the ligand. The complexation of diquinolinyl pyridine **6** (dqp)

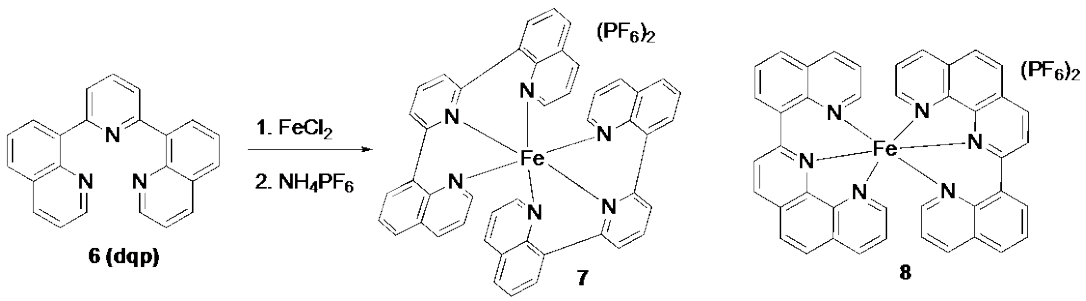

with $FeCl_2$ led to the diamagnetic complex $[Fe(dqp)_2]^{2+}$ **7** where the formation of 6-membered chelate rings and π-overlap between the two ligands enforced a well organized octahedral geometry around Fe^{II}. A closely related complex of quin-phen (**8**) was also prepared but both systems showed very short excited state lifetimes rendering them less useful for photoredox catalysis.

We prepared a series of ligands **9-11** that were isomers of ppq in which the connectivity between the pyridine, quinoline, and 1,10-phenanthroline moieties was varied.

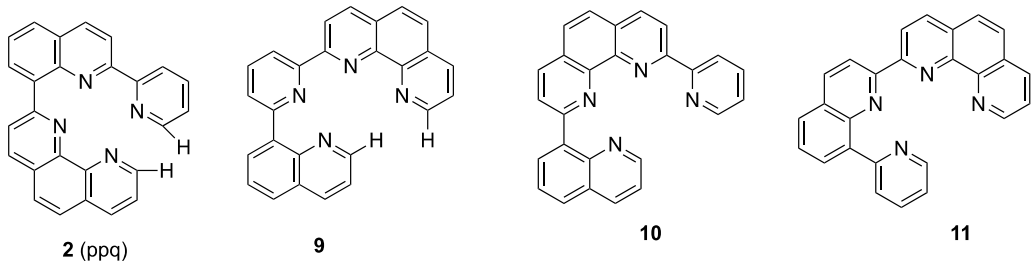

With regard to chelate ring size, **2** is a 5-6-5 system while **9-11** are 6-5-5. Thus **2** has a more square planar arrangement of the four pyridine rings and **9-11** have a slightly skewed tetradentate geometry. Complexation studies with these systems pointed towards metal complexes of **2** often being the most active, leading us to consider closing the macrocyclic ring of **2** to create a cyclotetrapyridine whose core structure can be represented by

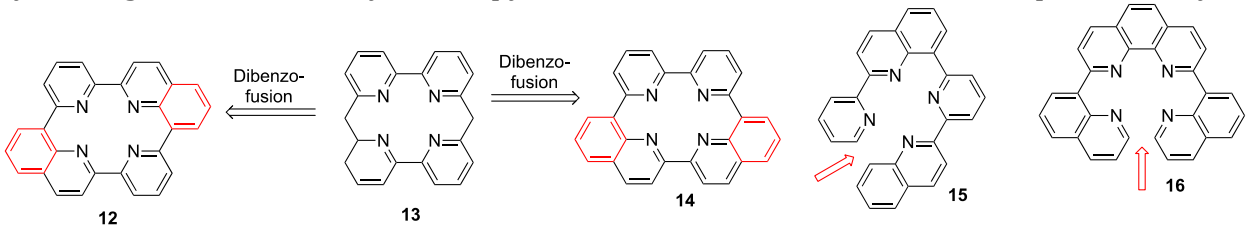

13. To produce a fully conjugated π-system we will need to fuse two benzo-rings to the core structure as represented by either **12** or **14**. We have prepared **15** which is a dimer of 2,2'-pyridylquinoline and also the diquinolinylphenanthroline **16** which is related to dqp described above. Closing the final bond has proved a challenge due to the demand of forcing four nitrogen lone pairs to point towards one another. We have examined a simpler system **18** that would also present the square planar tetradentate binding cavity found in **13**. The cyclo-self-condensation of **17** might be expected to provide **18** but the free base could not be detected either under acid or base conditions. In this case we can overcome the lone pair repulsion effect by using a metal ion as a template. Thus in the presence of $ZnCl_2$ **17** will form the complex **19** as evidenced both by NMR and MS. Other metal ions (Co^{II} or Fe^{III}) can be used to prepare complexes that may show activity as catalysts for water splitting.

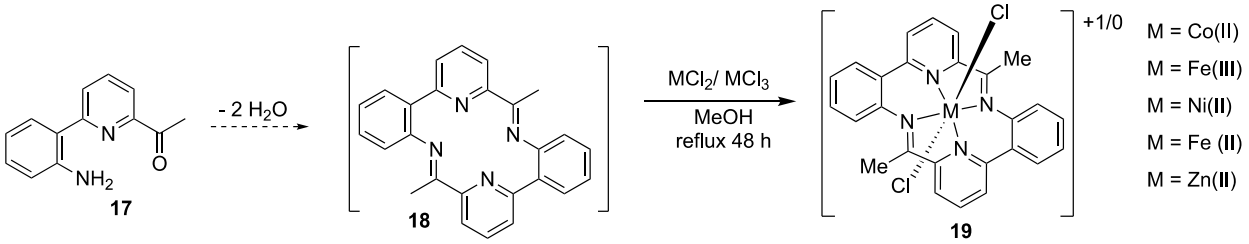

DOE Sponsored Publications 2015-2018

1. "Solvent-induced Changes in Photophysics and Photostability of Indole-naphthyridines," Golec, B.; Kijak, M.; Vetokhina, V.; Gorski, A.; Thummel, R.; Herbich, J.; Waluk, J. *J. Phys. Chem. B* **2015**, *119,* 7283-7293.

2. "Ruthenium Catalysts for Water Oxidation Involving Tetradentate Polypyridine-type Ligands," Tong, L.; Zong, R.; Zhou, R.; Kaveevivitchai, N.; Zhang, G.; Thummel, R. P. *Faraday Discussions*, **2015**, *185,* 87-104.

3. "Light-driven Proton Reduction in Aqueous Medium Catalyzed by a Family of Cobalt Complexes with Tetradentate Polypyridine-type Ligands," Tong, L.; Kopecky, A.; Zong, R.; Gagnon, K. J.; Ahlquist, M. S. G.; Thummel, R. P. *Inorganic Chemistry,* **2015**, *54,* 7873-7884.

4. "Iron Complexes of Square Planar Tetradentate Polypyridyl-type Ligands as Catalysts for Water Oxidation," Wickramasinghe, L. D.; Zhou, R.; Zong, R.; Vo, P.; Gagnon, K.; Thummel, R. P. *J. Am. Chem. Soc.* **2015**, *137,* 13260-132.

5. "Electronic Influences of Bridging and Chelating Diimine Ligand Coordination in Formamidinate- bridged Rh_2(II,II) Dimers," White, T. A.; Dunbar, K. R.; Thummel, R. P.; Turro, C. *Polyhedron* **2016**, *103,* 172-177.

6. "New Ru^{II} Complex for Dual Activity: Photoinduced Ligand Release and $^1O_2$ Production," Loftus, L. M.; White, J, K.; Albani, B. A.; Kohler, L.; Kodanko, J. J.; Thummel, R. P.; Dunbar, K. R.; Turro, C. *Chemistry – A European Journal,* **2016** *22,* 3704–3708.

7. "Mononuclear Ruthenium Polypyridine Complexes that Catalyze Water Oxidation," Tong, L.; Thummel, R. P. *Chemical Science,* **2016**, *7,* 6591-6603.

8. "Uncovering the Role of Oxygen Atom Transfer in Ru-based Catalytic Water Oxidation," Moonshiram, D.; Pineda-Galvan, Y. : Erdman, D.; Palenik, M.; Zong, R.; Thummel, R. P.; Pushkar, Y. *J. Am. Chem. Soc.* **2016**, *138,* 15605-15616.

9. "The synthesis, photophysical properties and water oxidation studies of a series of novel photosensitizer– catalyst assemblies," Nair, N. V.; Zhou, R.; Thummel, R. P. *Inorg. Chim. Acta* **2017**, *454,* 27-39.

10. "Evidence for Oxidative Decay of a Ru-Bound Ligand During Catalyzed Water Oxidation," Kagalwala, H.; Tong, L.; Zong, R.; Kohler, L.; Ahlquist, M. S. G.; Fan, T.; Gagnon, K. J.; Thummel, R. P. *ACS Catalysis* **2017**, *7,* 2606-2615.

11. "A ruthenium water oxidation catalyst containing a bipyridine glycoluril ligand," Mane, V. S.; Kumbhar, A. S.; Thummel, R. P. *Dalton Trans.* **2017**, *46***,** 12901-12907.

12. “Photochemical and Photobiological Activity of Ru(II) Homoleptic and Heteroleptic Complexes Containing Methylated Bipyridyl-type Ligands,” Kohler, L.; Nease, L.; Vo, P.; Garafolo, J.; Heidary, D. K.; Thummel, R. P.; Glazer, E. C. *Inorg. Chem.* **2017**, *56*, 12214-12223.

13. "Chemical evolution of the 7-coordinate Ru=O species in water oxidation catalysis," Pineda-Galvan, Y.; Karbakhsh Ravari, A.; Shmakov, S.; Lifshits, L.; Kaveevivitchai, N. ; Thummel, R.; Pushkar, Y. *ACS Catalysis* (submitted).

14. “Metal Ion Size-Based Selectivity effects for 5- and 6-membered Chelate Rings. A Fluorescence, Crystallographic, and Thermodynamic Study,” Triplett, T. N.; Gaver, Jr., C. R.; Brenneman, A. L.; Balance, D. G.; Zong, R.; Reibenspies, J. H.; Thummel, R. P.; and Robert D. Hancock, *Dalton Trans.* (submitted).

Measuring and increasing water oxidation catalyst viability

Douglas B. Grotjahn, Diane K. Smith, Dale A. Chatfield, Jayneil M. Kamdar, David C. Marelius, Thomas Chi Cao, Aaron G. Nash, Sima Yazdani
Department of Chemistry and Biochemistry
San Diego State University
San Diego, CA 92182-1030

The overall goal of our work is to increase the effectiveness of molecular water oxidation catalysts (WOC). One criticism of using carbon-containing ligands is that ligand carbon or carbons can be oxidized during water oxidation, either leading to new, unknown catalytically active complexes, or to metal oxide materials. Considering catalysis as a race between a desired process (here, water oxidation) and any undesired ones (e.g., ligand oxidation), one may win the race by increasing the rate of desired catalysis of water oxidation, and / or slowing the rate of undesired catalyst degradation. Most WOC research focuses on making faster catalysts. While we also have faster catalysts in mind, our project has two major objectives:

(1) slowing the rate of undesired catalyst degradation by exploring new catalysts designed to be more robust, and

(2) developing, benchmarking and applying new tools and methods for measuring catalyst viability, that we expect will become useful for other researchers concerned about WOC viability.

For WOC testing, using sacrificial oxidants and measuring oxygen formation is operationally easy, but there are limitations with respect to available oxidation potential and pH that we want to overcome. We are applying both sacrificial oxidant and electrochemical approaches (RRDE, CV, controlled potential electrolysis, spectroelectrochemistry) to WOC testing. We seek to use cost-effective GC and MS equipment to monitor formation not only of O_2, but more importantly for this project, CO_2 that may be a product of ligand degradation. Carboxylates are frequently used as part of the WOC ligand sphere, yet as far as we are aware, no one has evaluated rigorously whether decarboxylation occurs in the WOC context; in contrast, decarboxylations are well known in organic chemistry (e.g. Kolbe electrolysis, and modern uses of organic carboxylates as precursors for catalytic intermediates that have metal-carbon bonds).

Objective 1, Slowing the rate of catalyst degradation will be pursued using one or more of the following strategies:

(1A) use chelating ligands to reduce the chance of ligand loss,
(1B) replace carboxylates with other anionic groups,
(**1C**) create ligands that predominantly use oxygen atoms in the first coordination sphere, rather than more readily oxidizable nitrogens,
(1D) reduce the number of C-C and C-N pi bonds in the ligand framework, or shield them,
(1E) substitute susceptible C-H bonds on the ligand periphery, e.g. with C-F or C-CF_3 bonds.

Objective 2, Tools and methods for measuring catalyst viability include the following strategies:

(2A) We will compare HPLC analyses, UV-vis spectra and / or CV data before and after periods

of controlled potential electrolysis at oxidizing potentials; the utility of this approach is that we can observe the survival and evolution of catalyst (if any) as a function of the number of turnovers;

(2B) We will use ***in situ*** **ESI-MS analysis of reaction mixtures** either as a continuous microscopic flow or as aliquots, looking for catalyst speciation over time. These techniques applied to *electrochemical* reactions appear to be novel in WOC context. When using *sacrificial oxidants*, ESI-MS has been used occasionally in the WOC field, for example for pyridyl ruthenium species by groups of Berlinguette, Muckerman/Fujita/Thummel, and Akermark, and for Cp*Ir catalysts by us and others; evidence was obtained for intermediates, particularly M=O species, but also for metal complexes in which the original ligands had been partially or largely transformed. In our lab, on two diastereomeric polypyridyl Ru WOC with CAN as the oxidant, we have obtained evidence using ESI-MS for the surprising formation of an oxidized intermediate from only one diastereomer and not the other, better-performing catalyst isomer.

(2C) Trace gas analysis by GC-MS or GC of WOC reaction *headspace* over time for the presence of traces of CO_2 or other small-molecule gases besides product O_2, is not new, but at best it is done rarely, not routinely, not in a quantitative fashion, and to our knowledge only when the pH of the mixture is low (e.g., near pH 1 in ceric ammonium nitrate), conditions where CO_2 can escape the liquid where it is formed. What about WOC reactions conducted under more alkaline conditions, where CO_2 rapidly becomes bicarbonate/carbonate, hence would be invisible during headspace analysis? As far as we are aware, we have little or no idea how much dissolved CO_2 / (bi)carbonate forms in WOC reactions at near-neutral or alkaline pH. The challenges we will address in the project period will be described.

In separate parallel studies, **analysis of isotopically labelled CO_2 by GC-MS** will be relevant for rigorous evaluation of the stability of the metal-carboxylate moiety in WOC. The need for isotopically labelled carboxylates to lower the CO_2 detection limit will be described in this talk, as will our progress in making labelled water oxidation catalysts for study.

DOE Sponsored Publications

1. Kamdar, J. M.; Aspacio, D. S.; Boisaubert, P.; Spire, M. T.; Marelius, D.M.; Golen, J.; Moore, C. E.; Rheingold, A. L.; Smith, D. K.; Grotjahn, D.B. “Synthesis, characterization, and water oxidation reactivity of ruthenium complexes bearing 2,2’-bipyridine-6,6’-dipyrazolato and 6,6'-imidazolato ligands,” in preparation.

2. Rajor, H.; Kamdar, J. M.; Moore, C. E.; Rheingold, A. L.; Smith, D. K.; Grotjahn, D. B. "Improving the hydrolytic stability of water oxidation catalysts bearing 2,2'-bipyridine-6,6'-diphosphonate esters by increasing steric bulk on the phosphorus atom", in preparation.

3. Saeedifard, F.; Cao, T. C.; Kamdar, J. M.; Smith, D. K.; Moore, C. E.; Rheingold, A. L.; Grotjahn, D. B. “Increasing ligand denticity for water oxidation catalysts using P(V) as a connecting element,” in preparation.

From the Fundamental Radiation Chemistry of Acetonitrile to Mechanistic Pulse Radiolysis Studies of CO_2 Reduction Catalysts

David C. Grills, Mehmed Z. Ertem, Sergei V. Lymar, Dmitry E. Polyansky, and Etsuko Fujita
Chemistry Division
Brookhaven National Laboratory
Upton, NY 11973-5000

Our research seeks a fundamental understanding of the processes involved in the capture and chemical conversion of solar energy, often using transition metal complexes as catalysts. Since these processes can involve multiple redox states, many of which are transient in nature, pulse radiolysis (PR) is a powerful method for their rapid production and subsequent interrogation by time-resolved spectroscopic methods.[4] While UV-vis transient absorption (TA) is an important technique for monitoring radiolytically-generated intermediates, we have developed a nanosecond time-resolved infrared (TRIR) detection capability for PR.[12] PR-TRIR targets improved characterization to gain a better mechanistic understanding of energy-related processes, which is crucial for developing more efficient solar energy conversion.

We are applying PR-TRIR to a diverse range of systems, including fundamental studies of the radiation chemistry of non-aqueous solvents,[2] and the investigation of other physical processes that underpin energy conversion, such as ion pairing[8,13] and charge delocalization.[6,11] In addition to these fundamental investigations, we are using PR-TRIR to characterize specific intermediates involved in artificial photosynthetic processes, such as metal-hydrides[4] and metal-CO_2 adducts, and to reveal mechanistic details of CO_2 reduction,[1,4,5,12] not only in organic solvents but also in aqueous solution.

Fundamental Radiation Chemistry of Acetonitrile

Radiolytic Formation of the Carbon Dioxide Radical Anion in Acetonitrile: The carbon dioxide radical anion ($CO_2^{\bullet-}$) is often used as a versatile reductant ($E°(CO_2/CO_2^{\bullet-})$ = –1.90 V vs SHE) for mechanistic pulse radiolysis studies in water, where $CO_2^{\bullet-}$ can be generated through both the reduction of dissolved CO_2 by the solvated electrons (e_s^-), and the oxidation of added formate ion (HCO_2^-) via H-atom transfer scavenging of the radiolytically-generated radicals, $OH^\bullet$ and $H^\bullet$. While water is a heavily-used solvent, a large number of energy-related catalytic processes, e.g., CO_2 reduction, are carried out in organic solvents such as CH_3CN. Unfortunately, the fundamental radiation chemistry of CH_3CN and the radiolytic production of $CO_2^{\bullet-}$ in this solvent are not well understood, limiting its use as a medium for pulse radiolysis. The properties and reactivity of $CO_2^{\bullet-}$ in CH_3CN are also of importance for understanding electrochemical CO_2 reduction in polar aprotic solvents. In this work, we have used PR-TRIR to unambiguously identify $CO_2^{\bullet-}$ in CH_3CN by its antisymmetric stretch at 1650 cm^{-1} following the reduction of CO_2 by e_s^- (Fig. 1).[2] In neat CH_3CN, $CO_2^{\bullet-}$ decays on a ~10 μs time scale via recombination with solvent-derived radicals ($R^\bullet$) and solvated protons. Upon addition of HCO_2^-, the radiation yield of $CO_2^{\bullet-}$ is substantially increased by H-atom transfer from HCO_2^- to $R^\bullet$ ($R^\bullet$ +

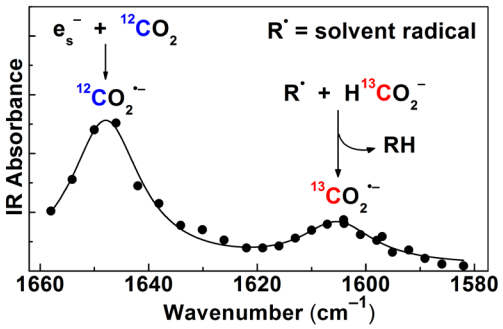

Fig. 1: TRIR spectrum recorded 60 ns after PR of CD_3CN containing 28 mM $^{12}CO_2$ and 50 mM $H^{13}CO_2^-$.[2]

$HCO_2^- \rightarrow RH + CO_2^{\bullet-}$), which occurs in two kinetically separated steps due to the different H-atom abstracting abilities of the various $R^\bullet$ (Fig. 1 shows initial step with isotopically-labeled $H^{13}CO_2^-$). The removal of solvent radicals by HCO_2^- also results in over a hundredfold increase in the $CO_2^{\bullet-}$ lifetime. $CO_2^{\bullet-}$ scavenging experiments suggest that at 50 mM HCO_2^-, ~60% of the solvent-derived radicals are engaged in $CO_2^{\bullet-}$ generation. These studies open up the possibility of CH_3CN becoming a standard solvent for pulse radiolysis, and work is currently under way to identify alternative radical scavengers that will further enhance the yield of reducing species from $R^\bullet$, and also allow the production of oxidants for the investigation of oxidative processes.

Mechanistic Pulse Radiolysis Investigations of CO_2 Reduction Catalysts

Accessing the Two-Electron Reduced, Catalytically Active Form of Group 7 CO_2 Reduction Catalysts by Pulse Radiolysis: In previous PR-TRIR work on the electrochemical CO_2 reduction precatalyst, Mn(^{t}Bu$_2$-bpy)(CO)$_3$(HCO$_2$) (^{t}Bu$_2$-bpy = 4,4′-^{t}Bu$_2$-2,2′-bipyridine), we identified all intermediates and monitored the kinetics of Mn-radical dimerization to [Mn(^{t}Bu$_2$-bpy)(CO)$_3$]$_2$, following one-electron reduction of the precatalyst by PR and ejection of HCO_2^-. More recently, we introduced bulky, methoxy-substituted groups at the 6,6′-positions of the bpy ligand in [*fac*-Mn({(MeO)$_2$Ph}$_2$bpy)(CO)$_3$(CH$_3$CN)](OTf).[5] Not only did these groups prevent **Mn**–**Mn** dimerization, but hydrogen-bonding interactions between the MeO substituents and certain Brønsted acids, e.g., phenol, provided access to the so-called *protonation-first* CO_2 reduction pathway, saving up to 0.55 V in overpotential compared to the conventional *reduction-first* pathway.[5] This family of catalysts offers promise as a cheaper alternative to their heavily-investigated Re-based counterparts, warranting mechanistic PR investigations deeper into the catalytic cycle. However, PR generally only produces one-electron redox species. To access the two-electron reduced, catalytically active species, **Mn**$^-$, we are developing strategies that involve either (i) the synthesis of **Mn**–**Mn** dimers, in which the Mn centers are already in a reduced oxidation state (**Mn**^{0}), such that one-electron reduction of the dimer by PR yields one equivalent of **Mn**$^-$, or (ii) the use of bulky groups in the 6,6′-positions of the bpy ligand that prevent dimerization of the one-electron reduced species, allowing disproportionation to occur to yield one equivalent of **Mn**$^-$ (e.g., Fig. 2 where bulky mesityl groups were used).[1] In the future, we will perform PR-TRIR investigations on these systems in the presence of CO_2 and Brønsted acids to understand mechanistic pathways and the role of second coordination sphere interactions.

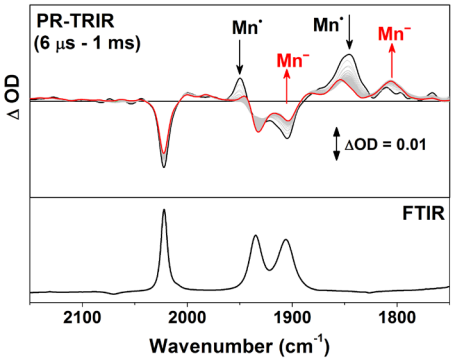

Fig. 2: Lower panel: FTIR spectrum of Mn(mes$_2$-bpy)(CO)$_3$(HCO$_2$) (mes = mesityl) in argon-saturated CH_3CN in the presence of 50 mM HCO_2^-. Top panel: Step-scan FTIR spectra recorded between 6 μs and 1 ms after PR of this solution. **Mn**$^\bullet$ = Mn(mes$_2$-bpy)(CO)$_3$, and **Mn**$^-$ = [Mn(mes$_2$-bpy)(CO)$_3$]$^-$.[1]

Unravelling the Mechanism of CO_2 Reduction by Co Macrocycles: Another class of catalysts for CO_2 reduction that we are investigating are the cobalt macrocycles, such as Co^{II}(HMD)$^{2+}$ (HMD = 5,7,7,12,14,14-hexamethyl-1,4,8,11-tetraazacyclotetradeca-4,11-diene). PR-TRIR of the chemically-prepared CO_2 adduct, Co(HMD)(CO$_2$)$^+$, has allowed us to identify a previously unknown reaction pathway in the catalytic cycle upon one-electron reduction, resulting in the production of the CO complex, Co^I(HMD)(CO)$^+$.

DOE Sponsored Publications 2015-2018

1. "Mechanistic Aspects of CO_2 Reduction Catalysis with Manganese-Based Molecular Catalysts" Grills, D. C.; Ertem, M. Z.; McKinnon, M.; Ngo, K. T.; Rochford, J. *Coord. Chem. Rev.* **2018**, under revision.
2. "Radiolytic Formation of the Carbon Dioxide Radical Anion in Acetonitrile Revealed by Transient IR Spectroscopy" Grills, D. C.; Lymar, S. V. *Phys. Chem. Chem. Phys.* **2018**, Advance Article. DOI: 10.1039/C8CP00977E
3. "Investigation of Excited State, Reductive Quenching, and Intramolecular Electron Transfer of Ru(II)-Re(I) Supramolecular Photocatalysts for CO_2 Reduction Using Time-Resolved IR Measurements" Koike, K.; Grills, D. C.; Tamaki, Y.; Fujita, E.; Okubo, K.; Yamazaki, Y.; Saigo, M.; Mukuta, T.; Onda, K.; Ishitani, O. *Chem. Sci.* **2018**, *9*, 2961-2974.
4. "Application of Pulse Radiolysis to Mechanistic Investigations of Catalysis Relevant to Artificial Photosynthesis" Grills, D. C.; Polyansky, D. E.; Fujita, E. *ChemSusChem* **2017**, *10*, 4359-4373.
5. "Turning on the Protonation-First Pathway for Electrocatalytic CO_2 Reduction by Manganese Bipyridyl Tricarbonyl Complexes" Ngo, K. T.; McKinnon, M.; Mahanti, B.; Narayanan, R.; Grills, D. C.; Ertem, M. Z.; Rochford, J. *J. Am. Chem. Soc.* **2017**, *139*, 2604-2618.
6. "Probing Intermolecular Electron Delocalization in Dimer Radical Anions by Vibrational Spectroscopy" Mani, T.; Grills, D. C. *J. Phys. Chem. B* **2017**, *121*, 7327-7335.
7. "Experimental Insight into the Thermodynamics of the Dissolution of Electrolytes in Room-Temperature Ionic Liquids: From the Mass Action Law to the Absolute Standard Chemical Potential of a Proton" Matsubara, Y.; Grills, D. C.; Koide, Y. *ACS Omega* **2016**, *1*, 1393-1411.
8. "Identification of Ion-Pair Structures in Solution by Vibrational Stark Effects" Hack, J.; Grills, D. C.; Miller, J. R.; Mani, T. *J. Phys. Chem. B* **2016**, *120*, 1149-1157.
9. "Electrocatalytic Reduction of Carbon Dioxide with a Well-Defined PN^3-Ru Pincer Complex" Min, S.; Rasul, S.; Li, H.; Grills, D. C.; Takanabe, K.; Li, L.-J.; Huang, K.-W. *ChemPlusChem* **2016**, *81*, 166-171.
10. "Thermodynamic Aspects of Electrocatalytic CO_2 Reduction in Acetonitrile and with an Ionic Liquid as Solvent or Electrolyte" Matsubara, Y.; Grills, D. C.; Kuwahara, Y. *ACS Catal.* **2015**, *5*, 6440-6452.
11. "Electron Localization of Anions Probed by Nitrile Vibrations" Mani, T.; Grills, D. C.; Newton, M. D.; Miller, J. R. *J. Am. Chem. Soc.* **2015**, *137*, 10979-10991.
12. "Development of Nanosecond Time-Resolved Infrared Detection at the LEAF Pulse Radiolysis Facility" Grills, D. C.; Farrington, J. A.; Layne, B. H.; Preses, J. M.; Bernstein, H. J.; Wishart, J. F. *Rev. Sci. Instrum.* **2015**, *86*, 044102.
13. "Vibrational Stark Effects to Identify Ion Pairing and Determine Reduction Potentials in Electrolyte-Free Environments" Mani, T.; Grills, D. C.; Miller, J. R. *J. Am. Chem. Soc.* **2015**, *137*, 1136-1140.

Photosynthetic Systems for Solar Fuel Production:
A Combined Study of Molecular Catalysts by Advanced EPR and DFT Modeling

Oleg G. Poluektov, Jens Niklas, Karen L. Mulfort, Lisa M. Utschig, and David M. Tiede
Chemical Sciences and Engineering Division, Argonne National Laboratory
Argonne, IL 60439
Kristy L. Mardis
Department of Chemistry & Physics, Chicago State University
Chicago, IL 60628

Overall research goals: Current research in our group aims to reveal fundamental mechanisms for solar-to-chemical energy conversion which consists of capture, conversion, and storage of solar energy in high-energy molecular bonds. Specifically our research is focused on: (1) photoinduced charge separation in artificial photosynthetic systems and at photo-active organic interfaces, (2) mechanisms of PCET in these systems, and (3) structure-function relationships in molecular catalysts for proton reduction and water oxidation. To this end, we are applying a combination of in-house novel design and synthesis, advanced EPR characterization, and DFT modeling to elucidate fundamentals which are crucial for understanding the inherent mechanisms for coupling captured photons to fuel generation (Fig.1).

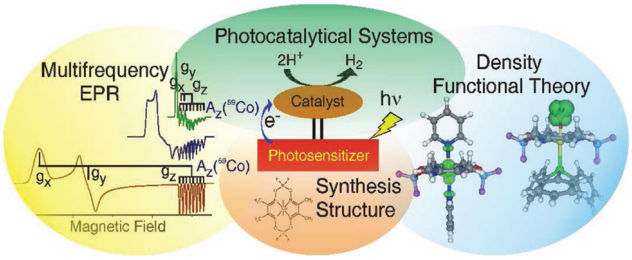

Figure 1. Our research approach combines Synthesis/Design, Advanced EPR, and DFT modeling.

Significant achievements 2015-2018: *Photoinduced charge separation and ET dynamics.*[6,7,9,11,16,20] While EPR spectroscopy has nanosecond or lower time-resolution, the light-induced electron spin-polarization pattern is sensitive to the dynamics of primary charge separation (chemically-induced dynamic electron polarization, CIDEP) which allows ET characterization down to the picosecond scale. Slower ET dynamics can be acquired by analysis of the spin-correlated radical pair spectral transformations and direct detection of the kinetics and pathways by more conventional EPR techniques. Recently, we have applied these techniques to clarify the mechanisms and dynamics of photoinduced charge separation and recombination in model/artificial photosynthetic systems as well as in OPV photoactive layers/films.

Molecular catalysts for proton reduction.[1-3,5,8,12,14,15,19,21-23] One key element of solar-to-fuel conversion systems is the catalyst. Both cobaloximes and Ni-bis(diphosphine) complexes are among the best molecular transition metal complexes for the reduction of protons to molecular hydrogen. The efficiency of the catalyst, a key issue for molecular catalysts, is determined to a large extent by its electronic structure. The electronic structure, in turn, is strongly influenced by its surroundings; in particular, the ligand(s) directly bound to the central metal ion as well as hydrogen bonding to ligand atoms and dielectric properties of the medium. To examine the electronic structure of cobaloxime and Ni-bis(diphosphine) molecules and establish correlations between structure and surroundings with catalytic activity we have used multi-frequency EPR/ENDOR spectroscopy at X-band (9 GHz), Q-band (34 GHz), and D-band (130 GHz) combined with X-ray crystallography and DFT calculations.

To assess the strength and nature of ligand cobalt interactions, the BF_2-capped cobaloxime, $Co(dmgBF_2)_2$, was studied in a variety of solvents and solvent mixtures with a range of polarities and stoichiometric amounts of potential ligands to the cobalt ion. This allows the differentiation of labile and strongly coordinating axial ligands for the Co(II) complex. We observed that labile, or weakly coordinating, ligands such as methanol result in larger g-tensor anisotropy than strongly coordinating ligands such as pyridine. In addition, a coordination number effect was seen for the strongly coordinating ligands with both singly ligated $LCo(dmgBF_2)_2$ and doubly ligated $L_2Co(dmgBF_2)_2$. We find that the strength of the axial ligand(s) is directly related to the catalytic proton reduction efficiency of cobaloximes. These experimental results are compared with a comprehensive set of DFT calculations on $Co(dmgBF_2)_2$ model systems with various axial ligands. DFT modeling demonstrates that experimental values for the "key" magnetic parameters, such as g-tensor and ^{59}Co hyperfine coupling tensor, allow identification of the conformation of the axially ligated $Co(dmgBF_2)_2$ complexes as well as its environment. We constructed correlation plots which make it possible to identify ligands, and molecular environment of cobaloxime in catalytically active solar energy conversion systems even without time-consuming DFT analysis (Fig.2).

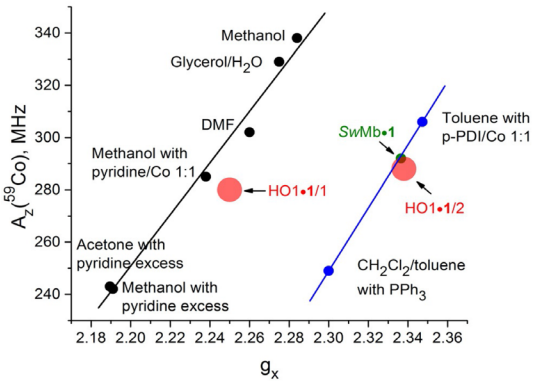

Figure 2. Correlation plots allows identifying ligands, conformation, and environment properties of cobaloxime in catalytically active solar energy conversion systems.

Crystallographic, DFT computational, and multifrequency EPR spectroscopic studies of hydrogen oxidation catalysts from the Ni-bis(diphosphine) family have provided a number of insights into their intrinsic properties and how these differ from those of proton reduction catalysts of the Ni-bis(diphosphine) family. Our EPR spectroscopic data do not exhibit evidence of coordination to the Ni(I) center by the potentially ligating solvents acetonitrile and butyronitrile. Results show that the molecular and electronic structures of the Ni complexes are as strongly dependent on the nature of the second-coordination-sphere (remote amine groups) as they are upon the first-coordination-sphere (phosphine groups). Knowledge gained by these studies has been used to characterize the cobaloxime and Ni-bis(diphosphine) based complexes with light-harvesting and charge separation motifs in artificial and photosynthetic protein frameworks.

A similar approach was used to investigate novel cobaloxime-type catalyst (Co^{III}(prdioxH)) containing different axial ligands, such as thiocyanate, pyridine and chloride, in distinct oxidation states obtained via bulk electrolysis. EPR was also applied to characterize a number of metal-organic catalysts developed at Argonne.

Science objectives for 2018-2019:

- We will continue to explore spin-quantum and CIDEP effects to clarify the mechanism and dynamics of PCET in artificial photosynthetic systems.
- We are going to apply the suite of advanced EPR techniques, including ENDOR, ESEEM and DEER spectroscopy, to structurally characterize newly synthesized solar energy conversion systems.

DOE Sponsored Publications 2015-2018

1. R. R. Langeslay, H. Sohn, B. Hu, J. S. Mohar, M. Ferrandon, C. Liu, H. Kim, J. Niklas, O. G. Poluektov, E. E. Alp, A. P. Sattelberger, A. S. Hocka, and M. Delferro, "Nuclearity Effects in Supported, Single-Site Fe(II) Hydrogenation Catalysts", *ChemCom*, 2018 March submitted.
2. Y. Zhao, H. Sohn, B. Hu, J. Niklas, O. Poluektov, J. Tian, M. Delferro, A. Hock, "Zirconium Modification Promotes Catalytic Activity of Single-Site Cobalt Heterogeneous Catalyst for Propane Dehydrogenation", *ACS Catalysis*, 2017 December submitted.
3. H. Baydoun, J. Burdick, B. Thapa, L. Wickramasinghe, D. Li, J. Niklas, O. Poluektov, H. B. Schlegel, and C. N. Verani "Immobilization of an Amphiphilic Cobalt Catalyst on Carbon Black for Ligand-assisted Water Oxidation", *Inorg. Chem.* Submitted March 2018.
4. G. Wolfowicz, C. P. Anderson, A. L. Yeats, S. J. Whiteley, J. Niklas, O. G. Poluektov, F. J. Heremans, and D. D. Awschalom "Optical charge state control of spin defects in 4H-SiC", *Nature Communications,* **2017**, 8, 1876, DOI: 10.1038/s41467-017-01993-4.
5. Z. Huang, D. Liu, J. Camacho-Bunquin, G. Zhang, D. Yang, J. López- Encarnación, Y. Xu, M. Ferrandon, J. Niklas, O. Poluektov, J. Jellinek, A. Lei, E. Bunel, M. Delferro. "Supported Single-Site Ti(IV) on a Metal–Organic Framework for the Hydroboration of Carbonyl Compounds," *Organometallics,* **2017**, 36 (20), 3921–3930.
6. S. A. J. Thomson, J. Niklas, K. L. Mardis, C. Mallares, I. D. W. Samuel, and O. G. Poluektov "Charge Separation and Triplet Exciton Formation Pathways in Small Molecule Solar Cells as Studied by Time-resolved EPR Spectroscopy", *J. Phys. Chem. C*, **2017**, 121 (41), 22707-22719
7. J. Ho, E. Kish, D. Méndez-Hernández, K. Wong-Carter, *S.* Pillai*, G.* Kodis, J. Niklas, O. G. Poluektov, D. Gust, T. A. Moore, A. L. Moore, V. S. Batista, B. Robert*, "*Triplet-Triplet Energy Transfer in Artificial and Natural Photosynthetic Antennas*", PNAS,* **2017**, 114 (28), E5513-E5521.
8. H. Sohn, J. Camacho-Bunquin, R. R. Langeslay, P. A. Ignacio-de Leon, J. Niklas, O. Poluektov, C. Liu, J. G. Connel, H. Kim, P. Stair, M. Ferrandon, and M. Delferro "Isolated, Well-Defined Organovanadium(III) on Silica: Single-Site Catalysts for Hydrogenation of Alkenes and Alkynes" *Chem. Comm*., **2017**, 53, 7325-7328.
9. M. Ortiz, S. Cho, J. Niklas, S. Kim, O. G. Poluektov, W. Zhang, G. Rumbles, J. Park "Through-Space Ultrafast Photoinduced Electron Transfer Dynamics of a C_{70}-Encapsulated Bisporphyrin Covalent Organic Polyhedron in a Low-Dielectric Medium" *JACS*, **2017**, 139, 4286−4289.
10. E. Boros, R. Srinivas, H. Kim, A. Raitsimring, A. Astashkin, O. Poluektov, J. Niklas, A. Horning, B. Tidor, P. Caravan, "Intramolecular Hydrogen Bonding Restricts Gd–Aqua-Ligand Dynamics", *Angew. Chem. Int. Ed.*, **2017**, 56, 5603-5606.
11. J. Niklas, O. G. Poluektov, "Charge Transfer Processes in OPV Materials as Revealed by EPR Spectroscopy", *Advanced Energy Materials*, Invited Review, **2017**, 7, 1602226.
12. N. Singh, J. Niklas, Oleg Poluektov, K. M. van Heuvelen, A. Mukherjee, "Mononuclear Nickel (II) and Copper (II) Coordination Complexes Supported by Bispicen Ligand Derivatives: Experimental and Computational Studies", *Inorganica Chimica Acta*, **2017**, 455, 221-230.

13. C. Yu, M. Graham, J. Zadrozny, J. Niklas, M. Krzyaniak, M. Wasielewski, O. Poluektov, D. Freedman, "Long Coherence Times in Surface-Compatible Nuclear Spin-Free Vanadium Qubits", *JACS,* **2016**, 138 (44), 14678–14685.

14. M. Bacchi, E. Veinberg, M. J. Field, J. Niklas, T. Matsui, D. M. Tiede, O. G. Poluektov, M. Ikeda-Saito, M. Fontecave, and V. Artero, "Artificial Hydrogenases Based on Cobaloximes and Heme Oxygenase", *ChemPlusChem*, **2016**, 81(10), 1083-10898.

15. D. Basu, S. Mazumder, J. Niklas, H. Baydoun, D. Wanniarachchi, X. Shi, R.J. Staples, O.G. Poluektov, H.B. Schlegel, C.N. Verani "Evaluation of the coordination preferences and catalytic pathways of heteroaxial cobalt oximes towards hydrogen generation" *Chemical Science*, **2016**, 7, 3264-3278.

16. K. L. Mardis, J. N. Webb, T. Holloway, J. Niklas, O. G. Poluektov, "Electronic Structure of Fullerene Acceptors in Organic Bulk-Heterojunctions: A Combined EPR and DFT Study", *J. Phys. Chem. Lett.,* **2015**, 6 (23), 47-30-4735.

17. J. Zadrozny, J. Niklas, O. G. Poluektov, D. Freedman, "Millisecond Coherence Time in a Tunable Molecular Electronic Spin Qubit" *ACS Central Science*, **2015**, 1, 488-492.

18. R. J. Ellis, T. Demars, G. Liu, J. Niklas, O. G. Poluektov, I. A. Shkrob, "In the Bottlebrush Garden: The Structural Aspects of Coordination Polymer Phases formed in Lanthanide Extraction with Alkyl Phosphoric Acids", *J. Phys. Chem. B,* **2015**, 119 (35), 11910-11927.

19. J. Niklas, M. Westwood, K.L. Mardis, T. Brown, A. Pitts-McCoy, M.D. Hopkins, O.G. Poluektov, "X-Ray Crystallographic, Multifrequency Electron Paramagnetic Resonance, and Density Functional Theory Characterization of the $Ni(P^{Cy}_2N^{tBu}_2)_2^{n+}$ Hydrogen Oxidation Catalyst in the Ni(I) Oxidation State", *Inorganic Chemistry,* **2015**, 54 (13), 6226-6234.

20. J. Niklas, S. Beaupré, M. Leclerc, T. Xu, L. Yu, A. Sperlich, V. Dyakonov, O.G. Poluektov, "Photoinduced Dynamics of Charge Separation: From Photosynthesis to Polymer-Fullerene Bulk Heterojunctions", *J. Phys. Chem. B,* **2015**, 119 (24), 7407-7416.

21. J. Camacho-Bunquin, N. A. Siladke, G. Zhang, J. Niklas, O. G. Poluektov, S. T. Nguyen, J. T. Miller, and A. S. Hock, "Synthesis and Catalytic Hydrogenation Reactivity of a Chromium Catecholate Porous Organic Polymer", *Organometallics*, **2015,** 34 (5), 947–952.

22. D. Basu, S. Mazumder, X. Shi, H. Baydoun, J. Niklas, O. Poluektov, H. B. Schlegel, C. N. Verani, "Ligand Transformations and Efficient Proton/Water Reduction with Cobalt Catalysts Based on Pentadentate Pyridine-Rich Environments", *Ang. Chem. Int. Ed.*, **2015**, 54 (7), 2105 –2110.

23. B. Hu, A. Getsoian, N.M. Schweitzer, U. Das, H.S. Kim, J. Niklas, O.G. Poluektov, L.A. Curtis, P.C. Stair, J.T. Miller, A.S. Hock, "Selective Propane Dehydrogenation with Single Site Co(II) on SiO_2 by a Non-redox Mechanism", *Journal of Catalysis,* **2015**, 322, 24-37.

Mechanisms of Photocatalytic Assemblies for Solar Fuel Production

Victor S. Batista, Charles A. Schmuttenmaer, Subhajyoti Chaudhuri, Svante Hedström, Jianbing Jiang, Shin Hee Lee, Adam J. Matula, Coleen T. Nemes, Kevin P. Regan, John R. Swierk, Gary W. Brudvig, and Robert H. Crabtree.

Department of Chemistry and Energy Sciences Institute
Yale University
New Haven, CT and 06520

We have made significant progress in understanding the fundamental science needed to develop better photocatalytic assemblies using a combination of synthetic, electrochemical, spectroscopic, and theoretical techniques found in our laboratories. These include both methodological developments as well as collaborative work to probe and characterize the functionality of molecular assemblies for solar fuel production.

We performed systematic studies of the effect of chromophore–oxide distance combining synthesis, characterization, spectroscopy, and computational modeling of electron-injection dynamics from free-base trimesitylporphyrins with varying linker lengths into tin(IV) oxide (SnO_2) [**41**]. We find a clear correlation between linker length and injection rates, providing insights that could be exploited in the optimization of dye-sensitized photoelectrochemical cells.

We probed a series of linkers (phenylene and benzanilidylene) and anchoring groups (carboxylate, hydroxamate, phosphonate, and silatrane) for direct interfacial electron transfer (IET) from CF_3-substituted, high-potential porphyrins into SnO_2 semiconductor surfaces [**54**] (Figure 1). From time-resolved terahertz (THz) measurements and quantum dynamics simulations, injection yields were determined. We found that IET occurs through space rather than through the linkers, due to the tilted orientation of the adsorbed porphyrins in direct contact with the metal oxide surface. As a result, the anchoring groups have a less significant effect on IET dynamics than for adsorbates exhibiting through-linker injection. Direct IET offers the advantage of the selection of anchoring groups based solely on chemical/ photoelectrochemical stability and synthetic viability, irrespective of the electronic coupling of the anchoring group to the metal oxide surface.

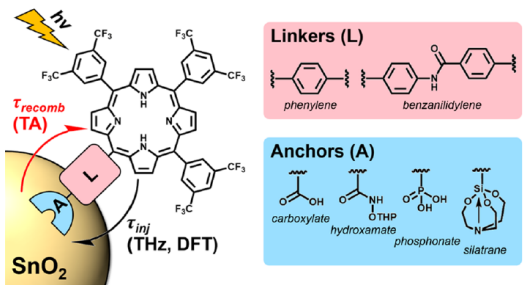

Figure 1. Series of linkers and anchors for investigating IET.

Terahertz spectroscopy is broadly applicable for the study of a wide variety of materials, but spectroelectrochemistry has not been performed in the THz range because of the lack of a THz-transparent electrochemical cell. While THz-transparent electrodes do exist, they have never been utilized in a complete three-electrode cell, which is the configuration required for accurate potential control in aqueous media. We have designed and constructed a THz-transparent electrochemical cell and have performed THz spectroelectrochemistry of a SnO_2 thin film [**55**]. The cell utilizes a custom-made reference electrode and tubing which allows the

composition of electrolyte to be changed during an experiment. THz spectroelectrochemical measurements showed a decrease in THz transmission at potentials where SnO_2 conduction band states were potentiostatically filled (Figure 2).

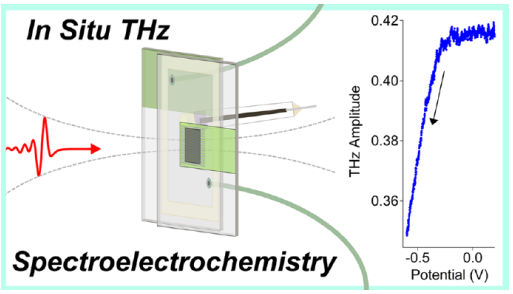

Figure 2. Schematic diagram of THz-transparent spectroelectrochemical cell.

The transient photoconductive properties of tin(IV) oxide (SnO_2) mesoporous films have been studied by time-resolved THz spectroscopy [**48**]. We gained insight into carrier dynamics by measuring overall injection and trapping lifetimes using optical pump–THz probe spectroscopy, as well as the frequency-dependent complex conductivity at various pump–probe delay times. It was found that the method of charge generation, either direct above band gap excitation (at 267 nm) or dye-sensitized electron injection (at 400 nm), has a dramatic effect on the overall injection and trapping dynamics of mobile charge carriers on the picosecond to nanosecond time scale. We found that the transient photoconductivity deviates from the behavior described by standard conductivity models such as the Drude and Drude–Smith models. This is due to the contribution from a photoinduced change in the permittivity of the SnO_2 films.

We have developed a Monte Carlo method for calculating electron transfer (ET) rates including modulation by molecular vibrations. Our density functional theory (DFT) Marcus–Jortner–Levich (MJL) approach provides robust and accurate predictions of ET rates spanning over 4 orders of magnitude in the 10^6–10^{10} s^{-1} range [**35**]. The contribution of individual modes to the rate provided insights into the interplay between vibrational degrees of freedom and changes in electronic state. The reported findings are relevant to a broad range of systems in photocatalysis.

We implemented a nonequilibrium Green's function methodology at the DFT level in order to examine charge-transport and rectification properties of a series of conjugated D–A systems [**39**]. We investigated 42 molecular junctions formed by D–A dyads bridging model gold electrodes, showing how transport properties are determined by chemical composition, symmetry of frontier orbitals, and molecular conformation. Key properties were compared to experimental data. Notably, an inverse correlation between conductance and rectification was found, with relatively large rectification ratios caused by the asymmetry of frontier orbitals near the Fermi level. We discussed design principles that should be valuable for the rational design of molecular D–A systems.

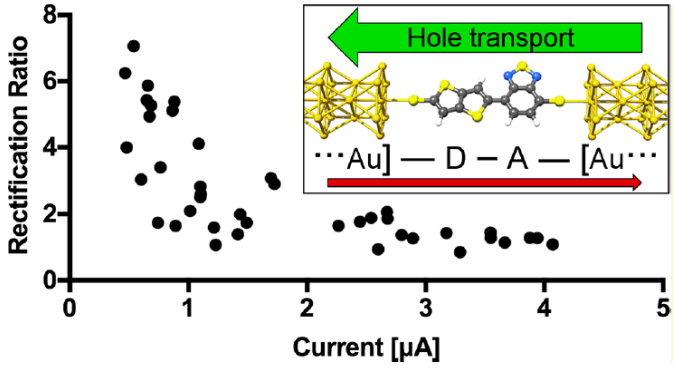

Figure 3. Rectification ratio as a function of current.

DOE Sponsored Publications 2015-2018

1. Blakemore, J. D.; Crabtree, R. H.; Brudvig, G. W., Molecular Catalysts for Water Oxidation. *Chem. Rev.* **2015,** *115*, 12974-13005.
2. Brennan, B. J.; Durrell, A. C.; Koepf, M.; Crabtree, R. H.; Brudvig, G. W., Towards Multielectron Photocatalysis: A Porphyrin Array for Lateral Hole Transfer and Capture on a Metal Oxide Surface. *Phys. Chem. Chem. Phys.* **2015,** *17*, 12728-12734.
3. Brennan, B. J.; Lam, Y. C.; Kim, P. M.; Zhang, X.; Brudvig, G. W., Photoelectrochemical Cells Utilizing Tunable Corroles. *ACS Appl. Mater. Inter.* **2015,** *7*, 16124-16130.
4. Ding, W.; Koepf, M.; Koenigsmann, C.; Batra, A.; Venkataraman, L.; Negre, C. F. A.; Brudvig, G. W.; Crabtree, R. H.; Schmuttenmaer, C. A.; Batista, V. S., Computational Design of Intrinsic Molecular Rectifiers Based on Asymmetric Functionalization of *N*-Phenylbenzamide. *J. Chem. Theor. Comp.* **2015,** *11*, 5888-5896.
5. Koepf, M.; Lee, S. H.; Brennan, B. J.; Méndez-Hernández, D. D.; Batista, V. S.; Brudvig, G. W.; Crabtree, R. H., Preparation of Halogenated Fluorescent Diaminophenazine Building Blocks. *J. Org. Chem.* **2015,** *80*, 9881-9888.
6. Li, C.; Koenigsmann, C.; Ding, W.; Rudshteyn, B.; Yang, K. R.; Regan, K. P.; Konezny, S. J.; Batista, V. S.; Brudvig, G. W.; Schmuttenmaer, C. A., Facet-Dependent Photoelectrochemical Performance of TiO_2 Nanostructures: An Experimental and Computational Study. *J. Am. Chem. Soc.* **2015,** *137*, 1520-1529.
7. Materna, K. L.; Brennan, B. J.; Brudvig, G. W., Silatranes for Binding Inorganic Complexes to Metal Oxide Surfaces. *Dalton Trans.* **2015,** *44*, 20312-20315.
8. Milot, R. L.; Schmuttenmaer, C. A., Injection Dynamics in High-Potential Porphyrin Photoanodes. *Acc. Chem. Res.* **2015,** *48*, 1423-1431.
9. Nemes, C. T.; Koenigsmann, C.; Schmuttenmaer, C. A., Functioning Photoelectrochemical Devices Studied with Time-Resolved Terahertz Spectroscopy. *J. Phys. Chem. Lett.* **2015,** *6*, 3257-3262.
10. Osowiecki, W. T.; Sheehan, S. W.; Young, K. J.; Durrell, A. C.; Mercado, B. Q.; Brudvig, G. W., Surfactant-Mediated Electrodeposition of a Water-Oxidizing Manganese Oxide. *Dalton Trans.* **2015,** *44*, 16873-16881.
11. Poddutoori, P. K.; Thomsen, J. M.; Milot, R. L.; Sheehan, S. W.; Negre, C. F. A.; Garapati, V. K. R.; Schmuttenmaer, C. A.; Batista, V. S.; Brudvig, G. W.; van der Est, A., Interfacial Electron Transfer in Photoanodes Based on Phosphorus(V) Porphyrin Sensitizers Co-Deposited on SnO_2 with the Ir(III)Cp* Water Oxidation Precatalyst. *J. Mat. Chem. A* **2015,** *3*, 3868-3879.
12. Sheehan, S. W.; Thomsen, J. M.; Hintermair, U.; Crabtree, R. H.; Brudvig, G. W.; Schmuttenmaer, C. A., A Molecular Catalyst for Water Oxidation That Binds to Metal Oxide Surfaces. *Nature Comm.* **2015,** *6*.
13. Sinha, S. B.; Shopov, D. Y.; Sharninghausen, L. S.; Vinyard, D. J.; Mercado, B. Q.; Brudvig, G. W.; Crabtree, R. H., A Stable Coordination Complex of Rh(IV) in an N, O-Donor Environment. *J. Am. Chem. Soc.* **2015,** *137*, 15692-15695.
14. Young, K. J.; Brennan, B. J.; Tagore, R.; Brudvig, G. W., Photosynthetic Water Oxidation: Insights From Manganese Model Chemistry. *Acc. Chem. Res.* **2015,** *48*, 567-574.
15. Antoniuk-Pablant, A.; Terazono, Y.; Brennan, B. J.; Sherman, B. D.; Megiatto, J. D.; Brudvig, G. W.; Moore, A. L.; Moore, T. A.; Gust, D., A New Method for the Synthesis of β-Cyano Substituted

Porphyrins and Their Use as Sensitizers in Photoelectrochemical Devices. *J. Mat. Chem. A* **2016,** *4*, 2976-2985.

16. Brennan, B. J.; Koenigsmann, C.; Materna, K. L.; Kim, P. M.; Koepf, M.; Crabtree, R. H.; Schmuttenmaer, C. A.; Brudvig, G. W., Surface-Induced Deprotection of THP-Protected Hydroxamic Acids on Titanium Dioxide. *J. Phys. Chem. C.* **2016,** *120*, 12495-12502.
17. Detz, R. J.; Sakai, K.; Spiccia, L.; Brudvig, G. W.; Sun, L.; Reek, J. N., Towards a Bioinspired-Systems Approach for Solar Fuel Devices. *ChemPlusChem* **2016,** *81*, 1024-1027.
18. Jiang, J.; Crabtree, R. H.; Brudvig, G. W., One-Step Trimethylstannylation of Benzyl and Alkyl Halides. *J. Org. Chem.* **2016,** *81*, 9483-9488.
19. Jiang, J.; Swierk, J. R.; Hedström, S.; Matula, A. J.; Crabtree, R. H.; Batista, V. S.; Schmuttenmaer, C. A.; Brudvig, G. W., Molecular Design of Light-Harvesting Photosensitizers: Effect of Varied Linker Conjugation on Interfacial Electron Transfer. *Phys. Chem. Chem. Phys.* **2016,** *18*, 18678-18682.
20. Jiang, J.; Swierk, J. R.; Materna, K. L.; Hedström, S.; Lee, S. H.; Crabtree, R. H.; Schmuttenmaer, C. A.; Batista, V. S.; Brudvig, G. W., High-Potential Porphyrins Supported on SnO_2 and TiO_2 Surfaces for Photoelectrochemical Applications. *J. Phys. Chem. C.* **2016,** *120*, 28971-28982.
21. Koenigsmann, C.; Ding, W.; Koepf, M.; Batra, A.; Venkataraman, L.; Negre, C. F. A.; Brudvig, G. W.; Crabtree, R. H.; Batista, V. S.; Schmuttenmaer, C. A., Structure–Function Relationships in Single Molecule Rectification by *N*-Phenylbenzamide Derivatives. *New J. Chem.* **2016,** *40*, 7373-7378.
22. Koepf, M.; Koenigsmann, C.; Ding, W.; Batra, A.; Negre, C. F. A.; Venkataraman, L.; Brudvig, G.; Batista, V. S.; Schmuttenmaer, C.; Crabtree, R. H., Controlling the Rectification Properties of Molecular Junctions through Molecule−Electrode Coupling. *Nanoscale* **2016,** *8*, 16357-16362.
23. McCool, N. S.; Swierk, J. R.; Nemes, C. T.; Saunders, T. P.; Schmuttenmaer, C. A.; Mallouk, T. E., Proton-Induced Trap States, Injection and Recombination Dynamics in Water-Splitting Dye-Sensitized Photoelectrochemical Cells. *ACS Appl. Mater. Inter.* **2016,** *8*, 16727-16735.
24. McCool, N. S.; Swierk, J. R.; Nemes, C. T.; Schmuttenmaer, C. A.; Mallouk, T. E., Dynamics of Electron Injection in SnO_2/TiO_2 Core/Shell Electrodes for Water-Splitting Dye-Sensitized Photoelectrochemical Cells. *J. Phys. Chem. Lett.* **2016**, 2930-2934.
25. Mi, Y.; Liu, W.; Yang, K. R.; Jiang, J.; Fan, Q.; Weng, Z.; Zhong, Y.; Wu, Z.; Brudvig, G. W.; Batista, V. S., Ferrocene Promoted Long-Cycle Lithium–Sulfur Batteries. *Angew. Chem.* **2016,** *128*, 15038-15042.
26. Michaelos, T. K.; Lant, H.; Sharninghausen, L. S.; Craig, S. M.; Menges, F. S.; Mercado, B. Q.; Brudvig, G. W.; Crabtree, R. H., Catalytic Oxygen Evolution from Manganese Complexes with an Oxidation Resistant N, N, O Donor Ligand. *ChemPlusChem* **2016,** *81*, 1129-1132.
27. Regan, K. P.; Koenigsmann, C.; Sheehan, S. W.; Konezny, S. J.; Schmuttenmaer, C. A., Size-Dependent Ultrafast Charge Carrier Dynamics of WO_3 for Photoelectrochemical Cells. *J. Phys. Chem. C.* **2016,** *120*, 14926-14933.
28. Ryu, W.-H.; Gittleson, F. S.; Thomsen, J. M.; Li, J.; Schwab, M. J.; Brudvig, G. W.; Taylor, A. D., Heme Biomolecule as Redox Mediator and Oxygen Shuttle for Efficient Charging of Lithium-Oxygen Batteries. *Nature Comm.* **2016,** *7*, 12925.
29. Swierk, J. R.; McCool, N. S.; Nemes, C. T.; Mallouk, T. E.; Schmuttenmaer, C. A., Ultrafast Electron Injection Dynamics of Photoanodes for Water-Splitting Dye-Sensitized Photoelectrochemical Cells. *J. Phys. Chem. C.* **2016,** *120*, 5940-5948.

30. Swierk, J. R.; Regan, K. P.; Jiang, J.; Brudvig, G. W.; Schmuttenmaer, C. A., Rutile TiO_2 as an Anode Material for Water-Splitting Dye-Sensitized Photoelectrochemical Cells. *ACS Energy Lett.* **2016,** *1*, 603-606.

31. Tsubonouchi, Y.; Lin, S.; Parent, A. R.; Brudvig, G. W.; Sakai, K., Light-Induced Water Oxidation Catalyzed by an Oxido-Bridged Triruthenium Complex With a Ru–O–Ru–O–Ru Motif. *Chem. Commun.* **2016,** *52*, 8018-8021.

32. Weng, Z.; Jiang, J.; Wu, Y.; Wu, Z.; Guo, X.; Materna, K. L.; Liu, W.; Batista, V. S.; Brudvig, G. W.; Wang, H., Electrochemical CO_2 Reduction to Hydrocarbons on a Heterogeneous Molecular Cu Catalyst in Aqueous Solution. *J. Am. Chem. Soc.* **2016,** *138*, 8076-8079.

33. Brennan, B. J.; Regan, K. P.; Durrell, A. C.; Schmuttenmaer, C. A.; Brudvig, G. W., Solvent Dependence of Lateral Charge Transfer in a Porphyrin Monolayer. *ACS Energy Lett.* **2017,** *2*, 168-173.

34. Jewess, M.; Crabtree, R. H., Electrocatalytic Nitrogen Fixation for Distributed Fertilizer Production? *ACS Sustainable Chem. Eng.* **2016,** *4*, 5855–5858.

35. Chaudhuri, S.; Hedström, S.; Méndez-Hernández, D. D.; Hendrickson, H. P.; Jung, K. A.; Ho, J.; Batista, V. S., Electron Transfer Assisted by Vibronic Coupling from Multiple Modes. *J. Chem. Theor. Comp.* **2017,** *13*, 6000-6009.

36. Crabtree, R. H., Homogeneous Transition Metal Catalysis of Acceptorless Dehydrogenative Alcohol Oxidation: Applications in Hydrogen Storage and to Heterocycle Synthesis. *Chem. Rev.* **2017,** *117*, 9228-9246.

37. Crabtree, R. H., Hypervalency, Secondary Bonding and Hydrogen Bonding: Siblings Under the Skin. *Chem. Soc. Rev.* **2017,** *46*, 1720-1729.

38. Crabtree, R. H., Nitrogen-Containing Liquid Organic Hydrogen Carriers: Progress and Prospects. *ACS Sustainable Chem. Eng.* **2017,** *5*, 4491-4498.

39. Hedström, S.; Matula, A. J.; Batista, V. S., Charge Transport and Rectification in Donor–Acceptor Dyads. *J. Phys. Chem. C.* **2017,** *121*, 19053-19062.

40. Jiang, J.; Materna, K. L.; Hedström, S.; Yang, K. R.; Batista, V. S.; Brudvig, G. W., Molecular Antimony Complexes for Electrocatalysis: Activity of a Main Group Element in Proton Reduction. *Angew. Chem. Int. Ed.* **2017,** *56*, 9111-9115.

41. Lee, S. H.; Regan, K. P.; Hedström, S.; Matula, A. J.; Chaudhuri, S.; Crabtree, R. H.; Batista, V. S.; Schmuttenmaer, C. A.; Brudvig, G. W., Linker Length-Dependent Electron-Injection Dynamics of Trimesitylporphyrins on SnO_2 Films. *J. Phys. Chem. C.* **2017,** *121*, 22690-22699.

42. Lim, G. N.; Hedström, S.; Jung, K. A.; Smith, P. A. D.; Batista, V. S.; D'Souza, F.; van der Est, A.; Poddutoori, P. K., Interfacial Electron Transfer Followed by Photooxidation in N, N-Bis (p-anisole) aminopyridine–Aluminum (III) Porphyrin–Titanium (IV) Oxide Self-Assembled Photoanodes. *J. Phys. Chem. C.* **2017,** *121*, 14484-14497.

43. Liu, W.; Jiang, J.; Yang, K. R.; Mi, Y.; Kumaravadivel, P.; Zhong, Y.; Fan, Q.; Weng, Z.; Wu, Z.; Cha, J. J.; Zhou, H.; Batista, V. S.; Brudvig, G. W.; Wang, H., Ultrathin Dendrimer–Graphene Oxide Composite Film for Stable Cycling Lithium–Sulfur Batteries. *P. Natl. Acad. Sci. USA* **2017,** *114*, 3578-3583.

44. Materna, K. L.; Crabtree, R. H.; Brudvig, G. W., Anchoring Groups for Photocatalytic Water Oxidation on Metal Oxide Surfaces. *Chem. Soc. Rev.* **2017,** *46*, 6099-6110.

45. Materna, K. L.; Jiang, J.; Regan, K. P.; Schmuttenmaer, C. A.; Crabtree, R. H.; Brudvig, G. W., Optimization of Photoanodes for Photocatalytic Water Oxidation by Combining a Heterogenized

Iridium Water-Oxidation Catalyst with a High-Potential Porphyrin Photosensitizer. *ChemSusChem* **2017,** *10*, 4526-4534.

46. Michaelos, T. K.; Shopov, D. Y.; Sinha, S. B.; Sharninghausen, L. S.; Fisher, K. J.; Lant, H. M. C.; Crabtree, R. H.; Brudvig, G. W., A Pyridine Alkoxide Chelate Ligand That Promotes Both Unusually High Oxidation States and Water-Oxidation Catalysis. *Acc. Chem. Res.* **2017,** *50*, 952-959.
47. Shopov, D. Y.; Sharninghausen, L. S.; Sinha, S. B.; Borowski, J. E.; Mercado, B. Q.; Brudvig, G. W.; Crabtree, R. H., Synthesis of Pyridine-Alkoxide Ligands for Formation of Polynuclear Complexes. *New J. Chem.* **2017**, 41, 6709-6719.
48. Regan, K. P.; Swierk, J. R.; Neu, J.; Schmuttenmaer, C. A., Frequency-Dependent Terahertz Transient Photoconductivity of Mesoporous SnO_2 Films. *J. Phys. Chem. C.* **2017,** *121*, 15949-15956.
49. Sharninghausen, L. S.; Sinha, S. B.; Shopov, D. Y.; Mercado, B. Q.; Balcells, D.; Brudvig, G. W.; Crabtree, R. H., Synthesis and Characterization of Iridium (V) Coordination Complexes With an N, O-Donor Organic Ligand. *Angew. Chem.* **2017,** *129*, 13227-13231.
50. Sinha, S. B.; Shopov, D. Y.; Sharninghausen, L. S.; Stein, C. J.; Mercado, B. Q.; Balcells, D.; Pedersen, T. B.; Reiher, M.; Brudvig, G. W.; Crabtree, R. H., Redox Activity of Oxo-Bridged Iridium Dimers in an N, O-Donor Environment: Characterization of Remarkably Stable Ir (IV, V) Complexes. *J. Am. Chem. Soc.* **2017,** *139*, 9672-9683.
51. Wu, Y.; Jiang, J.; Weng, Z.; Wang, M.; Broere, D. l. L. J.; Zhong, Y.; Brudvig, G. W.; Feng, Z.; Wang, H., Electroreduction of CO_2 Catalyzed by a Heterogenized Zn–Porphyrin Complex with a Redox-Innocent Metal Center. *ACS Centr. Sci.* **2017,** *3*, 847-852.
52. Zhong, Y.; Yang, K. R.; Liu, W.; He, P.; Batista, V. S.; Wang, H., Mechanistic Insights into Surface Chemical Interactions Between Lithium Polysulfides and Transition Metal Oxides. *J. Phys. Chem. C.* **2017,** *121*, 14222–14227.
53. Weng, Z.; Wu, Y.; Wang, M.; Jiang, J.; Yang, K.; Huo, S.; Wang, X.-F.; Ma, Q.; Brudvig, G. W.; Batista, V. S.; Liang, Y.; Feng, Z.; Wang, H., Active Sites of Copper-Complex Catalytic Materials for Electrochemical Carbon Dioxide Reduction. *Nature Comm.* **2018,** *9*, 415.
54. Jiang, J.; Spies, J. A.; Swierk, J. R.; Matula, A. J.; Regan, K. P.; Romano, N.; Brennan, B. J.; Crabtree, R. H.; Batista, V. S.; Schmuttenmaer, C. A.; Brudvig, G. W., Direct Interfacial Electron Transfer from High-Potential Porphyrins into Semiconductor Surfaces: A Comparison of Linkers and Anchoring Groups. *J. Phys. Chem. C.* **2018,** *In Press*.
55. Nemes, C. T.; Swierk, J. R.; Schmuttenmaer, C. A., A Terahertz-Transparent Electrochemical Cell for In Situ THz Spectroelectrochemistry. *Anal. Chem.* **2018,** *In Press*.
56. Peris, E.; Crabtree, R. H., Key Factors in Pincer Ligand Design. *Chem. Soc. Rev.* **2018,** *In Press*.
57. Shopov, D. Y.; Sharninghausen, L. S.; Sinha, S. B.; Mercado, B. Q.; Balcells, D.; Brudvig, G. W.; Crabtree, R. H., A Dinuclear Iridium(V,V) Oxo-Bridged Complex Characterized Using a Bulk Electrolysis Technique for Crystallizing Highly Oxidizing Compounds. *Inorg. Chem.* **2018,** *In Press*.

Polyoxometalate systems, interfacial electron transfer and multi-electron catalysis

Tianquan Lian, Djamaladdin G. Musaev and Craig L. Hill
Department of Chemistry and Emerson Center for Scientific Computation
Emory University
Atlanta, GA 30322

Catalyst development. The Emory team reports two new classes of water oxidation catalysts (WOCs) that each break new ground: (1) Molecular, base-compatible WOCs. We have used pH-14 compatible polyniobates, an emerging class of polyoxometalates, "POMs", to stabilize first-row-transition oxide units at very basic pH. This has led to the design and production of highly robust and molecular WOCs, including $[H_9Cu_{25.5}O_8(Nb_7O_{22})_8]^{28-}$ (Figure 1, left) that works in strong base (pH 13) for lengthy periods. Remarkably under electrocatalytic water oxidation conditions, no Cu or CuO_x is deposited on the electrode despite being 8 pH units beyond where Cu(II) remains in aqueous solution. (2) Molecular, strong-acid compatible WOCs of all earth-abundant elements. The first WOCs that are molecular, carbon-free and expensive-element-free have been made and studied. Four insoluble salts of $[Co_9(H_2O)_6(OH)_3(HPO_4)_2(PW_9O_{34})_3]^{16-}$ (**YCo$_9$**, **LaCo$_9$**, **BaCo$_9$** and **CsCo$_9$**; Figure 1, right) are all effective WOCs at pH = 2 at reasonable overpotential (η = 0.523 V). **YCo$_9$** shows the most noteworthy activity (current density = 5 mA/cm^2, and faradaic efficiency = 93.6 %) and long-term stability under turnover conditions (H_2SO_4 buffer with KNO_3 (1 M) electrolyte, FTO as working electrode, Pt wire as cathode, Ag/AgCl (1.0 M) as reference, scan rate = 50 mV/s, applied potential = 1.753 V (vs RHE). The varying water oxidation activities of **MCo$_9$** salts have been evaluated as a function of the Lewis acidity and impact on the Co_9 unit redox potentials of the counter cations. Despite widely varying WOC activity, all four **MCo$_9$** salts exhibit identical Tafel slopes showing all electro-oxidize H_2O by the same mechanism. The oxygen evolution rate remains constant for hours without any fatigue or decomposition even in strong acid, *where metal oxides are unstable*.

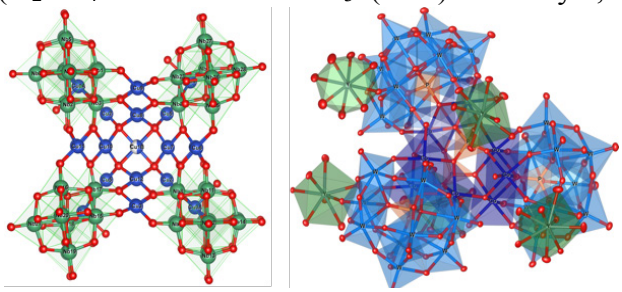

Figure 1. X-ray structures of new strong-base-compatible (left) and strong-acid-compatible molecular (right) WOCs. Left: $[H_9Cu_{25.5}O_8(Nb_7O_{22})_8]^{28-}$ (Cu, blue; Nb, green; O, red); Right: $Y_5K[Co_9(H_2O)_6(OH)_3(HPO_4)_2(PW_9O_{34})_3]$; (Y, green; WO_6, blue octahedra, CoO_6, purple octahedra; O, red).

Impact of ALD on photoelectrocatalytic systems. We just published a systematic study showing that ALD Al_2O_3 layers effectively immobilize and stabilize POM WOCs on photoelectrodes (hematite). Photocurrent densities and retention of POMs on these surfaces depend greatly on the depth of the ALD layer. Second, we investigated the effects of ALD Al_2O_3 on the structure of Re(2,2'-bipyridine-4,4'-bis-$CH_2PO(OH)_2$)$(CO)_3Cl$ (**ReC1P**)) on surfaces (TiO_2 nanocrystalline films and rutile (001) single crystals) by IR absorption and sum frequency generation (SFG) spectroscopy (Figure 2). The IR shows that ALD layers reduce the degree of **ReC1P** aggregation

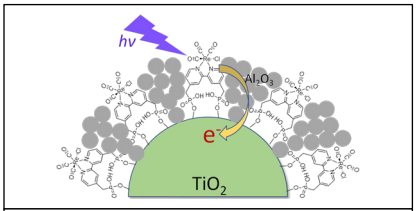

Figure 2. Schematic representation of the effect of atomic layer deposition on a **ReC1P**/TiO_2 nanocrystalline film.

on the TiO_2 film surface. In contrast, SFG studies show smaller effects of the ALD layer on **ReC1P**/TiO_2 (001) single crystals. Ultrafast IR transient absorption spectroscopy reveals that the ALD layer significantly slows down electron injection from **ReC1P** to the TiO_2. Our research demonstrates that although an ALD Al_2O_3 protection layer improves the stability of DSSCs and DSPECS, it also has a significant impact on adsorbate binding structure and charge separation kinetics.

Transient reflectance probe of charge carrier dynamics in GaP/TiO_2 photoanodes. The team has developed a new method for studying carrier dynamics in planar photoanodes using transient reflection spectroscopy. Compared to transient absorption, this method is more sensitive to surface carrier density that can be more directly correlated to catalysis. We showed that transient reflectance change can be used to follow charge carrier dynamics and their amplitude can be directly correlated to IPCE for water oxidation on a TiO_2 ALD coated GaP single crystal (Figure 3). Our finding suggests that IPCE is determined by the amount of separated charge carriers and that screening of the interfacial electrical field by high charge carrier density is a key loss mechanism.

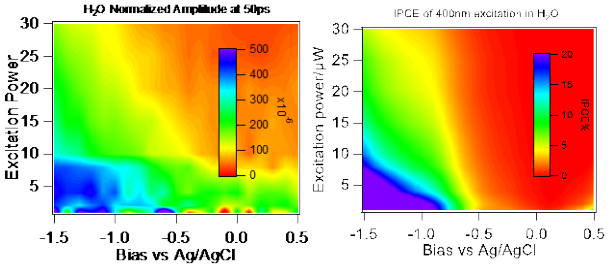

Figure 3. Correlation between IPCE and transient reflectance change at various biases and excitation power.

Computational/Theoretical Studies. Computation and theory developments are integral parts of our program and are aimed at guiding experiments to design more effective WOCs, and faster interfacial electron transfer (IET) at key junctions including WOCs/sensitizers and quantum dots (QDs)/electron scavengers. In the report period, we: (1) investigated the stability and reactivity of a new type of WOC with a structurally-dynamic active site (Figure 4; central yellow circle). We found (a) that the complexes $\{(FeM)[\gamma\text{-}SiW_{10}O_{36}]\}^{n-}$ with a $[(Fe_3M_3)(OH)_9]$ active core (where M = Fe, Co and Ni) in their high-spin ground electronic states are stable relative to three monomers, and (b) determined the $[(Fe_3M_3)(OH)_9] + 3[\gamma\text{-}SiW_{10}O_{36}]$ dissociation limit; and (2) developed a Bulk Adjusted (BA)-LCAO model to study QD-to-molecule electron/hole transfer. This approach applies a scaling and parametrical function to the 2-center interaction potentials (derived from *ab initio* data), strictly according to atomic valences acquired naturally in a bulk structure, to closely match both the available experimental and high-level calculation data. To evaluate the method, we parameterized a BA-LCAO Hamiltonian by finding the best scaling function of Wurtzite CdSe by fitting its band structure to a high-level DFT reference. We have shown that this method effectively reproduces the band structure and key properties including the valence and conduction band edges. Currently, we are expanding this method to core-shell type QDs of CdSe/CdS, CdSe/ZnS and other compositions.

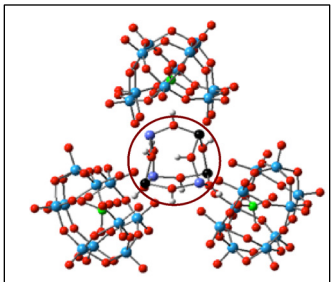

Figure 4. The $\{(FeM)[\gamma\text{-}SiW_{10}O_{36}]\}^{n-}$ complex with a $[(Fe_3M_3)(OH)_9]$ active core, where M= Fe, Co and Ni.

DOE Sponsored Publications 2015-2018

1. Fielden, J; Sumliner, J. M.; Han, N.; Geletii, Y. V.; Xiang, X.; Musaev, D. G.; Lian, T.; Hill, C. L. "Water Splitting with Polyoxometalate-Treated Photoanodes: Enhancing Performance through Sensitizer Design" *Chem. Sci.*, **2015**, *6*, 5531–5543. **DOI:** 10.1039/c5sc01439e

2. Lauinger, S. M.; Sumliner, J. M.; Yin, Q.; Xu, Z.; Liang, G.; Glass, E. N.; Lian, T.; Hill, C. L. "Enhanced Stability of Immobilized Polyoxometalates on TiO_2 Nanoparticles and Nanoporous Films for Robust, Light-Induced Water Oxidation" *Chem. Mater.* **2015**, *27,* 5886−5891. **DOI:** 10.1021/acs.chemmater.5b01248

3. Lv, H.; Chi, Y.; van Leusen, J.; Kögerler, P.; Chen, Z.; Bacsa, J.; Guo, W.; Lian, T.Q; Hill, C. L. "$[\{Ni_4(OH)_3AsO_4\}_4(B\text{-}\alpha\text{-}PW_9O_{34})_4]^{28-}$ a New Polyoxometalate Structural Family with Catalytic Hydrogen Evolution Activity" *Chem. Eur. J.* **2015**, *21*, 17363–17370. **DOI:** 10.1002/chem.20150301

4. Kaledin, A. L.; Lian, T.; Hill, C. L.; Musaev, D. G. "A Hybrid Quantum Mechanical Approach: Intimate Details of Electron Transfer Between Type I CdSe/ZnS Quantum Dots and an Anthraquinone Molecule" *J. Phys. Chem*, *B.*, **2015**, Published online January 21, 2015 **DOI:**10.1021/jp511935z

5. Guo, W.; Lv, H.; Chen, Z.; Lauinger, S. M.; Luo, Z.; Sumliner, J. M.; Lian, T.; Hill, C. L. "Self-assembly of Polyoxometalates, Pt Nanoparticles and Metal-Organic Frameworks in a Hybrid Material for Synergistic Hydrogen Evolution", *J. Mater. Chem. A*, **2016**, *4*(16), 5952-5957. **DOI:** 10.1039/C6TA00011H

6. Glass, E. N.; Fielden, J.; Huang, Z.; Xiang, X.; Musaev, D. G.; Lian, T.; Hill, C. L. "Transition Metal Substitution Effects on Metal-to-Polyoxometalate Charge Transfer", *Inorg. Chem.* **2016**, *55* (9), 4308–4319. **DOI:** 10.1021/acs.inorgchem.6b00060

7. Lv, H.; Gao, Y.; Guo, W.; Lauinger S. M.; Chi, Y.; Bacsa, J.; Sullivan, K. P.; Wieliczko, M.; Musaev, D. G.; Hill, C. L. "A Cu-based Polyoxometalate Catalyst for Efficient Catalytic Hydrogen Evolution" *Inorg. Chem.*, **2016**, *55* (13), 6750–6758. **DOI:** 10.1021/acs.inorgchem.6b01032

8. Soriano-López, J.; Musaev, D. G.; Hill, C. L.; Galán-Mascarós, J. R.; Carbó, J. J. Poblet, J. M. "Tetracobalt-polyoxometalate catalysts for water oxidation: Key Mechanistic Details" *J. Catalysis*, **2017**, *350*, 56-63. https://doi.org/10.1016/j.jcat.2017.03.018

9. Wieliczko, M.; Geletii, Y. V.; Bacsa, J.; Musaev, D. G.; Hill, C. L. "Effects of Competitive Active-Site Ligand Binding on Proton- and Electron-Transfer Properties of the $[Co_4(H_2O)_2(PW_9O_{34})_2]^{10-}$ Polyoxometalate Water Oxidation Catalyst" *J. Cluster Sci.*, **2017**, *28*, 839-852. **DOI:**10.1007/s10876-016-1135-3

10. Lauinger, S. M.; Piercy, B. D.; Li, W.; Yin, Q.; Collins-Wildman, D. L.; Glass, E. N.; Losego, M. D.; Wang, D.; Geletii, Y. V.; Hill, C. L. "Stabilization of Polyoxometalate Water Oxidation Catalysts on Hematite by Atomic Layer Deposition", *ACS Applied Materials & Interfaces*, *ACS Appl. Mater. Interfaces*, **2017**, *9* (40), 35048–35056. **DOI:** 10.1021/acsami.7b12168

11. Lauinger, S. M.; Yin, Q.; Geletii, Y. V.; Hill, C. L "Polyoxometalate Catalysts in Solar Fuel Production" *Advances in Inorganic Chemistry*, van Eldik, R. and Cronin, C.; Eds.; **2017**, *69*, Chapter 5. **DOI**.org/10.1016/bs.adioch.2016.12.002

12. Liu, B.; Glass, E. N.; Wang, R-p.; Cui, Y-t.; Harada, Y.; Huang, D-j.; Schuppler, S.; Hill, C. L.; de Groot, F. F. M. "Cobalt-to-vanadium charge transfer in polyoxometalate water oxidation catalysts revealed by 2p3d resonant inelastic x-ray scattering" *Physical Chemistry and Chemical Physics*, **2018**, *20*, 4554-4562 http://dx.doi.org/10.1039/C7CP06786K

13. Sullivan, K. P.; Wieliczko, M.; Geletii, Y. V.; Kim, M.; Collins-Wildman, D. L.; Hill, C. L. "Stability and reactivity of the $[Co_4V_2W_{18}O_{68}]^{10-}$ water oxidation catalyst in solution" *ACS Catalysis*, **2018**, *00*, 000 (invited paper; in preparation).

14. Yanyan Jia, Jinquan Chen, Kaifeng Wu, Alex Kaledin, Jamal Musaev, Zhaoxiong Xie, and Tianquan Lian, "Enhancing Photo-reduction Quantum Efficiency Using Quasi-Type II Core/Shell Quantum Dots", *Chem. Sci*. **2016** Published online 2 March 2016. **DOI**: 10.1039/C6SC00192K.

15. Jia Song, Aimin Ge, Brandon Piercy, Mark D. Losego, and Tianquan Lian, "Effects of Al_2O_3 Atomic Layer Deposition on Interfacial Structure and Electron Transfer Dynamics at Re-Bipyridyl Complex/TiO_2 Interfaces", *Chemical Physics,* **2018**, *accepted. doi.org/10.1016/j.chemphys.2018.03.033*

16. Zihao Xu, Bingya Hou, Stephen Cronin and Tianquan Lian, "Interfacial Electrical Field Enhanced Water Splitting Efficiency in TiO_2-GaP Electrode Studied by in situ Transient Reflectance Spectroscopy", *J. Am. Chem. Soc.*, **2018**, *in preparation*.

17. Alexey L. Kaledin, Craig L. Hill, Tianquan Lian, Djamaladdin G. Musaev, "Bulk Adjusted Linear Combination of Atomic Orbitals Approach for nanoparticles", *J. Computational Chem.*, **2018**, *submitted.*

18. Alexey L. Kaledin, Craig L. Hill, Tianquan Lian, Djamaladdin G. Musaev, "Polyoxometalates with a structurally dynamic water oxidation $[(Fe_3M_3)(OH)_9]$ active core, where M = Fe, Ni and Co", *Inorg. Chem.,* **2018**, *in preparation*.

Coupled transport-transformation phenomena in a dye-sensitized solar conversion systems

Frances Houle
Chemical Sciences Division
Lawrence Berkeley National Laboratory
Berkeley, CA 94720

Solar-driven transformations in nanostructured condensed phases and at their interfaces offer the potential for efficient and inexpensive conversion of photon energy to chemical energy. Of particular interest are molecular systems for conversion of sunlight to electricity such as dye-sensitized solar cells (DSSC), and, more recently, dye-sensitized photoelectrosynthesis cells (DSPEC), because they offer flexible and easily fabricated architectures. These cells operate through multiscale, multiphase couplings of excitation, charge flow and chemical reactions, which govern the efficiency with which these nanostructured systems convert solar photons into electricity or chemicals. Numerous in-depth investigations have been invaluable for elucidating key physics and chemistry phenomena in dye-sensitized systems, and have inspired new materials concepts. What they have not yet done is explain at a molecular level how the dye, nanoparticles, electrolyte and reduction at the companion counter electrode work together to produce observed photocurrents and reaction products. Such knowledge would help identify system elements that most strongly influence efficiency, which may be emergent. It would also help develop a deeper understanding of how the kinetics connect across length and time scales in these systems, revealing how brief, local events influence what is measured.

To begin to build a connection, I have constructed a reaction-diffusion modeling framework that integrates the major physical phenomena from nano- to micro/macro- scale in space and time. This framework, illustrated in Figure 1 for a DSSC, is a platform that can provide both spatial and temporal details on how photocurrents are generated. Using it, some insights to non-ideal behaviors such as the current vs time curve drawn in the Figure may be obtained.

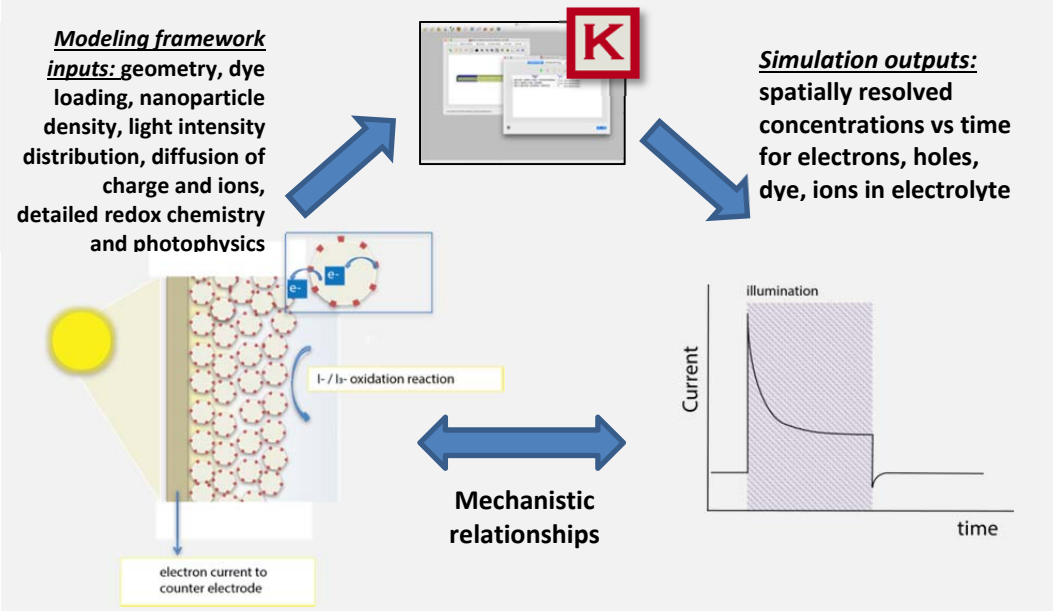

Figure 1. Modeling strategy for DSSCs. The system's chemistry and physics are connected to experimental observables using stochastic reaction-diffusion simulations.

A stochastic algorithm* is used to solve the master equation for the reaction-diffusion system. This technique is particularly well-suited to systems that are driven by sporadic events such as photon absorption. The methodology supports a wide range of time and length scales in a single calculation, allowing nm-scale phenomena in a device many microns thick to be examined, as well as inclusion of ultrafast photophysics coupled to slow liquid-phase redox processes. When the system's spatial and compositional characteristics and validated elementary reaction steps are used, the simulations provide predictions as a function of an absolute time base that enables computed and experimental data to be directly compared.

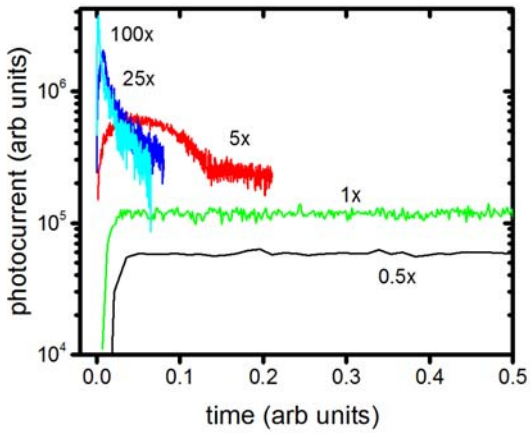

Figure 2. Simulated photocurrents vs time for photoexcitation rate constants varying from 0.5 to 100x $1s^1$. Units are currently arbitrary but will be quantified during the process of validation of the model against experiment.

Using literature data for cell geometry, reactant concentrations and rate constants, initial simulation studies focus on the response of a TiO_2-dye-I^-/I_3^- redox system to a range of light intensities. The light flux is assumed to be uniformly absorbed, and the dye photoexcitation rate constant is varied from 0.5-100 s^{-1}, where 1 s^{-1} is typical of DSSC operating conditions. The higher photoexcitation rates correspond to light concentration. As shown in Figure 2, at the lowest excitation rate the system's reactions are balanced and the photocurrent is constant for the specific anode configuration used, which represents a system that has sparse, large ($200nm^2$ cross sectional area) pores and minimal electron recombination. There are charge loss paths in the electrolyte, however, that reduce efficiency. As the excitation rate is increased, the iodide electrolyte becomes strongly polarized, eventually resulting in confinement of dye oxidation-reduction events to the external surface of the anode because the electrolyte in the interior is depleted of redox-active I^-. As a result, the photocurrent decays in time and does not exceed a limiting value despite higher light intensity. The simulations are used to predict spatially-resolved details about the chemical components of the DSSC under *operando* conditions.

These initial calculations provide a baseline that will be used as a reference while the model's physical and chemical details are being developed in future work. This will allow factors that are kinetically significant to be distinguished from those that are less important as the model is extended. The framework is modular and does not use adjustable parameters, so once it is validated against experiment it can be used directly to predict the results of changes in device configurations and components such as dye and redox couples. It will also serve as a starting point for simulations of DSPEC water splitting systems, which have more complex interfacial chemistry.

* W. D. Hinsberg and F. A. Houle, Kinetiscope, 2017. Available in open access at www.hinsberg.net/kinetiscope.

Well-defined Plasmonic-Excitonic Hybrid Nanosystems as Plexitonic Model Systems

Christopher W. Leishman[1], Nikunjkumar Visaveliya[1], Kara Ng[1], Pooja Gaikwad[1], Amedee des Georges[2], Alexander Govorov[3], and Dorthe M. Eisele[1]

(1) Department of Chemistry and Biochemistry, The City College of New York (CCNY) of The City University of New York (CUNY), 160 Convent Avenue, New York, NY 10031, U.S.A.; (2) Structural Biology Initiative, CUNY Advanced Science Research Center (ASRC), 85 St. Nicholas Terrace, New York, NY 10031, U.S.A.; (3) Department of Physics and Astronomy, Ohio University, Ohio University at Athens, Athens OH 45701, U.S.A.

Motivation. The interactions between excitonic and plasmonic nanoscale systems in close proximity result in coupled optical transitions (plexcitons) having novel properties distinct from those of either component system. Among these properties, particularly promising for solar energy conversion are plasmonic enhancement of excitonic transitions, tunability of resonance energies at plasmonic hot spots for photocatalysis, and enforced directionality of excitation energy transport. The pivotal next step for exploiting the full potential of these promising hybrid nanosystems is to gain a fundamental understanding of their complex plexcitonic properties.

Scope of the Project. Overall goal of this project is to understand plasmon-exciton interactions in nanoscale systems, in particular the relationship (i) between the plasmon-exciton interaction and the specific *plasmonic* nanostructure and, in a second step, (ii) between the plasmon-exciton interaction and the specific *excitonic* nanomaterial. In contrast to recent research efforts, our project aims at a concerted treatment of hybrid nanosystems by bringing together both Materials Research and Physical Research approaches. To this end, we take a distinct approach to the material synthesis. Recent research efforts take advantage of a typical *Plasmon-centric assembly* approach (**Figure 1a**), where excitonic material is added to or assembled in the presence of the plasmonic material, *i.e.* by close-packing adsorption (self-assembling) of dye molecules on metal nanoparticle (MNP) surfaces. Here, we develop a *Nanoconjugation* approach for the synthesis of hybrid model systems, where both components—the excitonic system and the plasmonic system—are treated on a more even footing: in solution, the two components are electrostatically linked by a spacer material such as an organic scaffolding (non-excitonic material with controllable thickness) as illustrated in **Figure 1b**.

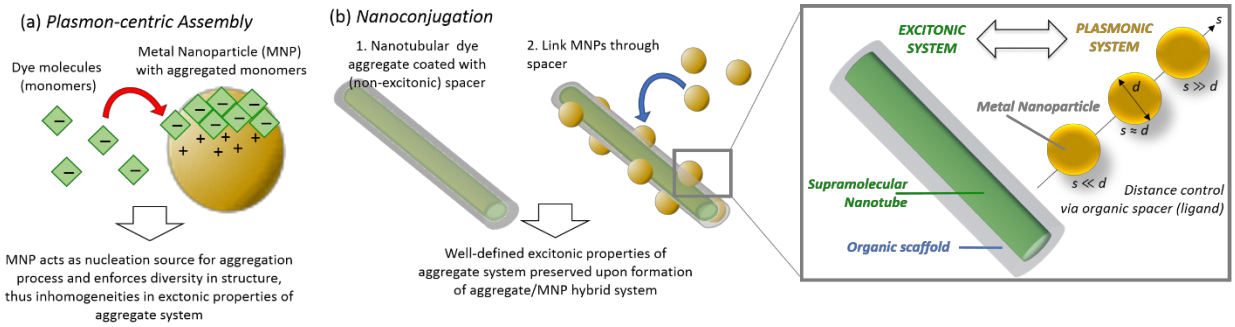

Figure 1. Different approaches for plexcitonic material synthesis. (a) Typical Plasmon-centric approach versus (b) this project's Nanoconjugation approach.

Recent results. As the plasmonic component, we synthesize silver MNPs at different sizes and shapes (spheres and nanorods) under batch conditions. As the excitonic component, we synthesize two kinds of nanotubular aggregates self-assembled from amphiphilic cyanine dye C8S3 molecules (**Figure 2a**) and porphyrin dye TSPP molecules (**Figure 2b**), respectively. In general, supramolecular aggregates consist of molecular sub-units (monomers) which self-assemble under thermodynamic equilibrium conditions by weak (non-covalent) interactions into close-packed (aggregated) molecules. Linking MNPs to the soft supramolecular nanotubes can easily change the nanotube's structural details such as details of its molecular packing. Due to the nanotube's delicate structure-function relationship, any minor structural alterations can change the nanotube's excitonic properties. However, our *Nanoconjugation* approach allows us to preserve the nanotube's well-characterized structure, which is key to allow for systematically investigate the details of how plexcitonic states arise from the two component of the hybrid model system. Currently, we are developing new methods of *Nanoconjugation* by employing several different kinds of non-excitonic material to encapsulate supramolecular nanotubes to stabilize their delicate structural and therefore excitonic properties. Specifically, we encapsulated the nanotubes in solution with non-excitonic materials such as silica while monitoring their optical properties via steady-state absorption spectroscopy in order to probe any structural changes during the encapsulation process. This encapsulation process is a pivotal first step towards the well-defined linking of the plasmonic MNPs to these excitonic nanotubes.

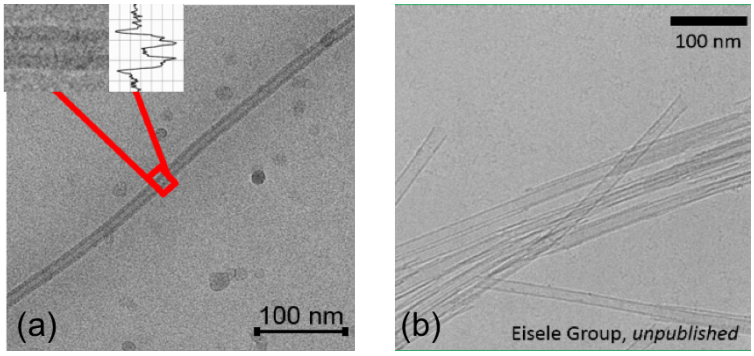

Figure 2: CryoTEM images of two kinds of well-characterized Frenkel excitonic supramolecular nanotubes. Nanotubes self-assembled from (a) cyanine C8S3 and (b) porphyrin TSPP. [Eisele *et al.* unpublished]

Future plans. The immediate next steps will be to synthesize the plexcitonic model systems by electrostatically linking our plasmonic MNPs via organic ligands with these encapsulated excitonic nanotubes in solution. We will then perform thorough sample characterization including studying the morphological, structural as well as optical properties of our plexcitonic model system on both, the ensemble (in solution) as well as on the individual object (immobilized onto solid substrates). Specifically, this will involve characterizing the nanoscale luminescence of the plexcitonic systems by near-field scanning optical microscopy (NSOM) as well as detailed analysis of their photophysical dynamics by femtosecond transient absorption spectroscopy. Our first samples will enable determination of relevant length and time scales for plexcitonic states and processes in these hybrid systems. These data will also serve as a baseline for structural homogeneity of the materials as we develop sophisticated Microfluidic methods to attain precise control over both the preparation of component materials and their nanoconjugation into hybrid structures.

DOE Sponsored Publications.

No publications yet. This is a new project (project start: September 15th, 2017).

Water Oxidation in Catalyst Modified Metal Organic Frameworks

Shaoyang Lin, Pavel Usov, Spencer Ahrenholtz, Amanda J. Morris
Department of Chemistry
Virginia tech
Blacksburg, VA 24060

We have explored the incorporation of known homogeneous, molecular water oxidation catalysts into stable zirconium-based metal organic framework backbones, namely, Ru(terpyridine)(dicarboxybipyridine)(H_2O)-doped UiO-67 and PCN-224-Ni. Importantly, Zr-frameworks exhibit superior stability relative to previously employed MOF water oxidation catalysts. We extensively characterized the MOFs pre- and post- electrolysis with powder X-ray diffraction, SEM, XPS, and ICP-MS (MOF and electrolyte solution) and demonstrated that there is no observable degradation of the parent MOF. Additional findings regarding the two projects are summarized below:

Ru(terpy)(dcbpy)(H_2O)-doped UiO-67. Herein, we explored electron transport and catalysis as a function of catalyst loading. Similar to what we observed for energy transfer (other DOE-sponsored work), as the loading of the catalyst was increased, the available pathways for charge transport also increased. CVs were performed at scan rates ranging from 10 to 1000 mV/s on the MOF thin films with different electroactive site coverages. An analysis of the data revealed a change in dependence of peak current to the log of the scan rate from 1 to 0.5 as catalyst loading was increased. The change indicates that the mechanism of charge transfer shifted from a surface-dominant process (slope of 1) to a diffusion controlled ambipolar redox-hopping process (slope of 0.5), **Figure 5**. The rate of charge transport estimated from the apparent diffusion coefficient was 1.3 (±0.5) ×10^{-9} cm^2/s. The observation of diffusion controlled charge transport provides some of the first support for *in*-MOF reduction and catalytic activity. As catalyst loading is increased, up to 32.1% of the poly-dispersed catalyst population was accessible and active. Thus, molecularly-modified MOF platforms can be utilized to realize high packing densities of electroactive water oxidation catalysts on electrodes. The highest electroactive site coverage of the film recorded here is more than **120 times higher** than a full packing monolayer of the homogenous analog on the same FTO electrode (~1×10^{-10} mol/cm^2).

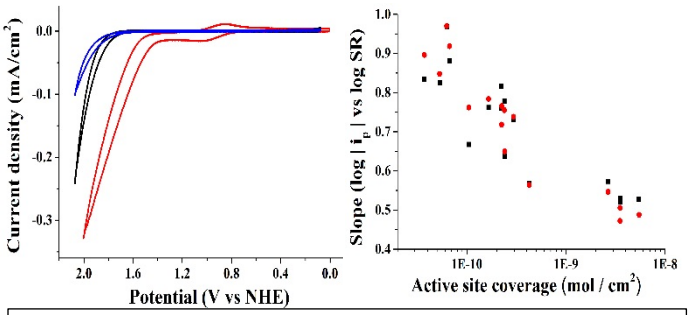

Figure 1. (Left) Cyclic voltammetry of FTO (black), UiO-67 thin film (blue), Ru-UiO-67 thin film (red) measured in 0.1 M $NaClO_4$, 50 mM MOPS buffer (pH 6.8) at a scan rate of 100 mV/s. The take-off in current at ~1.4 V vs. NHE is due to H_2O oxidation. **(Right)** The slope of log $|i_p|$ vs. log (scan rate) plot as a function of electroactive site coverage level (red, cathodic peak; black anodic peak for $Ru^{II/IV}$ couple at ~0.8 V vs. NHE at pH 6.8).

RuTERPY-UiO-67 oxidized water with activity similar to the homogeneous molecular analog. The Ru-doped MOF thin film produced 0.7 (± 0.5) µmol of O_2, over the course of the CPE experiments, compared to 0.17 (± 0.09) µmol for the UiO-67 thin film and 0.481 (± 0.009) µmol for unmodified FTO. Comparing the Faradaic efficiency of these three different electrodes (55 ± 6% for Ru-UiO-67, 48.7 ± 0.8% for FTO, 27 ± 6% for UiO-67), the values also supports the

conclusion that the incorporated Ru WOC played a critical role in the electrochemical WOR. Rotating ring disc experiments (RRDEs) confirmed the production of oxygen simultaneous to the increase in current observed for RuTERPY-UiO-67. Since not all the Ru WOCs in MOF thin film are electroactive, the electroactive site coverages of the thin films were used to calculate the turnover frequency (TOF) of the Ru-UiO-67 thin film, which was found to be 0.2 (± 0.1) s^{-1}.

PCN-224-Ni. In this work, we observed evidence of synergistic electron transfer/proton abstraction process occurring inside PCN-224-Ni between the linker and the inorganic node. Films of PCN-224-Ni were grown in situ on FTO and were found to electrochemically facilitate the water oxidation reaction at near neutral pH. The mechanism of water oxidation at PCN-224-Ni was found to proceed via the initial oxidation of the porphyrin linker followed by binding of water to the Ni(II) of Ni(II)TCPP, **Figure 2**. Subsequent proton transfer to the Zr nodes enabled the eventual release of O_2. The observed cooperative chemistry demonstrates a new strategy for water oxidation catalyst development via the incorporation of independent species (linker and node) competent in one component of the overall desired reactivity into MOF catalytic assemblies. The approach mirrors work on the effect of second coordination sphere manipulation on the activity of molecular catalysts, but on the supramolecular scale. Ultimately, the proton transfer limited the catalytic ability of the material. As available protonation sites were occupied, the catalytic activity diminished and limiting the possible turn-over to one.

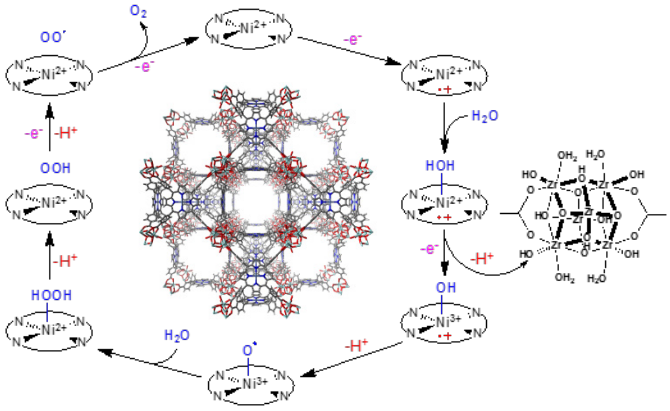

Figure 2. The catalytic cycle proposed for water oxidation by PCN-224-Ni. At neutral pH, the zirconium-node was the putative proton acceptor. (Center) The crystal structure of PCN-224-Ni, showing channels of 19Å.

DOE Sponsored Publications 2015-2018

1. Zhu, J.; Shaikh, S.; Mayhall, N. J.; Morris, A. J. Energy Transfer in Metal-Organic Frameworks. In Elaboration and Applications of Metal-Organic Frameworks; Series on Chemistry, Energy and the Environment; World Scientific, 2017; Vol. Volume 2, pp 581–654.

2. Zhu, J.; Usov, P.; Xu, W.; Celis-Salazar, P.J.; Lin, S.; Kessinger, M.C.; Landaverde-Alvardo, C.; Cai, M.; May, A.M.; Slebodnick, C.; Zhu, D.; Senanyake, S.D.; Morris, A.J.* "A New Class of Metal-Cyclam based Zirconium Metal-Organic Frameworks for CO_2 Adsorption and Chemical Fixation." J. Am. Chem. Soc., 2018, 140, 993-1003

3. Lin, S; Ravari, A.K., Zhu, J.; Usov, P.; Cai, M.; Ahrenholtz, S.R.; Pushkar, Y.; Morris, A.J.* "Insights into MOF Reactivity: Chemical Water Oxidation Catalysis $[Ru(tpy)(dcbpy)OH_2]^{2+}$ Modified Metal-Organic Framework." ChemSusChem, 2018, 11, 463-471.

4. Rowe, J. M.; Soderstrom, E. M.; Zhu, J.; Usov, P. M.; Morris, A. J.* "Synthesis, Characterization and Luminescent Properties of Two New Zr(IV) Metal-Organic Frameworks Based on Anthracene Derivatives." Can. J. Chem. 2017. DOI: 10.1139/cjc-2017-0445

5. Zhu, J.; Maza, W.A.; Morris, A.J.* “Light-harvesting and Energy Transfer in Ruthenium(II)-polypyridyl-doped Zirconium(IV) Metal-organic Frameworks: A look toward solar cell applications.” J. Photochem. Photobiol. A: Chem, 2017, 344, 64-77.

6. Usov, Pavel M.; Huffman, Brittany; Epley, C.C.; Kessinger, Matthew C.; Zhu, Jie; Maza, W.A.; Morris, A.J.* "Study of Electrocatalytic Properties of Metal–Organic Framework PCN-223 for the Oxygen Reduction Reaction." ACS Appl. Mater. Interfaces, 2017, 9, 33539-33543.

7. Rowe, J.M.; Hay, J.M.; Maza, W.A.; Chapleski, R.C.; Soderstrom, E.; Troya, D.; Morris, A.J.* “Systematic Investigation of the Excited-State Properties of Anthracene-Dicarboxylic Acids.” J. Photochem. Photobio. A: Chem., 2017, 337, 207-215.

8. Lin, S.; Pineda-Galvan, Y.; Maza, W.A.; Epley, C.C.; Zhu, J.; Kessinger, M.C.; Pushkar, Y.; Morris, A.J.* “Electrochemical Water Oxidation by a Catalyst-Modified Metal Organic Framework Thin Film.” ChemSusChem, 2017, 10, 514-522.

9. Usov, P.M.; Ahrenholtz, S.R.; Maza, W.A.; Stratakes, B.; Epley, C.C.; Kessinger, M.C.; Zhu, J.; Morris, A.J.* “Cooperative Electrochemical Water Oxidation by Zr Nodes and Ni-porphyrin Linkers of a PCN-224 MOF Thin Film.” J. Mater. Chem. A, 2016, DOI: 10.1039/c6ta05877a.

10. Padilla, R.; Maza, W.A.; Dominijanni, A.J.; Winkel, B.S.J; Morris, A.J.*; Brewer, K.J. “Pushing the Limits of Structurally-Diverse Light-Harvesting Ru(II) Metal-Organic Chromophores for Photodynamic Therapy.” J. Photochem. Photobiol. A.: Chem., 2016, 322, 67-75.

11. Maza, W.A.; Morris, A.J.*; Mul, G.* (2016) Photocatalytic Conversion of CO_2 to Fuels by Novel Green Photo-active Nanomaterials, in Sustainable Energy and Environment Remediation (1st Edition), Edited by Nuraje, N.; Asmatula, R.; Mul, G., Royal Society of Chemistry, 202-239.

12. Maza, W.A.; Haring, A.J.; Ahrenholtz, S.R.; Epley, C.C.; Lin, S.Y.; Morris, A.J.* "Ruthenium(II)-polypyridyl metal-organic frameworks as a new class of sensitized solar cells." Chem. Sci. 2016, 7, pp 719-727.

13. Maza, W. A.; Padilla, R.; Morris, A.J.* "Concentration dependent dimensionality of resonance energy transfer in a post-synthetically doped morphologically homologous analogue of UiO-67 MOF with a ruthenium (II) polypyridyl complex." J. Am. Chem. Soc. 2015, 137 (25), pp 8161–8168.

Fundamental Studies of Light-induced Charge Transfer, Energy Transfer, and Energy Conversion with Supramolecular Systems

Joseph T. Hupp
Department of Chemistry
Northwestern University
Evanston, IL 60093

This project is focused on advancing our understanding of: a) broad-spectrum, molecule-based light harvesting, b) long range, directional energy transfer and transport, c) rate-tunable, directional charge transfer and transport, in complex, yet well defined, many-component molecular systems of potential relevance for photochemical and photo-electrochemical energy conversion, and d) synthesized arrays of atomically well-defined clusters as computationally tractable models for metal-oxide photo-electrodes. The project approach centers on the creation and functional evaluation of extended, ordered molecular chromophoric and/or redox arrays. The project builds on synthesis advances in metal-organic framework (MOF) chemistry that permit complex structures to be constructed in automated, reproducible, and molecularly precise fashion as oriented, composition-tunable, thin films on electrodes or other platforms. Ultimately, these advances should provide a basis for assembling systems that functionally mimic the antenna behavior of the natural photosynthetic system, as well as the redox gradient construct that enables charge separation and energy conversion to be accomplished. The meeting presentation will touch on one or more of the following studies:

1. *Modulating rates of charge hopping.* Charge transport, an essential element of photoelectrochemical energy conversion via electrode-supported MOFs metal–organic frameworks, can be a kinetic bottleneck, especially when coupling to catalytic reactions. The limitation is understandable, as most MOFs are electrical insulators, at least at relevant electrochemical potentials. One approach for engendering conductivity in MOFs is through charge hopping between isolated redox-active sites in the framework. Nevertheless, the outcome often is only modest conductivity, with the behavior being attributed to weak electronic coupling between redox-active sites. At the same time, the slow charge-hopping associated with low conductivity may be desirable if back-electron (or hole) transfer to a catalytic or chromophoric component is important. Ideally, redox-based MOF conductivity, and the underlying charge-

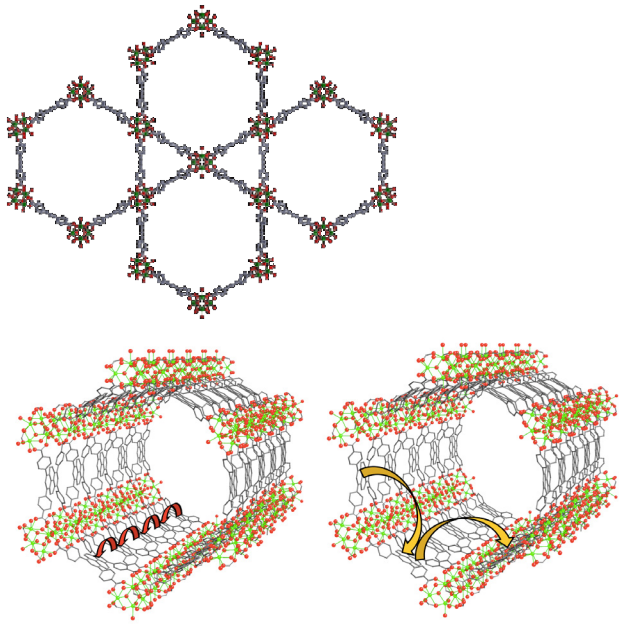

Cartoons of directional charge transport in the MOF, NU-1000, *i.e.* along hexagonal channel axis (left) or laterally from channel to channel. For simplicity, hopping steps in only single channels are sketched.

hopping process, would be tunable over an extended range, so as to obtain optimal behavior for a given application. We find that modulation of redox conductivity in electrode-supported, thin-films of the water-stable, Zr-based "platform MOF," NU-1000, by taking advantage of its anisotropic crystal shape and by employing complementary film deposition techniques. We find that electronic coupling between redox-active linkers is significantly greater along the MOF crystallite *c*-axis than through the *ab* plane. One consequence, is that solvothermally grown films (*c*-axis normal to the supporting electrode) are ~100-fold more conductivity in electrochemical applications than films of the same MOF that have been organized films formed via electrophoretic deposited MOF films (*c*-axis parallel to the supporting electrode).

2. *Boosting molecular-exciton transport distances.* Porphyrins are attractive model chromophores for understanding light-harvesting and energy transfer/transport within MOFs. We find that preferentially oriented, electrode-supported, pillared-paddlewheel MOF architectures are advantageous for constraining energy *transport* to directions to and from the underlying electrode (the *z* direction), as opposed to random transport based on identical rates for energy *transfer* (*i.e.* exciton hopping) in the *x*, *y,* and *z* directions. An immediate consequence is scaling of root-mean-square displacements of excitons as $N^{1/2}$ rather than $N^{1/6}$ where N is the number of exciton hops achieved within the brief lifetime of the photo-generated exciton. The change in scaling greatly increases energy-transport distances. We find that transport can be substantially further boosted by altering the lengths of MOF pillars (nonchromophoric organic linkers oriented in the *z* direction). Somewhat surprisingly, given short hopping distances, the behavior can be effectively modeled by treating tetra-phenyl-porphyrin units as point dipoles.

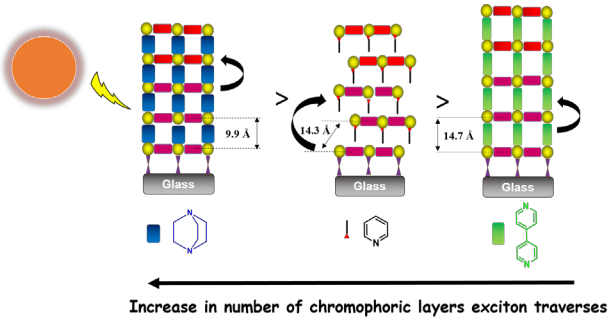

3. *Coupling redox hopping to chemical steps to modulate kinetics.* We recently described the installation of a ferrocene derivative on and within the archetypal metal–organic framework (MOF), UiO-66, by solvent assisted ligand incorporation (SALI). Thin films of the resulting material show a redox peak characteristic of the Fc/Fc^+ couple as measured by cyclic voltammetry. Consistent with restriction of redox reactivity solely to Fc molecules sited at or near the external surfaces of MOF crystallites, chronoamperometry measurements indicate that less than 20% of the installed Fc molecules are electrochemically active. Charge-transport diffusion coefficients, D_{ct}, of 9 x 10^{-10} cm^2/s and 125 x 10^{-10} cm^2/s were determined from potential step measurements, stepping oxidatively and reductively, respectively. The fourteen-fold difference in D_{ct} values contrasts with the expectation, for simple systems, of identical values for oxidation-driven versus reduction-driven charge transport. The origin of the striking difference is in coupling of a chemical step, ion insertion or expulsion, to the charge-hopping process. The findings have implications for the design of MOFs suitable for delivery of redox equivalents to framework-immobilized electrocatalysts and/or delivery of charges from chromophoric MOF films to electrodes.

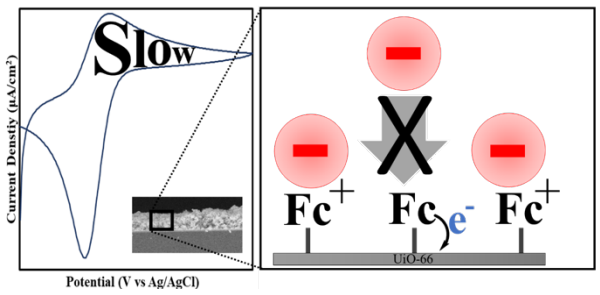

DOE Sponsored Publications 2015-2018

"Post-Assembly Atomic Layer Deposition of Metal-Oxide Coatings Enhances the Performance of an Organic Dye-Sensitized Solar Cell by Suppressing Dye Aggregation," Ho-Jin Son, Chul Hoon Kim, Dong Wook Kim, Nak Cheon Jeong, Chaiya Prasittichai, Langli Luo, Jinsong Wu, Omar K. Farha, Michael R. Wasielewski, Joseph T. Hupp, *ACS Applied Materials & Interfaces*, **2015**, *7*, 5150–5159. DOI: 10.1021/am507405b

"Metal-organic Framework Materials for Light-Harvesting and Energy Transfer," Monica C. So, Gary P. Wiederrecht, Joseph E. Mondloch, Joseph T. Hupp, Omar K. Farha, *Chem. Commun*., **2015**, *51*, 3501-3510. DOI: 10.1039/C4CC09596K

"Dynamics of Back Electron Transfer in Dye-Sensitized Solar Cells Featuring 4-tert-Butyl-pyridine and Atomic-Layer-Deposited Alumina as Surface Modifiers," *J. Phys. Chem. B*, **2015**, *119*, 7162–7169. DOI**:** 10.1021/jp506083a

"Electrochemically Addressable Trisradical Rotaxanes Organized Within a Metal-Organic Framework," P. R. McGonigal, P. Deria, I. Hod, P. Z. Moghadam, A.-J. Avestro, N. E. Horwitz, I. C. Gibbs-Hall, A. K. Blackburn, D. Chena, Y. Y. Botros, M. R. Wasielewski, R. Q. Snurr, J. T. Hupp, O. K. Farha, and J. F. Stoddart, *Proc. Natl. Acad. Sci. USA*, **2015**, *112*, 11161-8. DOI: 10.1073/pnas.1514485112

"Porphyrin-based metal-organic framework thin films for electrochemical nitrite detection," C-W. Kung, T-H. Chang, L-Y. Chou, J. T. Hupp, O. K. Farha, K-C. Ho, *Electrochemistry Communications*, **2015**, *58*, 51–56. DOI: http://dx.doi.org/10.1016/j.elecom.2015.06.003

"Enhancement of the Yield of Charge Separation in Zinc Porphyrin-CdSe Quantum Dot Donor-Acceptor Complexes by a Dithiocarbamate Linkage," Shengye Jin, Mario Tagliazucchi, Ho-Jin Son, Rachel D. Harris, Kenneth O. Aruda, David J. Weinberg, Alexander B. Nepomnyashchii, Omar K. Farha, Joseph T. Hupp, Emily A. Weiss, *J. Phys. Chem. C*, **2015**, *119*, 5195–5202. DOI: 10.1021/acs.jpcc.5b00074

"Bias-switchable Permselectivity and Redox Catalytic Activity of a Ferrocene-Functionalized, Thin-Film Metal Organic Framework Compound," Idan Hod, Wojciech Bury, Daniel M. Gardner, Pravas Deria, Vladimir Roznyatovskiy, M. R. Wasielewski, O. K. Farha, J. T. Hupp, *J. Phys. Chem. Lett.*, **2015**, *6*, 586–591. **DOI:** 10.1021/acs.jpclett.5b00019

"One Electron Changes Everything. A Multispecies Copper Redox Shuttle for Dye-Sensitized Solar Cells," William L. Hoffeditz, Michael J. Katz, Pravas Deria, George E. Cutsail III, Michael J. Pellin, Omar K. Farha, and Joseph T. Hupp, *J. Phys. Chem. C*, **2016**, *120*, 3731–3740. DOI: 10.1021/acs.jpcc.6b01020

"Toward Metal–Organic Framework-Based Solar Cells: Enhancing Directional Exciton Transport by Collapsing Three-Dimensional Film Structures" Subhadip Goswami, Lin Ma, Alex B. F. Martinson, Michael R. Wasielewski, Omar K. Farha, and Joseph T. Hupp *ACS Appl. Mater. Interfaces*, **2016**, *8*, 30863–30870. DOI: 10.1021/acsami.6b08552

"Barrier-layer-mediated Electron Transfer from Semiconductor Electrodes to Molecules in Solution. Sensitivity of Mechanism to Layer Thickness", Jason R. Avila, Michael J. Katz, Omar K. Farha, Joseph T. Hupp, *J. Phys. Chem. C*, **2016**, *120*, 20922–20928. **DOI:** 10.1021/acs.jpcc.6b02651

"Modulating the Rate of Charge Transport in a Metal–Organic Framework Thin Film Using Host:Guest Chemistry," I. Hod, O. K. Farha and J. T. Hupp, *Chem. Commun*., **2016**, *52*, 1705-1708. **DOI:** 10.1039/C5CC09695B

"Layer-by-Layer Assembled Thin Films of Perylene Diimide- and Squaraine-Containing Metal-Organic-Framework-like Materials: Solar Energy Capture and Directional Energy Transfer," Hea Jung Park, Monica C. So, David Gosztola, Gary P. Wiederrecht, Jonathan D. Emery, Alex B. F. Martinson, Süleyman Er, Christopher E. Wilmer, Nicolaas A. Vermeulen, Alán Aspuru-Guzik, J. Fraser Stoddart, Omar K. Farha, and Joseph T. Hupp, *ACS Appl. Mater. Interfaces*, **2016**, *8*, 24983–24988. DOI: 10.1021/acsami.6b03307

"Engendering Long-Term Air and Light Stability of a TiO_2-supported Porphyrinic Dye via Atomic Layer Deposition," William L. Hoffeditz, Ho-Jin Son, Michael J Pellin, Omar K. Farha, and Joseph T. Hupp *ACS Appl. Mater. Interfaces*, **2016**, *8*, 34863-34869. DOI: 10.1021/acsami.6b10844

"A Redox-Active Bistable Molecular Switch Mounted Inside a Metal-Organic Framework," Qishui Chen, Junling Sun, Peng Li, Idan Hod, Peyman Z. Moghadam, Zachary S. Kean, Randall Q. Snurr, Joseph T. Hupp, Omar K. Farha, and J. Fraser Stoddart *J. Am. Chem. Soc.*, **2016**, *138*, 14242–14245. DOI: 10.1021/jacs.6b09880

"Proton Conducting Self-Assembled MOF/Polyelectrolyte Hollow Hybrid Nanostructures," Unal Sen, Mustafa Erkartal, Chung-Wei Kung, Vijay Ramani, Joseph T. Hupp, and Omar K. Farha, *ACS Appl. Mater. Interfaces*, **2016**, *8*, 23015–23021. DOI: 10.1021/acsami.6b05901

"G-Quadruplex Organic Frameworks," Yi-Lin Wu, Noah E. Horwitz, Kan-Sheng Chen, Diego A. Gomez-Gualdron, Norman S. Luu, Lin Ma, Timothy C. Wang, Mark C. Hersam, Joseph T. Hupp, Omar K. Farha, Randall Q. Snurr, Michael R. Wasielewski, *Nature Chemistry*, published online, Dec. 19, **2017**, *9*, 466. DOI: 10.1038/NCHEM.2689

"Rendering High Surface Area, Mesoporous Metal-Organic Frameworks Electronically Conductive," T. Wang, I. Hod, C. Audu, N. Vermeulen, S. T. Nguyen, O. K. Farha, J. T. Hupp, *ACS Applied Materials & Interfaces* **2017**, *9*, 12584-12591. DOI: 10.1021/acsami.6b16834

"Determining the Conduction Band Potential of Nb_2O_5 Fabricated by Atomic Layer Deposition via Electrochemical Impedance Spectroscopy and Mott-Schottky Analysis," William L. Hoffeditz, Michael J. Pellin, Omar K. Farha, Joseph T. Hupp, *Langmuir*, **2017**, *33*, 9298-9303. DOI: 10.1021/acs.langmuir.7b00683.

"Intramolecular Energy and Electron Transfer Within a Diazaperopyrenium-Based Cyclophane," Gong, Xirui, Ryan M. Young, Karel J. Hartlieb, Claire Miller, Yilei Wu, Hai Xiao, Peng Li, Nema Hafezi, Jiawang Zhou, Lin Ma, Tao Cheng, William A Goddard III, Omar K Farha, Joseph T Hupp, Michael R Wasielewski, J Fraser Stoddart, *Journal of the American Chemical Society*, **2017**, *139*, 4107-4116. DOI: 10.1021/jacs.6b13223

"Postsynthetic Tuning of Metal–Organic Frameworks for Targeted Applications," Islamoglu, Timur, Subhadip Goswami, Zhanyong Li, Ashlee J. Howarth, Omar K. Farha, and Joseph T. Hupp, *Accounts of Chemical Research*, **2017**, *50*, 805-813. DOI: 10.1021/acs.accounts.6b00577

"Tunable Crystallinity and Charge Transfer in Two-Dimensional G-Quadruplex Organic Frameworks," Yi-Lin Wu, N. Scott Bobbitt, Jenna L. Logsdon, Natalia E. Powers-Riggs, Jordan N. Nelson, Xiaolong Liu, Timothy C. Wang, Randall Q. Snurr, Joseph T. Hupp, Omar K. Farha, Mark C. Hersam, Michael R. Wasielewski, *Angewandte Chemie International Edition*, **2018**, *57*, 3985-3989. DOI: 10.1002/anie.201800230

"Electroactive Ferrocene at or near the Surface of Metal–Organic Framework UiO-66," Rebecca H. Palmer, Jian Liu, Chung-Wei Kung, Idan Hod, Omar K. Farha, Joseph T. Hupp, *Langmuir*, **2018**, *34*, 4707-4714. DOI: 10.1021/acs.langmuir.7b03846

"Examination and Mitigation of Electron Interception Processes in Dye-Sensitized Solar Cells Through Redox Shuttle and Photoelectrode Modification," William L. Hoffeditz, Ph.D. Thesis, Dept. of Chemistry, Northwestern University, Evanston, IL 60208.

Metal-Tipped and Electrochemically Wired Semiconductor Nanocrystals: Modular Constructs for Directed Charge Transfer

Neal R. Armstrong, Jeffrey Pyun, S. Scott Saavedra
Department of Chemistry/Biochemistry
University of Arizona
Tucson, Arizona 85721

DOE supported research efforts are focusing on: i) development of new synthetic routes to symmetrically and asymmetrically metal- and metal oxide- tipped CdSe and CdS nanorods (NRs); ii) development of new measurement science approaches for characterization of band edge energies (E_{CB}/E_{VB}) which control energy conversion efficiencies (including spectroelectrochemical approaches for estimation of E_{CB}, and UV-photoemission approaches to estimation of E_{VB}) -- these approaches allow unique quantification of mid-gap state densities, especially following addition of metal (catalyst) tips; iii) development of new routes to monodisperse CdSe@CdS tetrapods (TPs), providing precise control over energetics (Type I versus quasi-Type II heterojunctions) via control of CdSe seed size (Fig. 1). Creation of these new nanostructured materials has enabled experiments which probe dynamics of charge formation, charge harvesting and recombination (collaborations with the Lian group, Emory) all of which point to the important role that defect sites along the NR or TP arm play in limiting energy conversion efficiencies. New routes for passivation of these states have been developed, and we now return to "wiring" of these TP constructs to (oxide) hole-harvesting/electron-blocking contacts, using complementary approaches to mitigation of recombination sites on the TP, recombination (and short circuit) sites on the contact and efficient harvesting of photogenerated charges.

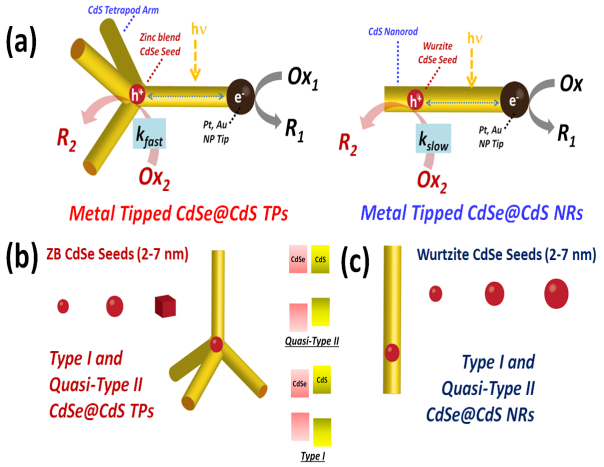

Fig. 1 -- (a) Schematics for photocatalysis at metal-tipped CdSe@CdS TPs and NRs, where slow hole extraction is observed from CdSe seeds due to deep hole traps. (b) Synthesis of CdSe@CdS TPs of varying ZB CdSe seed sizes. (c) Synthesis of CdSe@CdS NRs of varying wurtzite CdSe seed sizes. These synthetic approaches enable a systematic approach to the characterization of the factors that limit energy conversion efficiencies in these and related nanomaterials. Key findings suggest that the size of the CdSe seed ultimately controls both the growth of the rod (or arms of the tetrapod), and the energetics of the resultant heterostructure (Type I or quasi-Type II heterojunctions), which ultimately control the probability for hole-trapping at the seed. The differences in seed size also can control the rate and extent of asymmetric metal tipping (Au, Pt) of these constructs, and by inference, the efficiency of photo-induced charge separation. Recent photoemission spectroscopy, and spectroelectrochemical studies, however, demonstrate that the process of metal tipping may introduce new mid-gap (MIS-like) states within the bandgap region, tailing out to E_F, which represent spatially heterogeneous PtS_x-like states, and which are also likely to be charge traps. Addition of ZnS "shells" around the NR or TP appear to be one route to mitigation of these trap states, and we are evaluating these and related electrochemical wiring and passivation strategies for creation of planar arrays of metal-tipped TP photoelectrochemical platforms.

Ultrafast Vibrational Nano-Thermometers Probe Triplet Separation vs. Relaxation During Singlet Fission

Eric R. Kennehan, Grayson S. Doucette, Christopher Grieco and John B. Asbury
Department of Chemistry
The Pennsylvania State University
University Park, PA 16802

The objective of this research is to understand and control the electronic states and their dynamics that lead to triplet exciton multiplication by singlet fission to enable design rules for development of new singlet fission chromophores. Predictive correlations are sought about how molecular structure and crystalline packing arrangements influence the rate and yield of correlated triplet pair (CTP) separation using ultrafast mid-infrared (mid-IR) spectroscopy, which probes vibrational modes of singlet fission chromophores as local 'nano-thermometers.' This approach permits direct examination of relaxation processes that compete with CTP separation on ultrafast time scales.

We demonstrate that ultrafast vibrational spectroscopy in the mid-IR spectral range provides the opportunity to probe the dynamics of electronic states involved in all stages of the singlet fission reaction through their unique vibrational frequencies. This capability was first demonstrated using a model singlet fission chromophore, 6,13-bis(triisopropylsilylethynyl) pentacene (TIPS-Pn). The alkyne groups of the TIPS side chains are coupled to the conjugated framework of the pentacene cores, enabling direct examination of the dynamics of triplet excitons that have successfully separated from CTP intermediates in crystalline films of TIPS-Pn. Relaxation processes during the separation of triplet excitons and triplet-triplet annihilation after their separation result in the formation of hot ground state molecules that also exhibit unique vibrational frequencies.

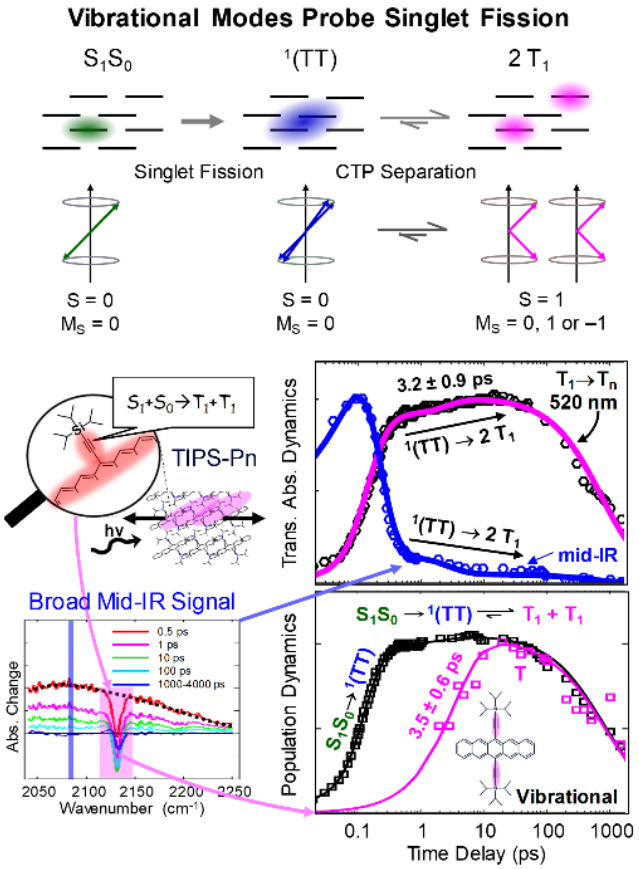

Furthermore, we demonstrate that complete CTP separation occurs on the 100 ps to 1 ns time scales, even in pentacenes for which the primary singlet fission events occur on the ~100 fs time frame. These findings reveal that electronic relaxation processes that compete with singlet fission need to be controlled on longer time scales than previously believed.

Finally, we demonstrate that the dynamics of CTP separation in TIPS-Pn are controlled by triplet energy transfer. This was demonstrated by comparing CTP separation rates with the diffusion constants of triplet excitons in different polymorphs exhibiting markedly different electronic coupling among the molecules.

Sensitization Strategies for Energy Level Alignment of Photoactive Molecules at Oxide Semiconductor Surfaces

Jonathan Viereck,[1] Sylvie Rangan,[1] Yuan Chen,[2] Robert A. Bartynski[1] and Elena Galoppini[2]

[1]Department of Physics & Astronomy and Laboratory for Surface Modification, Rutgers University-New Brunswick, Piscataway, NJ
[2]Department of Chemistry, Rutgers University-Newark, Newark, NJ

Electron transfer at the interface between a chromophore and large bandgap nanostructured metal oxide semiconductors remains at the center of intense research in numerous areas of solar energy conversion, including photocatalysis, photovoltaics, and artificial photosynthesis. A key goal of our DOE-supported research is to address different ways of controlling the energy level alignment between an adsorbed chromophore and an oxide semiconductor surface through a combination of synthetic design and surface studies. This poster will describe two strategies explored on single crystal oxide semiconductor [TiO_2(110)] surfaces to achieve our goal: **(I)** a synthetically accessible **"mixed-layer" approach,** where the oxide surface is sensitized by sequential exposure to solutions of dipole-linkers and chromophoric species, and **(II)** a synthetically challenging, but more elegant, **"chromophore-dipole"** approach where both the dipole-linker and chromophore are part of the same molecule. In approach (**I**), several dipole-containing molecules including helical peptides and $Si(Me)_3$ terminated molecules with dipole-linkers, were co-deposited with ZnTPP terminated molecules on TiO_2(110) (See Fig. 1). Surfaces sensitized with either molecule alone indicated that the molecules remain intact when they bind to the surface and form a monolayer coverage. However, sequential sensitization is accompanied by surface contamination, resulting in inconsistent and non-reproducible energy level shifts. The poster will describe alternative approaches, where a dipole layer is deposited in vacuum to functionalize and passivate the surface prior to binding the chromophore. Our most recent work involving the adsorption of perylene-based chromophores, as well as perylene-terminated helical peptide chains (see Fig. 2), on the TiO_2 surface will be also presented.

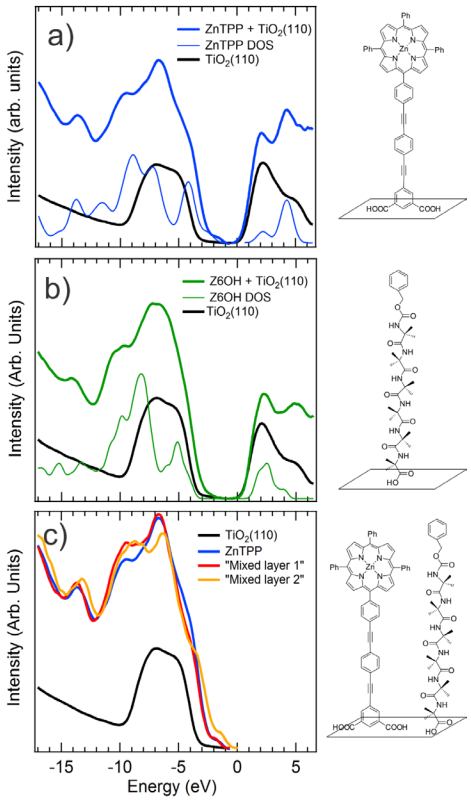

Fig. 1: Electronic structure of peptides and chromophore-bridge-anchor molecules on TiO_2(110).

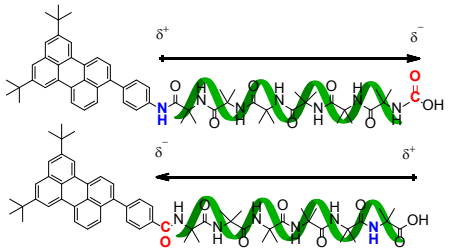

Fig. 2: Perylene-terminated helical peptide chains having opposite molecular dipoles.

n- and p-Type Impurity Doping in PbSe Quantum Dots

Daniel M. Kroupa[1,2], Haipeng Lu[1], Arthur J. Nozik[1,2], Xihan Chen[1], Gerard Carroll[1], Alexander Efros[3], Elisa Miller[1], Matthew C. Beard[1]

1. Chemistry and Nanoscience Center
National Renewable Energy Laboratory Institution
Golden, CO, 80007
2. Department of Chemistry
University of Colorado, Boulder,
Boulder, CO, 80401
3. Naval Research Laboratory
Washington, D.C.

Electronic impurity doping of bulk semiconductors is an essential component of semiconductor science and technology. Yet there are only a handful of studies demonstrating control of electronic impurities in semiconductor nanocrystals. Here, we studied electronic impurity doping of colloidal PbSe quantum dots (QDs) using postsynthetic cation exchange reactions in which Pb^{2+} cations are exchanged either for Ag^{+} or In^{3+} cations, to achieve p or n-type doping. We found that varying the concentration of dopant ions exposed to the as-synthesized PbSe QDs controls the extent of exchange. The electronic impurity doped QDs exhibit the fundamental spectroscopic signatures associated with injecting a free charge carrier into a QD under equilibrium conditions, including a bleach of the first exciton transition and the appearance of a quantum-confined, low-energy intraband absorption feature. Photoelectron spectroscopy confirms that Ag^{+} acts as a p-type dopant for PbSe QDs and infrared spectroscopy is consistent with $k \cdot p$ calculations of the size-dependent intraband transition energy. The electronic doping effect can be probed by spectroelectrochemical measurements, and for In^{3+} show characteristic n-type signatures, including both induced absorption and the shift of Fermi level. We find that to bleach the first exciton transition by an average of 1 carrier per QD requires that approximately 10% of the Pb^{2+} be replaced by Ag^{+}. We hypothesize that the majority of incorporated Ag^{+} remains at the QD surface and does not interact with the core electronic states of the QD. Instead, the excess Ag^{+} at the surface promotes the incorporation of < 1% Ag^{+} into the QD core where it causes p-type doping behavior. The dopants also induce an additional nonradiative relaxation pathways reducing the carrier lifetime.

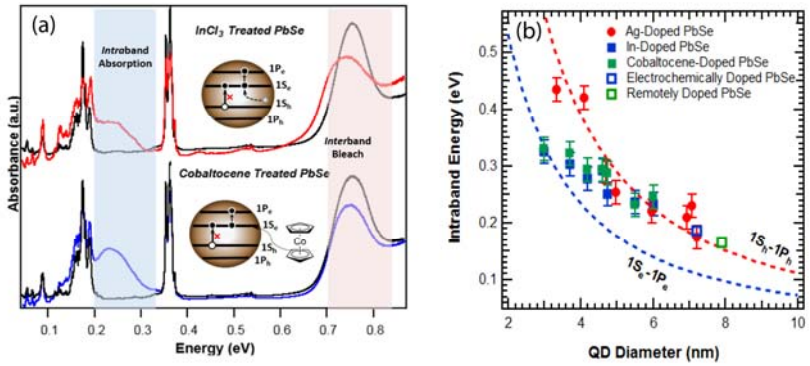

Figure. Left, comparison of the bleach and induced absorption for In3+ doped PbSe QDs and remote doping using colbaltocene to achieve n-type dopants. Intraband transition energy as a function of size for n and p-type doping.

C-H Bond Formation with CO_2: Mechanistic Insights and Structure-Function Correlations

Natalia D. Loewen, Cody R. Carr, Atefeh Taheri, Louise A. Berben
Department of Chemistry
University of California Davis
Davis, CA 95616

Our goal is to enable solar energy storage as fuel by selectively producing C-H bonds from CO_2 in water. We need to understand which kinetic and thermodynamic parameters are important in designing (electro)catalysts. This work builds on the catalytic activity of $[Fe_4N(CO)_{12}]^-$ (**1**$^-$) which selectively produces formate from CO_2 at -1.2 V vs. SCE in aqueous solutions, and is stable for over 24 h. Mechanistic investigations of this cluster guide future catalyst design.

Our current working hypothesis is that the reduced hydride, $[H\text{-}Fe_4N(CO)_{12}]^-$ (H-**1**)$^-$ is a key intermediate. Further investigations revealed that the (H-**1**)$^{1-/2-}$ redox couple is -0.91 V and this indicates that (H-**1**)$^{2-}$ can potentially be accessed at -1.2 V (Figure 1 left). Using IR-SEC we showed that (H-**1**)$^{2-}$ is very hydridic and that if (H-**1**)$^{2-}$ were formed it would react quickly to afford H_2. Since H_2 is not observed, we propose that (H-**1**)$^{2-}$ is not an intermediate in the reduction of CO_2 to formate and that (H-**1**)$^-$ remains the most likely intermediate. We have also established that hydride transfer to CO_2 is the rate determining step and inferred that hydride transfer is limited by $[CO_2]$, and that increased local $[CO_2]$ near active sites may provide faster and more selective catalysts for C-H bond formation in aqueous solutions: well designed CO_2-binding sites may turn H_2 evolution catalysts into selective C-H bond forming catalysts. With an Eyring analysis we provided a *kinetic* rationale for the faster rates of formate formation in water compared with MeCN, where we and others have previously given *thermochemical* rationale.

Moving toward next generation catalysts we installed functional groups that might increase local $[CO_2]$. CO_2 binding constants (K_{CO2}) were measured electrochemically for clusters substituted with dimethylaniline or pyridine: K_{CO2} for **1**$^-$, $[(Ph_2AnP)\text{-}\mathbf{1}]^-$, and $[(Ph_2pyP)\text{-}\mathbf{1}]^-$ are < 1, 2, and 8, respectively (Figure 1 middle and right). The Faradaic efficiency for formate with each cluster is 97, 30, and 0%, respectively, with the balance of the current going to H_2. This currently limited data set suggests an inverse correlation between CO_2 binding affinity and selectivity for CO_2 reduction which might result from decrease in the local pH as the local concentration of CO_2 is enhanced. Reactions at higher bulk pH and with additional derivatives are ongoing.

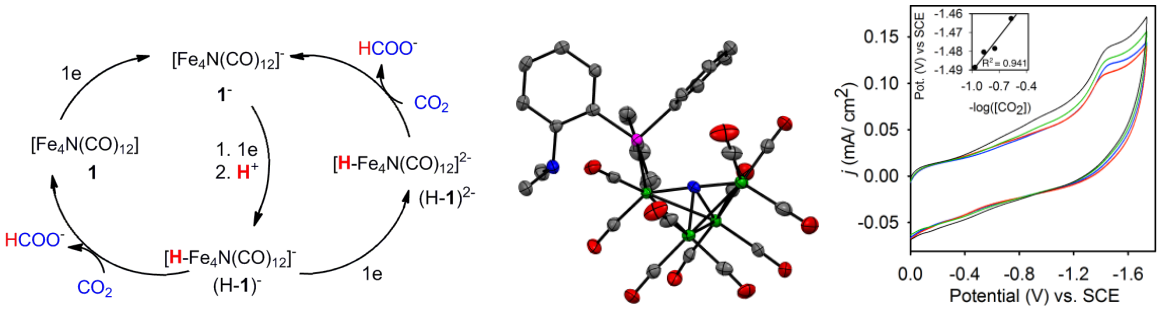

Figure 1. (**right**) Proposed mechanisms for reduction of CO_2 to formate by **1**$^-$. Left cycle: possible ECCE mechanism, and right cycle: possible ECEC mechanism. (**middle**) Structure of $[(Ph_2AnP)\text{-}\mathbf{1}]^-$. (**right**) CVs of 0.1 mM $[(Ph_2pyP)\text{-}\mathbf{1}]^-$ in dry MeCN, with increasing CO_2 (balance is N_2). Inset: peak potential vs. $-\log([CO_2])$ has slope 61 mV which represents one CO_2 molecule per cluster.

Ultrafast Charge Transfer and Slow Recombination at Semiconducting Single-Walled Carbon Nanotube Heterojunctions with Perylene Diimides

Jeffrey L. Blackburn,[#] Hyun Suk (Albert) Kang, [#] Dylan Arias, [#] Thomas J. Sisto,[*] Samuel Peurifoy,[*] Boyuan Zhang,[*] Colin Nuckols[*]
National Renewable Energy Laboratory, Materials Science Center; Golden, CO 80401
* Columbia University, Dept. of Chemistry; New York, New York 10027

Semiconducting single-walled carbon nanotubes (s-SWCNTs) are strong near-IR and visible absorbers, and have high mobilities for excitons and charges. As such, thin films of s-SWCNTs can be used in solar energy harvesting schemes to produce electricity or fuels. They are also informative model systems for understanding interfacial charge and energy transfer in quantum-confined semiconductors with low dielectric screening of excitons. Two of the primary areas we focus on within our research program involve the transport of energy (both excitons and charges) within s-SWCNT networks and the generation of long-lived charge separated states. This poster will highlight one of our recent studies exploring ultrafast charge transfer across carefully prepared and well-characterized interfaces between s-SWCNTs and non-fullerene small molecule acceptors. Non-fullerene electron acceptors have facilitated a recent surge in the efficiencies of organic solar cells, although fundamental studies of the nature of exciton dissociation at interfaces with non-fullerene electron acceptors are still relatively sparse.

In this study, we investigate excited-state photodynamics at the heterojunction between (6,5) s-SWCNTs and two perylene diimide (PDI)-based electron acceptors (**hPDI2-pyr-hPDI2** and **Trip-hPDI2**, Fig. 1). Transient absorption measurements demonstrate that photoinduced charge transfer occurs at the photoexcited bilayer interfaces, producing long-lived separated charges with lifetimes exceeding 1.0 μs. Both exciton dissociation and charge recombination occur more slowly for the **hPDI2-pyr-hPDI2** bilayer than for the **Trip-hPDI2** bilayer. To explain such differences, we discuss the potential roles of the thermodynamic charge transfer driving force available at each interface and the different molecular structure and inter-molecular interactions of PDI-based acceptors. Importantly, our results demonstrate that aggregates formed within the **hPDI2-pyr-hPDI2** help to delocalize the transferred electron away from the dissociation site, reducing the rate of geminate recombination. This is an important design rule for prolonging the charge-separated state in organic heterojunctions.

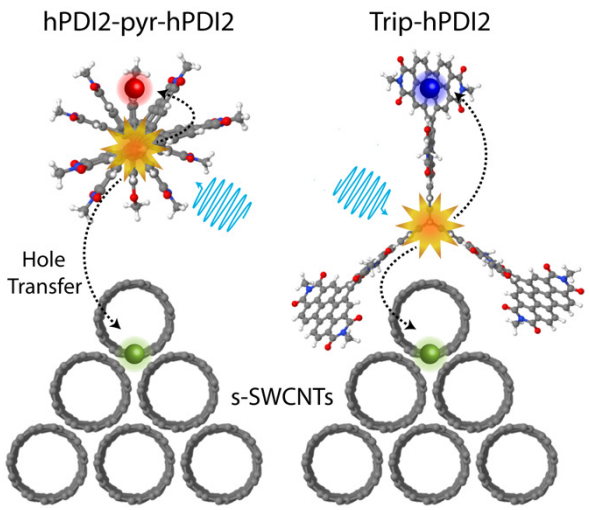

Figure 1. Ultrafast charge separation across s-SWCNT/PDI interfaces by picosecond photoinduced hole transfer.

Long-lived Charge Separation at Heterojunctions Between Semiconducting Single-walled Carbon Nanotubes and Perylene Diimide Electron Acceptors. Hyun Suk Kang, Thomas J. Sisto, Samuel Peurifoy, Dylan H. Arias, Boyuan Zhang, Colin Nuckolls, Jeffrey L. Blackburn. *J. Phys. Chem. C*, Article ASAP
DOI: 10.1021/acs.jpcc.8b01400 (Prashant Kamat festschrift)

Charge Transfer Processes in Catalyst-Coated Photoelectrodes for Solar Water Splitting

Shannon W. Boettcher
Department of Chemistry and Biochemistry
University of Oregon
Eugene, OR 97403

Light-absorbing semiconductor electrodes coated with electrocatalysts are key components of photoelectrochemical energy conversion and storage systems. Efforts to optimize these systems have been slowed by an inadequate understanding of the semiconductor-electrocatalyst interface. The semiconductor-electrocatalyst interface is important because it separates and collects photoexcited charge carriers from the semiconductor. The photovoltage generated across the interface drives "uphill" photochemical reactions, such as water splitting to form hydrogen fuel.

In this poster I will describe our latest efforts to understand the microscopic processes and materials parameters governing interfacial electron transfer between light-absorbing semiconductors, electrocatalysts, and solution, using new experimental "dual-working-electrode photoelectrochemistry" approaches. First, I report how direct electrical measurements show that $NiFeO_x$ catalyst layers deposited on α-Fe_2O_3 are efficient collectors of photoexcited holes, which then drive catalytic oxygen evolution.[1] These measurements directly address a longstanding debate on whether such layers on α-Fe_2O_3 indeed are acting as catalysts or only affecting the interface energetics / passivating surface states. Second, I will illustrate a previously unrecognized shunt recombination mechanism that limits the performance of many catalyst-coated oxide photoelectrodes.[2] Third, I report a new (photo)electrochemical atomic force microscopy technique to monitor hole accumulation, and the resulting potential changes, in catalyst layers in-situ with a conductive nanotip electrode probe (Fig. 1).[3] This technique enables the study of catalysts and photoelectrodes that were impossible to analyze by the macroscopic approach used previously.

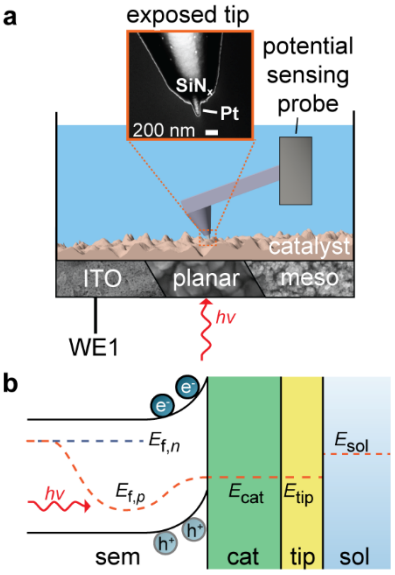

Fig. 1. Schematic illustration of (photo)electrochemical AFM technique developed to monitor interface electronic behavior and dynamics *in situ*.

1. Qiu, J.; Hajibabaei, H.; Nellist, M. R.; Laskowski, F. A. L.; Hamann, T. W.; Boettcher, S. W., Direct in Situ Measurement of Charge Transfer Processes During Photoelectrochemical Water Oxidation on Catalyzed Hematite. *ACS Cent. Sci.* **2017,** *3* (9), 1015-1025.
2. Qiu, J.; Hajibabaei, H.; Nellist, M. R.; Laskowski, F. A. L.; Oener, S. Z.; Hamann, T. W.; Boettcher, S. W., Catalyst Deposition on Photoanodes: The Roles of Intrinsic Catalytic Activity, Catalyst Electrical Conductivity, and Semiconductor Morphology. *ACS Energy Lett.* **2018**, DOI: 10.1021/acsenergylett.8b00336.
3. Nellist, M. R.; Laskowski, F. A. L.; Qiu, J.; Hajibabaei, H.; Sivula, K.; Hamann, T. W.; Boettcher, S. W., Potential-sensing electrochemical atomic force microscopy for in operando analysis of water-splitting catalysts and interfaces. *Nature Energy* **2018,** *3* (1), 46-52.

Modular Nanoscale and Biomimetic Systems for Photocatalytic Hydrogen Generation

Kara L. Bren, Richard Eisenberg, Todd D. Krauss
Department of Chemistry
University of Rochester
Rochester, NY14627-0216

Hydrogen (H_2) is a promising fuel and an important feedstock in the chemical industry. Currently, H_2 is primarily derived from natural gas, which itself is a valuable resource. In this collaborative project, we are developing new approaches to prepare H_2 from water in reactions driven by light. We are drawing on materials science, synthetic chemistry, biochemistry, and photochemistry to develop and investigate integrated systems for H_2 fuel production.

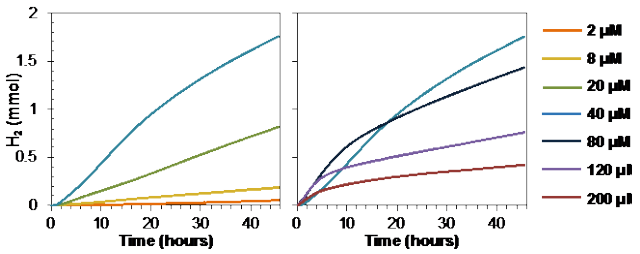

Fig. 1: Photocatalytic H_2 generation with CdSe QDs (1 μM) and varying concentrations of Ni-DHLA. Plots are separated for clarity.

Success with quantum dot (QD) photosensitizers for H_2 evolution has motivated our efforts to improve the performance of these systems. We studied efficiency of photocatalytic H_2 production using 4.4-nm CdSe QDs as photosensitizers and Ni-dihydrolipoic acid (Ni-DHLA) catalyst, and found that the efficiency increases with increasing Ni-DHLA:QD molar ratios (Fig. 1). Transient absorption spectroscopy of the electron transfer dynamics shows increasing electron transfer efficiencies for increased catalyst concentrations. These results suggest that increasing catalyst concentrations increases the probability of electron transfer from these larger QDs to Ni-DHLA, overcoming decreased surface electron density for large diameter QDs. Success with QD photosensitizers also inspired our development of a "rainbow" photocathode for delivering electrons to catalysts. This approach generates an energy gradient to funnel electrons to the surface and enhance charge separation (Fig. 2). This photocathode has been paired with molecular catalysts to enhance photon-to-H_2 efficiency.

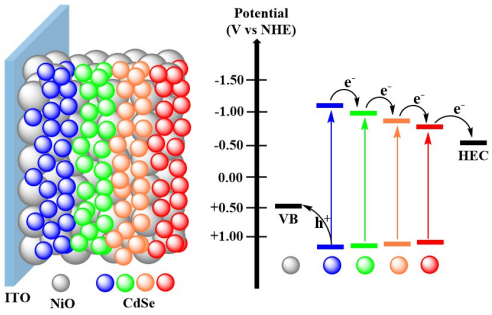

Fig. 2: Schematic of QD-sensitized rainbow photocathode employed for H_2 generation.

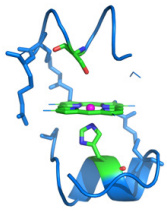

Fig. 3: Synthetic mimochrome enzyme.

Catalyst development has focused on molecular and biomolecular catalysts using base metals. Inspired by the active site structure of hydrogenase, Fe bis(dithiolate) catalysts have been developed that yield TON values over 17,000 when paired with CdSe QDs. We also have expanded our suite of biomolecular H_2-evolving catalysts to include synthetic "mimochromes." We have shown cobalt mimochromes to have structure-dependent overpotentials that are lower than those of related catalysts. Other biomolecular catalysts have been incorporated into systems for light-driven H_2 production, yielding high TON values (>100,000) for light-induced H_2 production.

Electrocatalysis of Proton and CO_2 Reduction and using Main-Group and Non-Redox-Active Metal-Porphyrin Complexes

Gary W. Brudvig, Jianbing Jiang, Kelly L. Materna, Svante Hedström, Ke R. Yang, Victor S. Batista, Robert H. Crabtree and Charles A. Schmuttenmaer

Department of Chemistry and Energy Sciences Institute
Yale University
New Haven, CT 06520

In a suitable ligand environment, complexes of the main-group element antimony and the non-redox-active element zinc are shown to be viable electrocatalysts for H_2 evolution from acid (1) and CO_2 reduction to CO (2), respectively (Figure 1). We have developed molecular antimony complexes for proton reduction electrocatalysis, which show remarkable activity for a main group element. A series of antimony porphyrins with varying axial ligands were synthesized for electrocatalysis applications. The proton reduction catalytic properties of $TPSb(OH)_2$ (TP=5,10,15,20-tetra(p-tolyl)porphyrin) with two axial hydroxo ligands were studied in detail, demonstrating catalytic H_2 production. Experiments, in conjunction with quantum chemistry calculations, show that the catalytic cycle is driven via the redox activity of both the porphyrin ligand and the Sb center. A zinc−porphyrin complex (Zn(II) 5,10,15,20-tetramesitylporphyrin) adsorbed on carbon fiber paper functions as an electrocatalyst with a turnover frequency as high as 14.4 site^{-1} s^{-1} and a Faradaic efficiency as high as 95% for CO_2 reduction to CO at − 1.7 V vs. the standard hydrogen electrode in an organic/water mixed electrolyte. While the Zn center is critical to the observed catalysis, *in situ* and *operando* X-ray absorption spectroscopic studies reveal that it is redox-innocent throughout the potential range. Cyclic voltammetry indicates that the porphyrin ligand may act as a redox mediator. This study brings insight into the use of main group elements and the role of redox-active ligands for catalysis.

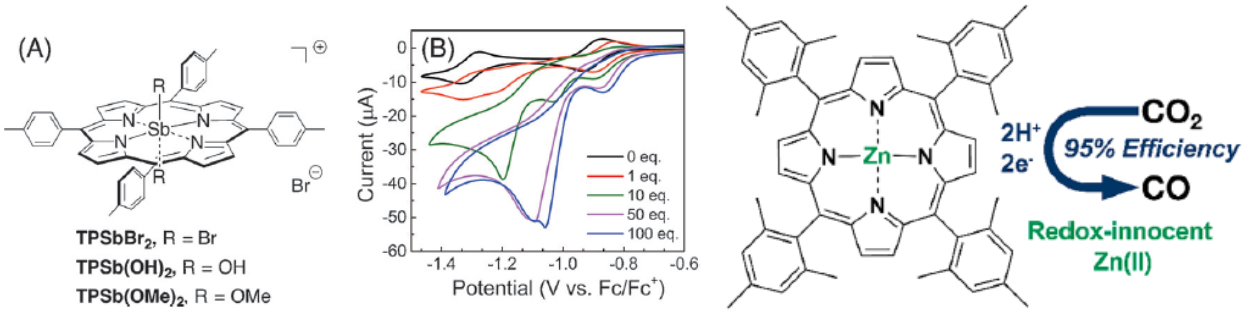

Figure 1. Left: A) Structures of the Sb-porphyrin complexes. B) TFA-dependent CV of 0.5 mM $TPSb(OH)_2$ in 0.1 M $TBAPF_6$ in acetonitrile. Right: Structure of the Zn-porphyrin complex and its electrocatalytic reduction of CO_2 to CO.

1. Jianbing Jiang, Kelly L. Materna, Svante Hedström, Ke R. Yang, Robert H. Crabtree, Victor S. Batista and Gary W. Brudvig (2017) Angew. Chem. Int. Ed. 56, 9111-9115.
2. Yueshen Wu, Jianbing Jiang, Zhe Weng, Maoyu Wang, Daniël L. J. Broere, Yiren Zhong, Gary W. Brudvig, Zhenxing Feng and Hailiang Wang (2017) ACS Cent. Sci. 3, 847-852.

Enhancing the Visible Light Absorption and Excited State Properties of Cu(I) MLCT Excited States

Sofia Garakyaraghi, Catherine E. McCusker, Saba Khan, Petr Koutnik, Anh Thy Bui, and Felix N. Castellano
Department of Chemistry
North Carolina State University
Raleigh, NC 27695

A computationally inspired Cu(I) metal-to-ligand charge transfer (MLCT) chromophore, $[Cu(sbmpep)_2]^+$ (sbmpep = 2,9-di(*sec*-butyl)-3,8-dimethyl-4,7-di(phenylethynyl)-1,10-phenanthroline), was synthesized in seven total steps, prepared from either dichloro- or dibromo-phenanthroline precursors. Complete synthesis, structural characterization, and electrochemistry, in addition to static and dynamic photophysical properties of $[Cu(sbmpep)_2]^+$ are reported on all relevant time scales. UV-vis absorbance spectroscopy revealed significant increases in oscillator strength along with a concomitant bathochromic shift in the MLCT absorption bands with respect to structurally related model complexes (ε = 16,500 M^{-1} cm^{-1} at 491 nm) as shown in the figure below. Strong red photoluminescence (Φ = 2.7%, λ_{max} = 687 nm) was observed from $[Cu(sbmpep)_2]^+$ which featured an average excited state lifetime of 1.4 □s in deaerated dichloromethane. Cyclic and differential pulse voltammetry revealed ~300 mV positive shifts in the measured one-electron reversible reduction and oxidation waves in relation to a Cu(I) model complex possessing identical structural elements without the π-conjugated 4,7-substituents. The excited state redox potential of $[Cu(sbmpep)_2]^+$ was estimated to be -1.36 V, a notably powerful reductant for driving photoredox chemistry. The combination of conventional and ultrafast transient absorbance and luminescence spectroscopy successfully map the excited state dynamics of $[Cu(sbmpep)_2]^+$ from initial photoexcitation to the formation of the lowest energy MLCT excited state and ultimately its relaxation to the ground state. These combined experiments showed a marked decrease in the time-scale of S-T intersystem crossing to τ_{ISC} = 1.5 – 3.2 ps, as independently measured by both fluorescence and transient absorption experiments, relative to the parent $[Cu(dsbtmp)_2]^+$ (dsbtmp = 2,9-di(*sec*-butyl)-3,4,7,8-tetramethyl-1,10-phenanthroline) complex (τ_{ISC} = 2 – 6 ps) published previously. This contribution demonstrates 4,7-phenanthroline modification, in conjunction with 2,9- and 3,8- steric supports, is an effective means to create a new body of tailor-made long-lifetime Cu(I) photosensitizers with somewhat deterministic photophysical properties, precisely designed for solar photochemistry applications.

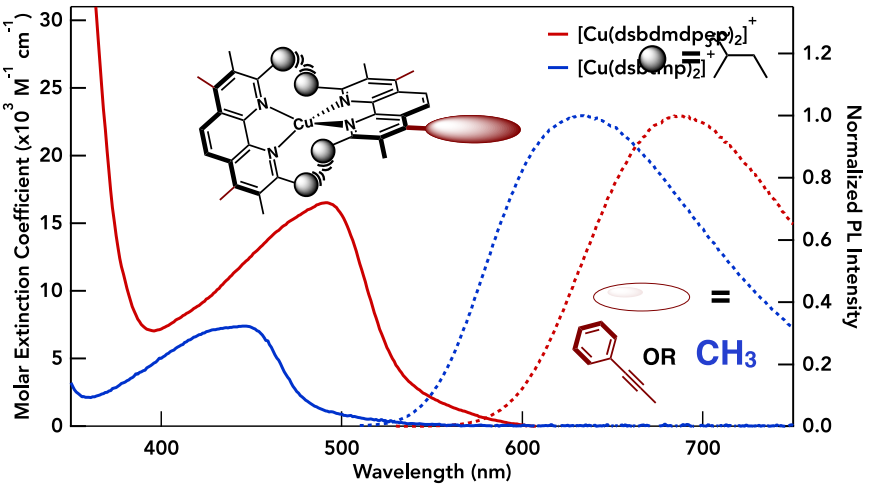

Thermochemical and Kinetics Factors Influencing the Proton-Coupled Electron Transfer Generation of Transition Metal Hydride Complexes

Jillian L. Dempsey, Noémie Elgrishi, William C. Howland Banu Kandemir, Daniel A. Kurtz, Brian D. McCarthy, and Eric S. Rountree
Department of Chemistry
University of North Carolina
Chapel Hill, NC 27599-3290

Proton-coupled electron transfer (PCET) reactions must be carefully considered in the development of catalysts that mediate production of fuels like H_2. This poster will describe two case studies that provide new insight to the kinetic and thermochemical factors influencing PCET reactions that generate transition metal hydride complexes—key intermediates in fuel production.

The applied potential at which $[Ni(P_2^{Ph}N_2^{Bn})_2(CH_3CN)]^{2+}$ ($P_2^{Ph}N_2^{Bn}$ = 1,5-dibenzyl-3,7-diphenyl-1,5-diaza-3,7-diphosphacyclooctane) catalyzes proton reduction varies as a function of proton source pK_a in acetonitrile. By contrast, most molecular catalysts exhibit catalytic onsets at potentials that are pK_a-independent. Through a combination of electrochemical and spectroscopic studies, we identified the Nernstian equilibria that give rise to this unique potential-pK_a behavior, generating a "coupled" potential–pK_a diagram by identifying the most thermochemically stable species as a function of applied potential and acid pK_a. These data provide new insight to why this catalyst uniquely exhibits pK_a-dependent catalytic activity, and identify the balance between proton transfer kinetics and thermodynamic stability of protonated products that influence observed proton-coupled electron transfer reactivity.

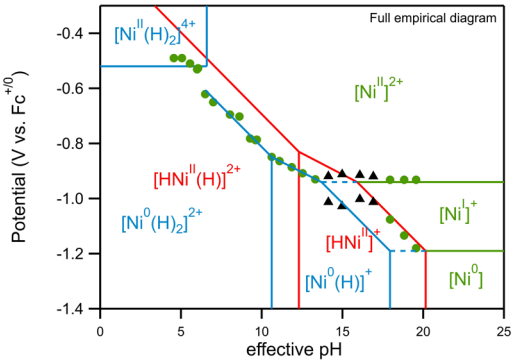

Coupled potential- pH diagram for $Ni(P_2^{Ph}N_2^{Bz})_2$ in acetonitrile; red lines are borders of metal-based PCET reactivity, and blue lines are thermochemical boundaries for ligand-based reactivity.

The proton-coupled electron transfer (PCET) reaction of $[Co(Cp)(dppe)]^+$ (Cp = cyclopentadienyl, dppe = 1,2-bis(diphenylphosphino)ethane) to form the corresponding cobalt(III)-hydride proceeds via a stepwise electron-transfer, proton-transfer process in acetonitrile. With weak acids, a linear free energy relationship between the second order rate constant for proton transfer and acid pK_a is observed. However, when the acid strength is increased, the second order rate constant becomes acid pK_a-independent. In order to more deeply understand the factors that give rise to this reactivity, we synthesized a series of analogous complexes with different phosphine substituents, allowing us to systematically tune the steric profile of the reactive cobalt center. Indeed, the ligand sterics influence the acid-independent k_{PT} value achieved with strong acids—the max k_{PT} decreases with increasing steric bulk. We posit that the acid independent second order rate constant k_{PT} for each complex reflects the intrinsic barrier for hydride formation—which necessitates electronic and structural rearrangements. This kinetic limitation to proton transfer informs us that PCET reactions involving protonation of metal centers are distinct from those of nitrogen and oxygen proton accepting sites.

Quantum Chemical Characterization of Photocatalytic CO_2 Reduction by Transition Metal Complexes: Mechanistic Insights from ^{13}C Kinetic Isotope Effects

Mehmed Z. Ertem
Chemistry Division, Energy & Photon Sciences,
Brookhaven National Laboratory, Upton, NY 11973-5000

Catalytic reactions of carbon dioxide reduction have attracted much attention as an important component of artificial photosynthesis and a variety of systems, both homogeneous and heterogeneous, have been shown to be active catalysts for CO_2 reduction. Despite the advances made in this field, the origins of the catalytic rate enhancement achieved by many of these systems remain to be fully understood. This is particularly true when it comes to mechanistic details of the bond-forming and bond-breaking steps accompanying the reduction of CO_2. Competitive kinetic isotope effects (KIEs) at natural abundance levels have provided direct information about the nature of the transition states in enzymatic and nonenzymatic reactions. The information gained from natural abundance KIEs is especially powerful when coupled with theoretical calculations. In the current work, computational investigation of high precision natural abundance competitive ^{13}C KIEs associated with photochemical CO_2 reduction by $[Ru(tpy)(bpy)Cl]^+$ (tpy = 2,2':6',2"-terpyridine, bpy = 2,2'-bipyridine) is presented (Fig. 1a).

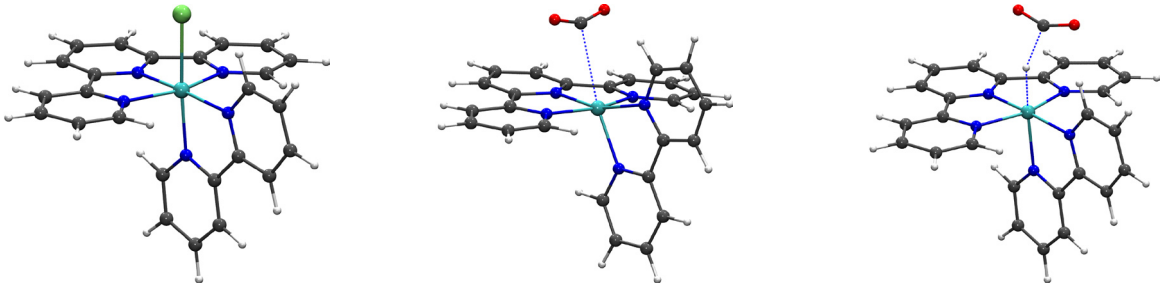

(a) **(b)** **(c)**

Figure 1. Optimized structures for **(a)** $[Ru(tpy)(bpy)Cl]^+$, **(b)** CO_2 binding to $[Ru(tpy)(bpy)]^0$ and **(c)** CO_2 insertion into the $[Ru(tpy)(bpy)H]^+$. Color code: Ru, cyan; Cl, green; N, blue; O, red; C, gray; and H, white.

Density functional theory (DFT) calculations in conjunction with continuum solvation methods for acetonitrile solvent were performed to map the energetics associated with a step-by-step mechanism of CO_2 reduction by $[Ru(tpy)(bpy)Cl]^+$. The ^{13}C equilibrium and kinetic isotope effects were calculated by employing the Transition State Theory and for each step of the catalytic mechanism, the vibrational frequencies of reactants and products were analyzed following the Bigeleisen and Goeppert-Mayer approach. Further analysis is performed via microkinetic simulations, calculation of commitment factors and effective rate constants for the proposed catalytic mechanism to gain insight into the contributions of distinct chemical steps and pathways on the observed isotope effects. The computations demonstrate that the first irreversible step in the CO formation pathway involves CO_2 binding to doubly reduced $[Ru(tpy)(bpy)]^0$ (Fig. 1b) with ^{13}C KIE of 1.068 whereas for formate generation CO_2 insertion into the $[Ru(tpy)(bpy)H]^+$ (Fig. 1c) constitutes the first irreversible step with ^{13}C KIE of 1.055. The nearly equal contribution from the two pathways results in an average value of KIE_{calc} = 1.062 in quite good agreement with experimental measurements $KIE_{expt} = 1.052 \pm 0.004$.

Acknowledgments: I thank Prof. Angeles-Boza (University of Connecticut) for insightful discussions and for providing experimental kinetic isotope effect results used in this study.

Quantum and Classical Spectroscopies

G.R. Fleming, O. Gamel, H.C.H. Chan, K.B. Whaley, G. McCrudden,
K. Orcutt, and P. Bhattacharyya
Molecular Biophysics and Integrated Bioimaging Division
Lawrence Berkeley National Laboratory
and
Department of Chemistry
University of California Berkeley
Berkeley CA 94720

This project aims to reveal the physical and chemical design principles that are utilized in natural photosynthetic light harvesting and trapping. We rely heavily on ultrafast spectroscopy and, theory and modeling. We are beginning experiments using entangled photon pairs (aka "quantum light") along with corresponding theory from our colleague K. Birgitta Whaley to explore fundamental aspects of light harvesting and charge separation.

A perennial question concerns the difference (if any) between excitation by sunlight and excitation by ultrashort pulse lasers. Given the very short timescales associated with electronic energy transport and the extremely weak nature (< 1 photon/mode) of sunlight it has been difficult to approach this question decisively. With Professor Whaley we have developed a unified approach to the absorption of single photons and subsequent excitation energy transfer in a photosynthetic light-harvesting complex. This involves a quantum description of both the light and the molecular system. A fundamental question relates to the meaning of ensemble averaged quantum efficiency. For example, does a near unity quantum efficiency imply that one photon corresponds to one electron transfer event? This is a quantum jump picture while an alternative picture is that multiple single photon events are required to place the full energy of a photon in to electronic excitation. With entangled photon pairs it is possible to think of addressing such a question experimentally as has been done for the quantum efficiency of frog rod cells by Krivitsky and coworkers.

In collaboration with G. Scholes, L. Chen and multiple others we explored the role of coherence and the possibility of utilizing it to enhance function. We are continuing to develop the formalism for two-dimensional electronic vibrational (2DEV) spectroscopy, particularly for investigating vibronic effects on energy transfer.

Figure 1.

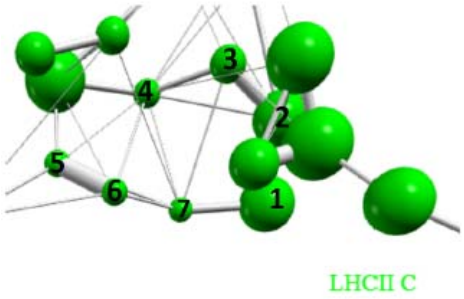

The seven chlorohylls of LHCII. Chlorophyll a 603 is labeled 7 in this figure. The size of spheres indicates the magnitude of the individual transition energies and the thickness of lines the electronic coupling between the pigments.

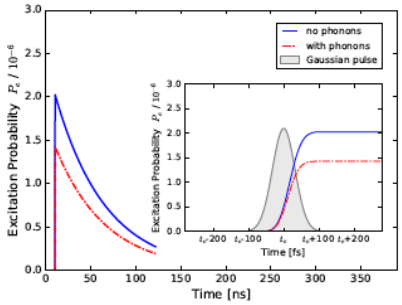

Excitation of a 603 in LHCII by a Gaussian coherent pulse with mean photon number <n> =1.
Blue: no phonon bath; Red: phonon bath at 300k.

Carbon Dioxide Dimer Radical Anion as Surface Intermediate of Photo-Induced CO_2 Reduction at Aqueous Cu Nanoparticle Catalyst by Rapid-Scan FT-IR Spectroscopy

Hua Sheng and Heinz Frei
Molecular Biophysics and Integrated Bioimaging Division
Lawrence Berkeley National Laboratory
Berkeley, CA 94720

Copper is unique among solid catalysts for CO_2 reduction as it offers a path beyond two-electron products CO or formic acid towards more energy dense molecules. In our effort to develop complete inorganic nanoscale assemblies for closing the photosynthetic cycle for CO_2 reduction by H_2O, we are seeking to detect and structurally identify catalytic surface intermediates on Cu nanoclusters and utilize this knowledge for guiding Cu particle modification for enhancing activity and generating more deeply reduced products.

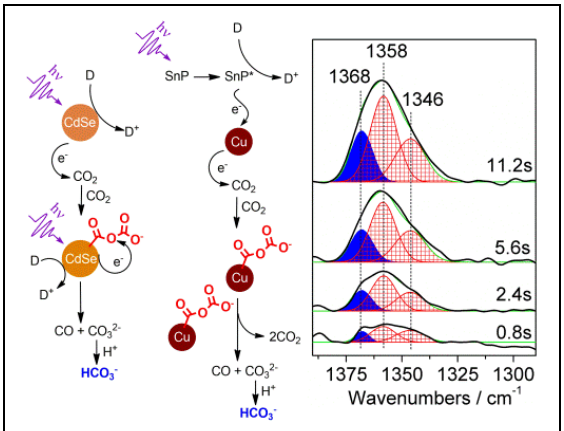

Figure: Observation of $C(=O)OCO_2^-$ surface intermediate of visible light-sensitized CO_2 reduction on aqueous Cu nanocatalysts and CdSe Q-dots, kinetic evaluation of the catalytic relevancy by rapid-scan FT-IR spectroscopy.

Monitoring of visible light sensitized reduction of CO_2 at Cu nanoparticles in aqueous solution by rapid-scan ATR FT-IR spectroscopy on the time scale of seconds allowed structural identification of a one-electron intermediate and demonstrated its kinetic relevancy for the first time. Isotopic labelling (^{12}C: 1632, 1358, 1346 cm^{-1}; ^{13}C: 1588, 1326, 1316 cm^{-1}) revealed a species of carbon dioxide dimer radical anion structure, most likely bound to the catalyst surface through carbon. Intermediacy of Cu-$C(=O)OCO_2^-$ surface species is in agreement with a recently proposed mechanism for electrocatalytic CO_2 reduction at Cu metal nanoparticles based on Tafel slope analysis. Spontaneous decrease of the intermediate after termination of the photosensitization pulse (Sn porphyrin excited at 405 nm) was accompanied by the growth of HCO_3^-. CO was produced as well, but sensitive detection required photolysis for tens of minutes. A direct kinetic link between a $C_2O_4^-$ surface intermediate and the CO product was also demonstrated for photocatalyzed CO_2 reduction at aqueous CdSe nanoparticles, where first order growth of a Cd-$C(=O)OCO_2^-$ species was accompanied by rise of CO (monitored by a fast Ni complex trap) and HCO_3^- showing a distinct induction period. The detection of the one-electron surface intermediate and confirmation of its catalytic relevancy was enabled by the delivery of electrons one-by-one by the photosensitization method. The formation of $C(=O)OCO_2^-$ adduct as one-electron intermediate provides an alternate, lower energy path for CO_2 reduction compared to CO_2^-. Reduction yields can be improved by enhancing the formation of $C_2O_4^-$ intermediate through increase of the density of surface adsorbed CO_2 molecules by using confined spaces such as exist for our core-shell nanotube array structures.

Sheng, H.; Oh, M. H.; Osowiecki, W. T.; Kim, W.; Alivisatos, A. P.; Frei, H. *J. Am. Chem. Soc.* **2018**. DOI: 10.1021/jacs.8b00271

Investigation of Ru(II)-Re(I) Supramolecular Photocatalysts for CO_2 Reduction using Time-Resolved IR Spectroscopy

Etsuko Fujita and David C. Grills
Chemistry Division
Brookhaven National Laboratory
Upton, NY 11973-5000

Supramolecular photocatalysts in which Ru(II) photosensitizer and Re(I) catalyst units are connected by a saturated ethylene linker are among the best known, most effective, and durable photocatalytic systems for CO_2 reduction. Time-resolved infrared (TRIR) spectroscopy is a powerful method for addressing chemistry associated with the Ru-based ^{3}MLCT excited state, quenching of the excited state, intramolecular electron transfer to the catalyst unit, and the catalytic reactions involving CO_2. IR vibrational bands are usually narrow and their frequencies are very sensitive to changes in electronic density at the metal center in transition metal complexes. We recently reported, for the first time, nanosecond TRIR spectra of Ru(II)-Re(I) binuclear complexes in CH_3CN following 532 nm laser excitation, in the absence (Figure 1, top) and presence (Figure 1, middle) of a sacrificial electron donor (*Chem. Sci.* **2018**, *9*, 2961-2974). While only the Ru center is excited by the 532 nm laser pulse, the CO stretching frequencies of the Re-carbonyl moiety are very sensitive to the electronic structure of the Ru and Re centers, as seen in Figure 1. In the absence of a reductant, photoexcitation of the binuclear complexes induced intramolecular electron transfer from the Ru ^{3}MLCT excited state to the Re center (~ 10^6 s^{-1}). In the presence of BNAH, intramolecular electron transfer from the reduced Ru unit to the Re unit is very fast (k_{ET} > 2 × 10^7 s^{-1}). This rapid intramolecular electron transfer is one of the most important advantages of the Ru(II)-Re(I) supramolecular photocatalysts with a saturated ethylene linker between each unit. In other words, contrary to a commonly held conception of the requirement for a π-conjugated linker for fast electron transfer reactions, a saturated ethylene linker adequately transfers photoproduced electrons to the catalyst unit in the photocatalytic reduction of CO_2. This work was carried out in collaboration of K. Koike (AIST) and O. Ishitani (Tokyo Inst. Tech.).

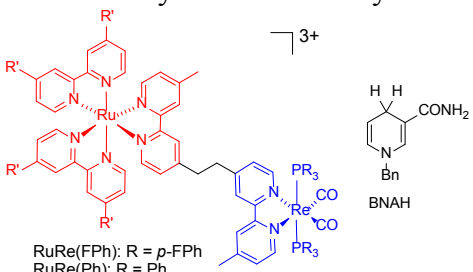

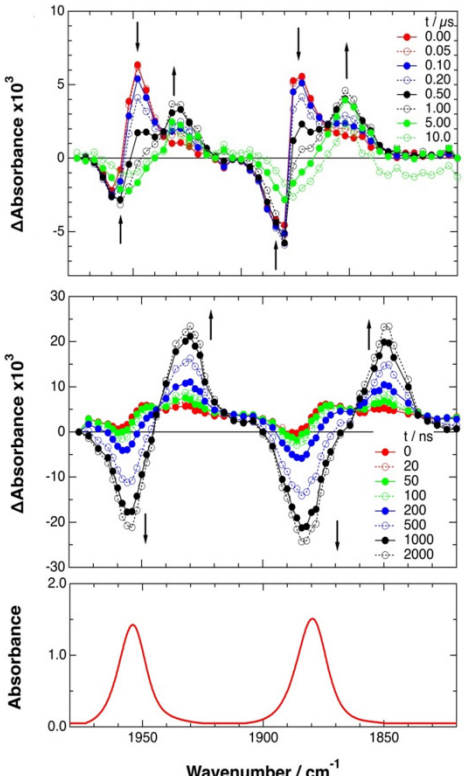

Figure 1. TRIR spectra recorded after 532 nm excitation of **RuRe(OEt)** in Ar-saturated CH_3CN without BNAH (top) and with BNAH (middle), and FT-IR spectrum of the ground state in CH_3CN (bottom).

Bridge Design for Photoactive Molecules at Semiconductor Interfaces

Elena Galoppini,[†] Robert A. Bartynski, [‡] Lars Gundlach,[#,+] Andrew Teplyakov,[+] Hao Fan,[†] Ryan Harmer,[†] Baxter Abraham,[+] Jesus Nieto-Pescador,[#] Zhengxin Li,[+] Chuan He.[+]

[†]*Chemistry Department, Rutgers University-Newark, Newark, NJ;* [‡] *Physics Department, Rutgers University-New Brunswick, Piscataway, NJ; Department of* [+]*Chemistry and* [#]*Physics, University of Delaware, Newark, DE.*

The objective of this research is to control at the molecular level, through synthetic design of organic linkers, the electronic properties of the interface between nanostructured metal oxide semiconductors, nanostructured and single crystal, and chromophoric compounds. The ultimate objective is gaining a fundamental understanding of charge transfer processes in hybrid organic-inorganic systems that are widely employed in solar photochemical energy conversion. The poster describes our progress in three areas of research.

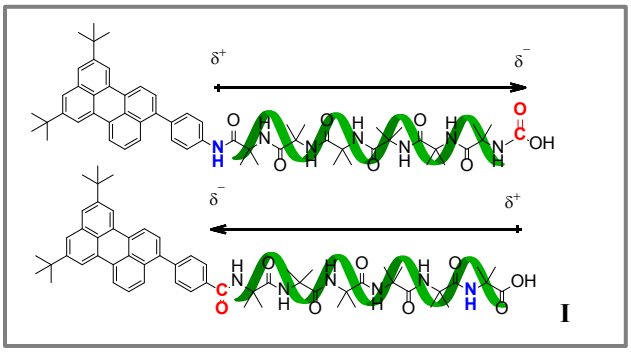

(I). The synthesis of chromophores (to date ZnTPP and perylene) that will be attached to the surface of semiconductors through $(Aib)_n$ 3_{10}-helical peptide bridge linkers as an approach to introduce in the bridge built-in dipoles that are tunable and that can be reversed.

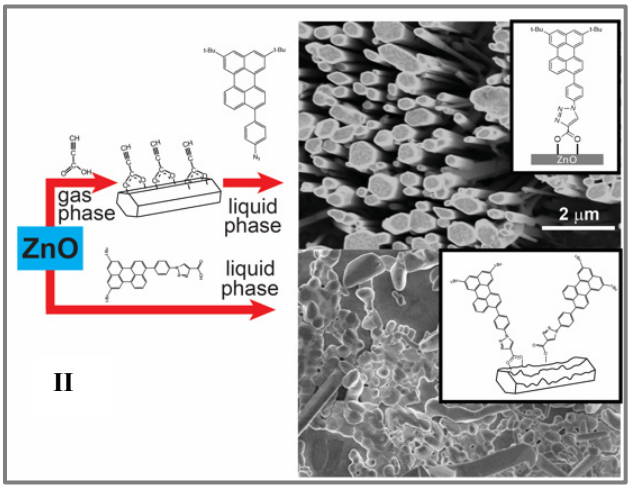

(II). The study of a series of perylene chromophores with bridges/anchor group combinations designed to tune vibronic coupling, and electronic coupling to acceptor states for an in-depth study of coherence in heterogeneous charge transfer in ultrafast laser spectroscopy experiments.

(III) In a new binding approach, ZnO nanorods were bound through a stepwise click approach that has allowed an excellent preservation of the surface morphology (probed by SEM, XPS and TA).

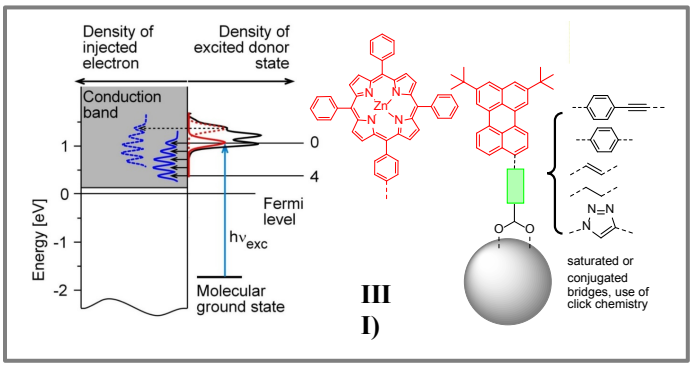

References (DOE): (1) C. He, B. Abraham, H. Fan, R. Harmer, Z. Li, E. Galoppini, L. Gundlach, A. Teplyakov *J. Phys. Chem. Lett.,* **2018**, *9*, 768–772. (2) B. Abraham, H. Fan, E. Galoppini, L. Gundlach, *J. Phys. Chem. A*, **2018**, *122*, pp 2039–2045. (3) J. Nieto-Pescador, B. Abraham, J. Li, A. Batarseh, R. A. Bartynski, E. Galoppini, L. Gundlach, *J. Phys. Chem. C*, **2016**, *120,* 48 – 55.

Chemical and Structural Factors of Excited State Transport

Casey L. Kennedy, Eric S. Massaro, Andrew H. Hill, Erik M. Grumstrup
Department of Chemistry and Biochemistry
Montana State University
Bozeman, MT 59717

Charge carrier and exciton transport is a key factor underpinning photophysical and photochemical processes in bulk chemical systems. In disordered materials like polymer films or lead halide perovskites, solution processing introduces significant chemical and structural heterogeneity that strongly perturbs transport characteristics on microscopic length scales. We'll report recent efforts at disentangling the relevant structural and chemical parameters in bulk PCDTBT polymer thin films as well as in individual domains of lead halide perovskites using time-resolved microscopy. In PCDTBT thin films, we have found significant heterogeneity in exciton transport rates, with diffusion constants varying over an order of magnitude from point to point on a single thin film. Aligning PCDTBT thin films using a grooved substrate results in an anisotropic factor of five increase in exciton transport along the polymer chain. Through ongoing theoretical efforts using a structurally-constrained Monte Carlo model, we set lower bounds on exciton hopping parameters which strongly point to highly delocalized excitons relaxing in a non-equilibrium manifold of states. In lead halide perovskites, we have correlated the local ambipolar diffusivity to a quantitative measure of the refractive index induced by photogenerated free charge carriers on individual perovskite domains. These correlated optical measurements provide a local probe of how perovskite chemistry systematically determines transport rates through a tightly-coupled interplay of effective mass, band structure, and lattice disorder.

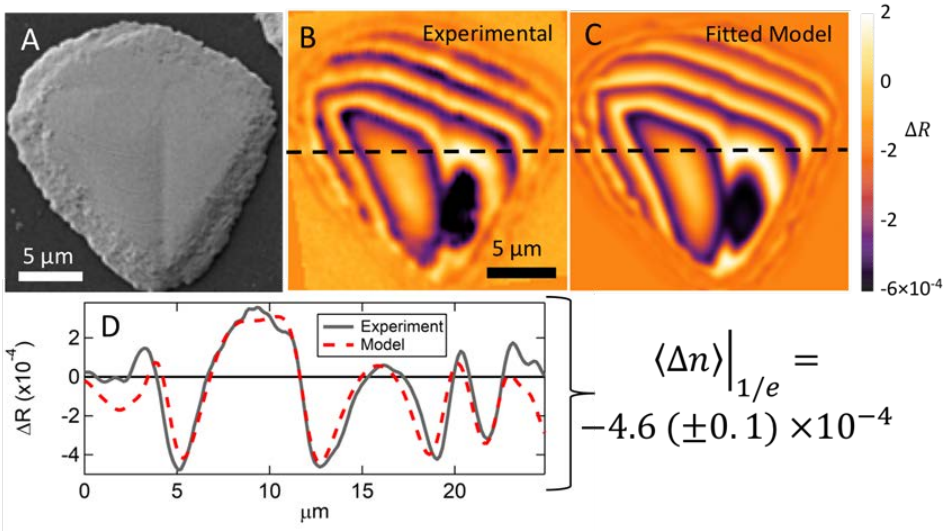

Structurally-correlated refractive index changes in lead halide perovskites. (A) SEM of a $CH_3NH_3PbI_3$ domain. (B) Experimental and (C) modeled ΔR image at Δt = 2 ps. (D) comparison of (B) and (C) along profile indicated by dashed black line. Transfer matrix analysis provides a quantitative measure of the free-carrier induced refractive index change.

Electronic and Vibrational Coherence in Heterogeneous Electron Transfer

Lars Gundlach[#+], Elena Galoppini[‡], Baxter Abraham[+], Jesus Nieto-Pescador[#], Zhengxin Li[+], Hao Fan[†], Ryan Harmer[†]

†Chemistry Department, Rutgers University-Newark, Newark, NJ; ‡ Physics Department, Rutgers University-New Brunswick, Piscataway, NJ; Department of +Chemistry and #Physics, University of Delaware, Newark, DE.

The goal of this project is to measure and distinguish vibrational excitation, vibrational coherence and electronic coherence in heterogeneous electron transfer (HET) by combining appropriate methods and model systems. Coherence is one aspect of HET that has yet to be fully explored and is of utmost importance for controlling materials properties and processes at the level of individual molecules and electrons. Here we present research accomplishments in measuring electronic-vibrational coupling in interfacial charge transfer reactions.

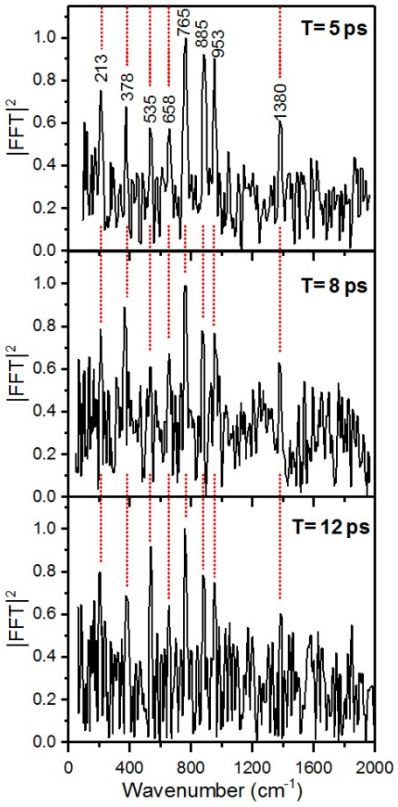

1. *Zn-porphyrin bound to TiO_2 excited state and cation vibrational dynamics.* The dominant modes in the cation spectrum measured by pump-DFWM at different delay times (Fig. right) are twisting modes between phenyl groups in the bridge and C-H bending modes on the chromophore's macrocycle. The 1380 cm^{-1} mode is assigned to the π-excited state while modes between 700 and 900 cm^{-1} are assigned to the bridge and are triggered by interfacial ET (1).

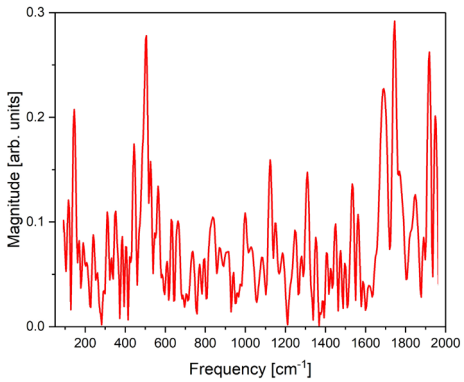

2. *Perylene-benzoic acid on TiO_2.* The figure on the left shows a resonant enhanced pump-DFWM difference spectrum of 2,5 di-tert-butyl perylene (DTB-Pe)-benzoic acid sensitized TiO_2 recorded at 500 fs after photoexcitation. The modes at 1533 cm^{-1}, 1311 cm^{-1}, and around 1700 cm^{-1} can be assigned to in-plane C-C-stretch modes of the chromophore.

3. *Structural dynamics and electron transfer studied by X-ray transient absorption spectroscopy (collaboration L. Chen and J. Rosenthal).* XTA difference spectra of the ground and excited stated of the nickel K-edge of a Ni-biladiene have been measured in solution and confirm that it is sensitive to excited state dynamics and can be used to study interfacial ET.

References (DOE): (1) C. He, B. Abraham, H. Fan, R. Harmer, Z. Li, E. Galoppini, L. Gundlach, A. Teplyakov *J. Phys. Chem. Lett.,* **2018**, *9*, 768. (2) B. Abraham, H. Fan, E. Galoppini, L. Gundlach, *J. Phys. Chem. A*, **2018**, *122*, 2039. (3) Abraham B., Nieto-Pescador J., Gundlach L, J. Lumin., **2017**, 187, 92. (4) J. Nieto-Pescador, B. Abraham, J. Li, A. Batarseh, R. A. Bartynski, E. Galoppini, L. Gundlach, *J. Phys. Chem. C*, **2016**, *120,* 48.

One-Electron Oxidation Coupled to Multiple Proton Transfers

S. Jimena Mora, Emmanuel Odella, Brian L. Wadsworth, Gary F. Moore,
Devens Gust, Thomas A. Moore, and Ana L. Moore

School of Molecular Sciences, ASU, Tempe, Arizona, 85257-1604

In photosystem II, tyrosine Z (Y_z) serves as a redox relay between the photo-oxidized primary donor ($P680^{\bullet+}$) and the oxygen-evolving complex (OEC). The oxidation of Y_z by $P680^{\bullet+}$ occurs with the transfer of a proton to its hydrogen-bonded partner, histidine (His190). The change in the protonation state of Y_z is thought to play several important roles. Kinetically, Y_z rapidly reduces $P680^{\bullet+}$ and thereby transfers the oxidizing power away from $P680^{\bullet+}$ and towards the OEC, thus lowering the yield of recombination. Thermodynamically, the Y_z-(His190) pair features PCET and thereby sets the $Y_z^{\bullet}/Y_z$ potential between those of $P680^{\bullet+}$ and the OEC.

To better understand this PCET process, and to adapt it to artificial photosynthetic systems, we designed and synthesized a series of benzimidazole-phenol (BIP) derivatives as mimics of the Y_z-His190 pair (the phenol mimics Y_z and the benzimidazole mimics His190). These models were studied theoretically, electrochemically and by IR spectroelectrochemical (IRSEC) techniques. We found that a concerted or effectively concerted one-electron, two-proton transfer (E2PT) process associated with the electrochemical oxidation of the phenol occurred in amino substituted BIPs, accompanied by a decrease in the redox potential of the phenoxyl radical/phenol couple by ~300 mV.[1,2] The loss of 300 mV in BIP is a high price to pay for a proton translocation of ~ 7Å, and it leaves the relay thermodynamically incapable of oxidizing water at pH near 7. Theoretical calculations predicted that substituents with reduced pK_a's, such as substituted imines attached to BIP, would still undergo an E2PT process while maintaining considerably higher potential for the phenoxyl radical/phenol couple. BIP-imine constructs were synthesized as alternative models of the Y_z-His190 pair, and preliminary results indicate that the phenol oxidation regains most of the 300 mV potential lost in the E2PT process of the amino-BIPs. IRSEC was used to identify the formation of the protonated imine while the benzimidazolium ion was not detected, which confirms the assignment of an E2PT process for imines substituted with electron donating groups. The mechanism switches to a predominately one-electron, one-proton (EPT) process when the basicity of the imine was reduced by substitution with electron withdrawing groups.

One of the aims of this study is to determine the number of proton transfers and their cost in redox potential that can be associated with a single oxidation event. To address this question, two new compounds were synthesized in which three proton transfer steps could occur. Preliminary theoretical, electrochemical and IRSEC experiments provide convincing evidence for an E3PT process in these systems.

(1) "Concerted One-Electron Two-proton Transfer Processes in Models Inspired by the Tyr-His couple of Photosystem II." Huynh, M. T.; Mora, S. J.; Villalba, M.; Tejeda-Ferrari, M. E.; Liddell, P. A.; Cherry, B. R.; Teillout,A-L.; Machan, C. W.; Kubiak, C. P.; Gust, D.; Moore, T. A.; Hammes-Schiffer, S.; Moore A. L., *ACS Cent. Sci.*, **2017**, *3*, 372–380.
(2) "Proton-Coupled Electron Transfer in Artificial Photosynthetic Systems," Mora S. J.; Odella E.; Moore, G. F.; Gust, D.; Moore, T. A.; Moore, A. L., *Acc. Chem. Res. Acc. Chem. Res.*, **2018**, *51*, 445–453.

Kinetic Control of Cobalt-based Redox Shuttles for DSSCs

Josh Baillargeon, Yuling Xie, Austin L. Raithel and Thomas W. Hamann
Department of Chemistry
Michigan State University
East Lansing, MI 48824

This poster will describe our recent efforts to manipulate the self-exchange kinetics of one-electron outersphere cobalt complexes and understand the effect on the charge transfer processes when employed as redox shuttles in dye-sensitized solar cells. The general goal of this project is to understand and design new redox shuttles capable of efficient dye regeneration with minimal overpotential which do not suffer from recombination. To this end, a new low spin (LS) cobalt(II) redox shuttle $[Co(PY5Me_2)(CN)]^+$, where $PY5Me_2$ represents the pentadentate ligand 2,6-bis(1,1-bis(2-pyridyl)ethyl)pyridine, has been synthesized and characterized for its potential application in DSSCs. Introduction of the strong field CN^- ligand into the open axial coordination site forced the cobalt(II) complex, $[Co(PY5Me_2)(CN)]^+$, to become LS, which is evidenced by the complex's magnetic susceptibility (1.91 ± 0.02 μB), determined by the Evans Method. Interestingly, dimerization and subsequent cobalt hexacyanide cluster formation of the $[Co(PY5Me_2)(CN)]^+$ monomer was observed upon long-term solvent exposure or addition of a supporting electrolyte for electrochemical characterization. Although long-term stability of the $[Co(PY5Me_2)(CN)]^+$ complex made it difficult to fabricate liquid electrolytes for DSSC applications, short-term stability in neat solvent afforded the opportunity to isolate the self-exchange kinetics of $[Co(PY5Me_2)(CN)]^{2+/+}$ via stopped-flow spectroscopy. Use of Marcus theory provided a smaller than expected self-exchange rate constant of 20 ± 5.5 $M^{-1}s^{-1}$ for $[Co(PY5Me_2)(CN)]^{2+/+}$, which we attribute to a Jahn-Tellar effect observed from the collected monomer crystallographic data. When compared side-by-side to cobalt tris(2,2'-bipyridine), $[Co(bpy)_3]^{3+}$, DSSCs employing $[Co(PY5Me_2)(CN)]^{2+}$ are expected to achieve superior charge collection, which result from a smaller rate constant, k_{et}, for recombination based upon simple dark *J-E* measurements of the two redox shuttles. Given the negative redox potential (0.254 V vs. NHE) of $[Co(PY5Me2)(CN)]^{2+/+}$ and the slow recombination kinetics, $[Co(PY5Me_2)(CN)]^{2+/+}$ becomes an attractive OSRS to regenerate near IR absorbing sensitizers in solid state DSSC devices.

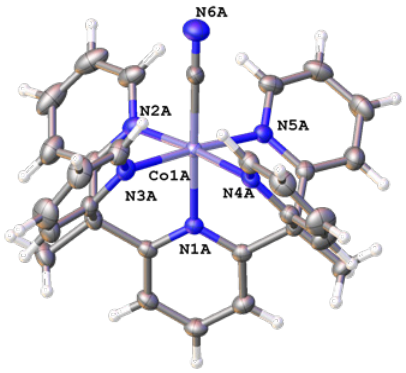

Single crystal representation of $[Co(PY_5Me_2)(CN)](OTf)$ provided by Olex2 and structurally refined by ShelXT software. Solvent and counter ions are excluded for clarity in each of the crystal structures above. Depicted ellipsoids are at the 50% probability level.

Fundamental Studies of Vibrational, Electronic, and Photophysical Properties of Tetrapyrollic Architectures

David F. Bocian,[1] Dewey Holten,[2] Christine Kirmaier,[2] and Jonathan S. Lindsey[3]
[1]Department of Chemistry, University of California, Riverside CA 92521-0403;
[2]Department of Chemistry, Washington University, St. Louis, MO 63130-4889;
[3]Department of Chemistry, North Carolina State University, Raleigh, NC 27695-8204

The long-term objective of our research program is to design, synthesize, and characterize tetrapyrrole-based molecular architectures that absorb sunlight, funnel energy, and separate charge with high efficiency and in a manner compatible with current and future solar-energy conversion schemes. This presentation focuses recent findings on tetrapyrrole-based panchromatic light-harvesting systems.

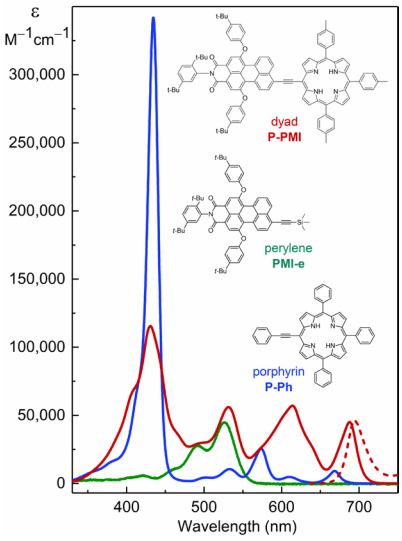

Three sets of tetrapyrrole–chromophore arrays have been examined that exhibit panchromatic absorption across large portions of the near-ultraviolet (NUV) to near-infrared (NIR) spectrum along with favorable excited-state properties for use in solar-energy conversion. The arrays vary the tetrapyrrole (porphyrin, chlorin, bacteriochlorin), chromophore (boron-dipyrrin, perylene, terrylene), and attachment sites (meso position, β-pyrrole position). In all, seven dyads, one triad and nine benchmarks in toluene and benzonitrile were studied using steady-state and time-resolved absorption and fluorescence spectroscopy. The results were analyzed with the aid of density functional theory (DFT) and time-dependent DFT (TDDFT) calculations. Natural transition orbitals (NTOs) were constructed to assess the net change in electron density associated with each NUV–NIR absorption transition. Porphyrin–perylene dyad **P-PMI** (top figure) displays spectral coverage evenly from 400–700 nm (average ε ~ 43,000 $M^{-1}cm^{-1}$). A significant contributor is a chromophore-induced reduction in the configuration interaction involving the four frontier molecular orbitals of benchmark porphyrins and associated constructive/destructive transition-dipole interference. **P-PMI** has an S_1 lifetime (τ_s) of 4.7 ns in toluene and 1.3 ns in benzonitrile. The NTOs for most arrays show that $S_0 \rightarrow S_1$ primarily involves the tetrapyrrole, but for **P-TMI** have electron density delocalized over the two units as a result of extensive orbital mixing. A change in tetrapyrrole to chlorin or bacteriochlorin and chromophore to BDPY or terrylene impacts the spectral and excited-state properties. A parallel study steps the number of perylenes per porphyrin from 1–4, which extends absorption farther into the NIR and enhances absorption in the green-orange spectral region (bottom figure). Collectively, the insights should aid the design of tetrapyrrole-based architectures for panchromatic light-harvesting systems for solar-energy conversion.

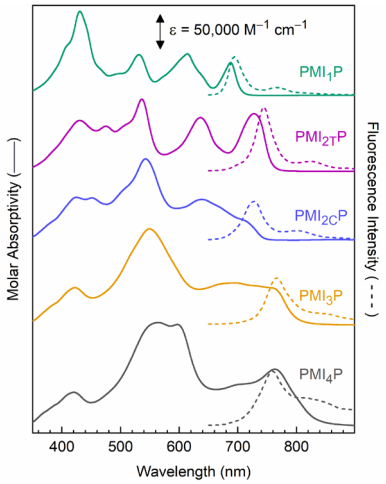

Spatial and Temporal Imaging of Multi-Scale Interfacial Charge Transport in Two-Dimensional Heterostructures

Tong Zhu, Long Yuan, Shibin Deng, Daria Blach and Libai Huang
Department of Chemistry, Purdue University, West Lafayette, IN 47907

Charge-transfer (CT) excitons at hetero-interfaces play a critical role in light to electricity conversion using organic and nanostructured materials. However, how CT excitons migrate at these interfaces is poorly understood. Atomically thin and two-dimensional (2D) nanostructures provide a new platform to create architectures with sharp interfaces for directing interfacial charge transport. Here we investigate the formation and transport of CT excitons in van der Waals (vdW) heterostructures based on semiconducting transition metal dichalcogenides (TMDCs) employing transient absorption microscopy (TAM) with a temporal resolution of 200 fs and spatial precision of 50 nm as schematically shown in Figure1.

We have recently imaged the transport of interlayer CT excitons in 2D organic-inorganic vdW heterostructures constructed from WS_2 layers and tetracene thin films[1]. To investigate driving force for exciton dissociation, we perform measurements on heterostructures constructed with different WS_2 thickness ranging from l layer to 7 layers. Photoluminescence (PL) measurements confirm the formation of interlayer excitons with a binding energy of ~ 0.3 eV. Electron and hole transfer processes at the interface between monolayer WS_2 and tetracene thin film are very rapid, with time constant of ~ 2 ps and ~ 3 ps, respectively. TAM measurements of exciton transport at these 2D interfaces reveal coexistence of delocalized and localized CT excitons, with diffusion constant of ~ 1 cm^2s^{-1} and ~ 0.04 cm^2s^{-1}, respectively. The high mobility of the delocalized CT excitons could be the key factor to overcome large CT exciton binding energy in achieving efficient charge separation.

We have also studied interlayer charge transfer and recombination in WS_2-graphene and WS_2-WSe_2 heterostructures. We have demonstrated broadband photocarrier generation directly from interlayer CT states in WS_2-graphene heterostructures[2]. Lifetime of the CT excitons has been found to be strongly dependent on interlayer stacking in epitaxial grown AA and AB stacking WS_2-WSe_2 heterostructures.

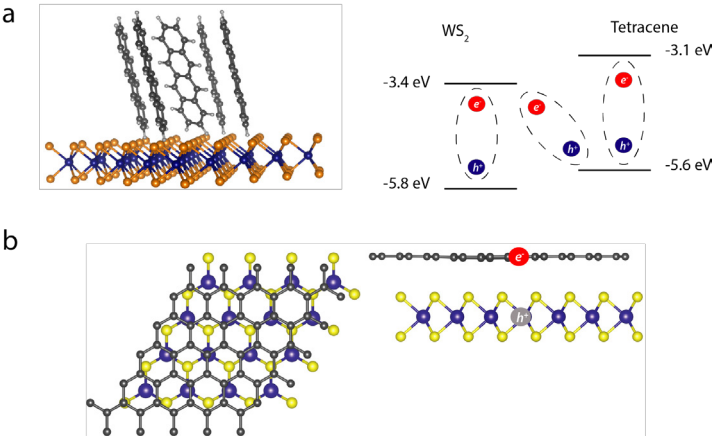

Figure 1. Schematic illustration of interfacial charge transfer in WS_2-tetracene (a) and WS_2-graphene (b) heterostructures.

References:

1. Tong Zhu, Long Yuan, Yan Zhao, Mingwei Zhou, Yan Wan, Jianguo Mei, and Libai Huang, Science Advances, 4, eaao3104 (2018).
2. Long Yuan, Ting-Fung Chung, Agnieszka Kuc, Yan Wan, Yang Xu, Yong P. Chen, Thomas Heine, Libai Huang, Science Advances, 4, e1700324, (2018).

Extraction of Triplet Excitons after Singlet Fission

Justin Johnson, Dylan Arias, Natalie Pace, Gerard Carroll, Daniel Kroupa, Jeffrey Blackburn, Matthew Beard, Garry Rumbles
Chemistry and Nanoscience Center
National Renewable Energy Laboratory
Golden, CO 80401

To utilize the two triplets born from a single photon following singlet fission (SF), schemes involving energy or charge transfer should be incorporated into the overall light harvesting system. We have recently approached this challenge from three directions: (i) a SF polymer that enables triplet-triplet separation across polymer chains in the solid-state; (ii) a quantum dot (QD)-polyacene ligand system that can undergo triplet energy transfer (TET) between both partners, depending upon the system design; and (iii) a dye-sensitized photoelectrode that has sensitizer SF compounds as the sensitizer. We have undertaken full spectroscopic evaluation of each system to test the fundamental principles of SF in the context of energy/charge transfer with suitable partners.

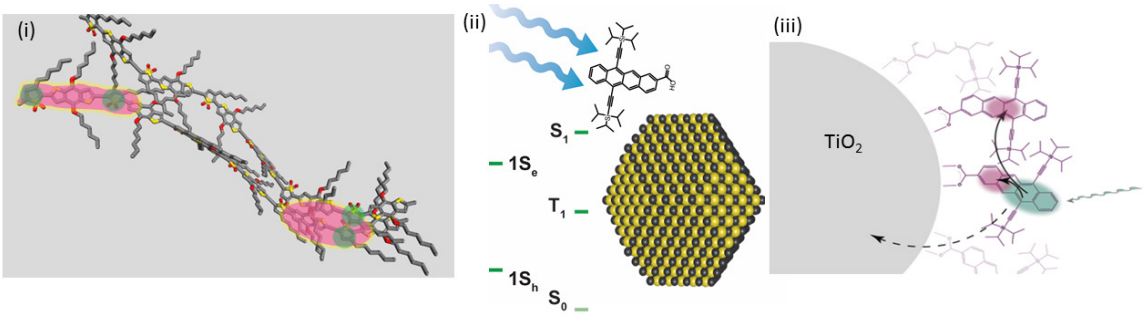

Figure 1. (i) Polymer SF with delocalized singlets (pink) and localized triplets (green) after intra- and interchain TET. (ii) Triplet energy transfer in a QD-tetracene complex. (iii) Electron injection in competition with SF for dyes on TiO_2.

For (i) we discovered that a known push-pull polymer can produce long-lived triplets if the polymer chains have interchain coupling that enables triplet hopping between chains. Without this coupling triplets undergo a fast geminate annihilation process in < 50 ps. The yield of long-lived triplets is about six-fold higher than in solution and two-fold higher than in a polymer with a bulky side-chain that prevents strong interchain interactions. For (ii) we found that for tetracene-based ligands attached to a PbS QD, SF does not compete with singlet energy transfer to the QD. However, subsequent reverse TET can occur efficiently in 50-200 ns, depending upon the band gap of the QD compared with the triplet energy of tetracene. Pentacene-based ligands show stronger signatures of SF on a ps time scale, but the subsequent transfer of both triplets to the QD results in Auger recombination, limiting the ultimate yield of long-lived excitons in the QD to one. For (iii) the polyacene-based dyes were covalently attached to mesoporous TiO_2 or SnO_2. After photoexcitation of the dye, electron transfer from the singlet occurs in ~3 ps for tetracene, outcompeting SF. For pentacene, SF effectively competes with singlet electron injection on a timescale of 6 ps, but the driving force for triplet exciton dissociation is insufficient to produce a high yield of charges in the semiconductor after SF. We have used insulating barrier layers and an applied bias to further characterize the interface between chromophore and semiconductor.

i. *J. Phys. Chem. Lett*. **2017**, 8, 6086. ii. *Nano Lett*. **2018**, *18*, 865. iii. *Chem. Sci*. **2018**, 9, 3004.

Establishing the Role of Mesoscopic TiO_2 in Metal Halide Perovskite Solar Cells

Rebecca A. Scheidt, Elisabeth Kerns, Subila Balakrishna and Prashant V. Kamat
Radiation Laboratory, and Department of Chemistry and Biochemistry
University of Notre Dame, Notre Dame, IN 46556

The metal halide perovskite solar cells often employ metal oxide such as TiO_2 to transport electrons to the contact electrode. The property of electron capture from excited metal halide perovskite plays an important role in delivering superior device performance. However, its role in perovskite solar cell is yet to be understood fully. The possibility of synthesizing $CsPbBr_3$ nanocrystals by hot injection method has allowed us to explore their photophysical properties [1-3].

When $CsPbBr_3$ nanocrystals are adsorbed onto mesoscopic TiO_2 film we observe quenching of emission as a result of charge injection from excited perovskite into mesoscopic TiO_2 film. This process is further confirmed by following the absorption changes under steady state irradiation of TiO_2 films modified with $CsPbBr_3$ nanocrystals. In air equilibrated conditions, the electrons injected into TiO_2 are scavenged away from the TiO_2, thus inducing oxidation of $CsPbBr_3$ nanocrystals. No such degradation is seen when $CsPbBr_3$ nanocrystals are coated on an inert support such as ZrO_2. Fundamental understanding of chemical transformations on TiO_2 surface is important in improving the stability of perovskite solar cells.

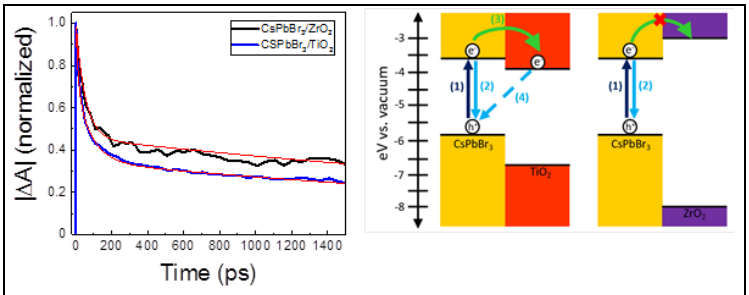

Figure 1. The comparison of bleaching recovery of $CsPbBr_3$ nanocrystals adsorbed on mesoscopic TiO_2 and ZrO_2 films following 387 nm laser pulse excitation (Left) allow us to establish the charge injection processes from excited $CsPbBr_3$ and TiO_2 as shown in the scheme(Right)

We have also probed the influence of applied bias on the charge recombination process in $CsPbBr_3$ deposited on FTO/TiO_2 films by carrying out spectroelectrochemical experiments. These experiments have allowed us to probe the influence of electron charging effect in TiO_2 layer on the charge injection process. Steady state and time-resolved transient absorption measurements that elucidate the role of TiO_2 in the solar cell operation will be discussed.

References

1. Balakrishnan, S. K.; Kamat, P. V., Ligand Assisted Transformation of Cubic CsPbBr3 Nanocrystals into 2-D $CsPb_2Br_5$ Nanosheets. *Chem.Mater.*, 2018, *30*, 74–78
2. Scheidt, R. A.; Samu, G. F.; Janáky, C.; Kamat, P. V., Modulation of Charge Recombination in $CsPbBr_3$ Perovskite Films with Electrochemical Bias. *J. Am. Chem. Soc.*, 2018, 140, 86–89.
3. Ravi, V. K.; Scheidt, R. A.; Nag, A.; Kuno, M.; Kamat, P. V., To Exchange or Not to Exchange. Suppressing Anion Exchange in Cesium Lead Halide Perovskites with $PbSO_4$–Oleate Capping. *ACS Energy Lett.*, 2018, 3, 1049-1055.

Photophysics of Charged Excitons in Single-Walled Carbon Nanotubes

Zhentao Hou, Amanda R. Amori, Nicole M. B. Cogan, and Todd D. Krauss
Department of Chemistry
University of Rochester
Rochester, New York 14627-0216

Single-walled carbon nanotubes (SWNTs) are fundamentally interesting and technologically relevant materials with size-tunable absorption and emission across visible and near infrared wavelengths. However, several important aspects of SWNT photophysical properties are not known well enough to predict how SWNTs will behave as part of a larger integrated solar photochemical system. Since SWNTs are comprised of all "surface" atoms, simple concepts such as the intrinsic photoluminescence efficiency (PL QY) are not understood for SWNTs, as they are strong functions of the local environment.

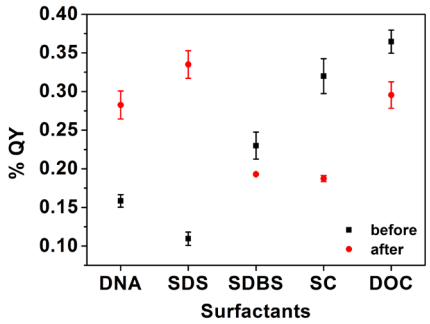

Figure 1: PL QY for SWNTs wrapped in various surfactants before and after addition of DTT.

We have found that addition of dithiothreitol (DTT) to DNA or sodium dodecyl sulfate (SDS) wrapped SWNTs causes PL brightening by several fold. In contrast, SWNTs dispersed in sodium dodecylbenzene sulfonate (SDBS), sodium cholate (SC) and sodium deoxycholate (DOC) solutions display fluorescence quenching upon addition of DTT. Time-resolved PL studies show that addition of DTT mitigates non-radiative decay processes, and also surprisingly increases the radiative decay rate for DNA and SDS-SWNTs (Figure 1). This combination leads to the increase of the PL QY. The opposite influences are found for the other SWNTs. The PL brightening (or quenching) is consistent with surfactant reorganization upon addition of DTT, which changes the local dielectric environment and the relative surfactant coverage on the SWNT.

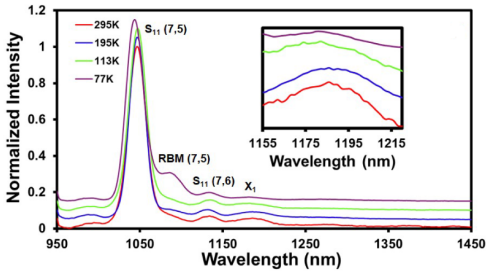

Figure 2: Normalized PL spectra of a (7,5) enriched ensemble SWNT sample at 295 K, 195 K, 113 K, and 77 K (all offset by 0.05 for clarity). The inset shows a zoom in of the PL sideband, located ~130 meV to the red of the bright S_{11} state.

Also, variable temperature PLE spectroscopy was used to investigate the origins of several sidebands featured in the PL spectra of chirality-enriched samples of SWNTs. While all ensemble PL spectra showed a temperature dependent "dark exciton" peak, called X_1, single molecule (SM) PL studies revealed that only a handful of NTs studied displayed X_1 emission. Lack of an X_1 contribution in the PL spectra from most individual NTs suggests that population of this state cannot be phonon-related. Therefore, we postulate that temperature dependence of the X_1 peak and the SM data are overall consistent with this dark exciton state being populated by a factor extrinsic to the NT: intervalley scattering from NT defects. By contrast, emission at X_1 involves creation of transverse optical phonon for momentum conservation. Our data suggests that the X_1 feature is a highly sensitive spectroscopic indicator for the presence of low numbers of defects in SWNTs.

Increasing the coverage of functional groups on modified molybdenum disulfide surfaces

Ellen X. Yan and Nathan S. Lewis
Department of Chemistry and Chemical Engineering
California Institute of Technology
Pasadena, CA 91125

Two-dimensionally layered transition-metal dichalcogenides (TMDs), especially TMDs containing a Group VI metal (MX_2; where M = Mo or W; X = S or Se), have been explored recently for use in a variety of devices and applications, including transistors, ultra-thin flexible electronics, sensors, drug-delivery, and bio-imaging. A variety of methods have been developed for covalent and non-covalent functionalization of the relatively inert basal plane of TMDs to improve the application-specific suitability of TMDs. Functionalization of TMDs typically first requires altering the properties of the semiconducting 2H phase of the TMD to create reactive sites, either by converting the TMD to a metallic 1T′ phase, or by increasing chalcogenide vacancies on the surface.

Our goal is to develop synthetic methods that increase the coverage of functional groups on covalently modified surfaces of the 1T′ and 2H phases of MoS_2 relative to existing methods. We are currently investigating reductant-activated addition, wherein one-electron reductants used as sacrificial electron donors that can transfer charge to the MoS_2. The reduced MoS_2 can then bind to electrophiles, similar to a known synthetic route where negative charge is transferred to involving MoS_2 by lithium intercalation.

Figure 1 shows preliminary results for reductant-activated addition of methyl and 4-fluorobenzyl groups to 1T' MoS_2, where the surface coverage was quantified using XPS. Our preliminary results indicate that we are able to achieve ~ 80% coverage for methyl-terminated 1T′ MoS_2, approximately twice the highest coverage previously reported, along with increased coverage on 1T′ MoS_2 functionalized with 4-fluorobenzylbromide using reductant-activated functionalization compared to the standard procedure. We also observe that the rate of reaction increases with increased reduction potential, resulting in higher coverages under the same conditions. In addition to the XPS data providing coverage, we can observe the covalent C-S bond and the carbon species through FTIR and solid-state ^{13}C-CPMAS NMR.

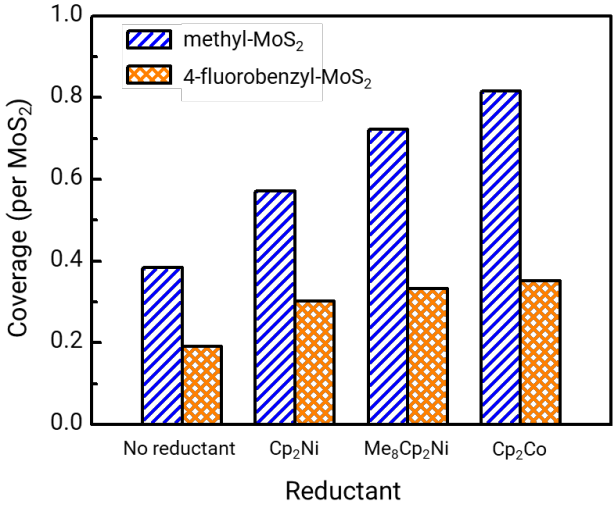

Figure 1. Coverage per MoS_2 as a function of the reductant used during functionalization of 1T′ MoS_2 for a methyl surface (blue) and a 4-fluorobenzyl surface (orange).

We are currently exploring reductant-activated addition to functionalize semiconducting 2H MoS_2 and are comparing the differences in reactivity and mechanisms for reductant-activated addition to the 1T' and 2H phases of MoS_2.

Exploring the Synergy between Semiconductor Surfaces and Molecular Catalysts for Efficient Solar CO_2 Reduction

Peipei Huang, Sebastian Pantovich, Ethan Jarvis, Shaochen Xu, Christine Caputo, Gonghu Li
Department of Chemistry, University of New Hampshire, Durham, NH 03824

A variety of hybrid photocatalysts have been reported using highly active molecular catalysts and robust surfaces. These hybrid systems demonstrated excellent properties in solar fuel production via water splitting and CO_2 reduction. Our project is focused on solar CO_2 reduction using macrocyclic complexes grafted on light-harvesting semiconductor surfaces. We collaborate with Dr. Tijana Rajh of Argonne National Lab to investigate structural features of such hybrid systems that are key to achieving efficient photocatalysis. We hypothesize that covalent linkages with appropriate *bend angles* and *flexibility* promote optimized interfacial electron transfer for fuel-producing reactions (**Figure 1**).

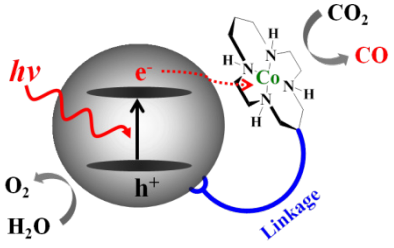

Figure 1. Design of hybrid photocatalysts for solar CO_2 reduction. M: Co(III),Cu(II).

In our research, TiO_2 is employed as the model support for a macrocyclic Co(III) complex for use in solar CO_2 reduction in the presence of a sacrificial electron donor (D in **Figure 2**). The orientation of the surface Co(III) site has been adjusted to establish correlation between the linkage structure and its photocatalytic performance. We have also synthesized nitrogen-doped tantalum oxide (N-Ta_2O_5, bandgap 2.4 eV) and graphitic carbon nitride (g-C_3N_4, bandgap 2.7 eV) as the semiconductor support for use in visible-light CO_2 reduction.

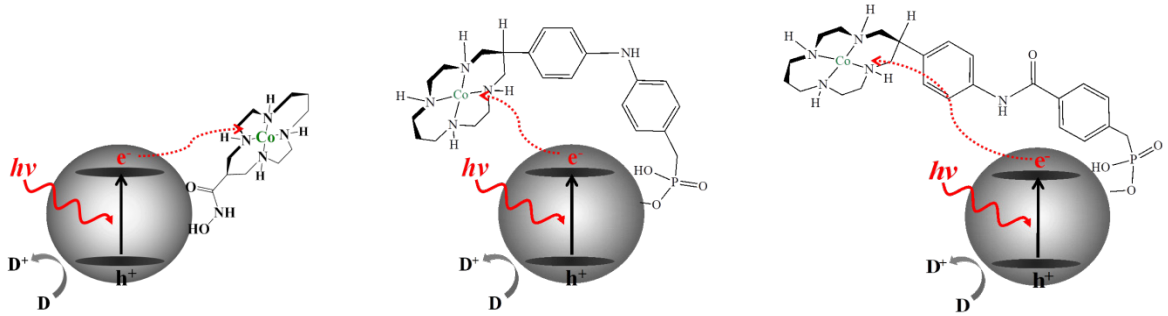

Figure 2. Different linkages between a macrocyclic Co(III) catalyst and TiO_2 surface.

Acknowledgements: This project is co-sponsored by the DOE EPSCoR Program.

References: (1) Stewart, B.; Huang, P.; He, H.; Fenton, T.; Li, G. "Visible-light Degradation of Orange II using an Fe(II)-terpyridine Complex Grafted onto TiO_2 Surface," *Can. J. Chem.* **2018**, in press; (2) Huang, P.; Pantovich, S.; Rajh, T.; Caputo, C.; Li, G. "Surface Molecular Catalysts for Solar CO_2 Reduction," **2018**, submitted; (3) Huang, P.; Fenton, T.; Li, G. "Photocatalytic CO_2 Reduction using Macrocyclic Co(III) Catalysts Supported on g-C_3N_4," **2018**, submitted; (4) Pantovich, S.; Jarvis, E.; Xu, S.; Huang, P.; Caputo, C.; Li, G. "The Effect of Linkages between a Surface Molecular Catalyst and TiO_2 on Photocatalytic CO_2 Reduction," **2018**, in preparation; (5) Yempally, V.; Dickie, D.; Chapman, C.; Caputo, C.A. "Incorporating Pendant Proton Relays in the Secondary Coordination Sphere of a Mn-Bipy Complex for Electrochemical CO_2 Reduction", **2018**, in preparation.

2D Morphology Enhances Light-Driven H_2 generation Quantum Efficiency in CdS Nanoplatelet-Pt Heterostructures

Tianquan Lian
Department of Chemistry
Emory University
1515 Dickey Dr. NE, Atlanta, Georgia 30222

The research effort in the past year can be divided in the following three areas 1) Mechanism of triplet energy transfer from QDs to molecular acceptors; 2) Mechanism of long distance charge separation and charge recombination in 2D nanosheet-metal heterostructures; and 3) Plasmonic hot electron driven ultrafast modulation of light amplitude, phase and polarization. In the following, we summarize the key progresses in the last two areas.

1) **Competition of Charge and Triplet Energy Transfer in QD/Acceptor complexes.** Because of the low singlet/triplet energy gap in QDs, they are ideal materials for sensitizing triplet states of molecules. However, triplet energy transfer often competes with charge transfer and the factors that determines the branching of these pathways are not well understood. We report an effecttive strategy to enhance triplet energy transfer using core/shell QDs. We show that a sub-monolayer CdS shell on PbS quantum dots (QDs) enhances triplet energy transfer (TET) by suppressing competitive charge transfer pathways. The CdS shell increases the linear photon upconversion quantum yield (QY) from 3.5% for PbS QDs to 5.0% for PbS/CdS QDs when functionalized with a tetracene acceptor, 5-CT. While transient absorption spectroscopy reveals that both PbS and PbS/CdS QDs show the formation of the 5-CT triplet (with rates of 5.91 ±0.60 ns-1 and 1.03 ±0.09 ns-1 respectively), ultrafast hole transfer occurs only from PbS QDs to 5-CT. Although the CdS shell decreases the TET rate, it enhances TET efficiency by suppressing hole transfer. Ongoing studies are investigating how other nanocrystal parameters (band alignment, morphology, energetics) can be used to further control these processes.

2) Light-driven H_2 Generation in CdS Nanoplatelet-Pt Heterostructures: Light-driven H2 generation using semiconductor nanocrystal heterostructures has attracted intense recent interest because of the ability to rationally improve their performance by tailoring their size, composition and morphology. We have shown previously that in zero- and one-dimensional (0D and 1D) nanomaterials, the lifetime of the photo-induced charge-separated state is often the key limiting factor for the solar-to-H_2 conversion efficiency. We report here that H_2 generation internal quantum efficiency (IQE) can exceed 40% at pH 8.8-13 and approach unity at pH 14.7 in 2D nanoplatelet (NPL)-Pt heterostructures. At pH<13, the IQE of NPL-Pt is significantly higher than those in 1D nanorods. Detailed time-resolved spectroscopic studies and modelling of the elementary charge separation and recombination processes show that compared to 1D nanorods, 2D morphology extends the charge-separated state, providing a new approach for designing efficient nanostructures for light-driven H_2 generation. Ongoing studies are investigating how nanosheet core/crown heterostructures can be used to further enhance the H_2 generation efficiency.

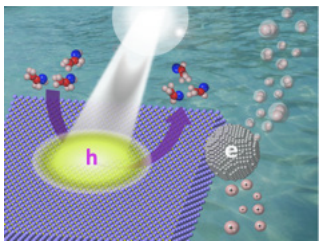

Figure 3. Light driven H2 generation from 2D nanosheet/Pt heterostructure.

Electron/hole selectivity in organic semiconductor contacts for solar energy conversion

Kira Egelhofer, Ellis Roe, Colin Bradley, and Mark C. Lonergan
Department of Chemistry and Biochemistry
University of Oregon
Eugene, OR 97403

The direct conversion of solar energy to electricity or fuels requires the selective collection of one of an electron or hole at an interface. The development of contacts that form such interfaces to solar absorbers presents significant challenges to our fundamental understanding of the integrated action of charge transfer processes at interfaces. The action of these processes in determining the selectivity and recombination characteristics of semiconductor interfaces is of particular interest. We have conducted studies on the relation of fundamental rate processes at semiconductor interfaces to their solar energy conversion properties, and the integrated measurement of these rate processes for organic semiconductor contacts in a silicon model system using the interdigitated back contact (IBC) solar cell, and on understanding bulk recombination centers in lead halide perovskite solar cells to lay a foundation for better understanding their interplay with recombination processes at contacts. In this presentation we focus on the relation between interfacial electron and hole exchange current densities and the energy conversion properties of an idealized solar cell (see Figure 1).

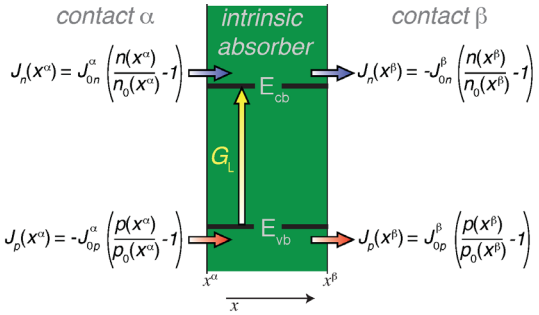

Figure 1. Four exchange current density model.

The conversion of solar energy into chemical or electrical energy typically requires an absorber with two contacts. Each contact can collect electrons and holes leading to four relevant rate processes at the contacts (see Figure 1). Classic theories of solar cells focus on one or two of these processes. We have developed a model of an idealized solar cell that relates the exchange current densities of all four electron/hole charge transfer processes and the power generation characteristics. An analytic expression for the current voltage behavior of a solar cell limited by selectivity and or recombination at its contacts is derived. The resulting current-voltage curve allows for the direct relation of performance parameters such as J_{sc}, V_{oc} (see Figure 2), and maximum power point to equilibrium exchange current densities associated with the contacts. These relations can be further related to the concepts of selectivity and recombination at the contacts, thereby clearly illustrating their role in energy conversion.

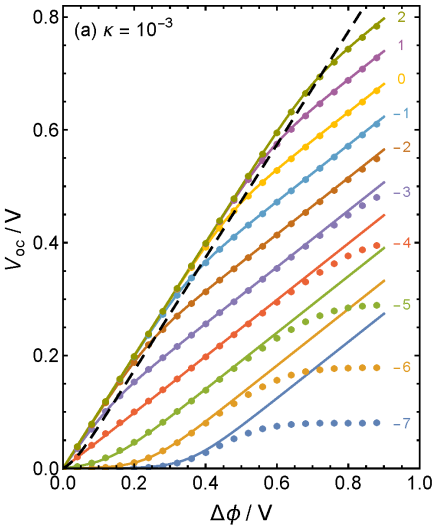

Figure 2 - Comparison of V_{oc} calculated from model (symbols) and numerical simulation (lines) as a function light intensity (different colors) and contact work function difference ($\Delta\phi$)

Advances in Sensitized Semiconductor Photocathodes

Sofiya Hlynchuk, Molly MacInnes, Robert Vasquez, Mitchell Lancaster,
Saurabh Acharya, and Stephen Maldonado
Department of Chemistry
University of Michigan
Ann Arbor, MI, 48109-1055

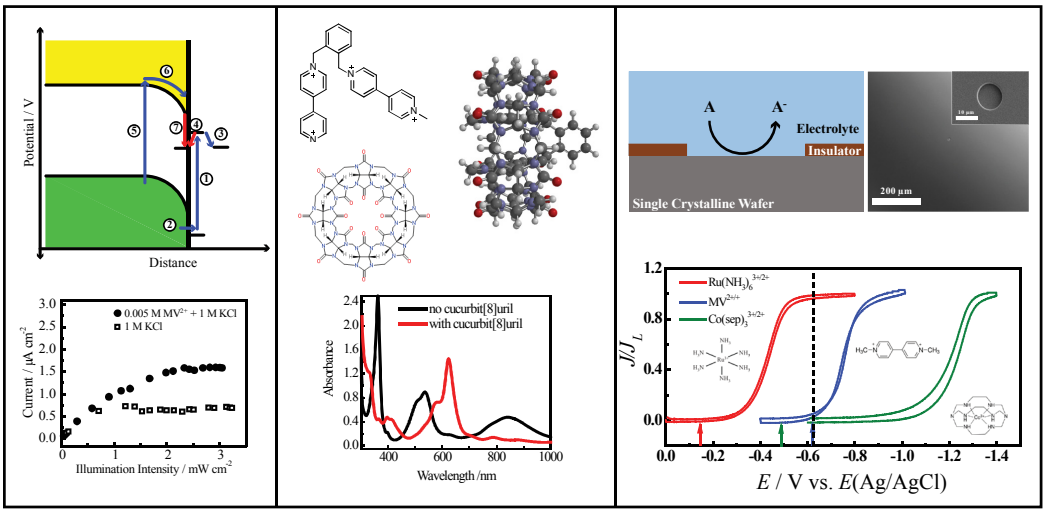

Figure 1. (left, top) Schematic depiction of a cathodic surface state acting as an electron acceptor for a physisorbed, photoexcited dye incapable of injecting an e^- directly into the conduction band. The blue arrows denote desirable processes for the flow of electrons in a conventional dye-sensitized photocathode. The red arrows indicate deleterious e^- trapping at a surface state. (left, bottom) The measured photocurrent at a p-GaP photocathode in water sensitized by physisorbed Fast Green FCF as a function of sub-bandgap light intensity. At low light intensities, the photocurrent is not affected by the presence of a dissolved redox mediator. At high light intensities, the photocurrent saturates at a low value without the presence of a dissolved redox mediator and is higher when a redox mediator is present. (middle, top) Depictions of an ortho-benzyl viologen dimer and cucurbit[8]uril besides a model of the lowest energy conformation of the reduced dimer inside cucurbit[8]uril. (middle, bottom) Comparison of the absorption spectra for solutions of the reduced the viologen dimers in the absence and presence of cucurbit[8]uril. (right, top) Schematic depiction and scanning electron micrographs of the semiconductor ultramicroelectrode (SUME) platforms developed in this work. (right, bottom) Comparison of the steady-state voltammograms for three distinct redox couples with n-Si SUMEs.

Dye sensitized photocathodes that operate in water represent an open area for development within the field of photoelectrochemistry. Three outstanding challenges exist: identification of a system(s) that allows systematic tuning of all operative features, identification of suitable cathodic redox mediators, and a means to discern kinetic information from conventional voltammetry. This poster presentation will highlight the recent progress our group has made on advancing these concepts. (*1*) Sensitization of p-type gallium phosphide (GaP) photoelectrodes with physisorbed dye will be detailed, highlighting a potential issue with dye regeneration through a cathodic surface degradation process. These data further motivate the development of passivation chemistry for GaP. (*2*) The design and demonstration of a macromolecular assembly of viologen dimers and cucurbiturils for realizing redox mediators with strong reducing power and stability even in the presence of O_2 will be shown. (*3*) The ongoing development of semiconductor ultramicroelectrodes (SUMEs) for making kinetic measurements will be described.

Nanostructured Solar Fuel Systems

Pengtao Xu, Yuguang C. Li, Zhifei Yan, Jeremy L. Hitt, Tian Huang, Christopher Gray, Langqiu Xiao, Kamryn Curry, August J. Rothenberger, and Thomas E. Mallouk,
Department of Chemistry, The Pennsylvania State University, University Park, PA 16802
Ryszard J. Wycisk and Peter N. Pintauro, Vanderbilt University, Nashville, TN 37203

This project investigates molecule-based (photo)electrochemical systems for overall water splitting and CO_2 electrolysis. We are developing photoanodes and photocathodes that combine molecular photosensitizers with core-shell and nanowire array oxide semiconductors, which are coupled to catalysts for water oxidation or CO_2 reduction. These problems are studied at the molecular level by transient spectroscopic and electrochemical methods, and at the system level in membrane-based electrolysis cells.

We have recently combined time-resolved transient absorbance spectroscopy (TAS) with intensity-modulated photovoltage spectroscopy (IMVS) and electrochemical impedance spectroscopy (EIS) to study the complex kinetics of charge separation and recombination at catalyst/dye/oxide semiconductor interfaces. Understanding these kinetics is important for improving the efficiency and stability of the water-splitting photoanode. TA and IMVS probe charge recombination in different spatial and temporal regimes. Regeneration of oxidized sensitzer molecules at the surface of a nanocrystalline TiO_2 electrode, measured by TAS, is three orders of magnitude faster than the recombination lifetime probed by IMVS, which is a capacitance-limited discharging process of trapped electrons in TiO_2. The rate and reaction order of the surface charge-recombination process change dramatically with core-shell electrodes. A photoanode based on a buried junction solid-state dye cell (right) was also developed and gave stable photocurrents for water oxidation in the mA/cm^2 range under AM 1.5 conditions.

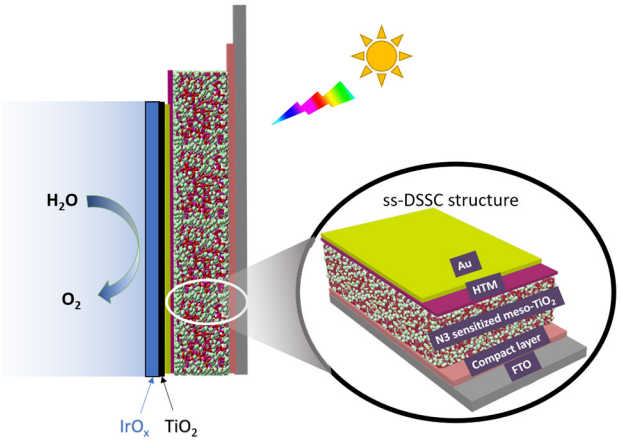

In studying these systems, we and other groups have discovered that bipolar membranes (BPM) can maintain stable currents and solution pH in water- and CO_2-(photo)electrolysis cells. Under reverse-bias conditions, water dissociation occurs in a catalytic layer at the interface between the cation- and anion-exchange layers of the BPM, driving H^+ and OH^- ions towards the cathode and anode, respectively. The crossover of anionic and neutral reduction products, such as formate and methanol, is problematic in conventional HCO_3^- electrolysis cells based on anion exchange membranes, but is suppressed in BPM-based cells. Recently we have studied electrolysis cells for gas-phase CO_2 based on "3D" BPMs with a high surface area catalytic interface. EIS measurements reveal the interplay of catalysis and electric field in water dissociation within the BPM and offer a prescription for the design of more efficient systems. Despite the high surface area interface and the high current density it sustains for CO_2 electrolysis, the crossover flux through the 3D BPM is an order of magnitude lower than with conventional membranes.

Rates and Mechanisms of Proton-Coupled Electron Transfer in Strongly Coupled Chromophore-Phenol Donor-Acceptor Pairs

Gerald F. Manbeck, Javier Concepcion, Etsuko Fujita
Chemistry Division
Brookhaven National Laboratory
Upton, NY 11973-5000

Challenges in the production of solar fuels include efficient coordination of ultrafast light absorption with slower catalytic reactions. Proton-coupled electron transfer (PCET) addresses this challenge because rates and driving forces can be controlled by regulating proton movement through hydrogen bond distances, pK_a's, and the stepwise or concerted nature of the mechanism. The donor side of Photosystem II (PSII) illustrates a specific example of PCET linking charge migration and catalysis. After excitation of P_{680} and oxidative quenching, the radical cation $P_{680}^{\bullet+}$ oxidizes the phenolic tyrosine Z (Tyr_Z) to the neutral radical, $Tyr_Z^{\bullet}$, by PCET with H^+ transferred to histidine-190 through a pre-formed hydrogen bond. $Tyr_Z^{\bullet}$ advances the oxygen-evolving complex (OEC) through four sequential oxidations to liberate O_2.

The PCET chemistry of the Tyr_Z / His_{190} pair stimulates interest in photochemical oxidations of model phenolic compounds. In a recent report, we detailed both the oxidation and reduction of a PSII-inspired chromophore-base-phenol complex with a pre-associated H-bond, $[Ru(bpy)_2(phen\text{-}imidazole\text{-}Ph(OH)(^tBu)_2)]^{2+}$ (**1**), in acetonitrile.[1] Strong coupling between flash-quenched produced Ru(III) and the phenol facilitated rapid oxidation of the phenol by an adiabatic stepwise pathway with $\Delta G = -0.01$ eV and $280 < H_{DA} < 540$ cm^{-1}. Reduction of the phenoxyl radical by a methyl viologen radical proceeded through concerted nonadiabatic PCET.

In this poster, we present PCET data for new complexes containing multiple (phen-imidazole-Ph(OH)(^{t}Bu)$_2$) ligands (**2**-**3**) and the N1-H congeners (**4**-**6**) (Chart 1) to study the rate enhancement by multiple donor sites as well as changes in the mechanism with variation in the acceptor basicity. For example, the PCET rate of **2** is over three times greater than that of **1** despite the similar driving force. Temperature dependent kinetics show that H_{DA} decreases to 150 cm^{-1} in **2**, and the faster PCET rate is attributed to a ~1 kJ mol^{-1} decrease in the activation energy and a 0.2 eV decrease in the reorganization energy, λ. The differences in rate and coupling are significant because it appears that the PCET occurs by a stepwise adiabatic mechanism in **1** but a nonadiabatic concerted mechanism in **2**. The new data show that the reactivity of these intramolecular PCET complexes is neither well-understood nor easily predicted by conventional assumptions. Our studies of **1**-**6** will be used to inform and guide the design of strongly coupled intramolecular PCET systems with the future goal of transferring the oxidative equivalent to catalysts or substrates.

Chart 1

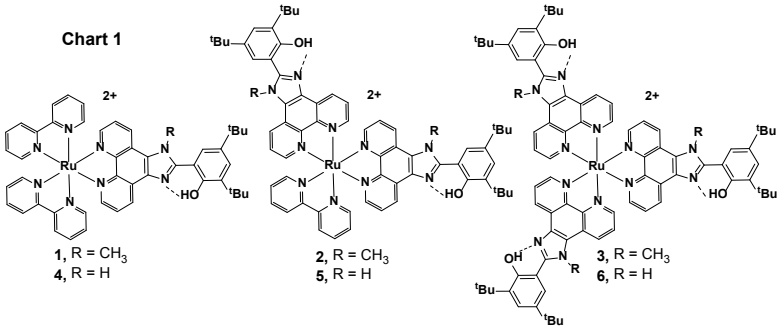

(1) Manbeck, G. F.; Fujita, E.; Concepcion, J. J. *J. Am. Chem. Soc.* **2016**, *138*, 11536.

Polarizability and low-frequency vibrations in electron-transfer reactions

D. V. Matyushov[1] and M. D. Newton[2]

[1]School of Molecular Sciences, Arizona State University, Tempe, AZ 85287
[2]Brookhaven National Laboratory, Chemistry Department, Upton, NY 11973-5000

This is the second year of the project in which our focus was shifted to the analysis of electrode reactions. We have studied electrode reactions in ionic liquids and more recently turned to identifying physical mechanisms and observable consequences of non-parabolicity of the free energy surfaces of electron transfer establishing the reaction activation barrier. This direction of research was largely motivated by our analysis of electron transfer in donor-acceptor complexes studied by Miller and co-workers performed in the first year of the project. We found that the maximum rate of activationless electron transfer is reached at a much lower driving force values than predicted by the standard theories. This finding potentially opens the door to new mechanisms to optimize the performance of solar energy conversion not understood from the standpoint of basic principles so far. Many current molecular champions of long-lived charge separated states employ conjugated and highly polarizable molecular fragments. Electrochemistry offers a convenient way to analyze the mechanistic parameters of such electron-transfer systems.

Experimental evidence invoked to test the theory is the asymmetry between anodic and cathodic branches of the electrode current recently observed for a number of redox systems studied by electrochemistry. In the first stage of this project, an analytical, exactly-solvable theory for electrode reactions involving polarizable reactants was proposed. The theory is formulated in terms of two reorganization energies, instead of one in the Marcus theory. It shows a clear asymmetry between the cathodic and anodic currents when the polarizability difference between the oxidations states is allowed. Another novel result of the theory is the predicted proximity of the electrode current branches to the empirical Butler-Volmer law, even though with non-equal transfer coefficients. The fact that an asymmetric Butler-Volmer law is often observed in electrode kinetics despite the expected symmetric Marcus-Hush behavior has puzzled many electrochemists and might find its explanation in the new theory.

The theory was further extended to the problem of electrode reactions in which the reactant's low-frequency vibrational mode changes its force constant as the result of altering the oxidation state. This physical mechanism has been explored by a long list of researchers for a number of decades, but no closed-form solution of the problem could be found. The general framework of the Q-model of electron-transfer reactions offers a fully analytical solution accounting for both the medium polarization and localized vibrations of the reactant. Other current projects, now in the finishing stage, include the application of the theory to electrochemistry of fullerenes and the development of a quantitative microscopic theory of dielectric screening effects in converting the redox potentials to the reaction free energy at finite donor-acceptor separations (so-called Rehm-Weller corrections).

Insights into Electronic and Structural Factors Governing Excited-state Dynamics in Fe(II) Polypyridyl Chromophores

Sara L. Adelman, Monica C. Carey, Jennifer N. Miller, and James K. McCusker*
Department of Chemistry
Michigan State University
East Lansing, Michigan 48824

Our research program continues to focus on elucidating the factors governing the dynamics of excited-state evolution in chromophores based on first-row transition metal ions. The motivation derives from the notion that the light-capture part of solar energy conversion is material-intensive; realization of successful approaches that are globally scalable therefore necessitates the use of earth-abundant components. For molecular chromophores employing transition metal ions, this places us in the first row of the d-block, where our DOE-supported work has demonstrated fundamental differences in the photophysics of this class of compounds as compared to their 2nd- and 3rd-row counterparts that undercuts their utility in virtually any solar energy conversion strategy. The origin(s) of these effects must be understood if the goal of effecting photo-induced charge separation using widely available materials is to be achieved.

There are two primary threads to our efforts, one focusing on electronic factors and the other on trying to understand the nature of the reaction coordinate along which excited-state evolution proceeds. This poster presentation will focus primarily on the second thrust, where we have been employing variable-temperature ultrafast time-resolved optical spectroscopy to gain insights into the activation parameters (and ultimately reorganization energies) associated with the photo-induced dynamics of a range of Fe(II) polypyridyl complexes.

Figure 1 shows data for ground-state recovery acquired on $[Fe(bpy)_3]^{2+}$ in CH_3CN solution as a function of temperature. In contrast to other reports in the literature, this compound does indeed exhibit a small but nonetheless measureable, non-zero barrier for high-spin to low-spin conversion in solution. Analyzing these data in the context of non-radiative decay theory allowed us to determine the magnitude of the electronic coupling interaction that facilitates this process as well as an experimental relationship between H_{ab} and the overall reorganization energy for the process that is highlighting changes in the degrees of freedom of the molecule that serve as the basis for the reaction coordinate. Analogous measurements made in a series of solvent families has furthermore allowed us to parse out outer-sphere contributions to the total reorganization energy, which we believe is a first for an excited-state process that does not involve charge separation. Details concerning these results will be presented, along with what we propose as the next steps in order to connect these insights and observations to the dynamics that control MLCT-state deactivation in this class of chromophores.

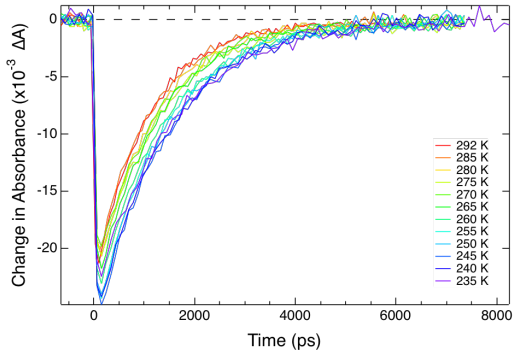

Figure 1. *Variable-temperature time-resolved absorption data for $[Fe(bpy)_3]^{2+}$ in CH_3CN solution.*

Electron Transfer Dynamics in Efficient Molecular Solar Cells

Eric Piechota, Tim Barr, Renato Sampaio and Gerald J. Meyer
Department of Chemistry
University of North Carolina at Chapel Hill
Chapel Hill, NC 27599

An objective of this Department of Energy supported research is to provide new mechanistic insights into surface mediated photochemical reactions at molecular-semiconductor interfaces. The scope is focused on the role surface electric fields play in dye-sensitized electron transfer at oxide interfaces. The electric fields are generated by excited state injection, electrochemical reduction, molecular dipoles, and/or ion surface adsorption. The dyes report on the field magnitude and direction through a spectral shift reminiscent of that observed in traditional Stark spectroscopy. Pulsed laser excitation experiments have been particularly valuable and provide kinetic data for ion-migration and dye reorientation that occurs in response to the electric field.

This poster presents a study designed to quantify the electric field as injected electrons inTiO_2 recombine with oxidized sensitizers. Light excitation of the characteristic metal-to-ligand charge-transfer (MLCT) absorption of $[Ru(NH_3)_5(ina)]^{2+}$, where ina is isonicotinic acid, anchored to mesoporous thin films of anatase TiO_2 nanocrystallites resulted in quantitative excited state injection in neat CH_3CN. A significant change in the molecular dipole, $\Delta\mu$ = 9.1 D was calculated by DFT and enabled the surface electric field to be quantified. The field present 70 ns after excited state injection was E = 0.35 MV/cm and this value decreased continuously with charge recombination. The kinetic behavior was most consistent with the surface anchored dyes experiencing a continuous contraction of an electric field generated by delocalized electrons, rather than a discrete number of sensitizers experiencing a localized field, as recombination proceeds. When Li^+ cations were present in the electrolyte, the field decayed more rapidly than did charge recombination and a longer-lived $[Ru^{III}(NH_3)_5(ina)|TiO_2(e^-)]$ charge separated state was observed, behavior attributed to cation screening of the electric fields. Taken together these observations suggest that the surface electric field controls charge recombination and may underlie the non-exponential kinetics commonly observed for this process.

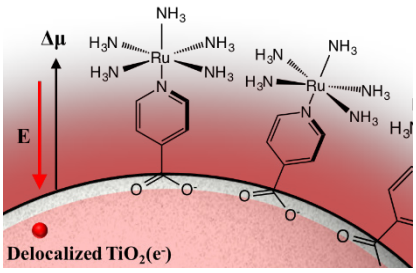

When the carboxylic acid in $[Ru(NH_3)_5(ina)]^{2+}$ was replaced with an ethyl ester group and the same experiments are performed, spectral changes consistent with the dye flipping over were observed. Interestingly, when the field was removed the dye molecules flip back over with dynamics that were time resolved. While an extensive literature exists for electric field '*poling*' in polymers and liquid crystals, to our knowledge this represents the first demonstration of related behavior at a semiconductor interface. The implications of these findings for solar energy conversion will be discussed.

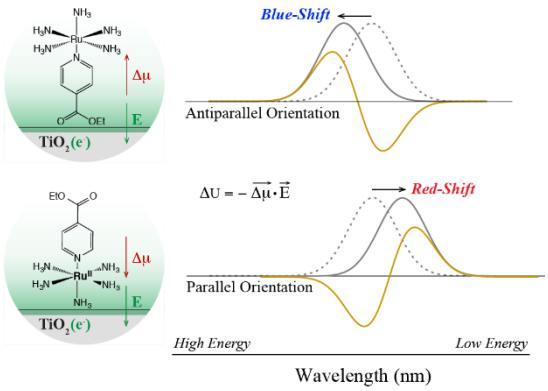

Functionalizing Oxide Surfaces with Molecular Assemblies: Applications in Energy Conversion

Thomas J. Meyer

Department of Chemistry
University of North Carolina at Chapel Hill
Chapel Hill, North Carolina, 27514

Abstract.

The performance of molecular-based solar energy conversion devices, such as dye-sensitized photoelectrosynthesis cells, is dictated in large part by the properties of the semiconductor-molecule interface. Manipulation of the interface at the surface is a key to improving their efficiencies. In our strategies, we use molecular dyes as light absorbers, redox mediators for enhancing charge-separation, and catalysts for carrying out chemical reactions at the surfaces of oxide electrodes. We have explored ways to prepare surface assemblies with those components, by using direct coordination of metal ion bridges and phosphonic /carboxylic acid anchoring groups, electrodeposition of inorganic catalysts coupled with surface-immobilized molecular dyes, and electro-polymerization of functional vinyl-derivatized molecular components. The direct surface synthesis of assemblies is desirable for its simplicity and with success, as a way to scale up for device purposes such as water splitting or carbon dioxide reduction.

In addition to synthesis, existing capabilities for characterizing the resulting molecularly modified surfaces have been applied, including spectroscopic, electrochemical, and rapid pulsed laser measurements, to explore the effect of chemical changes on surface properties. For those assembly-functionalized oxides, the photoinduced, interfacial electron transfer processes have been characterized by using time-resolved transient absorption /emission spectroscopies for investigation of the relationships between assembly structures, electron transfer dynamics and photoelectrocatalytic performances.

Molecular Photoelectrocatalysts for Hydrogen Evolution

Annabell G. Bonn, Bethany M. Stratakes, Kelsey R. Brereton, Teddy Wong,
Catherine L. Pitman, and Alexander J. M. Miller
Department of Chemistry
University of North Carolina at Chapel Hill
Chapel Hill, NC 27599-3290

Molecular photoelectrocatalysts facilitate both electrochemical hydride formation and photochemical H_2 evolution in a platform ripe for mechanistic examination and synthetic optimization. One aim is to identify monohydride complexes capable of photochemical H_2 release and understand the fundamental properties that engender productive H–H bond formation pathways from a single photon absorption. In parallel, we seek conditions under which photoactive hydrides can be regenerated electrochemically to achieve sustained catalytic H_2 evolution.

Initial studies on $[Cp^*Ir(bpy)H]^+$ and related hydrides, the first H_2 evolution photoelectrocatalysts, revealed a new H_2 release mechanism in which efficient bimetallic excited state electron transfer leads to H–H coupling. Inspired by the operative bimetallic pathway, we prepared new catalysts featuring two covalently linked Ir centers. At low catalyst loading, the bimetallic systems are >5-fold faster than the monometallic analogues, Fig. 1. Interestingly, there is evidence for competing intra- and intermolecular H_2 release. So far, catalysis has been carried out in water, even while a detailed thermodynamic and kinetic picture of the individual photochemical and electrochemical steps has been amassed in acetonitrile. Guided by thermodynamic parameters (e.g. acidity and hydricity), we have identified conditions for energy-storing catalysis in acetonitrile at electrochemical potentials *positive* of the thermodynamic potential for acid reduction, Fig. 2. Molecular systems that support electrochemical hydride generation and photochemical H_2 release remain rare, motivating efforts to discover new systems. We recently found that hydrides of type $[(arene)Ru(bpy)H]^+$, Fig. 3, can be generated electrochemically and also undergo photochemical H_2 release. Synthetic modifications tuned the photochemistry from arene photodissociation to selective H_2 release. Studies comparing the catalytic activity and reaction mechanism of Ir and Ru systems will be presented.

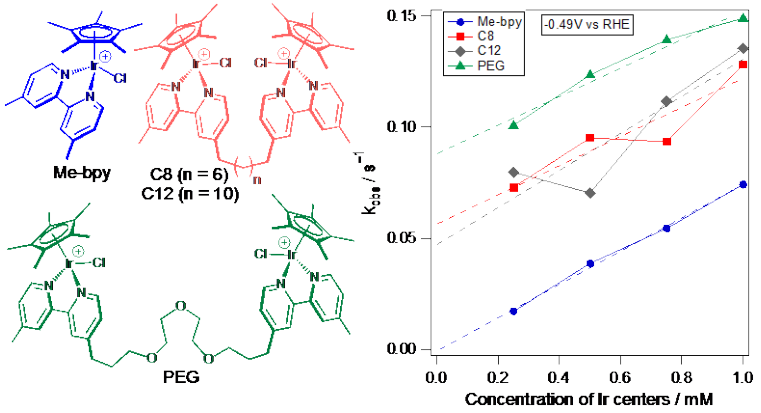

Fig. 1. Photoelectrocatalytic activity of mono- and bimetallic catalysts.

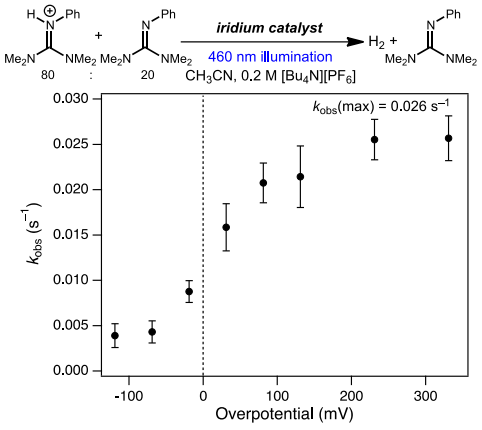

Fig. 2. Catalysis in acetonitrile solvent.

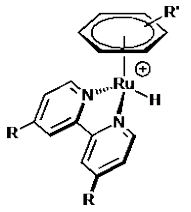

Fig. 3. Ruthenium catalyst structures.

Pulse Radiolysis Creates a Redox Ladder to the Top

Richard Marasas, Hung-Cheng Chen, and John R. Miller
Chemistry Department
Brookhaven National Laboratory
Upton, New York 11786

Redox potentials are widely used in chemistry to learn energetics of adding electrons or holes to molecules. They are usually measured electrochemically, most commonly by cyclic voltammetry. This work obtains very negative reduction potentials as part of our effort to better understand energetics of electron transfer chemistry through, principally, pulse radiolysis. In the radiation chemistry of water, the redox potential for the strongest, "top" reducing agent, the hydrated electron, has long been known. This is often not true for nonaqueous media. Free energy ladders have been constructed before for oxidation of molecules in acetonitrile, for reductions in the gas phase and for triplet energies. We describe here creation of a ladder for reductions in THF using methods pioneered by Dorfman and used in our laboratory but for much less negative potentials. The ladder connects known reduction potentials for molecules like biphenyl through a series of equilibria to the solvated electron in THF, thus determining its redox potential.

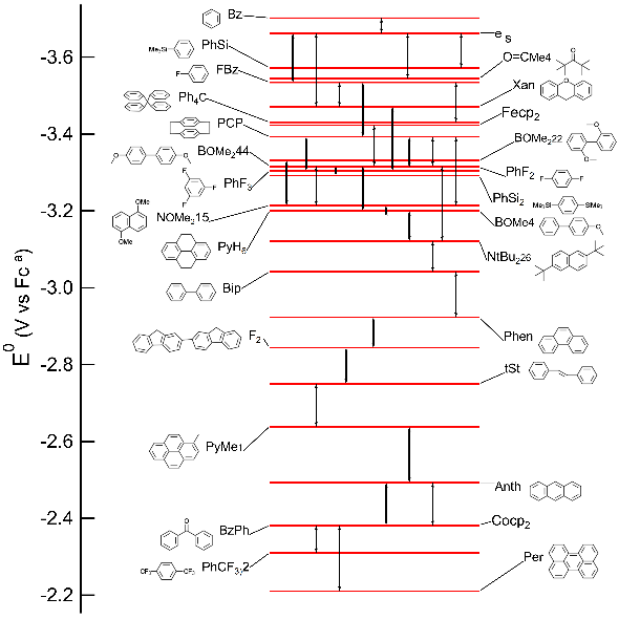

The ladder consists of free energy changes determined from equilibria of the type

$$D^{\bullet-} + A \rightleftharpoons D + A^{\bullet-} \qquad (1)$$

where the radical anion $D^{\bullet-}$ is an electron donor and A is an acceptor. The ladder enabled determination of reduction potentials for molecules which could not be measured electrochemically because the solvents or the electrolytes break down at very negative potentials. Each step in the ladder was smaller than ~200 meV because equilibrium constants much larger than 1000 become difficult to determine. We did not succeed to determine a redox potential for acetone due to destruction of the radical anions by proton transfer reactions. Determination for dihydroanthracene failed for similar reasons. The method succeeded for similar molecules having less acidic hydrogens. The data presented here is in the moderately polar solvent, THF, with no electrolyte. Comparing potentials from this ladder to results from electrochemical measurements find some curiosities which will be discussed.

Molecular Modules for Vectorial Photoinduced Electron Transfer and H_2 Photocatalysis

Karen L. Mulfort, Lars Kohler, Dugan Hayes, Ryan G. Hadt, Jens Niklas, Oleg G. Poluektov, Lin X. Chen, David M. Tiede
Division of Chemical Sciences and Engineering
Argonne National Laboratory
Argonne, IL 60439

This poster will describe our group's progress in the design and discovery of modular, molecular architectures for artificial photosynthesis, specifically recent work on 1) driving directional electron transfer from Cu(I)diimine photosensitizer modules and 2) mapping the impact of structure on activity in Co(II)poly(pyridyl) H_2 catalyst modules.

The visible-light accessible metal-to-ligand charge transfer (MLCT) states of Cu(I)diimine complexes suggest that they may be viable replacements for benchmark $Ru(bpy)_3^{2+}$-type photosensitizers, and we are particularly interested in understanding how to drive *directional* photoinduced electron transfer from molecular modules. To investigate this question, we synthesized four heteroleptic Cu(I)bis(phenanthroline) (CuHETPHEN) complexes with the well-known molecular electron acceptor 1,4,5,8-naphthalene-diimide (NDI) covalently bound to either the blocking ligand (2,9-dimesityl-1,10-phenanthroline, **bL**) or the secondary ligand (1,10-phenanthroline, **phen**, or 2,9-dimethyl-1,10-phenanthroline, **dmp**) (Figure 1). Analysis of the ultrafast transient absorption spectra demonstrates that charge transfer proceeds with strong directional preference, and charge separation is up to 35 times faster when NDI is linked to **bL**. Also, in polar solvent the charge-separated state of the dyads is stabilized by the large excited state structural distortion, resulting in dramatically longer lifetimes for dyads with minimal substitution about the Cu(I) center. This work using model electron acceptors establishes a set of design principles we will use to connect more challenging electron acceptors (i.e. proton reduction catalysts) to molecular chromophores based on the CuHETPHEN platform.

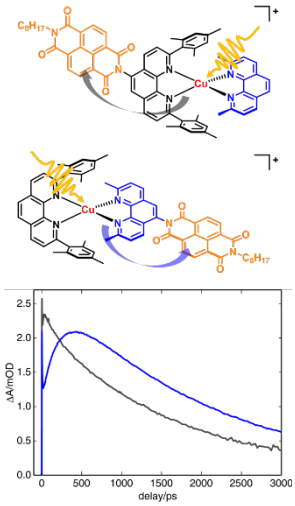

Figure 1. Top: chemical structure of CuHETPHEN-NDI dyads. Bottom: Comparison of kinetics of charge separation following 400 nm excitation to form NDI^- in CH_3CN. Gray trace of CuHETPHEN with NDI on blocking ligand, blue trace of NDI on secondary ligand.

Molecular catalysts enable an unparalleled opportunity to investigate, with very high resolution, how even very minor changes to the molecular structure influence catalytic activity. Here we describe the structure and H_2 photocatalytic activity of two closely-related Co(II) macrocycles formed via amine-linked bipyridine groups (Figure 2). Photocatalysis experiments show that these macrocycles are highly active for aqueous proton reduction at moderate pH levels, under certain conditions reaching over 2 x 10^4 H_2 TON when photo-driven by $Ru(bpy)_3^{2+}$. Current efforts are focused on linking these molecular catalysts directly to molecular chromophores.

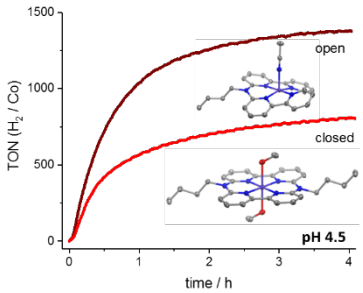

Figure 2. Comparison of H_2 photocatalysis of "open" and "closed" Co(II) macrocycles. $Ru(bpy)_3^{2+}$ photosensitizer, ascorbic acid used as sacrificial electron donor.

Isolating O–O Bond Activation

Daniel G. Nocera
Department of Chemistry and Chemical Biology
Harvard University
Cambridge, MA 02138

Solar-to-fuels generation requires the rearrangement of stable chemical bonds with light as the impetus for the fuel-forming reaction. All such reactions, regardless of the specific fuel, require the transfer of multiple electrons and protons. Energy barriers to such bond rearrangements are minimized only if electrons are efficiently coupled to protons. Catalysts can mediate this coupling, and as well as it does so, determines the solar-to-fuels efficiency. We have studied the proton-coupled electron transfer (PCET) mechanism for O–O bond cleavage in the oxygen reduction reaction (ORR) often mirrors O–O bond formation in the oxygen evolution reaction (OER) for both biological and chemical systems. For instance, Babcock first noted that the associative O_2 bond forming chemistry in Photosystem II has remarkable mechanistic similarities to the dissociative O_2 bond breaking chemistry in cytochrome c oxidase. The efficiency of associative and dissociative O–O bond activation depends on the critical coupling between the electron and the proton. When examining such PCET $O_2 \leftrightarrow H_2O$ conversions, rarely can the PCET event of O–O bond activation be isolated. We report here that ORR catalyzed by manganese(II) porphyrins and dicobalt complexes in the presence of Brønsted acids (HAs) does indeed allow the kinetics of O–O bond cleavage to be captured. Electrochemical kinetics data support a model where an oxygen bound to the reduced Mn(II) porphyrin platform is stabilized by a hydrogen bond to HA; in the case of the Mn hangman platforms, the HA is not needed as an internal hydrogen bond may be formed with the hanging acid group. The cleavage of the O–O bond of a subsequently formed Mn(III)-hydroperoxide is rate determining, as shown by foot-of-the wave analysis of catalytic cyclic voltammetric ORR profiles, thus allowing the kinetics for the PCET-induced O–O bond cleavage to be determined directly.

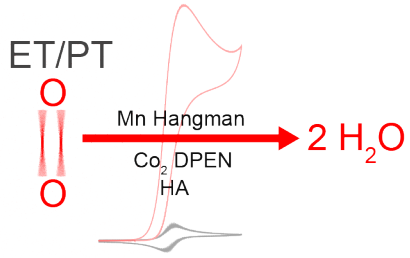

To isolate the types of oxygen intermediates in an OER/ORR cycle, we have turned to a dicobalt(III,III) core ligated by the polypyridyl ligand dipyridylethane naphthyridine (DPEN). Reduction by two electrons and subsequent protonation results in the release of one water moiety to furnish a dicobalt(II,II) center with an open binding site. Binding of O_2 to the open coordination site of the dicobalt(II,II) core results in the production of an oxygen adduct, which captures that of heterogeneous OER catalysts such as CoP_i. Electrochemical studies show that the addition of two electrons results in cleavage of the O–O bond, thus providing unique insight into O–O bond activation.

Semiconductor Quantum Dots for Advanced Concepts for Efficient Solar Photon Conversion: *Recent Advances in Using Hot Carriers in Solar Cells (Extraction and MEG)*

Arthur J. Nozik[1,2] and Matt Beard[2]

1. University of Colorado, Boulder
Department of Chemistry
&
2. National Renewable Energy Laboratory, Golden, CO

There are 2 fundamental approaches to utilize hot photogenerated electrons and/holes (charge carriers) in semiconductor-based solar photoconversion devices to generate additional electrical or chemical free energy in order to enhance their solar power conversion efficiencies (PCEs). The hot carriers are generated by absorbing solar photons with energies greater than the semiconductor bandgap and are utilized to generate additional free energy before the excess energy (in the form of kinetic energy) above the bandgap is lost through carrier-phonon scattering, and thus create heat rather than useful free energy. The two processes are: (1) to extract the hot carriers before they cool to the lattice temperature through phonon emission; or (2) use the excess hot carrier energy to create additional electron-hole pairs through a process in size-quantized semiconductor photon converters called Multiple Exciton Generation (MEG), since in quantized semiconductor nanocrystals the electron-hole pairs exist as excitons. In 2018 three manuscripts have been produced that report significant advances in the two approaches; these are: (1) Hot Carrier Enhanced Solar Cells. InGaAsP QWs in p-i-n solar cells wherein hot carriers generated in the QW produced an enhanced photovoltage and enhanced photocurrent (Guillemoles, Lombez , et al, Nature Energy 3, 236 (2018)); (2) Nearly Ideal Multiple Exciton Generation (MEG) Characteristic in 2-D Layered Van der Waal MoTe2 and WSe2 Crystals (Ji-Hee Kim et al, arkiv doi 1801.01675(002) (2018); and (3) Greatly Improved MEG Characteristic in Janus-type PbS|CdS heterojunction QDs (Beard, Klimov, Nozik, NREL team, submitted 2018). These advances will be discussed and analyzed regarding their significance and prognosis for future generation solar photoconverters with very high PCE.

Sensitization of Single Crystal Semiconductor Substrates with Single Wall Semiconductor Carbon Nanotubes

Lenore Kubie*, Kevin Watkins*, Mark Spitler, William Rice[#], Jeff Blackburn[+], Rachelle Ihly[+], Henry V. Wladkowski[#] and Bruce Parkinson*
Department of Chemistry* and Physics[#]
University of Wyoming
Laramie WY, 82071
and
[+]Energy Sciences Division
National Renewable Energy Laboratory
Golden, CO 80401

Semiconducting single-walled carbon nanotubes strongly absorb light in the spectral range spanning from the near-infrared to the ultraviolet. This broad absorption range, paired with their all-carbon composition, make single-walled carbon nanotubes attractive materials for light-harvesting. However, large exciton binding energies and the co-existence of metallic nanotubes have hindered the collection of free-carries from single-walled carbon nanotube films. We have demonstrated photoinduced charge transfer from single-walled carbon nanotube films into single-crystal metal oxide electrodes. Both multi-chiral and single-chirality carbon nanotube samples were used to sensitize atomically-flat GaP, SnO_2 and TiO_2 crystals. We find that while photocarrier collection occurs from both the first and second excitonic transitions of carbon nanotubes, more photocurrent is generated upon excitation of higher energy transitions in all cases. Furthermore, we show that there is a logarithmic relationship between the driving force for photoinduced charge transfer and photocarrier collection efficiency.

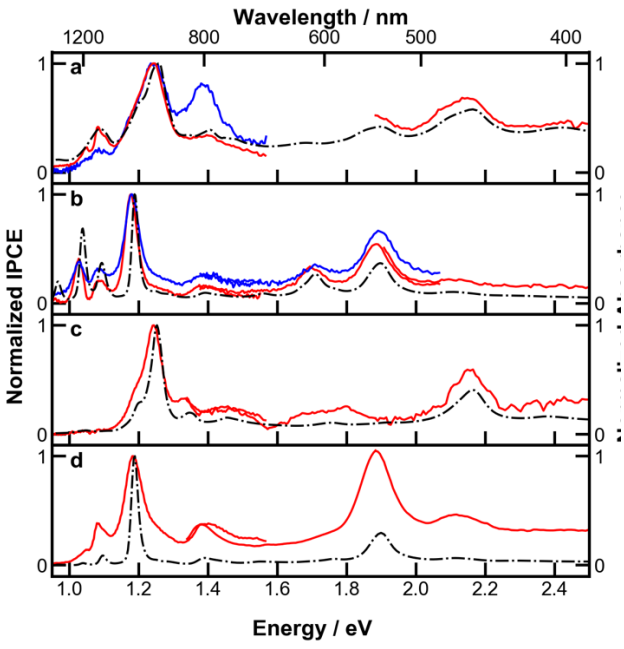

UV-vis spectra (black dashed lines), and normalized IPCE Spectra of various SWCNTs on SnO_2 (red) and TiO_2 (blue) where applicable. All spectra are normalized to the largest S_{11} peak and are collected in the electron injection regime unless otherwise noted. (A) Sodium cholate-wrapped CoMoCAT SWCNTs. SnO_2 spectra collected at +300 mV vs Ag-wire. TiO_2 spectra collected at +100 mV vs Ag-wire.; (B) PFO-wrapped HiPco SWCNTs SnO_2 spectra collected at 0.0 V vs Ag-wire. TiO_2 spectra collected at -600 mV vs Ag-wire (hole injection).;(C), Sodium cholate-wrapped (6,5)-enriched SWCNTs. SnO_2 spectra collected at 0.0 V vs Ag-wire.; (D) PFO-wrapped (7,5)-enriched SWCNTs. SnO_2 spectra collected at 0.0 V vs Ag-wire.

Reactive Intermediates in Catalytic CO_2 Reduction

Dmitry E. Polyansky, David C. Grills, James T. Muckerman and Etsuko Fujita
Chemistry Division, Energy & Photon Sciences Directorate
Brookhaven National Laboratory
Upton, NY 11973-5000

Transition-metal coordination compounds provide versatile platforms for mechanistic studies of reductive catalysis in artificial photosynthesis. In recent years, considerable advances have been made in the development of design principles that control the reactivity of a catalyst's metal center assisted by its ligand environment. However, the progress in mechanistic understanding of reductive catalysis has been significantly hindered owing to the poor characterization of reactive intermediates, especially those formed *following* the rate determining step of a catalytic cycle. Our work focuses on the application of transient methods, including laser and radiation techniques, augmented by advanced theoretical modeling to characterize transient intermediates formed during the catalytic reduction of CO_2 or protons.

In particular, the use of pulse radiolysis enables the production of highly reactive transient intermediates such as metal hydride, metal–CO_2 or metal–CO species.[1,2] This in turn allows the interrogation of the advanced stages of a catalytic cycle, where steady state concentrations of intermediates are typically small. Our recent laser flash photolysis and pulse radiolysis investigations of a CO_2 reduction catalyst $[Co^{II}(L)]^{2+}$ (L = 5,7,7,12,14,14-hexamethyl-1,4,8,11-tetraazacyclotetradeca-4,11-diene) in dry acetonitrile have shown that the generation of the doubly reduced $[Co^{II}(CO_2^{2-})L]$ intermediate, leads to the formation of $[Co^{I}(CO)L]^{+}$ *via* an unusual O^{2-} transfer reaction between the $[Co^{II}(CO_2^{2-})L]$ and $[Co^{III}(CO_2^{2-})L]^{+}$. Owing to the strong binding between the Co^{I} metal center and the CO ligand, the formation of the $[Co^{I}(CO)L]^{+}$ likely presents a deactivation pathway, resulting in the relatively low activity of this catalyst in dry organic solvents. The addition of a weak acid, e.g., water, increases the catalyst's activity by shifting the mechanism towards the protonation of the $[Co^{II}(CO_2^{2-})L]$ species. The reduction of $[Co^{II}L]^{2+}$ in aqueous solutions or in the presence of strong acids leads to H_2 evolution, signaling the efficient production of a metal hydride species followed by its protonation. This work demonstrates how the intricate interplay between reaction conditions and the reactivity of catalytic intermediates can control the mechanism of a CO_2 reduction reaction.

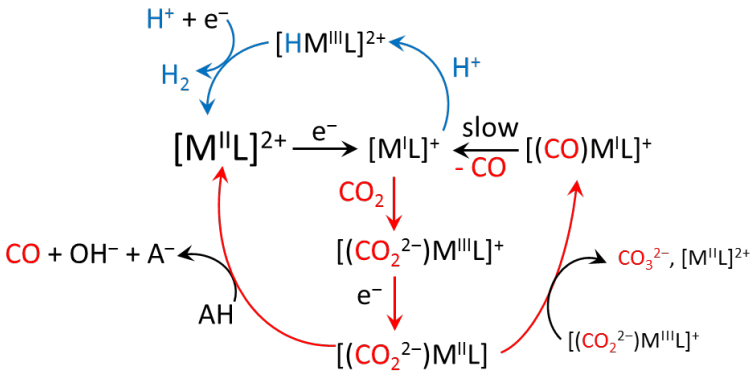

References.

1. Grills, D. C.; Polyansky, D. E.; Fujita, E. *ChemSusChem* **2017**, *10*, 4359 - 4373.
2. Lewandowska-Andralojc, A.; Baine, T.; Zhao, X.; Muckerman, J. T.; Fujita, E.; Polyansky, D. E. *Inorg. Chem*. **2015**, *54*, 4310−4321.

Excited State Dynamics of Photoexcited Charge Carriers in Halide Perovskites: Time-Domain Ab Initio Studies

Oleg Prezhdo
Department of Chemistry
University of Southern California
Los Angeles, CA 90089

Considering realistic aspects of perovskite structure,[1] we demonstrate that strong interaction at the perovskite/TiO_2 interface facilitates ultrafast charge separation,[2] that dopants can both decrease and increase charge recombination,[3-5] that grain boundaries constitute a major reason for charge losses,[5] that moderate humidity increases charge lifetime,[6] that trapping by defect, surprisingly, extends carrier lifetime,[7] that collective nature of dipole motions inhibits nonradiative relaxation,[8] that organic cation orientation has a strong effect on inorganic ion diffusion,[9] that surface passivation with Lewis base molecules decelerates nonradiative charge recombination,[10] that dual fluorescence originates from two types of perovskites substructures,[11] that charge separation at edges or 2D perovskites extends carrier lifetime, and that single-layer 2D perovskite is qualitatively different from multi-layer.[12]

1. *ACS Energy Lett.* **2017,** 2, 1588
2. *J. Phys. Chem. C* **2017,** 121, 3797
3. *J. Phys. Chem. Lett.* **2015,** 6, 4463
4. *ACS Nano* **2015,** 9, 11143
5. *J. Phys. Chem. Lett.* **2016,** 7, 3215
6. *J. Am. Chem. Soc.* **2016,** 138, 3884
7. *ACS Energy Lett.* **2017,** 2, 1270
8. *J. Phys. Chem. Lett.* **2017,** 8, 812
9. *ACS Energy Lett.* **2017,** 2, 1997
10. *J. Phys. Chem. Lett.* **2018,** 9, 1164
11. *J. Am. Chem. Soc.* **2017,** 139, 17327
12. *Nano Lett.*, in press

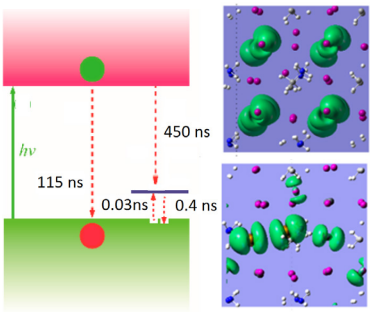

Fig. 1 Hole trapping by I interstitial in $MAPbI_3$ is fast, but recombination of trapped hole with electron is very slow, because they do not overlap. Hole can be trapped and detrapped multiple times before recombining, increasing carrier lifetime.

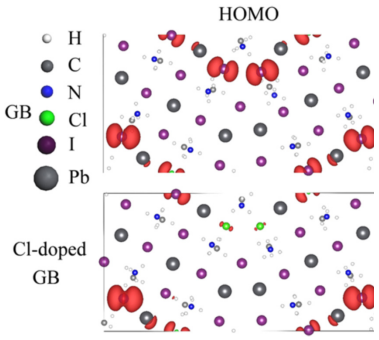

Fig. 2 Grain boundaries accelerate charge recombination in $MAPbI_3$, by creating trap states and enhancing electron-phonon coupling. Cl dopants aggregate at the boundary, push charges back to bulk, reducing recombination.

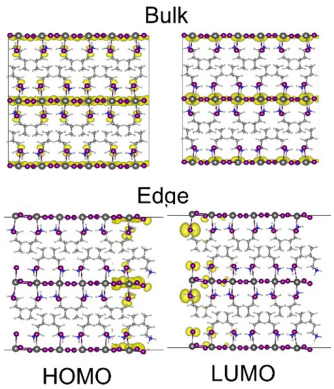

Fig. 3 Edge states in 2D peroskites separate charges, greatly extending their lifetimes. Single-layer behaves differently from multi-layer.

Free Charge Generation in Sensitized Conjugated Polymer Films

Garry Rumbles[1,2,3], Natalie Pace[2], Jessica Ramirez[2], and Obadiah Reid[1,3]
[1]Chemistry and Nanoscience Center,
National Renewable Energy Laboratory, Golden, Colorado, 80401
and
[2]Department of Chemistry and Biochemistry
[3]Renewable and Sustainable Energy Institute
University of Colorado Boulder, Boulder, CO 80309

Photoinduced electron transfer studies of conjugated polymers that have been sensitized with low concentrations of electron acceptor species have been studied using a variety of spectroscopies including photoluminescence (PL), transient absorption (TA), and time-resolved microwave conductivity (TRMC). The goal of the work is to understand what properties of the conjugated polymer in the solid-state promote the generation of long-lived free carriers, versus bound charge-transfer states that geminately recombine. We also investigate how the solid-state microstructure properties of the polymer host influence the carrier recombination process.

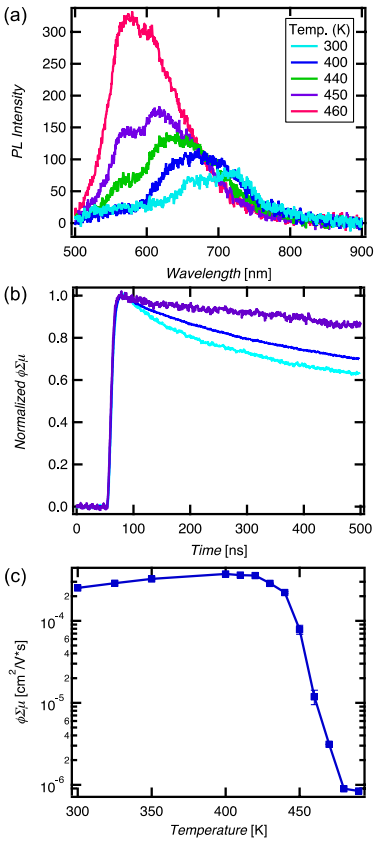

Figure 1 – Samples of poly(3-dodecyl thiophene) films sensitized with a silicon phthalocyanine. (a) PL Spectra as a function of temperature (b) Normalized, representative TRMC transients (c) (t=0) values as a function of temperature. Excitation at 450 nm for both PL and TRMC measurements.

We have demonstrated that the product of photoinduced electron transfer between a conjugated polymer host and a dilute molecular sensitizer is controlled by the solid-state microstructure of the polymer. Ordered semi-crystalline solids exhibit free charge generation, while disordered polymers in the melt phase do not. We used PL and TRMC measurements to sweep through polymer melt transitions *in situ* (see Figure 1). Free charge generation measured by TRMC turns off upon melting, whereas PL quenching of the molecular sensitizers remains constant, implying unchanged electron transfer efficiency. The key difference is the intermolecular order of the polymer host in the solid-state compared to the melt. We propose that this order-disorder transition modulates the localization length of the initial charge separated state, which controls the probability of free charge formation.

The carrier recombination process of a series of fullerene-sensitized polyfluorenes exhibits a characteristic charge transfer (CT) or exciplex emission for samples only where high carrier yields are generated. The kinetics of this emission have been modelled using a simple kinetic scheme that suggests that the intermediate CT/Exciplex state plays a critical role in both the production and recombination process. However, the characteristic, long-lived PL transients are controlled not by the intrinsic lifetime of the CT/exciplex state, but are a result of delayed luminescence from the non-geminate carrier recombination process.

Effects and External Control of Ultrafast, Coherent Nuclear Motion on Electronic Hybridization in Photochemical Processes

Matthew S. Kirscher, Wendu Ding, Craig T. Chapman, Xiao-Min Lin, Lin X. Chen, George C. Schatz, Richard D. Schaller
Nanoscience and Technology Division
Argonne National Laboratory
Lemont, IL 60439

Here, we investigate hybrid organic-metallic systems comprising metal particles that offer tunable, comparatively narrow plasmonic resonances and molecular species that form J-aggregate species.[1] We characterize the static properties of several different hybrids then analyze the ultrafast dynamics of these systems to determine the effects of coherent acoustic phonons on the electronic transitions. Specifically, gold bipyramids with systematically varied aspect ratios and corresponding localized surface plasmon resonance energies, functionalized with J-aggregated thiacarbocyanine dye molecules, produces two hybridized states that exhibit clear anti-crossing behavior with a Rabi splitting energy of 120 meV. In metal nanoparticles, photon absorption yields impulsively-generated coherent acoustic phonons that yield oscillations in the plasmon resonance energy. Upon coupling, these photogenerated oscillations alter the metal nanoparticle's energetic contribution to the hybridized system and, as a result, modulate the coupling between the plasmon and exciton. We demonstrate that such modulations in the hybridization are consistent across a wide range of bipyramid ensembles.

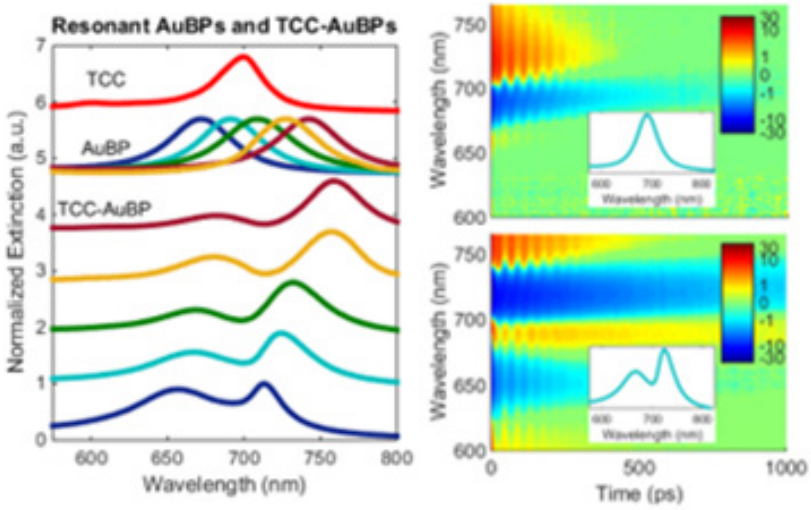

Through these studies, we demonstrate molecular sensitivity to the vibrational mode of a proximal, but externally designed inorganic solid undergoing acoustic deformation. We offer a qualitative explanation for the direction and magnitude of the observed changes in coupling. The resulting paradigm, which we describe as an oscillatory plasmonic−excitonic nanomaterial, could be used as a model system in the development of photochemistry facilitated by vibrational modes such as in vibrationally-manipulated donor-bridge-acceptor systems[2] as well as provide fundamental insight into plexcitonic systems or enable new applications owing to the inherent fine-tuning of the plasmonic resonance.

1. Kirschner et al. *Nano Lett.* **2018**, *18*, 442.

2. Delor et al. *Science* **2014**, *346*, 1492

Quasi-Particle Photophysics in Electronically and Morphologically Homogeneous Single-Walled Carbon Nanotubes

Yusong Bai, George Bullard, Jean-Hubert Olivier, and Michael J. Therien

Department of Chemistry, French Family Science Center, 124 Science Drive, Duke University, Durham, NC 27708-0346, USA

The formation of quasiparticles, such as polarons, excitons, and trions, is crucial to solar energy conversion reactions of single-walled carbon nanotubes (SWNTs), as these species respectively carry charge, excitation energy, and spin. Unraveling the spectroscopic and dynamic properties of these quasiparticles in SWNTs has proved challenging, largely due to the electronic and morphological heterogeneity of commonly interrogated carbon nanotube samples. We describe studies that exploit a binaphthalene-based polyanionic semiconducting polymer (*S*-PBN(b)-Ph_5) that exfoliates, individualizes, and disperses SWNTs via a single-chain helically chiral wrapping mechanism, giving rise to semiconducting polymer-SWNT superstructures in which the polymer maintains a fixed helical pitch length on the nanotube surface. The robust nature of these superstructures in various aqueous and organic solvents enables multiple rigorous separation procedures that permit isolation of highly-enriched (purity > 90%), length-sorted (700 ± 50 nm) (6,5) SWNTs: these *S*-PBN(b)-Ph_5-[(6,5) SWNTs] define uniquely engineered, consistent nanoscale carbon nanotube superstructures with which to probe spectroscopic signatures and dynamics of polarons, excitons, and trions. We demonstrate that charge carrier-doping densities (holes and electrons) may be rigorously controlled in these systems. Excited-state dynamical studies that vary both excitation fluence and excitation wavelength (i) elucidate SWNT trion formation and dynamics, and (ii) provide a straightforward means to quantitatively evaluate optically-driven free-carrier generation in neutral SWNTs as functions of exciton energy and medium dielectric strength.

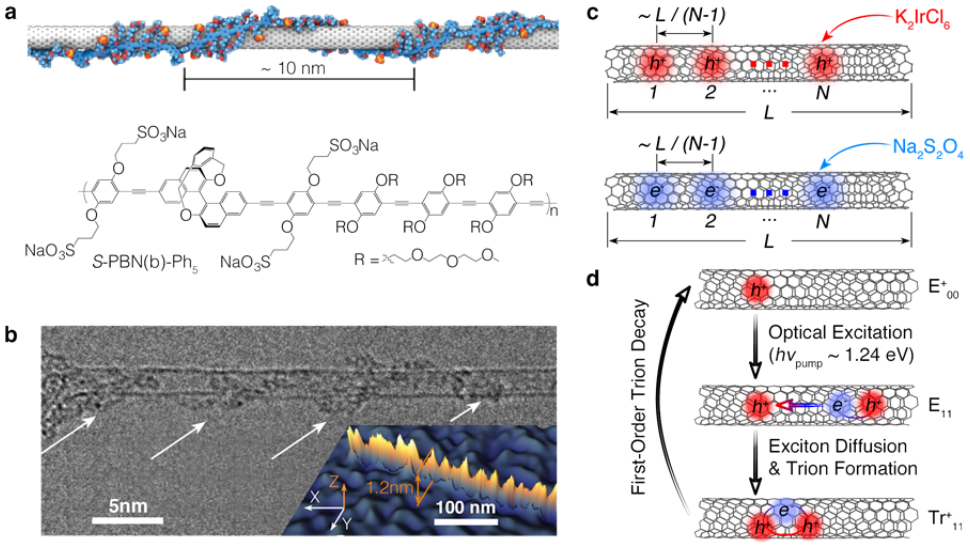

X-ray Structure and Photophysical Characterization of Catalysts and Photosensitizer Dyes Supported on Nano-to-Microporous Semiconductor and Conductive Oxides

David M. Tiede,[1] Gihan Kwon,[2,3] Alex B.F. Martinson,[2,3] Alex I. Smirnov,[4] Oleg Poluektov,[1] Jens Niklas,[1] Lars Kohler,[1] and Karen L. Mulfort[1]

[1]Chemical Sciences and Engineering and [2]Materials Sciences Divisions, Argonne National Laboratory, [3]Argonne Northwestern Solar Energy Research (ANSER) Center, [4]Department of Chemistry, NC State University

In this project we have been investigating approaches for *in situ* and *operando* X-ray structure characterization of catalysts and photosensitizer dyes supported on nano-to-microporous semiconductor and conductive oxides. We have developed high surface area TiO_2 semiconductor and ITO and IZO conducting oxide porous assemblies that duplicate oxide-supported dye and catalyst architectures widely used in dye sensitized solar cells (DSSC) and photoelectrochemial (PEC) electrodes, but have been tailored to allow interfacial X-ray structure characterization. In particular, we have developed these for combined X-ray spectroscopy (EXAFS) and scattering for atomic pair distribution function (PDF) analyses for solar (photo)catalysts. An example, Figure 1A, is shown by the accumulation of the N3 dye, cis-bis(isothiocyanato) bis(2,2'-bipyridyl-4,4'-dicarboxylato ruthenium(II), within a 50 μm thick anodic aluminum oxide, AAO, membrane with 80 nm diameter pores coated with a 8 nm TiO_2 overlayer by atomic layer deposition, Figure 1B. The N3 dye associates to the TiO_2-AAO membrane at a number density that is > 50-fold higher than the ~0.5 mM solubility limit. The high volume density allows accurate PDF analysis, Figure 1D, which provide clear resolution of both inner and outer coordination sphere distances. Each of the PDF peaks can be assigned to the coordination structure, and the PDF pattern for the surface tethered N3 dye was found to be equivalent to that in solution, allowing solvent-loaded, TiO_2-AAO membrane assemblies to be used as 2D materials that concentrate inorganic complexes in a solvated environment, and provides electronic coupling to a semiconductor layer for photophysical studies on excited-state charge injection to TiO_2. Preliminary experiments also demonstrate the ability to extend this approach to resolve high resolution PDF structure data for surface-bound "heterogenized" water oxidation (with G. Brudvig, Yale, and D. Wang, BC; and J. Concepcion, BNL), hydrogen evolving catalysts (with A. Miller, UNC).

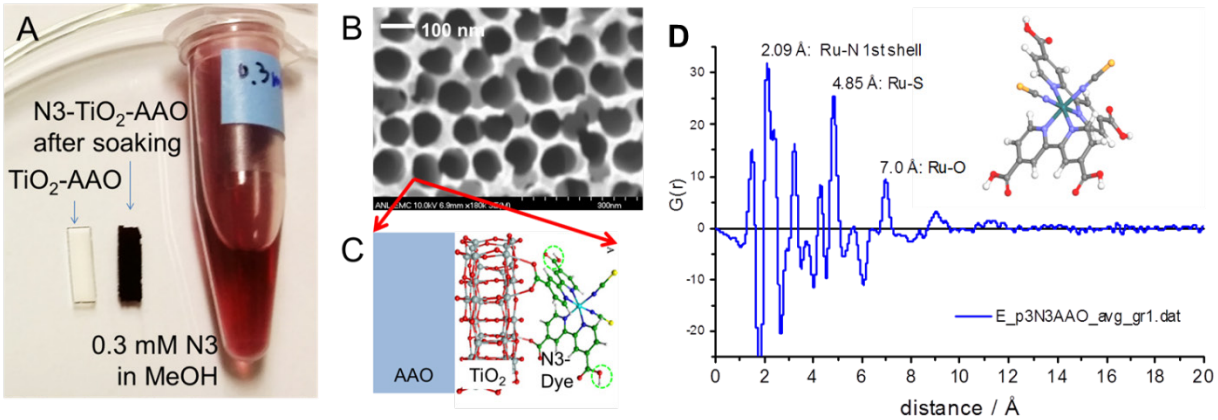

Photo-driven Charge Separation and Transport in G-Quadruplex Frameworks

Michael R. Wasielewski, Yi-Lin Wu, Natalia Powers-Riggs, and Jenna L. Logsdon
Department of Chemistry
Northwestern University
Evanston, IL 60208

Two-dimensional covalent organic frameworks often π-stack into crystalline solids that allow precise spatial positioning of donor-acceptor molecular building blocks. This behavior is critical for the formation of segregated charge conduits in which photo-generated holes and electrons can rapidly propagate to electrodes or to sites at which they can provide redox equivalents for catalysis. Inspired by the hydrogen-bonded G-quadruplexes found frequently in guanine-rich DNA, here we show that this structural motif can be exploited to guide the self-assembly of naphthalenediimide and perylenediimide electron acceptors end-capped with two guanine electron donors into crystalline G-quadruplex-based frameworks (GQFs), wherein the electron donors and acceptors form ordered, segregated, π-stacked arrays. Due to the strong association between molecules forming arrays of multi-point hydrogen bonds (K_a ~$10^{5–12}$ M^{-1}), non-covalent frameworks exploiting hydrogen bonding have attracted increasing attention. The planar geometry of multiply hydrogen-bonded arrays is suitable for generating 2D architectures, which subsequently π-stack into 3D ordered solids. This methodology is different from conventional assembly methods, where the 2D framework is constructed using reversible covalent linkages of boronate ester, imine, or triazine functionalities. Based on our previous experience with self-ordering G-quadruplex-based donor-acceptor assemblies, we reasoned that the π-stacking properties of the G-quadruplex, together with its hydrogen-bond forming ability, could be exploited for GQF synthesis.

In order to probe the how building block structure dictates overall 3D structural GQF assembly, 2,7-diaryl pyrene building blocks with high HOMO energies and large optical gaps were examined. The adjustable substitution on the aryl groups provides an opportunity to elucidate the framework formation mechanism; molecular non-planarity is found to be beneficial for restricting interlayer slippage, and the framework crystallinity is highest when intermolecular interaction and non-planarity strike a fine balance. When guanine-functionalized pyrenes are co-crystallized with naphthalenediimide, charge-transfer (CT) complexes are obtained. The photophysical properties of the pyrene-only and CT frameworks were characterized by UV-Vis and steady-state and time-resolved photoluminescence spectroscopies, and by EPR spectroscopy for the CT complex frameworks.

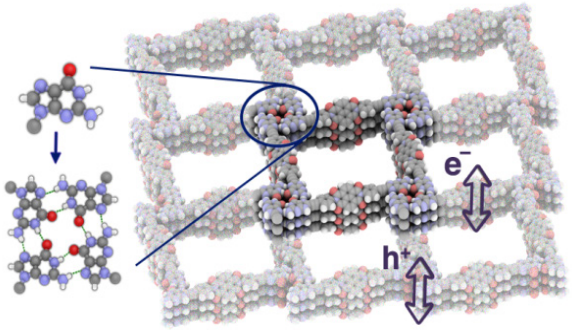

Fig. 1. Structure of a G-quadruplex framework containing naphthalenediimide electron acceptors.

Time-resolved optical and electron paramagnetic resonance spectroscopies show that photo-generated holes and electrons in the frameworks have long lifetimes (>10 μs) and display recombination kinetics typical of dissociated charge carriers. Moreover, the reduced acceptors form polarons in which the electron is shared over several molecules, making GQFs excellent photo-driven charge generation and transport systems.

Thermochemical Guidelines for Designing Efficient H_2 Evolution or Selective CO_2 Reduction Catalysts

Dr. Charlene Tsay, Bianca Ceballos, Drew Cunningham, Jenny Y. Yang
Department of Chemistry
University of California, Irvine
Irvine, CA 92617

Our goals are to 1) develop a thermochemical framework to guide the design of efficient molecular catalysts for aqueous H^+ to H_2 at various pH conditions or selective CO_2 reduction to HCO_2^- and 2) design new ligand architectures with functional groups in the secondary coordination sphere to orchestrate proton movement in multi-electron, multi-proton redox reactions.

Scheme 1

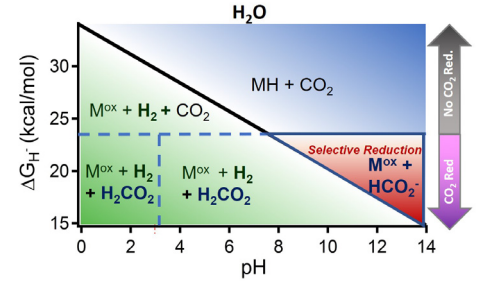

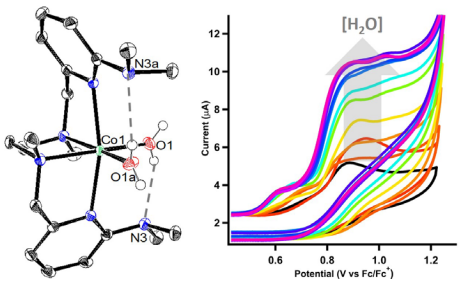

Figure 1. (left) Structural characterization depicting hydrogen-bonding interactions with bound aquo ligands, (right) cyclic voltammetry illustrating oxygen evolution electrocatalysis upon titration with water.

In order to understand the factors that determine selectivity between CO_2 and H^+ reduction, we have been investigating the reactivity of metal hydrides. Selectivity for CO_2 reduction is a difficult challenge because of the commonality of metal hydrides in both reaction pathways. Understanding their reactivity is key to controlling the bifurcating reaction pathways that ultimately determine selectivity. We depict our findings in a diagram (Scheme 1) that describes the thermodynamic products as a function of hydricity and delineating a region where combinations of hydricity and pK_a lead to thermodynamic favorability for selective CO_2 reduction over H_2 evolution. Our depiction is fundamentally a Pourbaix diagram except products are specified as function of hydricity instead of redox potential which provides a more instructive guide for targeted catalyst discovery. We establish the utility of our diagram by selecting a known metal hydride $[HPt(dmpe)_2]^+$ with an appropriate hydricity and demonstrate exclusive CO_2 reduction with high Faradaic efficiency and low overpotential.

In order to mimic aspects of a proton relay microenvironment, $[Co^{LDMA}(CH_3CN)_2][BF_4]_2$ (Figure 1) was synthesized. Structural characterization of the corresponding aqua complexes establish hydrogen bonding between the bound water and pendant base(s). Cyclic voltammetry reveals enhanced oxidative current upon titration with water and controlled potential electrolysis confirms evolution of O_2. The related complex with the same primary coordination environment as $[Co^{LDMA}(CH_3CN)_2][BF_4]_2$ but lacks pendant bases, is inactive. The structural and electrochemical studies illustrate the role positioned proton relays can play in promoting redox reactivity..

Participant List – 40th Solar Photochemistry P.I. Meeting

Neal Armstrong
University of Arizona
nra@email.arizona.edu

John Asbury
Pennsylvania State University
jasbury@psu.edu

Robert Bartynski
Rutgers University
bart@physics.rutgers.edu

Victor Batista
Yale University
victor.batista@yale.edu

Matthew Beard
National Renewable Energy Laboratory
matt.beard@nrel.gov

Louise Berben
University of California Davis
laberben@ucdavis.edu

Jeffrey Blackburn
National Renewable Energy Laboratory
jeffrey.blackburn@nrel.gov

David Bocian
University of California, Riverside
David.Bocian@ucr.edu

Shannon Boettcher
University of Oregon
swb@uoregon.edu

Stephen Bradforth
University of Southern California
bradfort@usc.edu

Kara Bren
University of Rochester
bren@chem.rochester.edu

Gary Brudvig
Yale University
gary.brudvig@yale.edu

Christine Caputo
University of New Hampshire
christine.caputo@unh.edu

Ian Carmichael
Notre Dame Radiation Laboratory
carmichael.1@nd.edu

Felix Castellano
NC State University
fncastel@ncsu.edu

Lin Chen
Argonne National Laboratory
reactioncenter@gmail.com

Kyoung-Shin Choi
University of Wisconsin-Madison
kschoi@chem.wisc.edu

Javier Concepcion
Brookhaven National Laboratory
jconcepc@bnl.gov

Jillian Dempsey
University of North Carolina
dempseyj@email.unc.edu

Dorthe Eisele
City College of New York, CUNY
eisele@eiselegroup.com

Richard Eisenberg
University of Rochester
eisenberg@chem.rochester.edu

Mehmed Zahid Ertem
Brookhaven National Laboratory
mzertem@bnl.gov

Christopher Fecko
U.S. Department of Energy
Office of Basic Energy Sciences
christopher.fecko@science.doe.gov

Graham Fleming
University of California, Berkeley
grfleming@lbl.gov

Heinz Frei
Lawrence Berkeley National Laboratory
HMFrei@lbl.gov

Renee Frontiera
University of Minnesota
rrf@umn.edu

Etsuko Fujita
Brookhaven National Laboratory
fujita@bnl.gov

Elena Galoppini
Rutgers University - Newark
galoppin@newark.rutgers.edu

Bruce Garrett
U.S. Department of Energy
Office of Basic Energy Sciences
bruce.garrett@science.doe.gov

Theodore Goodson III
University of Michigan
tgoodson@umich.edu

David Grills
Brookhaven National Laboratory
dcgrills@bnl.gov

Douglas Grotjahn
San Diego State University
dbgrotjahn@sdsu.edu

Erik Grumstrup
Montana State University
erik.grumstrup@montana.edu

Lars Gundlach
University of Delaware
larsg@udel.edu

Devens Gust
Arizona State University
gust@asu.edu

Thomas Hamann
Michigan State University
hamann@chemistry.msu.edu

Alexander Harris
Brookhaven National Laboratory
alexh@bnl.gov

Craig Hill
Emory University
chill@emory.edu

Dewey Holten
Washington University
holten@wustl.edu

Frances Houle
Lawrence Berkeley National Laboratory
fahoule@lbl.gov

Libai Huang
Purdue University
libai-huang@purdue.edu

Joseph Hupp
Northwestern University
hupp-ofc@northwestern.edu

Cynthia Jenks
Argonne National Laboratory
cjenks@anl.gov

Justin Johnson
National Renewable Energy Laboratory
justin.johnson@nrel.gov

Prashant Kamat
Notre Dame Radiation Laboratory
pkamat@nd.edu

David Kelley
University of California, Merced
dfkelley@ucmerced.edu

Christine Kirmaier
Washington University
kirmaier@wustl.edu

Bruce Koel
Princeton University
bkoel@princeton.edu

Todd Krauss
University of Rochester
krauss@chem.rochester.edu

Nathan S. Lewis
California Institute of Technology
nslewis@caltech.edu

Gonghu Li
University of New Hampshire
gonghu.li@unh.edu

Tianquan Lian
Emory University
tlian@emory.edu

Jonathan Lindsey
NC State University
jlindsey@ncsu.edu

Elisa Link
National Renewable Energy Laboratory
elisa.miller@nrel.gov

Mark Lonergan
University of Oregon
lonergan@uoregon.edu

Stephen Maldonado
University of Michigan
smald@umich.edu

Thomas Mallouk
Pennsylvania State University
tem5@psu.edu

Gerald Manbeck
Brookhaven National Lab
gmanbeck@bnl.gov

Dmitry Matyushov
Arizona State University
dmitrym@asu.edu

James McCusker
Michigan State University
jkm@chemistry.msu.edu

Gail McLean
U.S. Department of Energy
Office of Basic Energy Sciences
gail.mclean@science.doe.gov

Gerald Meyer
University of North Carolina at Chapel Hill
gjmeyer@email.unc.edu

Thomas J. Meyer
University of North Carolina Chapel Hill
tjmeyer@unc.edu

Josef Michl
University of Colorado
josef.michl@colorado.edu

Alexander Miller
University of North Carolina at Chapel Hill
ajmm@email.unc.edu

John Miller
Brookhaven National Laboratory
jrmiller@bnl.gov

Eric Miller
U.S. Department of Energy
Fuel Cell Technologies Office
eric.miller@ee.doe.gov

Michael Mirkin
Queens College-CUNY
mmirkin@qc.cuny.edu

Thomas Moore
Arizona State University
tmoore@asu.edu

Ana Moore
Arizona State University
amoore@asu.edu

Amanda Morris
Virginia Tech
ajmorris@vt.edu

Karen Mulfort
Argonne National Laboratory
mulfort@anl.gov

Djamaladdin Musaev
Emory University
dmusaev@emory.edu

Nathan Neale
National Renewable Energy Laboratory
nathan.neale@nrel.gov

Marshall Newton
Brookhaven National Laboratory
newton@bnl.gov

Daniel Nocera
Harvard University
dnocera@fas.harvard.edu

Arthur Nozik
National Renewable Energy Laboratory
and University of Colorado, Boulder
anozik@nrel.gov

Colin Nuckolls
Columbia University
cn37@columbia.edu

Frank Osterloh
University of California Davis
fosterloh@ucdavis.edu

Bruce Parkinson
University of Wyoming
bparkin1@uwyo.edu

Oleg Poluektov
Argonne National Laboratory
Oleg@anl.gov

Dmitry Polyansky
Brookhaven National Lab
dep@bnl.gov

Oleg Prezhdo
University of Southern California
prezhdo@usc.edu

Sylwia Ptasinska
University of Notre Dame
sptasins@nd.edu

Garry Rumbles
National Renewable Energy Laboratory
garry.rumbles@nrel.gov

Steven Scott Saavedra
Uiniversity of Arizona
saavedra@email.arizona.edu

Richard Schaller
Argonne National Laboratory
schaller@anl.gov

Charles Schmuttenmaer
Yale University
charles.schmuttenmaer@yale.edu

Gregory Scholes
Princeton University
greg.scholes.princeton@gmail.com

Diane Smith
San Diego State University
dksmith@mail.sdsu.edu

Michael Therien
Duke University
michael.therien@duke.edu

Mark Thompson
University of Southern California
met@usc.edu

Randolph Thummel
University of Houston
thummel@uh.edu

David Tiede
Argonne National Laboratory
tiede@anl.gov

William Tumas
National Renewable Energy Laboratory
bill.tumas@nrel.gov

Jao Van de Lagemaat
National Renewable Energy Laboratory
jao.vandelagemaat@nrel.gov

Michael Wasielewski
Northwestern University
m-wasielewski@northwestern.edu

Kevin Wilson
Lawrence Berkeley National Laboratory
krwilson@lbl.gov

Jenny Yang
University of California, Irvine
j.yang@uci.edu

Xiaoyang Zhu
Columbia University
xyzhu@columbia.edu